

LJUBLJANA SLOVENIA
JULY 17-21 2017

Liquids 2017

10TH LIQUID
MATTER
CONFERENCE

Conference book



Liquids Section of the
Condensed Matter Division



Univerza v Ljubljani

10th Liquid Matter Conference

July 17-21 2017

Ljubljana, Slovenia

Conference Book

Volume editors

N. Osterman, M. Vilfan and P. Ziherl

Ljubljana 2017

Conference Book

10th Liquid Matter Conference, Ljubljana, Slovenia, July 17-21 2017

Volume editors: N. Osterman, M. Vilfan and P. Ziherl

Published by European Physical Society, Mulhouse, France and Jožef Stefan Institute, Ljubljana, Slovenia

Ljubljana, 2017

Europhysics Conference Abstracts

Volume 41 F

Series Editor: D. Vernhet, Paris, France

Managing Editor: P. Helfenstein, Mulhouse, France

Cover design: A. Šiber

© European Physical Society

Printed in 700 copies

Published with financial support from Jožef Stefan Institute and University of Ljubljana

Free of charge

ISBN: 978-961-264-109-2

CIP - Kataložni zapis o publikaciji
Narodna in univerzitetna knjižnica, Ljubljana

544.2(082)

54-14(082)

LIQUID Matter Conference (10 ; 2017 ; Ljubljana)

Conference book / 10th Liquid Matter Conference, July 17-21 2017, Ljubljana, Slovenia ; volume editors N. Osterman, M. Vilfan and P. Ziherl. - Mulhouse : European Physical Society ; Ljubljana : Jožef Stefan Institute, 2017. - (Europhysics Conference Abstracts)

ISBN 978-961-264-109-2

1. Osterman, Natan

290562816

Preface

It is our pleasure to welcome you at the 10th Liquid Matter Conference. Organized jointly by the Liquids Section of the Condensed Matter Division of the European Physical Society, the Jožef Stefan Institute, and the University of Ljubljana in Ljubljana, Slovenia. Previous conferences in the series were hosted by Lyon (1990), Florence (1993), Norwich (1996), Granada (1999), Konstanz (2002), Utrecht (2005), Lund (2008), Vienna (2011), and Lisbon (2014). The purpose of the conference is to review recent advances in experimental, theoretical, and applied studies in the liquid state of matter, bringing together researchers working in the physics and chemistry of liquids as well as in several closely related fields such as soft condensed matter and biophysics. Over time, the topics represented at the conference have changed and so has their relative weight measured by the number of papers; this is the natural course of events in a conference series with such a long tradition. The 10th Liquid Matter Conference is an accurate representation of the current state of the field, and we hope that the participants will enjoy the scientific program as well as discussions with fellow researchers. We trust the conference will give rise to new ideas as well as initiate new and strengthen existing collaborations.

The scientific program of the conference consists of 1 prize lecture, 10 plenary lectures, 26 keynote lectures, and 95 contributed oral presentations selected by the International Program Committee. On June 1 2017, 664 poster contributions were submitted.

We gratefully acknowledge the multifaceted support from the Jožef Stefan Institute and the University of Ljubljana. We are thankful to the City of Ljubljana for letting us use the poster boards on the banks of Ljubljanica river for the Liquids Art Exhibition, which may contribute to the visibility of the science of liquid state. We also thank all the sponsors of the conference for the financial support.

Finally, we thank you for participating at the conference and for contributing to its scientific content. We hope that you will like it, and we wish you a productive and enjoyable stay in Ljubljana.

Igor Muševič

J. Stefan Institute and University of Ljubljana
Chairman of the 10th Liquid Matter Conference

Organization

The 10th Liquid Matter Conference is organized by the Liquids Section of the Condensed Matter Division of the European Physical Society, the Jožef Stefan Institute, and the University of Ljubljana in Ljubljana.

Committees

International program committee

C. Bechinger

D. Bartolo

P. G. Bolhuis

F. Caupin

L. Cipelletti

E. Eiser

D. Frenkel

G. Kahl

R. Di Leonardo

I. Mušević (Chair)

M. Müller

I. Pagonabarraga Mora

M. Ravnik

A. K. Soper

M. M. Telo da Gama

N. B. Wilding

I. Nezbeda

International advisory board

D. G. A. L. Aarts

J.-P. Barrat

F. Barocchi

P. Bartlett

L. Belloni

K. Binder

L. Bocquet

C. Dellago

S. Dietrich

M. Dijkstra

R. Dullens

M. D. Ediger

R. Evans

J. Forsman

A. Giacometti

J.-P. Hansen

S. Herminghaus

R. D. Kamien

R. Kapral

A. R. Khokhlov

D. Langevin

O. D. Lavrentovich

H. N. W. Lekkerkerker

Y. Levin

C. N. Likos

G. Maret

G. Pabst

A. Parola

S. Perkin

R. Podgornik

C. P. Royall

S. A. Safran

F. Sciortino

H. Tanaka

P. Tarazona Lafarga

P. I. C. Teixeira

D. N. Theodorou

C. Vega

E. R. Weeks

H. Wennerström

J. M. Yeomans

P. Ziherl

Local organizing committee

I. Muševič (Chair)

R. Podgornik (Vice-chair)

S. Žumer (Vice-chair)

M. Ravnik (Secretary)

P. Ziherl (Secretary)

D. Babić

M. Čepič

S. Čopar

M. Čopič

I. Drevenšek

B. Hribar Lee

M. Kavčič

S. Kralj

Z. Kutnjak

A. Mertelj

N. Osterman

M. Praprotnik

G. Skačej

D. Svenšek

M. Škarabot

J. Štrancar

T. Urbič

U. Tkalec

N. Vaupotič

A. Vilfan

M. Vilfan

B. Zalar

General Information

Venue

The conference will take place at the Cankarjev dom Cultural and Congress Centre (Prešernova 10, SI-1000 Ljubljana, Slovenia). The opening and the closing session as well as all plenary lectures will be held in the Linhart Hall. The three parallel sessions of the conference will be in the the Linhart Hall, the Štih Hall, and the Kosovel Hall. Poster sessions will be in the Grand Reception Hall (level 0) and in Foyer I (level -1) of the Cankarjev dom. During coffee breaks refreshments will be served in the Grand Reception Hall and in Foyer I.

Registration

The Registration Desk is located in the Grand Reception Hall. Registration will start on Sunday July 16 2017 at 14:00 and close at 19:00. On this day, the conference office located next to the Registration Desk will be open from 14:00 to 20:00.

From Monday July 17 2017 until Thursday July 20 2017 the Registration Desk will be open from 8:00 until 18:00 and on Friday July 21 2017 it will be open from 8:00 until 14:00.

On-site registration fees are as follows:

Regular participant	EUR 550
EPS Member	EUR 500
Student	EUR 350

The registration fee includes:

- Admission to all scientific sessions
- Conference materials (printed and electronic book of abstracts)
- Coffee breaks
- Welcome reception
- Certificate of attendance
- Lunches are not included

Also included in the registration bag is a map of nearby restaurants.

Certificate of attendance

A Certificate of Attendance will be issued to all registered participants.

Identification badge

A conference identification badge will be included in the conference material provided upon registration. There will be no admittance to the scientific sessions without the conference badge. Invitations to social events will be collected at the entrance.

Coffee breaks

During coffee breaks refreshments will be served in the Grand Reception Hall and in Foyer I.

Internet

Free on-site wireless access to internet is provided throughout Cankarjev dom. The name of the network is **CD_GUEST**. No login or password is needed.

Contact

Local Organizing Committee: I. Muševič, Jožef Stefan Institute, Jamova 39, SI-1000 Ljubljana, Slovenia; phone: +386 1 4773 572, mobile: +386 51 646 391, fax: +386 1 4773 191, email: igor.musevic@ijs.si.

Congress Agency: A. Kregar, Cankarjev dom Cultural and Congress Centre, Prešernova 10, SI-1000 Ljubljana, Slovenia; phone: +386 1 2417 133, fax: +386 1 2417 297; email: alenka.kregar@cd-cc.si.

Emergency contact

M. Kavčič, mobile: +386 30 721 107, email: masa.kavcic@ijs.si, liquids2017@ijs.si.

Presentations

Plenary, keynote, and contributed talks

Speakers can use their own laptops but are urged to test their presentation **at least a day in advance during one of the breaks** so as to ensure that the presentation is fully functional. During the break before their session, the speakers are asked to connect to the projector and check the quality of the image.

Technical support for speakers will be available at the Speakers Desk, located at the Registration Desk. If your talk has been scheduled for the morning session, you are requested to attend to the technical details one day before your presentation. If your presentation is scheduled Monday July 17 2017 in the morning, you are kindly requested to test it on Sunday July 16 2017, between 17:00 and 19:00. All tests will be performed in the session room where your talk will be delivered.

Please prepare your presentation in format 16:9, this will ensure the best quality picture. All the conference projectors operate best in a 16:9 aspect ratio, switching to another aspect ratio might reduce the image quality and size.

Should your computer have micro HDMI or another dedicated micro-connector for video output, please bring the standard adapter with you.

Users of Mac laptops and other laptops that do not have VGA or HDMI connections are requested to bring an original adapter for the VGA or HDMI connection in the session room.

A backup Windows laptop will be available in each lecture hall.

The duration of plenary lectures is 45 minutes (= 40 minute presentation + 5 minute discussion), the duration of keynote lectures is 30 minutes (= 25 minute presentation + 5 minute discussion), and the duration of contributed talks is 20 minutes (= 17 minute presentation + 3 minute discussion).

Poster presentations

The poster sessions will take place in the Grand Reception Hall and in Foyer I. Each poster will be displayed for two days in a row. Preferred dimensions of posters are 95 cm (width) by 140 cm (height). Scotch tape will be provided to attach posters to the boards.

The first poster session starting Monday July 17 2017 and ending Tuesday July 18 2017 will cover topics

1. Ionic Liquids, Liquid Metals	Foyer I
3. Liquid Crystals	Foyer I
7. Confined Fluids, Interfacial Phenomena	Grand Reception Hall
8. Supercooled Liquids, Glasses, Gels	Grand Reception Hall
10. Active Matter	Foyer I

The second poster session starting Wednesday July 19 2017 and ending Thursday July 20 2017 will cover topics

2. Water, Solutions	Foyer I
4. Polymers, Polyelectrolytes, Biopolymers	Foyer I
5. Colloids	Grand Reception Hall
6. Films, Foams, Surfactants, Emulsions	Grand Reception Hall
9. Driven Systems, Rheology, Nanofluidics	Foyer I
11. Biological and Biomimetic Fluids	Foyer I

The posters will be arranged by the poster number as indicated in the Book of Abstracts. The posters should be displayed between 8:00 and 9:00 on the first day of each poster session and removed from the boards no later than 19:00 on the second day of the session. All posters left on boards after this time will be removed by the organizers.

During the poster session, the authors are kindly asked to stay close to their poster.

EPS poster prize

The EPS Poster Prize in the amount of EUR 200 will be awarded to a PhD student who will present an outstanding poster. The poster must be prepared by the awardee whose student status is defined by student registration. The winning poster will be selected by the committee appointed by the organizers of the conference. The EPS Poster Prize will be awarded on Friday July 21 2017 just before the first plenary lecture.

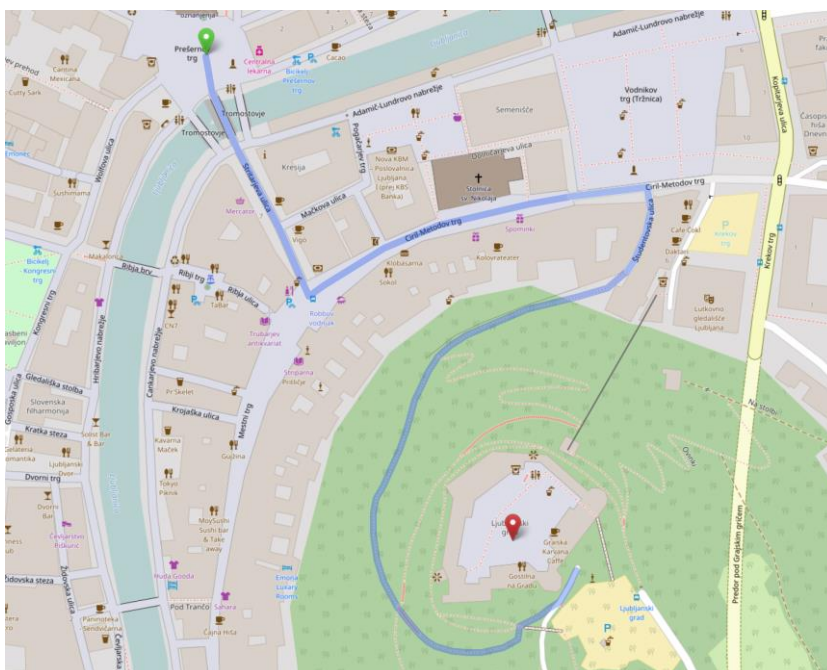
Social Program

Welcome reception

The Welcome Reception will take place Sunday July 16 2017 from 19:00 to 21:00 in the Grand Reception Hall at the ground floor of Cankarjev dom Cultural and Congress Centre. Snacks and drinks will be served.

Conference dinner

The conference dinner will be on Wednesday July 19 2017 in the court of the Ljubljana Castle on the castle hill, starting at 20:00. The Castle can be reached on foot from city center in 10 or 15 minutes; the shortest trail starts at Študentska Street at the southern edge of the Vodnikov Square (see map below). It can also be reached by funicular from Krekov Square (return ticket EUR 4); the funicular operates until 23.00. Bus transport from Cankarjev dom to the Ljubljana Castle and back will be provided, with buses leaving from the exit of the Cankarjev dom at Erjavčeva Street at 19:30. The price of Conference Dinner is EUR 50.



Sponsors

The Organizers are deeply appreciative of the sponsorship generously provided by the following companies:

Aresis



Extreme



Gorenje



RK Tech



List of Exhibitors

Aresis

Comsologic GmbH

Extreme

Institute of Physics, Chinese Academy of Sciences

IOP publishing

RK Tech

SCAN d.o.o.

Springer-Verlag GmbH

Program

Sunday July 16 - Afternoon

14:00 – 19:00	Registration
19:00 – 21:00	Welcome Reception

Monday July 17 - Morning

8:45 – 9:00 Linhart Hall		Opening	
9:00 – 9:45 Linhart Hall, P1			
G. Tarjus Supercooled liquids and the glass transition			
Chair: F. Caupin			
9:45 – 10:00		Break	
10:00 – 11:10 Kosovel Hall Session 8: Supercooled Liquids, Glasses, Gels	10:00 – 11:10 Linhart Hall Session 5: Colloids	10:00 – 11:10 Štíh Hall Session 1: Ionic Liquids, Liquid Metals	
Chair: D. Coslovich	Chair: A. Gambassi	Chair: G. Kahl	
10:00 – 10:30 K8.1 P. Charbonneau Recent advances on the glass problem	10:00 – 10:30 K5.1 C. Dellago How van der Waals interactions determine the unique properties of water: insights from neural network based computer simulations	10:00 – 10:30 K1.1 A. A. Kornyshev Liquid-based tuneable optical metamaterials: New scenarios navigated by theory	
10:30 – 10:50 O8.1 H. Shiba Unveiling dimensionality dependence of glassy dynamics: 2D infinite fluctuation eclipses inherent structural relaxation	10:30 – 10:50 O5.1 J. Loehr Topologically protected multiparticle transport of magnetic colloids	10:30 – 10:50 O1.1 H. Bartsch Insights on the diversity of smectic phases in ionic liquid crystals	
10:50 – 11:10 O8.2 C. Zhang Dynamical and structural signatures of the glass transition in emulsions	10:50 – 11:10 O5.2 A. Caciagli Optical trapping of colloids at a liquid-liquid interface	10:50 – 11:10 O1.2 J. Forsman An asymmetric primitive model approach to ionic liquids	
11:10 – 12:30			
Coffee break and posters (Topics 1, 3, 7, 8, 10)			
12:30 – 14:00			
Lunch break			

<p>14:00 – 14:45 Linhart Hall, P2 K. Stebe Assembly in confined soft matter hosts Chair: N. Wilding</p>		
<p>14:45 – 15:00 Break</p>		
<p>15:00 – 16:30 Kosovel Hall Session 10: Active Matter Chair: R. van Roij</p>	<p>15:00 – 16:30 Linhart Hall Session 5: Colloids Chair: S. Dietrich</p>	<p>15:00 – 16:30 Štíh Hall Session 7: Confined Fluids, Interfacial Phenomena Chair: M. Matsumoto</p>
<p>15:00 – 15:30 K10.1 H. Löwen Microswimmers in complex environments</p>	<p>15:00 – 15:30 K5.2 P. Tierno Engineering of frustration in colloidal artificial ices realized on microfeatured grooved lattices</p>	<p>15:00 – 15:30 K7.1 Q. Chen Direct imaging of crystallization kinetics and interfacial fluctuations of nanoparticle superlattices</p>
<p>15:30 – 15:50 O10.1 J. Simmchen Interactions of chemical microswimmers with microscale objects</p>	<p>15:30 – 15:50 O5.3 J. McBride Localised plasticity in crystals formed by wireframe particles</p>	<p>15:30 – 15:50 O7.1 P. Tarazona Three-dimensional structures of electrolyte aqueous solutions near a solid surface: 3D-AFM experiments and DFT results</p>
<p>15:50 – 16:10 O10.2 J. Stenhammar Pressure and phase equilibria in active brownian particles</p>	<p>15:50 – 16:10 O5.4 C. Evers Mad particles self-assemble into virus-like microcapsules</p>	<p>15:50 – 16:10 O7.2 N. A. M. Araujo How does shape anisotropy affect the aggregation of colloidal particles at the edge of an evaporating drop</p>
<p>16:10 – 16:30 O10.3 I. Buttinoni Confined and complex: When shape and interfaces modify active trajectories</p>	<p>16:10 – 16:30 O5.5 A. Nikoubashman Fabrication of homogeneous and structured polymeric nanoparticles through rapid solvent exchange</p>	<p>16:10 – 16:30 O7.3 L. G. MacDowell Observation of a roughening transition on the surface of ice</p>
<p>16:30 – 17:00 Coffee break</p>		
<p>17:00 – 18:00 Kosovel Hall Session 8: Supercooled Liquids, Glasses, Gels Chair: A. Furukawa</p>	<p>17:00 – 18:00 Linhart Hall Session 5: Colloids Chair: H. Diamant</p>	<p>17:00 – 18:00 Štíh Hall Session 7: Confined Fluids, Interfacial Phenomena Chair: B. Laird</p>
<p>17:00 – 17:20 O8.3 R. Bowles Structure and dynamics in glassy nanoparticles</p>	<p>17:00 – 17:20 O5.6 P. Bartlett Direct measurement of sub-Debye-length forces between charged colloids</p>	<p>17:00 – 17:20 O7.4 I. Martínez Energy transfer between colloids via critical interactions</p>
<p>17:20 – 17:40 O8.4 M. Fuchs Emergence of long-ranged strain and stress correlations at the glass transition</p>	<p>17:20 – 17:40 O5.7 J. Everts Non-touching charged colloidal particles near an oil-water interface</p>	<p>17:20 – 17:40 O7.5 E. Guillermin Negative pressure amplification by precipitation in a confined droplet and consequences for paleotemperatures reconstruction</p>
<p>17:40 – 18:00 O8.5 D. Coslovich Catching up with experiments: Equilibrium simulations of supercooled liquids beyond laboratory time scales</p>	<p>17:40 – 18:00 O5.8 A. Gambassi Nonadditivity of critical Casimir forces</p>	<p>17:40 – 18:00 O7.6 N. Shahidzadeh Evaporation of salt solutions from droplets and thin liquid films</p>

Tuesday July 18 - Morning

<div>9:00 – 9:45 Linhart Hall, P3</div> <div>O. Lavrentovich</div> <div>Command of swimming bacteria by liquid crystals with topological defects and patterns</div> <div>Chair: M. Wilson</div>		
<div>9:45 – 10:00</div> <div>Break</div>		
<div>10:00 – 11:10 Kosovel Hall</div> <div>Session 8:</div> <div>Supercooled Liquids, Glasses, Gels</div> <div>Chair: M. Fuchs</div>	<div>10:00 – 11:10 Linhart Hall</div> <div>Session 3:</div> <div>Liquid Crystals</div> <div>Chair: J. Yamamoto</div>	<div>10:00 – 10:50 Štíh Hall</div> <div>Session 1:</div> <div>Ionic Liquids, Liquid Metals</div> <div>Chair: J. Forsman</div>
<div>10:00 – 10:30 K8.2</div> <div>J. Rottler</div> <div>Cooperative dynamics and memory effects in the deformation and flow of amorphous materials</div>	<div>10:00 – 10:30 K3.1</div> <div>T. López-León</div> <div>Patterning the surface of chiral nematic shells via anchoring in moderation</div>	<div>10:00 – 10:30 K1.2</div> <div>B. Rotenberg</div> <div>Structural transitions at ionic liquid interfaces</div>
<div>10:30 – 10:50 O8.6</div> <div>F. Bomboi</div> <div>A biocompatible re-entrant DNA hydrogel</div>	<div>10:30 – 10:50 O3.1</div> <div>M. Dijkstra</div> <div>Colloidal liquid crystals: How flexible needles become obese, biaxial bricks schizophrenic, and chiral rods twisted</div>	<div>10:30 – 10:50 O1.3</div> <div>J. Comtet</div> <div>Nanoscale capillary freezing of ionic liquids confined between metallic interfaces and the role of electronic screening</div>
<div>10:50 – 11:10 O8.7</div> <div>V. Trappe</div> <div>Interplay of coarsening and aging impacting the mechanical properties of a colloidal gel</div>	<div>10:50 – 11:10 O3.2</div> <div>E. Grelet</div> <div>From soft to hard rod behavior in liquid crystalline suspensions of sterically stabilized colloidal filamentous particles</div>	
<div>11:10 – 12:30</div> <div>Coffee break and posters (Topics 1, 3, 7, 8, 10)</div>		
<div>12:30 – 14:00</div> <div>Lunch break</div>		

<p>14:00 – 14:45 Linhart Hall, P4 R. Dullens Two-dimensional melting of colloidal hard spheres Chair: R. Evans</p>		
<p>14:45 – 15:00 Break</p>		
<p>15:00 – 16:30 Kosovel Hall Session 8: Supercooled Liquids, Glasses, Gels Chair: H. Tanaka</p>	<p>15:00 – 16:30 Linhart Hall Session 5: Colloids Chair: T. Araki</p>	<p>15:00 – 16:30 Štih Hall Session 10: Active Matter Chair: E. Spohr</p>
<p>15:00 – 15:30 K8.3 P. Royall Fivefold symmetry and the fate of liquids</p>	<p>15:00 – 15:20 O5.9 J. Russo Two-dimensional melting in binary hard disks</p>	<p>15:00 – 15:20 O10.4 A. Morin Flocking through disorder</p>
<p>Break</p>		
<p>15:30 – 15:50 O8.8 H. Schöpe Correlation between dynamical and structural heterogeneities in metastable hard-sphere fluids</p>	<p>15:30 – 15:50 O5.10 G. Soligno Self-assembly of cubes into 2D hexagonal and honeycomb lattices by hexapolar capillary interactions</p>	<p>15:30 – 15:50 O10.5 D. Levis Synchronization and pattern formation in active matter</p>
<p>15:50 – 16:10 O8.9 J. de Graaf Fluid flow speeds up the gravitational collapse of colloidal gels</p>	<p>15:50 – 16:10 O5.11 E. Roldan Brownian Carnot engine</p>	<p>15:50 – 16:10 O10.6 D. Vågberg Flowing crystals – the liquid-solid transition of monodisperse active particles</p>
<p>16:10 – 16:30 O8.10 F. Zhang Temporarily arrested state in protein solutions studied using ultra-small angle X-ray scattering</p>	<p>16:10 – 16:30 O5.12 A. Scotti Ultra low crosslinked microgels: How soft are soft particles?</p>	<p>16:10 – 16:30 O10.7 J. Arlt Painting with bacteria</p>
<p>16:30 – 17:00 Coffee break</p>		
<p>17:00 – 18:00 Kosovel Hall Session 3: Liquid Crystals Chair: M. Mazza</p>	<p>17:00 – 18:00 Linhart Hall Session 7: Confined Fluids, Interfacial Phenomena Chair: P. Tarazona</p>	<p>17:00 – 18:00 Štih Hall Session 10: Active Matter Chair: I. Pagonabarraga</p>
<p>17:00 – 17:20 O3.3 L. Metselaar Nematic tactoids in an electric field</p>	<p>17:00 – 17:20 O7.7 E. Charlaix Dynamic flow of confined poly-electrolyte solutions: Interfacial friction and complex slip length</p>	<p>17:00 – 17:20 O10.8 J. Gomez-Solano Dynamics of self-propelled colloidal particles in viscoelastic fluids</p>
<p>17:20 – 17:40 O3.4 J. Yamamoto Phantasmagoric liquid crystals - continuous isotropic-nematic transition driven by shape transformation of micelles</p>	<p>17:20 – 17:40 O7.8 M. Janssen Temperature dependence and thermal response of electric double layer capacitors</p>	<p>17:20 – 17:40 O10.9 J. Ignés-Mullol Control of active nematics by means of addressable soft interfaces</p>
<p>17:40 – 18:00 O3.5 J. Jeong Chiral symmetry breaking of confined lyotropic chromonic liquid crystals: Effects of saddle-splay elastic modulus and dopants</p>	<p>17:40 – 18:00 O7.9 Y. Uematsu Power-law electrokinetic behavior as a direct probe of effective surface viscosity</p>	<p>17:40 – 18:00 O10.10 R. Cerbino Reawakening of motility in glassy confluent epithelia</p>

Wednesday July 19 - Morning

<div>9:00 – 9:45 Linhart Hall, P5</div> <div>D. Vlassopoulos</div> <div>Tuning the performance of polymers: On the role of thickness, associations and free ends</div> <div>Chair: K. Kremer</div>		
<div>9:45 – 10:00</div> <div>Break</div>		
<div>10:00 – 11:10 Kosovel Hall</div> <div>Session 3:</div> <div>Liquid Crystals</div> <div>Chair: J. Fukuda</div>	<div>10:00 – 11:10 Linhart Hall</div> <div>Session 5:</div> <div>Colloids</div> <div>Chair: C.-H. Chang</div>	<div>10:00 – 11:10 Štíh Hall</div> <div>Session 4:</div> <div>Polymers, Polyelectrolytes, Biopolymers</div> <div>Chair: C. Holm</div>
<div>10:00 – 10:30 K3.2</div> <div>I. Smalyukh</div> <div>Static and out-of-equilibrium behavior of topological solitons in partially ordered fluids</div>	<div>10:00 – 10:30 K5.3</div> <div>G. Volpe</div> <div>Experimental studies of critical Casimir forces in colloidal suspensions</div>	<div>10:00 – 10:30 K4.1</div> <div>T. Knowles</div> <div>Kinetics of protein aggregation</div>
<div>10:30 – 10:50 O3.6</div> <div>M. Nikkhou</div> <div>Annihilation dynamics of topological monopoles in nematic liquid crystal</div>	<div>10:30 – 10:50 O5.13</div> <div>E. Lattuada</div> <div>Can colloidal swarms settle faster than isolated particles?</div>	<div>10:30 – 10:50 O4.1</div> <div>D. Mukherji</div> <div>Drunken soft matter: Co-non-solvency based design of smart multi-responsive materials in aqueous alcohol mixtures</div>
<div>10:50 – 11:10 O3.7</div> <div>V. Raghunathan</div> <div>Hexatic phase of self-assembled micellar polymers</div>	<div>10:50 – 11:10 O5.14</div> <div>D. Kraft</div> <div>Self-assembly dynamics of flexible colloidal molecules</div>	<div>10:50 – 11:10 O4.2</div> <div>I. Coluzza</div> <div>Artificial chaperonins</div>
<div>11:10 – 12:30</div> <div>Coffee break and posters (Topics 2, 4, 5, 6, 9, 11)</div>		
<div>12:30 – 14:00</div> <div>Lunch break</div>		

<p>14:00 – 14:45 Linhart Hall, P6 E. Frey Self-organization and collective phenomena in active biopolymer fluids Chair: M. Müller</p>		
<p>14:45 – 15:00 Break</p>		
<p>15:00 – 16:30 Kosovel Hall Session 9: Driven Systems, Rheology, Nanofluidics Chair: A. Würger</p>	<p>15:00 – 16:30 Linhart Hall Session 4: Polymers, Polyelectrolytes, Biopolymers Chair: C. N. Likos</p>	<p>15:00 – 16:30 Štih Hall Session 4: Biological and Biomimetic Fluids Chair: R. Netz</p>
<p>15:00 – 15:30 K9.1 S. Fielding Edge fracture in complex fluids</p>	<p>15:00 – 15:30 K4.2 K. C. H. Daoulas Top-down coarse-grained descriptions of polymeric liquid crystals. A special case: Maier-Saupe models</p>	<p>15:00 – 15:30 K11.1 G. Gompper Blood cells und blood flow – cell deformation, shear thinning, and cell sorting</p>
<p>15:30 – 15:50 O9.1 S. Leitmann Nonlinear microrheological response to a step force</p>	<p>15:30 – 15:50 O4.3 C. Holm The influence of charged-induced variations in the local permittivity on the static and dynamic properties of polyelectrolyte solutions</p>	<p>15:30 – 15:50 O11.1 S. Shimobayashi Direct observations of transition dynamics from macro- to micro-phase separation in asymmetric lipid bilayers</p>
<p>15:50 – 16:10 O9.2 C. Ybert Nanoscale dynamics versus surface interactions: What dictates osmotic transport?</p>	<p>15:50 – 16:10 O4.4 F. Roosen-Runge On scenarios for dynamical arrest in protein solutions</p>	<p>15:50 – 16:10 O11.2 A. Sengupta Active shape control as an adaptive strategy in phytoplankton</p>
<p>16:10 – 16:30 O9.3 S. Jabbari-Farouji The role of intercrystalline tie chains on plastic deformation of semicrystalline polymers</p>	<p>16:10 – 16:30 O4.5 A. Archer Quasicrystal formation in soft matter and a “crystal-liquid” state</p>	<p>16:10 – 16:30 O10.11 F. Woodhouse Active matter logic for autonomous microfluidics</p>
<p>16:30 – 17:00 Coffee break</p>		
<p>17:00 – 18:00 Liquid Matter Prize lecture, Linhart Hall J. Klein Liquids under confinement: From reptation to osteoarthritis Chair: D. Frenkel</p>		
<p>20:00 – 23:00 Conference dinner</p>		

Thursday July 20 - Morning

<div>9:00 – 9:45 Linhart Hall, EPJE de Gennes Lecture, P7</div> <div>R. Golestanian</div> <div>Collective chemotaxis in active matter</div> <div>Chair: C. Bechinger</div>		
<div>9:45 – 10:00</div> <div>Break</div>		
<div>10:00 – 11:10 Kosovel Hall</div> <div>Session 10:</div> <div>Active Matter</div> <div>Chair: M. Dijkstra</div>	<div>10:00 – 11:10 Linhart Hall</div> <div>Session 5:</div> <div>Colloids</div> <div>Chair: W. Kegel</div>	<div>10:00 – 11:20 Štih Hall</div> <div>Session 6:</div> <div>Films, Foams, Surfactants, Emulsions</div> <div>Chair: E. Eiser</div>
<div>10:00 – 10:30 K10.2</div> <div>C. Cottin-Bizonne</div> <div>Suspensions of active particles</div>	<div>10:00 – 10:30 K5.4</div> <div>E. Zaccarelli</div> <div>In-silico synthesis of microgels</div>	<div>10:00 – 10:30 K6.1</div> <div>J. Brujic</div> <div>Folding emulsion polymers</div>
<div>10:30 – 10:50 O10.12</div> <div>C. Maass</div> <div>Chemotaxis and autochemotaxis in self propelling liquid crystal droplets</div>	<div>10:30 – 10:50 O5.15</div> <div>J. Meijer</div> <div>Observation of solid-solid transitions in 3D crystals of colloidal superballs</div>	<div>10:30 – 10:50 O6.1</div> <div>Y. Iwashita</div> <div>Micelles and emulsion droplets in amphiphilic Janus particle–water–oil ternary system</div>
<div>10:50 – 11:10 O10.13</div> <div>C. Maggi</div> <div>Active micromachines: Novel propulsion and control strategies</div>	<div>10:50 – 11:10 O5.16</div> <div>C. Dias</div> <div>Dynamics of self-organization of network fluids</div>	<div>10:50 – 11:20 K6.2</div> <div>I. Cantat</div> <div>Velocity measurements in draining foam films</div>
<div>11:10 – 12:30</div> <div>Coffee break and posters (Topics 2, 4, 5, 6, 9, 11)</div>		
<div>12:30 – 14:00</div> <div>Lunch break</div>		

<p>14:00 – 14:45 Linhart Hall, P8 T. Loerting Water's glass transitions Chair: A. Soper</p>		
<p>14:45 – 15:00 Break</p>		
<p>15:00 – 16:30 Kosovel Hall Session 2: Water, Solutions Chair: S. Woutersen</p>	<p>15:00 – 16:30 Linhart Hall Session 7: Confined Fluids, Interfacial Phenomena Chair: F. Mugele</p>	<p>15:00 – 16:30 Štih Hall Session 11: Biological and Biomimetic Fluids Chair: R. Piazza</p>
<p>15:00 – 15:30 K2.1 C. Valeriani Ice nucleation and water anomalies (EPS invited speaker)</p>	<p>15:00 – 15:30 K7.2 L. Isa Rough particles at liquid-liquid interfaces: Arrested adsorption and "universal" emulsion stabilization</p>	<p>15:00 – 15:30 K11.2 R. Netz The transition from hydrodynamic via interfacial to dry friction for sheared surfaces in water</p>
<p>15:30 – 15:50 O2.1 F. Sciortino Re-entrant limits of stability of the liquid phase and the speedy scenario in colloidal model systems</p>	<p>15:30 – 15:50 O7.10 S. Mandal Diverging time scale in the dimensional crossover for liquids in strong confinement</p>	<p>15:30 – 15:50 O11.3 J. Berret Wire active microrheology to differentiate viscoelastic liquids from soft solids: applications to biophysics</p>
<p>15:50 – 16:10 O2.2 M. Ricci Sweet taste and sugar hydration</p>	<p>15:50 – 16:10 O7.11 M. Engel Precise colloidal assemblies in emulsion droplets</p>	<p>15:50 – 16:10 O11.4 J. Dobnikar Selective activation of immune response by non-specific multivalent interactions</p>
<p>16:10 – 16:30 O2.3 M. Levesque Predicting solvation profiles and free energies of proteins – the molecular density functional theory route</p>	<p>16:10 – 16:30 O7.12 G. Trefalt Interactions between charged particles in like-charged polyelectrolyte solutions: Interplay between non-exponential double-layer and depletion forces</p>	<p>16:10 – 16:30 O11.5 A. Vijaykumar Multiscale MD-GFRD simulations of the effect of rebinding kinetics in dilute diffusion-reaction systems</p>
<p>16:30 – 17:00 Coffee break</p>		
<p>17:00 – 17:40 Kosovel Hall Session 2: Water, Solutions Chair: E. Guardia</p>	<p>17:00 – 18:00 Linhart Hall Session 7: Confined Fluids, Interfacial Phenomena Chair: P. Teixeira</p>	<p>17:00 – 18:00 Štih Hall Session 4: Polymers, Polyelectrolytes, Biopolymers Chair: R. Potestio</p>
<p>17:00 – 17:20 O2.4 F. Merzel Molecular mechanism of hydrophobic hydration</p>	<p>17:00 – 17:20 O7.13 F. Mugele Hofmeister series of wettability in mica-water-alkane systems</p>	<p>17:00 – 17:20 O4.6 A. J. Moreno Single-chain polymer nanoparticles: from simple models for intrinsically disordered proteins to new soft colloids</p>
<p>17:20 – 17:40 O2.5 V. Bianco Contribution of water on the selection and stability of proteins at ambient and extreme thermodynamic conditions</p>	<p>17:20 – 17:40 O7.14 A. Würger Visco-elastic drag force and crossover from no-slip to slip boundary conditions for flow near an air-water interface</p>	<p>17:20 – 17:40 O4.7 H. Meyer Local chain segregation and entanglements in a confined polymer melt</p>
	<p>17:40 – 18:00 O7.15 A. Giacomello Hysteresis phenomena concerning wetting of surfaces with nanoscale defects</p>	<p>17:40 – 18:00 O4.8 A. Chatterji Origin of spatial organization of DNA-polymer in chromosomes</p>

Friday July 21 - Morning

<i>9:00 – 9:45 Linhart Hall, P9</i> D. Bonn Friction: From ice skating to the building of the pyramids Chair: H. Pleiner		
<i>9:45 – 10:00</i> Break		
<i>10:00 – 11:30 Kosovel Hall</i> Session 9: Driven Systems, Rheology, Nanofluidics Chair: M. Schmidt	<i>10:00 – 11:30 Linhart Hall</i> Session 2: Water, Solutions Chair: P. Poole	<i>10:00 – 11:30 Štíh Hall</i> Session 6: Films, Foams, Surfactants, Emulsions Chair: M. M. Telo Da Gama
<i>10:00 – 10:30 K9.2</i> T. Squires Dynamic chemical micro- environments: Designing and visualizing solute and particle migration in non-equilibrium solutions	<i>10:00 – 10:30 K2.2</i> A. D. Stroock From plants to clouds – how nanostructured materials mediate transport and phase behavior in the environment	<i>10:00 – 10:30 K6.3</i> S. Cohen-Addad Playing with trapped gas species or elasticity to arrest coarsening in foams
<i>10:30 – 10:50 O9.4</i> S. Marbach Non-equilibrium separation: From biomimetic kidney-on-a-chip to active sieving	<i>10:30 – 10:50 O2.6</i> S. Woutersen Liquid-liquid transitions in aqueous solutions observed using infrared spectroscopy	<i>10:30 – 10:50 O6.2</i> E. Forel Coarsening and coalescence of a liquid 2D-foam
<i>10:50 – 11:10 O9.5</i> N. Bremond Liquid filled hourglass	<i>10:50 – 11:10 O2.7</i> I. Saika-Voivod Water nanodroplets and the equation of state of TIP4P/2005	<i>10:50 – 11:10 O6.3</i> A. Puisto Foam rheology: negative wake behind a penetrable obstacle
<i>11:10 – 11:30 O9.6</i> G. Nava Onset of non-Newtonian viscosity in a DNA transient network	<i>11:10 – 11:30 O2.8</i> E. Guardia Short range order, hydrogen bonding and rotational dynamics in plastic crystal phases of water	<i>11:10 – 11:30 O6.4</i> D. Filippi Wall roughness effects in micro- channel flows of soft glassy materials
<i>11:30 – 11:45</i> Break		
<i>11:45 – 12:30 Linhart Hall, P10</i> S. Perkin Ionic liquid puzzles Chair: F. Sciortino		
<i>12:30 – 13:00 Linhart Hall</i> Closing session		

Plenary Lectures

Supercooled liquids and the glass transition

G. Tarjus

LPTMC, CNRS/University Pierre and Marie Curie, Paris, France

When cooled fast enough to avoid crystallization, a liquid becomes increasingly viscous and eventually forms a glass. This “glass transition”, one of the oldest unsolved problems in condensed-matter physics, gives rise to a wide diversity of views. Accordingly, there is a lack of agreement on which would be the most profitable theoretical perspective. I will briefly describe the main pieces of the phenomenology and then discuss the progress made in the last decade, including new insights concerning the characteristic length scales associated with the glass transition. The emphasis will be placed on those theories that associate glass formation with growing collective behavior and emerging universality.

Assembly in confined soft matter hosts

K. J. Stebe

*Department of Chemical and Biomolecular Engineering, University of Pennsylvania,
Philadelphia, PA, USA*

We have been developing strategies for directed assembly in soft matter hosts. We define energy landscapes in confined soft matter by controlling geometries and boundary conditions. Colloids placed in these hosts create deformations fields and associated energy fields. These energy fields depend on the energy landscape in the host, which we use to direct assembly.

Here, we discuss three examples. First, we discuss curvature capillary interactions. Particles trapped on interfaces of isotropic fluids deform the interface, increasing the surface area and energy of the interface. Particles interact and assemble in highly organized assemblies guided by the interface curvature. This phenomenon is remarkably rich; particles can experience curvature capillary attraction, repulsion, and find equilibrium states. Second, we discuss Janus colloids on lipid bilayer vesicles. Particles adhered to vesicles also move along paths defined by the vesicle's shape; membrane bending and tension can play important roles. Third, we discuss particles in confined nematic liquid crystals (NLCs). Colloids distort the NLC host, and seed topological defects in the director field. By confining the NLC, an energy landscape can be defined. Colloids move to minimize distortion in this field. First steps in exploiting such interactions in the context of soft robotics are described.

Command of swimming bacteria by liquid crystals with topological defects and patterns

O. D. Lavrentovich

Liquid Crystal Institute, Kent State University, Kent, OH, USA

Self-propelled bacteria are marvels of nature. If we can control their dynamics, we could use it to power dynamic materials and microsystems of the future. Unfortunately, bacteria swimming is mostly random in isotropic liquids such as water and is difficult to control by factors other than transient gradients of nutrients. We propose to command the dynamics of bacteria by replacing water with a water-based lyotropic liquid crystals. The long-range orientational order of the liquid crystal can be designed as uniform or be pre-patterned into various structures by a plasmonic photoalignment technique [1]. In particular, molecular orientation can be pre-programmed to form arrays of topological defects. The experiments demonstrate that the liquid crystal patterns command the dynamics of bacteria, namely, the trajectories of swimming, the polarity of motion, and the distribution of bacteria in space [2]. Topological defects of integer strength serve as attractors of bacteria, while defect pairs pump the bacterial flows along a preselected polar axis. The study of bacteria-liquid crystal system might result in approaches to harness the energy of collective motion for micro-robotic, biomechanical, and sensing devices, as well as micro-mixing and transport of micro-cargo. The work is supported by the US National Science Foundation grant DMR-1507637.

- [1] C. Peng, Y. Guo, T. Turiv, M. Jiang, Q.-H. Wei, and O. D. Lavrentovich, *Adv. Mater.* **2017**, 1606112 (2017).
- [2] C. Peng, T. Turiv, Y. Guo, Q.-H. Wei, and O. D. Lavrentovich, *Science* **354**, 882 (2016).

Two-dimensional melting of colloidal hard spheres

A. L. Thorneywork, J. L. Abbott, D. G. A. L. Aarts, and R. P. A. Dullens

Department of Chemistry, Physical and Theoretical Chemistry Laboratory, University of Oxford, Oxford, United Kingdom

Despite the recent interest in the novel and unique properties of two-dimensional materials, the melting behaviour of the simplest two-dimensional material, hard disks, is still intensely disputed. Crucially, until now – more than half a century after the first simulations of hard-disk freezing were published – no reliable experimental observations of the phase diagram of two-dimensional hard spheres have been reported.

In this talk, I will describe how we determine the full phase behaviour of quasi-two-dimensional colloidal hard spheres [1, 2] by considering a tilted monolayer of particles in sedimentation-diffusion equilibrium [3]. In particular, we measure the equation of state from the density profiles and use time-dependent and height-resolved correlation functions to identify the liquid, hexatic and crystal phases. We find that the liquid-hexatic transition is first order and that the hexatic-crystal transition is continuous. Furthermore, we directly measure the width of the liquid-hexatic coexistence gap from the fluctuations of the corresponding interface, and thereby experimentally establish the full phase behaviour of hard disks [3].

- [1] A. L. Thorneywork, R. Roth, D. G. A. L. Aarts, and R. P. A. Dullens, *J. Chem. Phys.* **140**, 161106 (2014).
- [2] A. L. Thorneywork, R. E. Rozas, R. P. A. Dullens, and J. Horbach, *Phys. Rev. Lett.* **115**, 268301 (2015).
- [3] A. L. Thorneywork, J. L. Abbott, D. G. A. L. Aarts, and R. P. A. Dullens, *Phys. Rev. Lett.* **118**, 158001 (2017).

Tuning the performance of polymers: On the role of thickness, associations and free ends

D. Vlassopoulos^{1,2}

¹ FORTH, Institute of Electronic Structure & Laser, Heraklion, Greece

² University of Crete, Department of Materials Science & Technology, Heraklion, Greece

The ability to form entanglements is perhaps the most intriguing feature of long polymers. Whereas the notion of entanglements is not fully understood yet, their consequences on polymer dynamics are profound and can be explained at molecular level. The associated plateau modulus dictates to a large degree the extent of polymer deformation and flow, hence the final properties and performance. Varying it is a route to tailor processability. We discuss here three recent examples which represent current trends in the field: (i) Macromolecular thickness decreases the number of entanglements and makes polymers akin to supersoft elastomers, as demonstrated with bottlebrushes. Alternatively, dendronized polymers (DPs), comprising a backbone grafted with dendrons, exhibit orientational order, weak shear thinning and elasticity, which can vary by adjusting the degree of polymerization and dendron generation, allowing to span the gap from wormlike polymers to colloidal molecules [1-7]. (ii) Selective introduction of strong associating groups into the DPs leads to hardening in shear and ductile-to-brittle transition in extension. (iii) The absence of free ends has dramatic consequences on the way polymers relax stress. This is manifested with ring polymers which exhibit self-similar relaxation accompanied by a complex long-time response and weak thinning, due to unusual topological interactions [3-7]. Interestingly, mixtures of ring and linear polymers exhibit a plethora of interesting features, all of entropic origin; more remarkable is the addition of small amounts of rings to linear matrices which yields a large increase of viscosity, reflecting enhanced threading. These exciting phenomena can be explained and tuned molecularly and suggest that a strong synergy of polymer physics with chemistry is the way forward.

- [1] A. D. Schlüter, A. Halperin, M. Kröger, D. Vlassopoulos, G. Wegner, and B. Zhang, *ACS Macro Lett.* **3**, 991 (2014).
- [2] S. Costanzo, L. F. Scherz, T. Schweizer, M. Kröger, G. Floudas, A. D. Schlüter, and D. Vlassopoulos, *Macromolecules* **49**, 7054 (2016).
- [3] M. Kapnistos, M. Lang, D. Vlassopoulos, W. Pyckhout-Hintzen, D. Richter, D. Cho, T. Chang, J. Roovers, and M. Rubinstein, *Nat. Mater.* **7**, 997 (2008).
- [4] T. Ge, S. Panyukoy, and M. Rubinstein, *Macromolecules* **49**, 708 (2016).

- [5] J. D. Halverson, G. S. Grest, A. Y. Grosberg, and K. Kremer, Phys. Rev. Lett. **108**, 038301 (2012).
- [6] Y. Doi, K. Matsubara, Y. Ohta, T. Nakano, D. Kawaguchi, Y. Takahashi, A. Takano, and Y. Matsushita, Macromolecules **48**, 3140 (2015).
- [7] Z-C. Yan, S. Costanzo, Y. Jeong, T. Chang, and D. Vlassopoulos, Macromolecules **49**, 1444 (2016).

Self-organization and collective phenomena in active biopolymer fluids

E. Frey

Arnold-Sommerfeld-Center for Theoretical Physics and Center for NanoScience, Ludwig-Maximilians-Universität München, München, Germany

Active matter is a fascinating new field in soft matter physics aiming to understand how interacting active particles self-organise into an intriguing set of patterns and collective non-equilibrium states. Superficially, flocks of animals, self-propelled microorganisms or cytoskeletal systems appear to display similar phenomenologies, hinting towards universal organizing principles. However, upon closer inspection it has turned out that a more comprehensive understanding of the microscopic interaction between active particles beyond simple collision rules is needed to explain the emergent macroscopic order. In this context, the actomyosin motility assay [1] has played an important role. It is composed of two ingredients: actin filaments and molecular motor proteins. Actin filaments move on a lawn of active motors by consuming adenosine triphosphate. We have used the binary collision statistics determined in this assay [2] to predict the collective behavior by using a recently developed numerical scheme to solve the Boltzmann equation for active particles [3]. Contrary to common beliefs, we have found that the alignment effect of the binary collision statistics is too weak to account for the observed ordering transition [2]. This indicates that the dynamics of active matter requires a description that accounts for multi-filament collisions, and calls for a theoretical framework that goes beyond kinetic theories.

In this talk, we will discuss recent theoretical and experimental advances in understanding pattern formation and collective dynamics in active biopolymer systems [4]. We will explain how by tuning the polar or nematic nature of the binary interaction between active biopolymers one is able to precisely control the formation of distinct patterns. In addition, the macroscopic state of these systems exhibits an emergent symmetry that is not already dictated by the symmetry of the microscopic interaction as in equilibrium systems. Both agent-based computer simulations and experiments with the actomyosin motility assay consistently show chimera states in which polar and nematic structures coexist and are in dynamic equilibrium with each other. Our theoretical analysis indicates that multi-stability as well as the capability of varying the emerging order upon small variations in local interactions is a generic feature of active biopolymer liquids. Finally, we will discuss

how chirality in the biopolymers' trajectories leads to novel collective vorticity states [5].

- [1] V. Schaller, C. A. Weber, C. Semmrich, E. Frey, and A. R. Bausch, *Nature* **467**, 73 (2010).
- [2] F. Thüroff, C. A. Weber, and E. Frey, *Phys. Rev. X* **4**, 041030 (2014).
- [3] R. Suzuki, C. A. Weber, E. Frey, and A. R. Bausch, *Nat. Phys.* **11**, 839 (2015).
- [4] L. Huber, T. Krüger, R. Suzuki, A. R. Bausch, and E. Frey, unpublished.
- [5] J. Denk, L. Huber, E. Reithmann, and E. Frey, *Phys. Rev. Lett.* **116**, 178301 (2016).

EPJE Pierre-Gilles de Gennes Lecture: Collective chemotaxis in active matter

R. Golestanian

Rudolf Peierls Centre for Theoretical Physics, University of Oxford, Oxford, United Kingdom

In my talk, I will discuss the non-equilibrium dynamics of particles, which have two types of activity: (i) chemical activity in the form of releasing or consuming chemicals, and (ii) motility that is affected or caused by the chemical activity. These activities will mediate long-range interactions and lead to non-equilibrium fluxes, which join together to lead to interesting collective effects. I examine theoretically the consequences of this interaction, using several examples from synthetic and living systems, including: collective chemotaxis in a solution of catalytically active colloids that could lead to cluster formation, aster condensation, and spontaneous oscillations [1], swarming – in the form of a comet – of light-induced thermally active colloids with negative Soret coefficient due to a shadowing interaction [2], spontaneous formation of small static [3] and dynamic [4] clusters or “molecules” that can exhibit functionality that depends on geometry, and collective behaviour of a colony of cells that divide and interact chemotactically [5]. Finally, I will discuss the limit of slowly diffusing chemicals in the context of trail-following bacteria and how the interaction with the trail leads to complex dynamical behaviour at the single bacterium level [6] and provides a route to bacterial self-organization into micro-colonies [7].

- [1] S. Saha, R. Golestanian and S. Ramaswamy, *Phys. Rev. E* **89**, 062316 (2014).
- [2] J. A. Cohen and R. Golestanian, *Phys. Rev. Lett.* **112**, 068302 (2014).
- [3] R. Soto and R. Golestanian, *Phys. Rev. Lett.* **112**, 068301 (2014).
- [4] R. Soto and R. Golestanian, *Phys. Rev. E* **91**, 052304 (2015).
- [5] A. Gelimson and R. Golestanian, *Phys. Rev. Lett.* **114**, 028101 (2015).
- [6] W. T. Kranz, A. Gelimson, K. Zhao, G. C. L. Wong and R. Golestanian, *Phys. Rev. Lett.* **117**, 038101 (2016).
- [7] A. Gelimson, K. Zhao, C. K. Lee, W. T. Kranz, G. C. L. Wong and R. Golestanian, *Phys. Rev. Lett.* **117**, 178102 (2016).

Water's glass transitions

T. Loerting

Institute of Physical Chemistry, University of Innsbruck, Innsbruck, Austria

Water's anomalous nature is still not understood in spite of at least 200 years of scientific studies on the topic. Mixture models were proposed long ago, e.g., by Röntgen. Two liquid models of water have been considered especially after the simulation work by Poole et al. [1] This work indicates the possibility of a first-order liquid-liquid transition in the one-component system H_2O ending in a critical point. Currently, the best estimate for the location of this hypothesized point is 570 bar and 214 K. Experimental studies on this topic are hampered by the crystallization, which takes place on the microsecond time scale at such conditions. For this reason, a p - T field in the phase diagram of non-crystalline water has remained unexplored and is known as no-man's land. In this contribution I review our recent work on the metastable amorphous ices below the crystallization line (reviewed in Ref. [2]).

In particular, I show how we have optimized the preparation protocol for amorphous ices to increase their crystallization resistance, and hence to shrink the no-man's land [3]. These studies have allowed us to provide evidence for two distinct glass transitions at ambient pressure, which we interpret as evidence for the existence of two distinct (ultraviscous) liquids below 150 K [4]. We followed these glass transitions up to pressures of 2 GPa. In these studies we were able to locate a first-order phase transition between two non-crystalline forms of water at 140 K and 0.07 GPa [5]. We interpret these experiments as the first experimental evidence for co-existence of a low- and high-density liquid of water. In addition to our own interpretation I will highlight the controversies in the field and the open questions on the nature of these glass transitions.

- [1] P. H. Poole, F. Sciortino, U. Essmann, and H. E. Stanley, *Nature* **360**, 324 (1992).
- [2] K. Amann-Winkel, R. Böhmer, F. Fujara, S. Gainaru, B. Geil, and T. Loerting, *Rev. Mod. Phys.* **88**, 011002 (2016).
- [3] M. Seidl, A. Fayter, J. N. Stern, G. Zifferer, and T. Loerting, *Phys. Rev. B* **91**, 144201 (2015).
- [4] K. Amann-Winkel, C. Gainaru, P. H. Handle, M. Seidl, H. Nelson, R. Böhmer, and T. Loerting, *Proc. Natl. Acad. Sci. USA* **110**, 17720 (2013).
- [5] K. Winkel, E. Mayer, and T. Loerting, *J. Phys. Chem. B* **115**, 14141 (2011).

Friction: From ice skating to the building of the pyramids

D. Bonn

Institute of Physics, University of Amsterdam, Amsterdam, The Netherlands

Friction is responsible for 30% of the world energy consumption, but remains incompletely understood. Amonton's famous friction law states that the friction force is proportional to the normal force since both are proportional to the area of contact. The macroscopic friction coefficient is therefore determined by contact details at the microscopic scale. I will show some results where we use a new fluorescence technique that allows us to probe the real area of contact at the molecular scale. In our case, we conclude that important deviations from Amonton's law are observed. These findings can subsequently be used to better understand a number of long-standing friction problems. The slipperiness of ice, for instance, has fascinated scientists for over 130 years, but no real consensus has been reached as to its origin. I will show that the friction coefficient of steel on ice, which is particularly relevant for ice skating, can also be understood by looking at the deviations from Amonton's law. Finally, I will show that one of the findings from the ice skating experiment also allows us to understand why the ancient Egyptians wetted the desert sand with water before sliding heavy stones over it.

Ionic liquid puzzles

S. Perkin

Physical and Theoretical Chemistry Laboratory, University of Oxford, Oxford, United Kingdom

Ionic liquids can be loosely defined as salts that are in the liquid state under near-ambient conditions. They have a range of useful and tuneable physical properties, which has led to interest and application in areas from energy storage to synthesis to electronics. Yet many of their structural and dynamic characteristics have been challenging to explain with our existing theoretical toolkit, presenting several fascinating puzzles for those interested in the nature of the (ionic) liquid state.

I will outline some recent advances in understanding ionic liquids, illustrated by examples from leading researchers around the world as well as our own contributions in this direction. I will focus on ionic liquids and other concentrated electrolytes at interfaces and in confinement, as probed in our experiments using a Surface Force Balance. We reveal curious interfacial phenomena, such as a structural cross-over reminiscent of the packing effects in mixtures of big and small spheres [1], and bulk characteristics, such as anomalously long screening lengths which increase with increasing volume fraction of ions [2]. Finally, a currently-unsolved puzzle concerns large and unanticipated effects of electric fields across films of ionic liquid. Overall I will propose that ionic liquids present several exciting challenges for our understanding of concentrated electrolytes, as well as opening avenues for design of new materials with wide applications.

[1] A. Smith, A. Lee, and S. Perkin, *Phys. Rev. Lett.* **118**, 096002 (2017).

[2] A. Smith, A. Lee, and S. Perkin, *J. Phys. Chem. Lett.* **7**, 2157 (2016).

Liquid Matter Prize Lecture

Liquids under confinement: From reptation to osteoarthritis

J. Klein

Weizmann Institute of Science, Rehovot, Israel

Confinement of liquids can take many forms, and the behavior of the confined fluids may differ profoundly from their bulk behavior. An early example concerned the motion of highly entangled polymers, where topological constraints on chain motion confined them to “tubes”, resulting in a snake-like motion [1], termed reptation, controlling all aspects of their dynamics and flow. More conventional constraints on liquid motion, such as confining surfaces, can lead to dramatic changes in their dynamic properties. In particular, simple non-polar liquids may undergo an abrupt (reversible) dynamic phase transition when confined to a few (five to eight) molecular layers [2]. This can be understood in terms of van der Waals fields at surfaces, which act to densify the near-surface fluid layers. Remarkably, water, whose solid phase is less dense than the liquid phase, does not undergo this transition and remains fluid at all confinements [3]. Organic liquids (oils) solidified under such surface confinement experience stick-slip sliding under shear, a common effect that was long thought to arise from shear melting of the confined material. Recently we demonstrated in a model system that such shear melting does not occur, and the sporadic sliding motion is due rather to periodic interfacial slip [4]. Hydration shells surrounding charges, held through dipole-charge interactions, represent the ultimate confinement of water molecules. The properties of such shells, being both tenaciously held (thus resisting squeeze-out by normal stresses), and at the same time very fluid (thereby responding easily to shear), result in their having remarkable lubrication ability (hydration lubrication) [5]. We found that phosphocholine groups – the head-groups of phosphatidylcholines (PCs), the most common lipids in our bodies – which are especially well hydrated, are exceptionally efficient in this sense [6], and that as a result PC lipids can provide excellent lubricating layers. Boundary layers exposing PC lipid complexes have indeed been recently proposed to underlie the very lubricated surface of healthy articular cartilage [7,8]. We are currently examining how this idea may be used to alleviate osteoarthritis, the most common joint disease, affecting millions, and believed to arise from the breakdown of such lubrication, through the relation between biolubrication and gene regulation within the articular cartilage.

- [1] J. Klein, *Nature* **271**, 143 (1978).
- [2] J. Klein and E. Kumacheva, *Science* **269**, 816 (1995).
- [3] U. Raviv, P. Laurat, and J. Klein, *Nature* **413**, 51 (2001).
- [4] I. Goldian, N. Kampf, A. Yeredor, and J. Klein, *Proc. Natl. Acad. Sci. USA* **112**, 7117 (2015).
- [5] U. Raviv and J. Klein, *Science* **297**, 1540 (2002).
- [6] R. Goldberg, A. Schroeder, Y. Barenholz, and J. Klein, *Adv. Mater.* **23**, 3517 (2011).
- [7] J. Seror, L. Zhu, R. Goldberg, A. J. Day, and J. Klein, *Nat. Commun.* **6**, 6497 (2015).
- [8] S. Jahn, J. Seror, and J. Klein. *Annu. Rev. Biomed. Eng.* **18**, 235 (2016).

Keynote Lectures

Liquid-based tunable optical metamaterials: New scenarios navigated by theory

A. A. Kornyshev

Department of Chemistry, Imperial College London, London, United Kingdom

The notion of *metamaterials* has emerged in the context of new structures with unusual optical properties, such as specially designed plasmonic materials. But metamaterials can be considered more broadly, in the context of what is called *smart materials* which can perform different kind of novel functions at our will. N. Zheludev opened META-2014 congress with a statement: “The time of metamaterials is over. It is the time of ...*tunable* metamaterials”. Electrochemical liquid-based systems are in best position to deliver innovations on this front, to tune the properties of nano and micro- structures by varying electrode potential. My group at Imperial is involved broadly in collaborative research on a variety of such materials: electrovariable nanoplasmonic mirrors, optical switches, and trace analyte sensors [1-5]; but also on electrotuneable friction [6]; ultrananoporous supercapacitors [7,8], electro-actuators [9] and reverse electroactuators (AC-current generating “shoes”) [10]; electrochemical single molecule rectifiers [11].

In this keynote I discuss recent examples of electroactive/ electro-tuneable *optical metamaterials* based on electrolytic liquid | liquid or solid | liquid interfaces, the design of which has been navigated by the theory. The study of many of them is still in progress. These are *electrovariable* plasmonic mirrors-windows and optical filters, Fabry-Perrot resonators, tuneable colour mirrors, and SERS sensors for ultrasensitive detection of hazardous molecules.

Functioning of these structures is underpinned by voltage and composition controlled self-assembling of charged nanoparticles at liquid | liquid or solid | liquid interfaces. The theory of such assembly, as well as of its optical properties, is a key to rational design of such devices. My talk will overview the front of work based on collaboration of several laboratories, including J. Edel, A. R. Kucernak, and F. Bresme (Imperial), M. Urbakh (TAU), leading research associates Y. Montelongo and D. Sikdar, students, and other external collaborators, whose contributions will be highlighted in the talk.

[1] J. Edel, A. A. Kornyshev, A. Kucernak, and M. Urbakh, Chem. Soc. Rev. **45**, 1581 (2016).

[2] J. B. Edel, A. A. Kornyshev, and M. Urbakh, ACS Nano **7**, 9526 (2013).

[3] D. Sikdar and A. A. Kornyshev, Sci. Rep. **6**, 33712 (2016).

- [4] D. Sikdar, S. Bin Hasan, M. Urbakh, J. Edel, and A. A. Kornyshev, *Phys. Chem. Chem. Phys.* **18**, 20486 (2016).
- [5] L. Velleman, D. Sikdar, V. A. Turek, A. R. Kucernak, S. J. Roser, A. A. Kornyshev, and J. Edel, *Nanoscale* **8**, 19229 (2016).
- [6] O. Fajardo, F. Bresme, A. A. Kornyshev, and M. Urbakh, *J. Phys. Chem. Lett.* **6**, 3998 (2015).
- [7] M. V. Fedorov and A. A. Kornyshev, *Chem. Rev.* **114**, 2978 (2014).
- [8] S. Kondrat and A. A. Kornyshev, *Nanoscale Horizons* **1**, 45 (2016).
- [9] A. Lee, R. Colby, and A. A. Kornyshev, *Soft Matter* **9**, 3767 (2013).
- [10] A. B. Kolomeisky and A. A. Kornyshev, *J. Phys. Condens. Matter* **28**, 464000 (2016); corrigendum: **29** (2017).
- [11] K. C. M. Cheung, X. Chen, T. Albrecht, and A. A. Kornyshev, *J. Phys. Chem. C* **120**, 3089 (2016).

Structural transitions at ionic liquid interfaces

B. Rotenberg^{1,2}

¹ Sorbonne Universités, UPMC, CNRS, UMR PHENIX, Paris, France

² Réseau sur le Stockage Electrochimique de l'Energie (RS2E), CNRS, Paris, France

Room Temperature Ionic Liquids (RTILs) consist of mixtures of cations and anions without any solvent, with a low melting point so that, unlike common salts, they are liquid at ambient or moderate temperature. They are now widely used as electrolytes in electrochemical devices, in particular Electrochemical Double Layer Capacitors also known as supercapacitors [1,2].

In this context, understanding the structure, thermodynamics and dynamics of RTIL-metal interfaces is of primary importance. However the Gouy-Chapman-Stern theory, which remains the cornerstone of theoretical electrochemistry since over a century, is of limited help due to the strong ionic correlations within the fluid [3].

I will discuss the properties of such interfaces, emphasizing recent contributions of molecular simulations as well as some experimental evidence of voltage-driven structural changes. I will illustrate in particular the insights provided by the simulation of electrodes maintained at a constant potential and by the analysis of the electrode charge fluctuations in order to analyze and predict the evolution of the interfacial properties with applied voltage [4-6].

- [1] J. Chmiola, G. Yushin, Y. Gogotsi, C. Portet, P. Simon, and P. L. Taberna, *Science* **313**, 1760 (2006).
- [2] C. Merlet, B. Rotenberg, P. A. Madden, P.-L. Taberna, P. Simon, Y. Gogotsi, and M. Salanne, *Nat. Mater.* **11**, 306 (2012).
- [3] M. V. Fedorov and A. A. Kornyshev, *Chem. Rev.* **114**, 2978 (2014).
- [4] D. T. Limmer, C. Merlet, M. Salanne, D. Chandler, P. A. Madden, R. van Roij, and B. Rotenberg, *Phys. Rev. Lett.* **111**, 106102 (2013).
- [5] C. Merlet, D. T. Limmer, M. Salanne, R. van Roij, P. A. Madden, D. Chandler, and B. Rotenberg, *J. Phys. Chem. C* **118**, 18291 (2014).
- [6] B. Rotenberg and M. Salanne, *J. Phys. Chem. Lett.* **6**, 4978 (2015).

EPS Invited Speaker: Ice nucleation and water anomalies

C. Valeriani,^{1,2} E. Sanz,² C. Vega,² J. F. L. Abascal,² and F. Caupin³

¹ *Departamento de Física Aplicada I, Universidad Complutense de Madrid, Madrid, Spain*

² *Departamento de Química Física I, Universidad Complutense de Madrid, Madrid, Spain*

³ *ILM, Université Claude Bernard Lyon 1, Lyon, France*

Avoiding water freezing is the holy grail in cells cryopreservation and climate change modeling. Using a seeding approach [1], in which classical nucleation theory is combined with simulations of ice clusters embedded in supercooled water, we evaluate the nucleation rate at ambient pressure in a wide metastability range [2] and for several water models [3], and estimate the ice-liquid interfacial free energy up to coexistence conditions, in reasonable agreement with the reported experimental values.

Simulating supercooled water outside the experimental temperature window allows us to conclude that ice nucleation above 20 K, via the formation of either hexagonal or cubic ice [4], has necessarily to be heterogeneous [2]. Whereas applying high pressure is a strategy to slow down ice nucleation, due to an increase of the ice I-water interfacial free energy with pressure [5]. Experimental ice nucleation rates are closer to the ones obtained for TIP4P/ICE and mW water [6], water models with similar melting point and enthalpy but different freezing dynamics. Estimating the crystallisation time via the Avrami's expression, we conclude that the minimum crystallization time for TIP4P/ICE is about ten microseconds at 55 K below melting, compatible with the minimum cooling rate required to avoid ice formation [6].

Avoiding crystallisation is the route to unravel the nature of anomalies in supercooled water, such as maxima in the isothermal compressibility [7] (emerging from the no man's land at negative pressure) and a nonmonotonic density dependence of sound velocity [8], in contrast with a standard extrapolation of the equation of state.

[1] J. R. Espinosa, C. Vega, C. Valeriani, and E. Sanz, *J. Chem. Phys.* **144**, 34501 (2016).

[2] E. Sanz, C. Vega, J. R. Espinosa, R. Bernal, J. Abascal, and C. Valeriani, *J. Am. Chem. Soc.* **135**, 15008 (2013).

[3] J. R. Espinosa, E. Sanz, C. Valeriani, and C. Vega, *J. Chem. Phys.* **142**, 18C529 (2014).

[4] A. Zaragoza, M. Conde, J. Espinosa, C. Valeriani, C. Vega, and E. Sanz, *J. Chem. Phys.* **143**, 134504 (2015).

[5] J. Espinosa, A. Zaragoza, P. Rosales-Pelaez, C. Navarro, C. Valeriani, C. Vega, and E. Sanz, *Phys. Rev. Lett.* **117**, 135702 (2016).

[6] J. R. Espinosa, C. Navarro, E. Sanz, C. Valeriani, and C. Vega, *J. Chem. Phys.* **145**, 211922 (2016).

[7] M. A. Gonzalez, C. Valeriani, F. Caupin, and J. L. F. Abascal, *J. Chem. Phys.* **145**, 054505 (2016).

[8] G. Pallares, M. El Mekki Azouzi, M. A. Gonzalez, J. L. Aragonés, J. L. F. Abascal, C. Valeriani, and F. Caupin, *Proc. Natl. Acad. Sci. USA* **111**, 7836 (2014).

From plants to clouds – how nanostructured materials mediate transport and phase behavior in the environment

A. D. Stroock,^{1,2} O. Vincent,¹ S. Zhu,¹ M. Santiago,¹ A. Robin,³ H. Lu,³ and W. L. Black¹

¹ Robert Frederick Smith School of Chemical and Biomolecular Engineering, Cornell University, Ithaca, NY, USA

² Kavli Institute at Cornell for Nanoscale Science, Cornell University, Ithaca, NY, USA

³ Sibley School of Mechanical and Aerospace Engineering, Cornell University, Ithaca, NY, USA

To begin, I will introduce two contexts to motivate fundamental physical questions about the thermodynamics and transport phenomena of water interacting with nanostructured materials: first, the evaporation-driven flow – transpiration – of water from the soil, through plants and into the atmosphere, and its connections to draught response; and, second, the nucleation of condensation and freezing by aerosol particles in the atmosphere, and its connections to cloud formation and atmospheric modeling. Starting from the context of transpiration, I will use experiments in synthetic mimics of the vascular structure of plants to address questions about the breakdown of continuum behavior of liquids in nano-scale confinement, a much-debated topic over the past several decades. In particular, I will use a variety of measurements with a series of liquids to show that continuum thermodynamics and dynamics hold quantitatively in pores that are just 5-10 molecular diameters wide, if account is taken of a monolayer of immobilized molecules. In the context of aerosol-mediated nucleation ice from vapor, I will revisit a long history of measurements that have eluded theoretical explanation. Using experiments with well-characterized synthetic substrates, I will provide strong evidence that freezing on insoluble aerosols proceeds in a two-step process – following the Ostwald step rule – with condensation of a supercooled liquid that subsequently freezes. Importantly, when we account for capillary condensation in nanoscale pore structure, our results provide a coherent structure-property relationship for aerosol-mediated freezing across an important range of conditions found in the atmosphere. I will conclude with perspectives on the translation of these insights and experimental methods toward tools for environmental measurements and for material design in applications for heat transfer and the management of freezing.

Patterning the surface of chiral nematic shells via anchoring in moderation

G. Durey,¹ L. Tran,² M. O. Lavrentovich,² A. Darmon,¹ R. D. Kamien,¹
and T. Lopez-Leon²

¹ UMR CNRS 7083, Ecole Supérieure de Physique et de Chimie Industrielles de la Ville de Paris, PSL Research University, Paris, France

² Department of Physics and Astronomy, University of Pennsylvania, Philadelphia, PA, USA

Chirality is key to the organization and function of many biological systems. However, their complex nature often prevents a thorough understanding of their structure. In the lab, many of their features can be recaptured using cholesteric liquid crystals (CLCs). Interesting defect structures have been recently observed in spherical shells of cholesteric liquid crystal under planar boundary conditions, including defects with double helix structure or stacks of defect rings [1, 2]. Although shells can easily accommodate planar anchoring, the cholesteric order is necessarily frustrated when imposing normal molecular anchoring at the shell interfaces, since this boundary condition is incompatible with the tendency to twist of the liquid crystal [3, 4, 5].

In this work, we study spherical shells of CLC under weak normal anchoring conditions. We control the anchoring at the inner and outer boundaries using two independent methods: by changing the surfactant concentration or by raising the temperature close to the clearing point. When the anchoring energy is comparable to the elastic energy of the liquid crystal, we observe the formation of intricate surface patterns that stem from the competition between these two terms. In particular, we observe a state where long stripes on the shell can be filled with shorter, perpendicular substripes, and a focal conic domain state, where thin stripes wrap into at least two, topologically required, double spirals. We use a Landau-de Gennes model of the CLC to simulate the detailed director configurations as a function of anchoring strength. By increasing the degree of confinement in the CLC, we observe a transition where the stripe width decreases, first continuously, and then abruptly, to half the cholesteric pitch, indicating the unbending of the cholesteric layers. By abruptly changing the topological constraints on the shell, we are able to study the interconversion between director defects and pitch defects, a phenomenon usually restricted by the complexity of the cholesteric phase.

- [1] A. Darmon, M. Benzaquen, D. Seč, S. Čopar, O. Dauchot, and T. Lopez-Leon, *Proc. Natl. Acad. Sci. USA* **113**, 9469 (2016).
- [2] A. Darmon, M. Benzaquen, S. Čopar, O. Dauchot, and T. Lopez-Leon, *Soft Matter* **12**, 9280 (2016).
- [3] D. Seč, S. Čopar, and S. Žumer, *Nat. Commun.* **5**, 3057 (2014).
- [4] T. Orlova, S. J. Aszho, T. Yamaguchi, N. Katsonis, and E. Brasselet, *Nat. Commun.* **6**, 7603 (2015).
- [5] G. Posnjak, S. Čopar, and I. Muševič, *Sci. Rep.* **6**, 26361 (2016).

Static and out-of-equilibrium behavior of topological solitons in partially ordered fluids

I. I. Smalyukh,^{1,2,3} P. J. Ackerman,¹ H. O. Sohn,² and B. J.-S. Tai¹

¹ *Departments of Physics, Department of Electrical, Computer and Energy Engineering, Boulder, University of Colorado, Boulder, CO, USA*

² *Soft Materials Research Center and Materials Science and Engineering Program, University of Colorado, Boulder, CO, USA*

³ *Renewable and Sustainable Energy Institute, National Renewable Energy Laboratory and University of Colorado, Boulder, CO, USA*

Three-dimensional (3D) topological solitons are continuous but topologically nontrivial field configurations localized in 3D-space and embedded in a uniform far-field background. They behave like particles and cannot be transformed to a uniform state through smooth deformations. Many topologically nontrivial 3D-solitonic fields have been proposed. However, the experimental discovery of such solitons is hindered by the need of spatial imaging of the 3D fields. This lecture will start from discussing how we recently experimentally realized and numerically modeled stationary topological solitons in a fluid chiral ferromagnet formed by colloidal dispersions of magnetic nanoplates [1] and in chiral liquid crystals [2]. Such 3D solitons have closed-loop preimages, 3D regions with a single orientation of the magnetization field, which can be linked with each other integer number of times [1,2]. The lecture will discuss both the stability and the unexpected out-of-equilibrium behavior of topological solitons while the host medium responds to external stimuli, such as electromagnetic fields and light. Finally, I will discuss this behavior for localized structures with different knotting and linking of preimages quantified by topological Hopf invariants, as well as how our experimental platform may lead to solitonic condensed matter phases and technological applications.

[1] P. J. Ackerman and I. I. Smalyukh, *Nat. Mater* **16**, 426 (2017).

[2] P. J. Ackerman and I. I. Smalyukh, *Phys. Rev. X* **7**, 011006 (2017).

Kinetics of protein aggregation

T. P. J. Knowles^{1,2}

¹ *Department of Chemistry and Centre for Protein Misfolding Diseases, University of Cambridge, Cambridge, United Kingdom*

² *Cavendish Laboratory, University of Cambridge, Cambridge, United Kingdom*

Filamentous protein aggregation underlies a number of functional and pathological processes in nature. This talk focuses on the formation of amyloid fibrils, a class of beta-sheet rich protein filament. Such structures were initially discovered in the context of disease states where their uncontrolled formation impedes normal cellular function, but are now known to also possess numerous beneficial roles in organisms ranging from bacteria to humans. The formation of these structures commonly occurs through supra-molecular polymerisation following an initial primary nucleation step. In recent years it has become apparent that in addition to primary nucleation, secondary nucleation events which are catalysed the presence of existing aggregates can play a significant role in the dynamics of such systems. This talk describes our efforts to understand the nature of the nucleation processes in protein aggregation as well as the dynamics of such systems and how these features connect to the biological roles that these structures can have in both health and disease. A particular focus will be on the development of new microfluidics approaches to study heterogeneous protein self-assembly and their application to explore the molecular determinants of amyloid formation from peptides and proteins.

Top-down coarse-grained descriptions of polymeric liquid crystals. A special case: Maier-Saupe models

C. Greco,¹ Y. Jiang,² J. Z. Y. Chen,³ K. Kremer,¹ and K. Ch. Daoulas¹

¹ *Max Planck Institute for Polymer Research, Mainz, Germany*

² *School of Chemistry and Environment, Center of Soft Matter Physics and its Applications, Beihang University, Beijing, China*

³ *Department of Physics and Astronomy, University of Waterloo, Waterloo, Canada*

Polymeric liquid crystals (PLC) are interesting for fundamental theory of soft condensed matter and advanced applications, e.g. organic electronics [1]. Studying their mesoscale behavior with all-atom or moderately coarse-grained simulations is impractical due to the large systems that must be considered and protracted equilibration times. An alternative, is to employ mesoscopic models [2] where the amount of degrees of freedom is significantly reduced. Typically such descriptions are developed within top-down strategies, where some ingredients of the model are introduced phenomenologically to reproduce selected material properties.

Here we will discuss Maier-Saupe (MS) models – a special class of top-down models for mesoscopic simulations of polymer nematics. To represent polymer molecules MS models adopt the worm-like chain (WLC) description. The interplay between various microscopic factors favoring nematic alignment in the actual material, is captured via a phenomenological anisotropic non-bonded potential given by $vP_2(\cos \theta)$. Here θ is the angle between two interacting WLC segments, P_2 stands for the second-order Legendre polynomial, while v sets the strength of the potential. We will demonstrate [3-6] how the statistical mechanics of MS models can be investigated with particle-based simulations and Self Consistent Field (SCF) theory. The latter is a powerful method which can efficiently describe morphology and thermodynamic properties. Both techniques are complementary and can elucidate the effect of certain approximations. For example, benefiting from the computational efficiency of SCF it is straightforward to estimate [6] how the increased compressibility of MS models affects phase behavior. However, this efficiency stems from simplifications such as neglecting fluctuations and certain correlations.

We will highlight [5] the effect of these approximations by comparing the free-energy landscape in SCF theory with advanced free-energy calculations in particle-based simulations of MS models. The comparison will demonstrate that the missing

correlations in SCF cannot be taken into account through simple renormalization of model parameters.

- [1] N. Stingelin, Polym. Int. **61**, 866 (2012).
- [2] M. Müller, J. Stat. Phys. **145**, 967 (2011).
- [3] K. C. Daoulas, V. Rühle, and K. Kremer, J. Phys. Condens. Matter **24**, 284121 (2012).
- [4] P. Gemünden and K. C. Daoulas, Soft Matter **11**, 532 (2015).
- [5] C. Greco, Y. Jiang, J. Z. Y. Chen, K. Kremer, and K. C. Daoulas, J. Chem. Phys. **145**, 184901 (2016).
- [6] Y. Jiang, C. Greco, K. C. Daoulas, and J. Z. Y. Chen, Polymers **9**, 48 (2017).

How van der Waals interactions determine the unique properties of water: Insights from neural network based computer simulations

C. Dellago,¹ T. Morawietz,² A. Singraber,¹ and J. Behler³

¹ *Faculty of Physics, University of Vienna, Vienna, Austria*

² *Department of Chemistry, Stanford University, Palo Alto, CA, USA*

³ *Institute of Physical Chemistry, University of Göttingen, Göttingen, Germany*

While the interactions between water molecules are dominated by strongly directional hydrogen bonds, it has become clear that the relatively weak, isotropic van der Waals forces are essential for understanding the properties of liquid water and ice. This insight was mostly gleaned from ab initio computer simulations, which provide an unbiased description of water at the atomic level and yield information on the underlying molecular forces. However, the high computational cost of such simulations prevents the systematic investigation of the influence of van der Waals forces on the thermodynamic anomalies of water. In my talk, I will report on a neural network potential we have recently developed for liquid water and ice [1]. This approach, in which reference data obtained from electronic structure calculations are used to train a neural network for the prediction of energies and forces, yields the accuracy of ab initio simulations at a fraction of their cost. Using neural network potentials parameterized for several density functionals with and without van der Waals corrections, we have shown that van der Waals interactions are crucial for the formation of water's density maximum and its negative volume of melting. Both phenomena can be explained by the flexibility of the hydrogen bond network, which is the result of a delicate balance of weak van der Waals forces, causing a pronounced contraction of the second solvation shell upon cooling that induces the density maximum.

[1] T. Morawietz, A. Singraber, C. Dellago, and J. Behler, *Proc. Natl. Acad. Sci. USA* **113**, 8368 (2016).

Engineering of frustration in colloidal artificial ices realized on microfeatured grooved lattices

A. Ortiz Ambriz,¹ J. Loher,^{1,2} and P. Tierno^{1,3}

¹ *Departament de Física de la Matèria Condensada, Universitat de Barcelona, Barcelona, Spain*

² *Physikalisches Institut, Universität Bayreuth, Bayreuth, Germany*

³ *Institut de Nanociència i Nanotecnologia, IN²UB, Universitat de Barcelona, Barcelona, Spain*

Artificial spin ice systems, namely lattices of interacting single domain ferromagnetic islands, have been used to date as microscopic models of frustration induced by lattice topology, allowing for the direct visualization of spin arrangements and textures. However, the engineering of frustrated ice states in which individual spins can be manipulated in situ and the real-time observation of their collective dynamics remain challenging tasks. Inspired by recent theoretical advances, here we realize a colloidal version of an artificial spin ice system using interacting polarizable particles confined to lattices of bistable gravitational traps. We show quantitatively that ice-selection rules emerge in this frustrated soft matter system by tuning the strength of the pair interactions between the microscopic units [1].

Combining real-time experiments with simulations, we prove that these defects behave like emergent topological monopoles obeying a Coulomb law with an additional line tension. We further show how to realize a completely resettable “NOR” gate, which provides guidelines for fabrication of nanoscale logic devices based on the motion of topological magnetic monopoles [2].

[1] A. Ortiz-Ambriz and P. Tierno, *Nat. Commun.* **7**, 10575 (2016).

[2] J. Loehr, A. Ortiz-Ambriz, and P. Tierno, *Phys. Rev. Lett.* **117**, 168001 (2016) .

Experimental studies of critical Casimir forces in colloidal suspensions

G. Volpe

Department of Physics, University of Gothenburg, Gothenburg, Sweden

Recently, critical Casimir forces have been proved to be a powerful tool to control the self-assembly and complex behavior of microscopic and nanoscopic colloidal particles. Critical Casimir forces were theoretically predicted by Fisher and de Gennes in 1978 [1]: the confinement of thermal fluctuations in a binary liquid mixture may result in attractive or repulsive interactions with universal features. These thermal fluctuations typically occur on the molecular scale; however, on approaching a critical point of a second-order phase transition, they become relevant and correlated across a much larger (up to several micrometers) length scale characterized by a correlation length. The first direct experimental evidence for critical Casimir forces was provided only in 2008, using total internal reflection microscopy (TIRM) [2]. Since then, these forces have been investigated under various conditions, for example, by varying the properties of the involved surfaces or with moving boundaries. In addition, a number of studies of the phase behaviour of colloidal dispersions in a critical mixture indicate critical Casimir forces as candidates for tuning the self-assembly of nanostructures and quantum dots, while analogous fluctuation-induced effects have been investigated, for example, at the percolation transition of a chemical sol, in the presence of temperature gradients, and even in granular fluids and active matter. In this presentation, I will give an overview of this field with a focus on recent results on the measurement of many-body forces in critical Casimir forces [3] and on the direct measurement of critical Casimir forces between colloids [4].

- [1] M. E. Fisher and P. G. de Gennes, C. R. Acad. Sci. Paris B **287**, 207 (1978).
- [2] C. Hertlein, L. Helden, A. Gambassi, S. Dietrich, and C. Bechinger, Nature **451**, 172 (2008).
- [3] S. Paladugu, A. Callegari, Y. Tuna, L. Barth, S. Dietrich, A. Gambassi, and G. Volpe, Nat. Commun. **7**, 11403 (2016).
- [4] F. Schmidt, A. Magazzù, A. Callegari, L. Biancofiore, F. Cichos, and G. Volpe, arXiv 1705.03317 (2017).

***In-silico* synthesis of microgels**

E. Zaccarelli^{1,2}

¹ *CNR Institute for Complex Systems, Rome, Italy*

² *Department of Physics, Sapienza University of Rome, Rome, Italy*

Microgels are soft particles individually made by cross-linked polymer networks. They are nowadays widely used as a colloidal model system because of their swelling properties and their responsivity to external control parameters such temperature or pH. In the most used synthetic protocol, microgels have an inhomogeneous density profile characterized by a core-corona structure. The internal architecture thus affects the effective interactions between microgels, especially at high densities. In addition, temperature variations leading to a more compact structure will also change the effective interactions. For these reasons, the simple Hertzian model for elastic spheres is only applicable to the fluid regime [1]. In order to go beyond this simplified picture, we have recently synthesized microgels in-silico using different preparation protocols [2]. In this talk I will discuss the internal properties of these particles in relation to available experimental data for varying softness and temperature with the aim to provide a realistic model that will be used to determine more accurate effective interactions.

- [1] D. Paloli, P. S. Mohanty, J. J. Crassous, E. Zaccarelli, and P. Schurtenberger, *Soft Matter* **9**, 3000 (2013).
- [2] N. Gnan, L. Rovigatti, and E. Zaccarelli, in preparation (2017).

Folding emulsion polymers

A. McMullen and J. Brujic

Center for Soft Matter Research, Department of Physics, New York University, New York, NY, USA

Traditionally, assembly lines to build machines, from electronic circuits to motor vehicles, follow very specific instruction manuals, followed by robots or people. On the other hand, in biology, organisms self-assemble spontaneously according to the instructions encoded in their genes — following the laws of physics. Inspired by biology, we design and develop emulsions with specific DNA or protein-protein interactions that guide their spontaneous assembly into linear or branched freely-jointed polymers, with programmable sequences, capable of folding into more complex 3D architectures. The droplets can readily be solidified, therefore they offer a route to hands-off manufacturing of desired objects.

Velocity measurements in draining foam films

J. Seiwert,^{1,2} R. Kervil,^{1,3} S. Nou,¹ and I. Cantat¹

¹ *Institut de Physique de Rennes, Université de Rennes, Rennes, France*

² *Air Liquide, Centre de Recherche Paris-Saclay, Les Loges-en-Josas, France*

³ *Institut Lumière Matière, Université de Lyon, Villeurbanne, France*

Foam films are stable because surface tension gradients induce a net force on the trapped solution and balance the gravity [1]. The velocity within a vertical film, *relatively to the interface*, is a simple Poiseuille flow, with a typical velocity given by the Reynolds prediction $v_R = \rho g h^2 / \eta$, with ρ the fluid density, g the gravity, h the local film thickness, and η the fluid viscosity. If h is of the order of 1 μm , this Reynolds velocity is of the order of 10 $\mu\text{m/s}$ which is much lower than the measured velocities. The velocities in the film are thus controlled by the interface velocities, involving the rheological properties of the surfactants. It has been shown by Mysels et al. in a pioneering work [2] that in some cases the drainage time is proportional to the film width, which was qualitatively explained at that time by the dominant role of the menisci at the film boundaries. This implies a complex flow within the draining film that we measure here using a tracer-free innovative velocimetry technique.

Our measurements rely on a fluorescent labeled surfactant solution (sodium dodecyl sulfat (SDS) 10 g/L, fluorescein sodium 0.1 g/L, glycerol 10% wt). A dark spot is photobleached and acts as a perfect passive tracer during fractions of second, before disappearing by diffusion or mixing. This is repeated in time during the whole life time of the film, and at many locations, in order to obtained the velocity field in the whole film as a function of the time. The velocity field shows a downward velocity of the order of 1 mm/s in the central part of the 1 μm thick film. Refine measurements in the first millimetre close to the lateral meniscus evidence an upward velocity that may reach 10 mm/s. This coincide with an observable pinching of the film, in contact with the lateral meniscus. This marginal pinching has been described theoretically by Aradian et al. [3] and arises from the capillary suction in the meniscus.

The total flux of interface across an horizontal line is close to zero, thus validating the assumption of conserved interface area during the flow. With this assumption, the velocity field in the film can be deduced from the force balance on an elementary piece of foam. It is govern schematically by the following processes: The film near the meniscus get thinner because of the capillary suction, and its mass per unit area (2D density) is thus smaller than in the middle of the film. An Archimedean-like

force arises from this 2D-density discrepancy, based on gravity and surface tension gradient, at the origin of the upward motion. Finally the surface viscosity induces a friction between the fluid moving upward and the fluid moving downward and governs the velocity scale. We propose scaling laws for the associated velocities [4].

- [1] P.-G. de Gennes, *Langmuir* **17**, 2416 (2001).
- [2] K. J. Mysels, K. Shinoda and A. Frankel, *Soap films: Study of their thinning and a bibliography* (Pergamon, New York, 1959).
- [3] A. Aradian, E. Raphaël, and P.-G. de Gennes, *Europhys. Lett.* **55**, 83 (2001).
- [4] J. Seiwert, R. Kervil, S. Nou, and I. Cantat, *Phys. Rev. Lett.* **118**, 048001 (2017).

Playing with trapped gas species or elasticity to arrest coarsening in foams

S. Cohen-Addad,¹ H. Bey,^{1,2} R. Höhler,¹ O. Ronsin,¹ and F. Wintzenrieth¹

¹ *Institut des Nanosciences de Paris, Université Pierre et Marie Curie, Paris, France*

² *LR99ES16 Laboratoire Physique de la Matière Molle et de la Modélisation
Électromagnétique, Université de Tunis El Manar, Tunis, Tunisia*

Liquid foams are constituted of dense packings of gas bubbles in a surfactant solution. They can get turned into solid materials as their continuous phase is solidified. Both liquid and solid foams are sought for many applications ranging from material sciences to chemical engineering due to their unique rheological properties [1] or their ability to provide cellular materials with specific structural and mechanical properties [2]. Therefore, elaborating stable foams is crucial to meet their required properties. Here we study how coarsening in liquid foams can be slowed down by using a mixture of gas containing an insoluble species and how coarsening can even be arrested in a soft solid elastic foam. This raises the question whether elastic stresses and osmotic pressure can eventually overcome Laplace pressure differences that drive foam coarsening.

We describe recent experiments with ordered liquid foams where a gas mixture with controlled concentration is used to inflate the bubbles or where the continuous phase is made of a hydrogel. As the latter undergoes gelation, the foam becomes a solid elastic material. We investigate whether such liquid or solid foams may coarsen, and we determine their stability diagram as a function of the bubble size, the shear modulus of the foam and the insoluble gas concentration. We propose a linear stability criterion based on a coarse grained physical model that predicts the stability diagram. It is consistent with a previous prediction regarding Ostwald ripening in diluted emulsions [3]. Our model predicts that the domain of stable foams is governed by a characteristic elastocapillary radius given by the ratio of surface tension to foam shear modulus, in qualitative agreement with our experimental findings.

[1] S. Cohen-Addad and R. Höhler, *Curr. Opin. Colloid. Interf. Sci.* **19**, 536 (2014).

[2] M. Scheffler and P. Colombo, *Cellular Ceramics: Structure, Manufacturing, Properties and Applications* (Wiley, New York, 2005).

[3] A. Webster and M. Cates, *Langmuir* **14**, 2068 (1998).

Direct imaging of crystallization kinetics and interfacial fluctuations of nanoparticle superlattices

Q. Chen

University of Illinois, Department of Materials Science and Engineering, Urbana, IL, USA

We use a new nanoscopic imaging tool, liquid-phase transmission electron microscopy, to image and understand the crystal growth front and interfacial fluctuation of a nanoparticle superlattice. With single particle resolution and hundreds of nanoscale building blocks in view, we are able to identify the interface between ordered lattice and disordered structure and visualize the kinetics of single building block attachment at the lattice growth front. The spatial interfacial fluctuation profiles support the capillary wave theory, from which we derive a surface stiffness value consistent with scaling analysis. Our experiments demonstrate the potential of extending model study on collective systems to nanoscale with single particle resolution and to fundamental theories of condensed matter at a length scale linking atoms and micrometer-sized colloids.

Rough particles at liquid-liquid interfaces: Arrested adsorption and “universal” emulsion stabilization

M. Zanini,¹ C. Marschelke,² S. Anachkov,³ E. Marini,¹ A. Synytska,² and
L. Isa¹

¹ *Laboratory for Interfaces, Soft matter and Assembly, Department of Materials, ETH, Zurich, Switzerland*

² *Department of Polymer Interfaces, Leibniz Institute of Polymer Research, Dresden, Germany*

³ *Department of Chemical and Pharmaceutical Engineering, Faculty of Chemistry and Pharmacy, Sofia University, Sofia, Bulgaria*

Surface heterogeneities, including surface roughness, significantly affect the adsorption [1-3], motion [4,5] and interactions [6-9] of particles at fluid interfaces. These consequences of surface heterogeneities have been the focus of many studies, but there is still a lack of experimental systematic work where the roughness is tailored over a broad range of length scales and its effect on particle wettability is investigated at the single-particle level. Here, we synthesize a library of all-silica microparticles with uniform surface chemistry, but tuneable surface roughness and study their spontaneous adsorption at oil-water interfaces. Akin to contact-line pinning for macroscopic droplets on structured surfaces [10], we demonstrate that surface roughness strongly pins the particle contact lines and arrests their adsorption in long-lived metastable positions. We also directly show that the interface around each particle is deformed as predicted by the capillary theory [6,7]. Finally, pinning imparts tremendous contact angle hysteresis for rough particles adsorbing either from the polar, or the non-polar phase. For large enough roughness, this can practically invert the particle wettability, irrespective of their chemical nature, e.g. rough hydrophilic particles can behave as hydrophobic ones if adsorbing from the oil. As a unique consequence, the same rough particles can be used as “universal” stabilizers for both water-in-oil and oil-in-water emulsions by just changing the phase in which they are initially dispersed. These results both shed light on fundamental phenomena concerning particle adsorption and indicate new design rules for particle-based emulsifiers [11].

[1] Y. Nonomura, S. Komura, and K. Tsujii, *J. Phys. Chem. B* **110**, 13124 (2006).

[2] D. M. Kaz, R. McGorty, M. Mani, M. P. Brenner, and V. N. Manoharan, *Nat. Mater.* **11**, 138 (2012).

- [3] A. Wang, R. McGorty, D. M. Kaz, and V. N. Manoharan, *Soft Matter* **12**, 8958 (2016).
- [4] G. Boniello, C. Blanc, D. Fedorenko, M. Medfai, N. Ben Mbarek, M. In, M. Gross, A. Stocco, and M. Nobili, *Nat. Mater.* **14**, 908 (2015).
- [5] N. Sharifi-Mood, I. B. Liu, and K. J. Stebe, *Soft Matter* **11**, 6768 (2015).
- [6] D. Stamou, C. Duschl, and D. Johannsmann, *Phys. Rev. E* **62**, 5263 (2000).
- [7] P. A. Kralchevsky, N. D. Denkov, and K. D. Danov, *Langmuir* **17**, 7694 (2001).
- [8] W. Chen, S. Tan, Z. Huang, T.-K. Ng, W. T. Ford, and P. Tong, *Phys. Rev. E* **74**, 021406 (2006).
- [9] W. Chen, S. Tan, Y. Zhou, T.-K. Ng, W. T. Ford, and P. Tong, *Phys. Rev. E* **79**, 041403 (2009).
- [10] J. -F. Joanny and P. G. de Gennes, *J. Chem. Phys.* **81**, 552 (1984).
- [11] M. Zanini et al., submitted (2017).

Recent advances on the glass problem

P. Charbonneau^{1,2}

¹ *Department of Chemistry, Duke University, Durham, NC, USA*

² *Department of Physics, Duke University, Durham, NC, USA*

Recent advances in the mean-field theory of glasses predict the existence, deep in the glass phase, of a novel phase transition. This so-called Gardner transition signals the emergence of a complex free energy landscape composed of a marginally stable hierarchy of sub-basins. It is also thought to be the onset of the anomalous thermal and transport properties of amorphous solids as well as the origin of the unusual critical properties observed at the jamming transition. This talk offers an overview of our latest theoretical and numerical progress in understanding this novel materials feature [1].

- [1] P. Charbonneau, J. Kurchan, G. Parisi, P. Urbani, and F. Zamponi, *Annu. Rev. Condens. Matter Phys.* **8**, 265 (2017).

Cooperative dynamics and memory effects in the deformation and flow of amorphous materials

J. Rottler

Department of Physics and Astronomy, University of British Columbia, Vancouver, Canada

This presentation will explore particle scale processes during plastic deformation of amorphous materials with molecular simulations. Macroscopic flow occurs in the form of swift localized shear transformations in the background of a homogeneously deforming medium. We show that these plastic events correlate with subtle structural features that can be identified by soft quasilocalized vibrational modes [1]. The elastoplastic response of the medium to a plastic event, as well as their mutual correlations, exhibit quadrupolar symmetry that is characteristic of the shear stress redistribution following the local transformation [2, 3]. At finite temperature, structural recovery occurs spontaneously due to thermal activation, and the relaxation times grow as the glass slowly evolves or ages towards equilibrium. We show that the evolution of the relaxation time can be quantitatively described in a mean-field picture, where particle trajectories are computed from a continuous time random walk [4]. We then compare the relaxation times during different deformation protocols to the predictions of simple fluidity type models [5]. Time permitting, we also discuss briefly the role of inertia in the shear rheology of amorphous solids.

- [1] A. Smessaert and J. Rottler, *Soft Matter* **10**, 8533 (2014).
- [2] F. Puosi, J. Rottler, and J. L. Barrat, *Phys. Rev. E* **89**, 042302 (2014).
- [3] F. Puosi, J. Rottler, and J-L. Barrat, *Phys. Rev. E* **94**, 032604 (2016).
- [4] M. Warren and J. Rottler, *Phys. Rev. Lett.* **110**, 025501 (2013).
- [5] J. Rottler, *J. Chem. Phys.* **145**, 064505 (2016).

Fivefold symmetry and the fate of liquids

C. P. Royall,^{1,2,3,4} J. E. Hallett,^{1,3} F. Turci,^{1,3} N. Wood,^{1,3} J. Russo,⁵ and G. Tarjus⁶

¹ *H. H. Wills Physics Laboratory, Bristol, United Kingdom*

² *School of Chemistry, University of Bristol, Bristol, United Kingdom*

³ *Centre for Nanoscience and Quantum Information, Bristol, United Kingdom*

⁴ *Department of Chemical Engineering, Kyoto University, Kyoto, Japan*

⁵ *School of Mathematics University of Bristol, Bristol, United Kingdom*

⁶ *LPTMC, CNRS-UMR 7600, Université Pierre et Marie Curie, Paris, France*

That fivefold symmetry should play a crucial role in the non-equilibrium behaviour of condensed matter was proposed in the 1950s [1]. Six decades later, the basic mechanism of the solidification of liquids remains unexplained, either in the case that the material crystallises, or that it forms an amorphous solid, a glass [2]. We will explore the implications of fivefold symmetry in the solidification of liquids and discuss two recent developments. Crystallisation is among the most common everyday physical phenomena. Yet in the only material in which quantitative comparison has been made between experiment and theory — hard spheres — predictions of crystal nucleation rates are up to 20 orders of magnitude slower than measurements, the “second worst prediction in physics” [3]. This discrepancy casts doubt upon the theoretical methods concerned — importance sampling — which is important not only for crystallisation, because these methods are used to tackle a very wide range of problems, such as drug uptake in cells and chemical reaction pathways. We present results that show that fivefold symmetric arrangements of particles may hold the key to resolving this long-standing puzzle [4]. The nature of amorphous solids — glasses — is not understood: The possibility of a phase transition to a thermodynamically stable “ideal glass” is a contentious and challenging issue. Unlike everyday non-equilibrium glasses, such an ideal glass has a vanishing entropy — like a crystal — yet remains amorphous. Building on the ideas of Frank, the geometric frustration approach to the glass transition posits an avoided phase transition in a curved space inaccessible to experiment [5]. Here we show that such a “crystallisation” to a state comprised of fivefold symmetric icosahedra indeed occurs and consider the implications of this avoided transition in the Euclidean space relevant to experiments [6].

[1] F. C. Frank, Proc. R. Soc. A. **215**, 43 (1952).

[2] C. P. Royall and S. R. Williams, Phys. Rep. **560**, 1 (2015).

[3] J. Russo, A. Maggs, H. Tanaka, and D. Bonn, Soft Matter **9**, 7369 (2013).

[4] J. Taffs and C. P. Royall, Nat. Commun. **7**, 13225 (2016).

[5] G. Tarjus, S. A. Kivelson, Z. Nussinov, and P. Viot, J. Phys. Condens. Matter **17**, R1143 (2005)

[6] F. Turci, G. Tarjus, and C. P. Royall, accepted in Phys. Rev. Lett. (2017).

Edge fracture in complex fluids

S. M. Fielding, E. J. Hemingway, and H. Kusumaatmaja

Department of Physics, Durham University, Durham, UK

In the most common rheological experiment, a sample of complex fluid is sandwiched between plates and sheared. Plotting the steady state shear stress versus the imposed shear rate then gives the flow curve, which plays a central role in fundamentally characterising the flow behaviour of any complex fluid. Almost ubiquitously encountered beyond a certain (material and device dependent) shear rate, however, is the phenomenon of edge fracture: the free surface where the edge of the fluid sample meets the outside air destabilises, rendering accurate rheological measurement impossible. Anecdotal reports of this effect pervade the literature and are too numerous to recount. Indeed, it is (at least arguably) seen as the limiting factor in rotational rheometry.

In this work, we study theoretically the edge fracture instability using linear stability analysis and direct nonlinear simulations. We derive an exact expression for the onset of edge fracture in terms of the shear-rate derivative of the fluid's second normal stress difference, the shear-rate derivative of the shear stress, the jump in shear stress across the interface between the fluid and the outside medium (usually air), the surface tension of that interface, and the rheometer gap size. We provide a mechanistic understanding of the edge fracture instability, validated against our simulations. These findings, which are robust with respect to choice of rheological constitutive model, also suggest a possible route to mitigating the effect, potentially allowing experimentalists to achieve and accurately measure stronger flows [1].

[1] E. J. Hemingway, H. Kusumaatmaja, and S. M. Fielding, arxiv.org/abs/1703.05013.

Dynamic chemical micro-environments: Designing and visualizing solute and particle migration in non-equilibrium solutions

T. M. Squires

Department of Chemical Engineering, University of California, Santa Barbara, CA, USA

Microfluidic techniques enable exquisite control over the physical and chemical properties of experimental systems. We will describe new techniques we have developed to sculpt chemical environments in space and time [1], and interferometric methods to visualize these concentration fields as they evolve [2]. We will illustrate with direct, dynamic measurements of water sorping into ionic liquids, reagent depletion during interfacial polymerization reactions, and solvent diffusion through hydrogels.

We then use this solution-sculpting to study the diffusiophoretic migration of colloids under imposed chemical gradients [3, 4, 5]. Such phenomena occur quite generally in response to non-equilibrium chemical fluxes, and therefore arises in a wide variety of real-world systems. Nonetheless, diffusiophoresis has remained stubbornly difficult to observe or characterize directly. We will discuss the physico-chemical phenomena that underlie diffusiophoresis, and therefore how to intuitively design systems with desired diffusiophoretic properties.

Finally, we will build on this foundation to introduce conceptually new colloidal interactions that are non-equilibrium but long-lived, much longer-ranged than is possible in aqueous suspensions, and are chemically-specific[6]. We envision a broad role for such interactions in destabilizing suspensions, breaking emulsions, and extracting compounds.

- [1] J. S. Paustian, R. N. Azevedo, S.-T. B. Lundin, M. J. Gilkey, and T. M. Squires, *Phys. Rev. X* **3**, 1 (2014).
- [2] D. R. Vogus, V. Mansard, M. V. Rapp, and T. M. Squires, *Lab Chip* **15**, 1689 (2015).
- [3] J. S. Paustian, C. D. Angulo, R. Nery-Azevedo, N. Shi, A. I. Abdel-Fattah, and T. M. Squires, *Langmuir* **31**, 4402 (2015).
- [4] N. Shi, R. Nery-Azevedo, A. I. Abdel-Fattah, and T. M. Squires, *Phys. Rev. Lett.* **117**, 258001 (2016).
- [5] T. M. Squires, in *Soft materials - generation, physical properties and fundamental applications*, edited by A. Fernandez- Nieves (Wiley-VCH, Berlin, 2012).
- [6] A. Banerjee, I. Williams, R. N. Azevedo, M. E. Helgeson, and T. M. Squires, *Proc. Natl. Acad. Sci. USA* **113**, 8612 (2016).

Microswimmers in complex environments

H. Löwen,¹ C. Bechinger,² F. Guzman-Lastra,¹ L. M. C. Janssen,¹
A. Kaiser,³ C. Lozano,² and B. ten Hagen¹

¹ *Institute of Theoretical Physics II, Heinrich-Heine-Universität, Düsseldorf, Germany*

² *Physikalisches Institut, Universität Stuttgart, Stuttgart, Germany*

³ *Materials Science Division, Argonne National Laboratory, Argonne, IL, USA*

Active matter is a rapidly developing field in the research arena of nonequilibrium liquids. In particular, artificial man-made microswimmers can be brought into controlled motion in a liquid via external light fields.

Here we summarize some recent research results on synthetic colloidal microswimmers in various complex environments, for a recent review see [1]. First we explore cluster formation of "microswimmer molecules" as governed by dipolar and hydrodynamic interactions and discuss fission and fusion scenarios for these clusters [2]. Second, microswimmers are exposed to a motility landscape, as realized in experiments by an inhomogeneous light intensity field, and a strong phototactic response is found which can be exploited to guide and rectify microswimmers [3]. Finally, aging and rejuvenation phenomena known from glasses of passive particles will be studied for active particles where novel behaviour emerges from topological constraints [4].

- [1] C. Bechinger, R. Di Leonardo, H. Löwen, C. Reichhardt, G. Volpe, and G. Volpe, *Rev. Mod. Phys.* **88**, 045006 (2016).
- [2] F. Guzman-Lastra, A. Kaiser, and H. Löwen, *Nat. Commun.* **7**, 13519 (2016).
- [3] C. Lozano, B. ten Hagen, H. Löwen, and C. Bechinger, *Nat. Commun.* **7**, 12828 (2016).
- [4] L. M. C. Janssen, A. Kaiser, and H. Löwen, <http://arxiv.org/abs/1611.03528>.

Suspensions of active particles

F. Ginot, N. Waisbord, L. Bocquet, F. Detcheverry, C. Ybert, and
C. Cottin-Bizonne

Institut Lumière Matière, University of Lyon, CNRS, Lyon, France

We experimentally explore the phase behaviour of dense active suspensions of selfpropelled colloids. At intermediate densities we observe the formation of clusters, resulting from a permanent dynamical merging and separation of active colloids [1]. We have characterised in depth their kinetics of formation and their dynamics which shows vivid translational and rotational motions. These experimental results are discussed in the framework of a simple statistical model that captures quantitatively the measured dynamics. This sheds some new light on the internal organisation of the clusters and on the mechanisms underlying their formation.

In a second part I will present studies on driven active matter using a system based on the directional control of self-propelled magnetotactic bacteria. Remarkably, the bacteria orientation proceeds from a direct physical mechanism which can be characterised fully quantitatively. Exploring the active matter behaviour in motion under hydrodynamic and magnetic field stimuli we evidence suspension jetting and pearling instability [2].

- [1] F. Ginot, I. Theurkauff, D. Levis, C. Ybert, L. Bocquet, L. Berthier, and C. Cottin-Bizonne, Phys. Rev. X **5**, 011004 (2015).
- [2] N. Waisbord, C. T. Lefèvre, L. Bocquet, C. Ybert, and C. Cottin-Bizonne, Phys. Rev. F **1**, 053203 (2016).

Blood cells und blood flow – cell deformation, shear thinning, and cell sorting

D. A. Fedosov and G. Gompper

*Theoretical Soft Matter and Biophysics, Institute of Complex Systems,
Forschungszentrum Jülich, Jülich, Germany*

The flow behavior of blood cells is important in many biomedical applications. For example, blood flow is strongly affected by diseases such as malaria or diabetes, where red blood cell (RBC) deformability is strongly reduced. Of fundamental interest is therefore the relation between flow behavior, cell elasticity and deformability, hydrodynamic cell-cell interactions [1], and possibly active fluctuations [2]. We study these mechanisms by combination of particle-based mesoscale simulation techniques for the fluid hydrodynamics and triangulated-surface models for the RBC membrane [1].

Blood viscosity decreases with shear stress, a property essential for an efficient perfusion of the vascular tree by the heart. In the classical picture, shear-thinning arises due to RBCs alignment and elongation in the flow direction together with a tank-treading motion of their membranes. However, the link between cellular-scale dynamics and shear-thinning actually remains unsettled. We show that shear-thinning at high shear rates is the result of a rich dynamic behavior of RBCs convoluted with a large distribution of shapes [3,4].

Deterministic lateral displacement (DLD) devices have been proposed recently for a label-free sorting of micro-particles. However, the design of such microfluidic devices is based on theories developed for rigid spherical particles with size as a separation parameter. We demonstrate the use of cell mechanical and dynamical properties as biomarkers for separation [5]. In particular, we show that the viscosity contrast and associated cell dynamics clearly determine the RBC trajectory through a DLD device.

- [1] D. A. Fedosov, H. Noguchi, and G. Gompper, *Biomech. Model. Mechanobiol.* **13**, 239 (2014).
- [2] H. Turlier, D. A. Fedosov, B. Audoly, T. Auth, N. S. Gov, C. Sykes, J. F. Joanny, G. Gompper, and T. Betz, *Nat. Phys.* **12**, 513 (2016).
- [3] D. A. Fedosov, W. Pan, B. Caswell, G. Gompper, and G.E. Karniadakis. *Proc. Natl. Acad. Sci. USA* **108**, 11772 (2011).
- [4] L. Lanotte, J. Mauer, S. Mendez, D.A. Fedosov, J.-M. Fromental, V. Claveria, F. Nicoud, G. Gompper, and M. Abkarian, *Proc. Natl. Acad. Sci. USA* **113**, 13289 (2016).
- [5] E. Henry, S. H. Holm, J. P. Beech, J. O. Tegenfeldt, D. A. Fedosov, and G. Gompper, *Sci. Rep.* **6**, 34375 (2016).

The transition from hydrodynamic via interfacial to dry friction for sheared surfaces in water

A. Schlaich, J. Kappler, and R. R. Netz

Department of Physics, Free University Berlin, Berlin, Germany

The friction force between hydrated surfaces under shear is important in various fields ranging from biolubrication to flocculation and jamming. For large surface separation friction is well described by hydrodynamics and dominated by water viscosity. As the normal pressure increases the surface separation goes down and the interfacial properties of water, which are different from bulk [1], become relevant and modify the friction force. When the normal pressure is so high that all water is squeezed out, dry friction is obtained. We establish the general framework that describes the separation-dependent crossover between these three regimes. We concentrate on neutral yet polar surfaces which exhibit stable water films and are governed by strong hydration repulsion [2] and report extensive atomistic non-equilibrium molecular dynamics simulations. It turns out that it is important to correctly account for the constant water chemical potential as the water number changes according to the applied normal pressure [3].

[1] C. Sendner, D. Horinek, L. Bocquet, and R. R. Netz, *Langmuir* **25**, 10768 (2009).

[2] M. Kanduč and R. R. Netz, *Proc. Natl. Acad. Sci. USA* **112**, 12338 (2015).

[3] E. Schneck, F. Sedlmeier, and R. R. Netz, *Proc. Natl. Acad. Sci. USA* **109**, 14405 (2012).

Contributed Talks

Session 1: Ionic Liquids, Liquid Metals

Insights on the diversity of smectic phases in ionic liquid crystals

H. Bartsch,^{1,2} M. Bier,^{1,2} and S. Dietrich^{1,2}

¹ *Max Planck Institute for Intelligent Systems, Stuttgart, Germany*

² *Institute for Theoretical Physics IV, University of Stuttgart, Stuttgart, Germany*

Ionic liquid crystals (ILCs) can be described as anisotropic molecules, which carry charges and therefore combine properties of liquid crystals, e.g. mesophases, and ionic fluids, e.g. low melting temperatures and tiny triple-point pressures. However, the combination of both, orientational degrees of freedom and electrostatics renders a particular challenge for theoretical studies.

Recently a promising model of ILCs has been proposed and studied within the framework of density functional theory [1]. It turns out, that the phase diagram is strongly affected by the molecules' properties, i.e. the length-to-breath ratio, the position of charges and the interaction strengths. Here, we report on very recent findings on the phase behavior of ILCs obtained by means of density functional theory and Monte Carlo simulations. The most striking is the occurrence of a novel, second smectic A phase at low temperature, whose layer spacing is larger than that of the ordinary high-temperature smectic A phase and increasing upon decreasing temperature at constant packing fraction or pressure.

[1] S. Kondrat, M. Bier, and L. Harnau, *J. Chem. Phys.* **132**, 184901 (2010).

An asymmetric primitive model approach to ionic liquids

H. Lu,¹ B. Li,¹ C. E. Woodward,² S. Nordholm,³ and J. Forsman¹

¹ *Theoretical Chemistry, Lund University, Lund, Sweden*

² *PEMS, University of New South Wales, Sydney, Australia*

³ *Department of Chemistry, Gothenburg University, Gothenburg, Sweden*

An asymmetric restricted primitive model (ARPM) of electrolytes is proposed as a simple three-parameter (charge q , diameter d and charge displacement b) model of ionic liquids and solutions. Charge displacement allows electrostatic and steric interactions to operate between different centres, so that orientational correlations arise in ion-ion interactions. In this way the ionic system may have partly the character of a simple ionic fluid/solid and of a polar fluid formed from ion pairs. The present exploration of the system focuses on the ion pair formation mechanism, the relative concentration of paired and free ions and the consequences for the cohesive energy, and the tendency to form fluid or solid phase. In contrast to studies of similar (though not identical) models in the past, we focus on behaviours at room temperature. By MC and MD simulations of such systems composed of monovalent ions of hard-sphere (or essentially hard-sphere) diameter equal to 5 Å and a charge displacement from hard-sphere origin ranging from 0 to 2 Å we find that ion pairing dominates for b larger than 1 Å. When b exceeds about 1.5 Å, the system is essentially a liquid of dipolar ion pairs, with a small presence of free ions. We also investigate dielectric behaviours of corresponding liquids, composed of purely dipolar species. Many basic features of ionic liquids appear to be remarkably consistent with those of our ARPM at ambient conditions, when b is around 1 Å.

We have furthermore studied the behaviours of ARPM models in heterogeneous environments, with a particular focus on the differential capacitance at isolating or conducting surfaces. The latter system is particularly interesting, given the potential use of ionic liquids in Electric Double Layer Capacitors (supercapacitors). At a conducting surface, there is a competition between ion pairing, and “pairing” with self-images at the dielectric interface. We have developed a density functional theory for these systems, that includes an explicit representation of ion pairs, free ions, and an approximate treatment of (screened) image interactions. The latter is shown to provide the correct limiting interaction between neutral conducting surfaces, i.e. the zero frequency van der Waals interaction. We compare results for capacitance and surface interactions for conducting and isolating surfaces, and with explicit or implicit treatments of the ion pairs, with some very interesting findings. A natural extension of the ARPM is a model in which b is different for cations and anions. We have recently begun exploring such systems.

Nanoscale capillary freezing of ionic liquids confined between metallic interfaces and the role of electronic screening

J. Comtet,¹ A. Niguès,¹ V. Kaiser,¹ B. Coasne,² L. Bocquet,¹ and A. Siria¹

¹ *Laboratoire de Physique Statistique, Ecole Normale Supérieure, Paris, France*

² *Laboratoire Interdisciplinaire de Physique, Université Grenoble Alpes, Grenoble, France*

Room temperature ionic liquids (RTIL) received considerable attention as a new class of materials with fundamental importance for energy storage and active lubrication. Their unique properties result from the competition of strong electrostatic interactions with properly designed molecular structure to avoid crystallization at room temperature. They are however unusual liquids, which challenge fundamentally the classical frameworks of electrolytes. In particular their behavior at electrified interfaces remains elusive with very rich and exotic responses relevant to their electrochemical activity. In this work, we use quartz tuning fork based AFM nanorheological measurements to explore the properties of RTIL in nanometric confinement. We unveil a dramatic change of the RTIL towards a solid-like phase below a threshold thickness, pointing to capillary freezing in confinement. This threshold thickness is found to be intimately related to the metallic nature of the confining materials, with more metallic surfaces facilitating capillary freezing. This behavior is interpreted theoretically in terms of the shift of the freezing transition, taking into account the influence of the electronic screening on RTIL wetting of the confining surfaces, as described by the simple Thomas-Fermi approach. Our findings provide fresh views on the properties of confined RTIL with important implications for their static and dynamical properties inside nanoporous metallic structures. This also suggests applications to tune nanoscale lubrication with the phase-changing RTIL, by varying the nature as well as the patterning of the substrate, and the application of active polarisation.

[1] J. Comtet, A. Niguès, V. Kaiser, B. Coasne, L. Bocquet, and A. Siria, arXiv:1611.08448 (2016).

Session 2: Water, Solutions

Re-entrant limits of stability of the liquid phase and the Speedy scenario in colloidal model systems

L. Rovigatti,¹ V. Bianco,² J. M. Tavares,³ and F. Sciortino⁴

¹ *Rudolf Peierls Centre for Theoretical Physics, University of Oxford, Oxford, United Kingdom*

² *Faculty of Physics, University of Vienna, Vienna, Austria*

³ *Instituto Superior de Engenharia de Lisboa, Lisbon, Portugal*

⁴ *Dipartimento di Fisica, Sapienza-Università di Roma, Rome, Italy*

The origin of density anomalies in water has animated the debate in the scientific community. Different thermodynamic consistent scenarios have been proposed leading to intense discussions which extends up to present days. The first thermodynamic scenario coherently accounting for the observed density, compressibility and specific heat anomalies of water was proposed in 1982 by Robin Speedy [1]. In this very elegant piece of work, Speedy focused on the limit of stability of the liquid phase — which in mean-field coincides with the gas-liquid spinodal line — a line emanating from the gas-liquid critical point. Speedy proposed a re-entrant gas-liquid spinodal as a possible explanation of the apparent divergence of the compressibility and specific heat on supercooling water. Such a counter-intuitive possibility, e.g. a liquid that becomes unstable to gas-like fluctuations on cooling at positive pressure, has never been observed, neither in real substances nor in off-lattice simulations. In this communication I will present recent numerical and analytical calculations [2] showing that the re-entrant spinodal scenario can be observed in patchy colloidal particles. Specifically, I will demonstrate that two different models (a model for Janus particle and a model for ring-forming colloids) both show (i) a re-entrant limit of stability of the liquid phase and (ii) a re-entrant binodal, providing a neat in silico (and in charta) realization of such unconventional thermodynamic scenario.

[1] R. J. Speedy, *J. Phys. Chem.* **86**, 3002 (1982).

[2] L. Rovigatti, V. Bianco, J. M. Tavares, and F. Sciortino, *J. Chem. Phys.* in press (2017).

Sweet taste and sugar hydration

M. A. Ricci,¹ F. Bruni,¹ S. Imberti,² S. E. McLain,³ and N. Rhys³

¹ *Dipartimento di Scienze, Università Roma Tre, Rome, Italy*

² *STFC, Rutherford Appleton Laboratory, ISIS Facility, Didcot, United Kingdom*

³ *Department of Biochemistry, University of Oxford, Oxford, United Kingdom*

Among our senses, taste has the primary function of driving our appetite, protecting from poisons and contributing to the overall enjoyment of a meal. Sweet taste permits the identification of energy-rich nutrients, umami allows the recognition of amino acids, salt taste ensures the proper dietary electrolyte balance, and sour and bitter warn against the intake of potentially poisonous chemicals. In particular the perception of sweet or bitter taste is ascribed to taste receptor cells expressing T1R2 + T1R3 or T2R receptors which, after binding to the sweet or bitter molecule, activate Guanine proteins for signal transmission to the brain [1]. What is still debated is why a sugar is perceived sweeter than another or elicits a bitter aftertaste. This is a quite intriguing question, given that substantial taste differences seem to be determined by apparently small differences in the molecular stereochemistry of sugars: the case of mannose is paradigmatic as α -mannose is sweet while its anomer β -mannose is bitter [2, 3].

A solid molecular theory of the sweet taste is still lacking and the best model available is the so-called sweetness triangle [4, 5] and its evolution, namely the multipoint interaction model [6]. Both models establish a relation between molecular structure and taste, by requiring the presence of specific Hydrogen bond donor and acceptor sites, plus a hydrophobic or steric hindrance. These structural characteristics can be verified by determining the hydration properties of sugars.

In this communication we present the results of neutron diffraction experiments on three monosaccharides, showing the correlation between the number and directionality of the Hydrogen bonds formed with water and the degree of sweetness of the sugars.

[1] J. Chandrashekar, M. A. Hoon, N. J. P. Ryba, and C. S. Zuker, *Nature* **444**, 288 (2006).

[2] R. G. Steinhardt, A. D. Calvin, and E. A. Dodd, *Science* **135**, 367 (1962).

[3] R. A. Stewart, C. K. Carrico, R. L. Webster, and R. G. Steinhardt, *Nature* **234**, 220 (1971).

[4] R. S. Shallenberger and T. E. Acree, *Nature* **216**, 480 (1967).

[5] L. B. Kier, *J. Pharm. Sci.* **61**, 1394 (1972).

[6] C. Nofre and J.-M. Tinti, *Food Chem.* **56**, 263 (1996).

Predicting solvation profiles and free energies of proteins – the molecular density functional theory route

C. Gageat,¹ D. Borgis,² and M. Levesque¹

¹ *Ecole Normale Supérieure, Paris, France*

² *Maison de la Simulation, Saclay, France*

Biochemical processes in the human body happen in an embedding medium, a large number of solvent molecules, for instance water, that crowd the environment. To take into account this environment at the molecular scale, several possibilities are offered to in-silico experimentalists:

(i) One can forget about the molecular nature of the solvent: no hydrogen bonding, no crowding effect, etc. These primitive methods like polarizable continuums focus on macroscopic properties of the solvent like its dielectric permittivity: That's quite crude, but fast and arbitrarily configurable.

(ii) Go very precise, using all-atom simulations like molecular dynamics. That increases the numerical cost by 4 orders of magnitude with respect to solution (i) but you have all the details you want; If it fits in nowadays computers.

(iii) I will present a new paradigm, the molecular density functional theory (MDFT). For the same numerical cost as primitive models, our implicit-explicit theory aims at producing, rigorously, the equilibrium properties of all-atom simulations for solute of any size and any shape, like proteins.

[1] G. Jeanmairet, M. Levesque, and D. Borgis, *J. Chem. Phys.* **21**, 139 (2013).

[2] G. Jeanmairet, M. Levesque, R. Vuilleumier, and D. Borgis, *J. Phys. Chem. Lett.* **4**, 619 (2013).

Molecular mechanism of hydrophobic hydration

F. Merzel

National Institute of Chemistry, Ljubljana, Slovenia

In spite of intensive research for more than 50 years, the hydrophobic effect and its physical origin remains a matter of debate. Molecular solutes are known to have a strong effect on structural and dynamical properties of the surrounding water [1,2]. Depending on perturbations by a solute the water hydrogen-bond network can either locally relax to configurations of optimal intermolecular angles or decouple from the network. In our recent study [3] we have identified the presence of strengthened water hydrogen bonds near hydrophobic solutes by using both IR spectroscopy and ab-initio molecular dynamics simulations. The water molecules involved in the enhanced hydrogen bonding display extensive structural ordering while their mobility is restricted. We observe that an individual pair of water molecules can make stronger hydrogen bond to each other if it is not overcoordinated by neighboring water molecules. Molecules occupying the non-tetrahedral sites cause an unfavorable electrostatic screening of the hydrogen bond. While such intercalating water molecules are generally present in the bulk water, they are absent around hydrophobic solute due to the excluded volume of solute molecule. As a consequence, hydrogen bonds between water molecules around apolar solute can become stronger than in the bulk. Our results strongly support the classical view of hydrophobic hydration.

[1] A. Godec, J. C. Smith, and F. Merzel, Phys. Rev. Lett. **107**, 267801 (2011).

[2] A. Godec and F. Merzel, J. Am. Chem. Soc. **134**, 17574 (2012).

[3] J. Grdadolnik, F. Merzel, and F. Avbelj, Proc. Natl. Acad. Sci. USA **114**, 322 (2017).

Contribution of water on the selection and stability of proteins at ambient and extreme thermodynamic conditions

V. Bianco

Faculty of Physics, University of Vienna, Vienna, Austria

Proteins that are functional at ambient conditions do not necessarily work at extreme conditions of temperature T and pressure P . Furthermore, there are limits of T and P above which no protein has a stable functional state. Here we show that these limits and the selection mechanisms for working proteins depend on how the properties of the surrounding water change with T and P . We find that proteins selected at high T are super-stable and are characterized by an optimal segregation of a hydrophilic surface and a hydrophobic core. Surprisingly, a larger segregation reduces the stability range in T and P . Our computer simulations, based on a new protein design protocol, explain the hydropathy profile of proteins as a consequence of a selection process influenced by water, offering an alternative rationale to the evolutionary action exerted by the environment in extreme conditions. Our results are potentially useful for engineering proteins and drugs working at extreme conditions.

- [1] V. Bianco and G. Franzese, Phys. Rev. Lett. **115**, 108101 (2015).
- [2] V. Bianco, G. Franzese, C. Dellago, and I. Coluzza, submitted (2016).
- [3] V. Bianco, S. Iskov, and G. Franzese, J. Biol. Phys. **38**, 27 (2012).
- [4] V. Bianco and G. Franzese, Sci. Rep. **4**, 4440 (2014).
- [5] I. Coluzza, PLOS ONE, **9**, e112852 (2014).
- [6] G. Franzese and V. Bianco, Food Biophys. **8**, 153 (2013).
- [7] G. Franzese and V. Bianco, Food Biophys. **6**, 186 (2011).

Liquid-liquid transitions in aqueous solutions observed using infrared spectroscopy

S. Woutersen,¹ M. Hilbers,¹ J. R. Bruijn,¹ T. H. van der Loop,¹ Z. Zhao,² and C. A. Angell²

¹ *Van 't Hoff Institute for Molecular Sciences, University of Amsterdam, Amsterdam, The Netherlands*

² *School of Molecular Sciences, Arizona State University, Tempe, AZ, USA*

There is evidence (mostly from simulations) that supercooled water can undergo a phase transition between two different liquid states at a temperature well below the homogeneous-nucleation temperature $T_{\text{hom}} \sim 230$ K [1]. Since at room temperature only one liquid-water phase is known to exist, the phase line between the two liquid states must terminate at a temperature below T_{hom} ; the critical point at the end of the phase line would cause diverging susceptibilities and so explain the anomalies at higher temperatures.

Here, we investigate liquid-liquid transitions in aqueous solutions by means of infrared spectroscopy, using the OH-stretching mode of water as a probe of the local hydrogen-bond structure. We find that the previously reported liquid-liquid transition in glycerol solution [2] involves a metastable low-temperature liquid, which rapidly converts into a suspension of nanoscopic ice crystals [3]. Such phase separation can be prevented by using salts that are “commensurate” with the hydrogen-bond structure of water (as evidenced by their ideal-solution behavior and their IR spectra). In particular, aqueous solutions of $\text{N}_2\text{H}_5\text{TFA}$ exhibit a specific-heat peak at ~ 180 K [4], suggesting a phase transition. The IR spectra show that this specific-heat peak indeed arises from a transition between two different liquid phases, that both appear to be homogeneous at the molecular level, and that are reversibly inter-convertible [5]. The IR spectra also show that the low-temperature liquid has a hydrogen-bond structure similar to (but more disordered than) that of low-density amorphous water. This structural similarity suggests a connection [6] between the observed liquid-liquid transition and the HDA-LDA transition in water [7]; and based on the equivalence of high ionic concentrations with the application of high pressure [8] this connection suggests that a liquid-liquid transition also exists in neat water, providing a unified explanation for its well-known anomalous properties.

[1] P. H. Poole, F. Sciortino, U. Essmann, and H. E. Stanley, *Nature* **360**, 324 (1992).

- [2] K.-I. Murita and H. Tanaka, Nat. Commun. **4**, 2844 (2013); Y. Suzuki and O. Mishima, J. Chem. Phys. **141**, 094505 (2014).
- [3] J. R. Bruijn, T. H. van der Loop, and S. Woutersen, J. Phys. Chem. Lett. **7**, 795 (2016).
- [4] Z. Zhao and C. A. Angell, Angew. Chem. Int. Ed. **55**, 2474 (2016).
- [5] S. Woutersen, M. Hilbers, Z. Zhao, and C. A. Angell, arXiv:1605.08985.
- [6] J. W. Biddle and V. Holten & M. A. Anisimov, J. Chem. Phys. **141**, 074504 (2014).
- [7] K. Amann-Winkel, R. Böhmer, F. Fujara, C. Gainaru, B. Geil, and T. Loerting, Rev. Mod. Phys. **88**, 011002 (2016).
- [8] R. Leberman and A. K. Soper, Nature **387**, 364 (1995).

Water nanodroplets and the equation of state of TIP4P/2005

S. M. Malek,¹ P. H. Poole,² and I. Saika-Voivod¹

¹ *Department of Physics and Physical Oceanography, Memorial University of Newfoundland, St. John's, Canada*

² *Department of Physics, St. Francis Xavier University, Antigonish, Canada*

We carry out extensive molecular dynamics simulations of nanoscale liquid droplets of the TIP4P/2005 model of water, with number of molecules ranging from $N = 64$ to 2880 and temperatures down to 180 K. As droplet size decreases, the Laplace pressure induced by the liquid-vapour surface tension increases. For sufficiently small droplets, the density within droplets exceeds the critical density associated with the liquid-liquid critical point proposed to occur deep in the supercooled region of the model. Since crystallization is suppressed for such small droplets, they provide a possible experimental probe for determining the equation of state for water where crystallization is otherwise unavoidable, and hence could provide direct evidence for the much-investigated second critical point scenario. However, it is unclear whether such small systems can provide any information on bulk water. We report on our progress in determining the relationships between N , temperature, pressure, and density, including the emergence of anomalous behaviour emblematic of bulk liquid water. For example, we identify the threshold size of a nanodroplet above which a density maximum can be observed.

Short range order, hydrogen bonding and rotational dynamics in plastic crystal phases of water

E. Guardia,¹ A. Henao,¹ L. C. Pardo,¹ and I. Skarmoutsos²

¹ *Departament de Física, Universitat Politècnica de Catalunya, Barcelona, Spain*

² *Institut Charles Gerhardt Montpellier, Université de Montpellier, Montpellier, France*

In plastic or orientationally disordered phases, the centers of mass of molecules are translationally ordered, as in a solid crystal, but the molecular orientations are disordered as in a liquid. The appearance of plastic phases in computer simulations of water at high pressures has been reported by several authors [1,2]. In the present contribution, we analyze the short range order, the hydrogen bond network and the rotational dynamics of water molecules in two different plastic phases: a bcc plastic phase at $T = 440$ K and $P = 8$ GPa and a fcc plastic phase at $T = 460$ K and $P = 8$ GPa. To this end, we have performed a series of molecular dynamics simulations with the TIP4P/2005 force field. The positional and orientational order of water molecules within the first solvation shell was determined with the same procedure as in a previous study of liquid water at ambient conditions [3]. The local structural order was also studied in terms of the trigonal and tetrahedral order parameters [4], revealing an interplay between local orientational order and hydrogen bonding. The rotational dynamics was investigated from the calculation of molecular reorientational times around different molecular directions [5]. For the sake of comparison, we have also analyzed ice VII at $T = 340$ K and $P = 7$ GPa and a liquid phase at $T = 440$ K and $P = 8$ GPa. Our present results are compared with recent neutron scattering experiments of water [6] and aqueous salt solutions [7] in the GPa range.

- [1] Y. Takii, K. Koga, and H. Tanaka, J. Chem. Phys. **128**, 204501 (2008).
- [2] J. L. Aragones, M. M. Conde, E. G. Noya, and C. Vega, Phys. Chem. Chem. Phys. **11**, 543 (2009).
- [3] L. C. Pardo, A. Henao, S. Busch, E. Guardia, and J. Ll. Tamarit, Phys. Chem. Chem. Phys. **16**, 24479 (2014).
- [4] I. Skarmoutsos, M. Masia, and E. Guardia, Chem. Phys. Lett. **648**, 102 (2016).
- [5] E. Guardia, I. Skarmoutsos, and M. Masia, J. Phys. Chem. B **119**, 8926 (2015).
- [6] L. E. Bove, S. Klotz, Th. Strässle, M. Koza, J. Teixeira, and A. M. Saitta, Phys. Rev. Lett. **111**, 185901 (2013)
- [7] S. Klotz, K. Komatsu, F. Pietrucci, H. Kagi, A. A. Ludl, S. Machida, T. Hattori, A. Sano-Furukawa, and L. E. Bove, Sci. Rep. **6**, 32040 (2016).

Session 3: Liquid Crystals

Colloidal liquid crystals: How flexible needles become obese, biaxial bricks schizophrenic, and chiral rods twisted

M. Dijkstra,¹ R. van Roij,² S. Dussi,¹ S. Belli,² and M. Dennison¹

¹ *Soft Condensed Matter, Debye Institute for Nanomaterials Science, Utrecht University, Utrecht, The Netherlands*

² *Institute for Theoretical Physics, Utrecht University, Utrecht, The Netherlands*

We extend and apply Onsager's seminal work to a variety of systems, including mixtures of semiflexible rods, polydisperse biaxial bricks, and chiral rods. To be more specific, we study suspensions of semiflexible colloidal rods and biopolymers using Onsager theory for a segmented-chain model. We calculate full phase diagrams for mixtures of thin and thick fd virus particles, finding quantitative agreement with experimental observations. We show that flexibility, which renders the rods effectively shorter, thicker, and obese depending on the state point, is crucial to understanding the topologies of the phase diagrams [1].

In addition, we study by means of Onsager theory within the restricted orientation (Zwanzig) model the effect of size polydispersity on the phase behavior of a suspension of boardlike particles. We show that polydispersity induces a novel topology in the phase diagram of prolate bricks, with two Landau tetracritical points in between which oblate uniaxial nematic order is favored over the expected prolate order. Hence, the prolate bricks become schizophrenic and act as oblate bricks [2]. This phenomenon causes the opening of a huge stable biaxiality regime in between uniaxial nematic and smectic states, thereby explaining the experimental observations of a remarkably stable biaxial nematic phase in a colloidal system of goethite particles.

Finally, we develop a novel Onsager theory combined with a Monte Carlo integration method to obtain the equilibrium cholesteric pitch as a function of thermodynamic state and microscopic details [4]. Applying the theory to hard helices, we observe both right- and left-handed cholesteric phases that depend on a subtle combination of particle geometry and system density [3]. In particular, we find that entropy alone can even lead to a (double) inversion in the cholesteric sense of twist upon changing the packing fraction. We thus find that chiral rods can get twisted with the same, opposite, or mixed handedness compared to the microscopic handedness of the particle. We show how the competition between single-particle properties (shape) and thermodynamics (local alignment) dictates the macroscopic

chiral behavior. Our results provide new insights into the role of entropy in the microscopic origin of this state of matter. Additionally, we introduce a novel chiral hard-particle model, namely particles with a twisted polyhedral shape and obtain, for the first time, a stable fully-entropy-driven cholesteric phase by computer simulations. By slightly modifying the triangular base of the particle, we are able to switch from a left-handed prolate to a right-handed oblate cholesteric phase using the same right-handed twisted prism model [4].

- [1] M. Dennison, M. Dijkstra, and R. van Roij, Phys. Rev. Lett. **106**, 208302 (2011).
- [2] S. Belli, A. Patti, M. Dijkstra and R. van Roij, Phys. Rev. Lett. **107**, 148303 (2011).
- [3] S. Dussi, S. Belli, R. van Roij, and M. Dijkstra, J. Chem. Phys. **142**, 074905 (2015).
- [4] S. Dussi and M. Dijkstra, Nat. Commun. **7**, 11175 (2016).

From soft to hard rod behavior in liquid crystalline suspensions of sterically stabilized colloidal filamentous particles

E. Grelet and R. Rana

Centre de Recherche Paul-Pascal, CNRS and University of Bordeaux, Bordeaux, France

Rod-like viruses with their features like outstanding monodispersity and their ability to self-organize into ordered structures, motivate the strong interest they have raised as model systems for soft condensed matter [1]. Aqueous suspensions of filamentous viruses form a variety of liquid crystalline phases [1,2], including three hexagonal phases which have been recently evidenced beyond the smectic-A phase: smectic-B, hexatic columnar and crystalline phases [2-4].

We will show recent experimental investigations on the phase behavior of such semi-flexible viruses which have been coated with neutral hydrophilic polymers by irreversibly binding poly(ethylene glycol) [5]. Depending on the size of the grafted polymer, up to three different phase transitions are observed (isotropic-to-chiral nematic, chiral nematic-to-smectic, and smectic-to-columnar) [6]. Each phase transition is shown to be independent of the ionic strength, confirming the steric stabilization of the viral colloids [6]. A *direct* i.e. without any free parameters, comparison with theory and computer simulations of the volume fraction associated with the phase transition can be performed [7, 8], showing a quantitative agreement with hard rod behavior at low polymer chain size, and some deviation stemming from soft repulsion by increasing the polymer thickness coating the rod. Specifically, we will demonstrate that the columnar mesophase is not stabilized by electrostatic repulsion [9], and we will discuss the conditions of its existence.

- [1] Z. Dogic and S. Fraden, *Curr. Opin. Colloid Interface Sci.* **11**, 47 (2006).
- [2] E. Grelet, *Phys. Rev. Lett.* **90**, 168301 (2008).
- [3] S. Naderi, E. Pouget, P. Ballesta, P. van der Schoot, M.P. Lettinga, and E. Grelet, *Phys. Rev. Lett.* **111**, 037801 (2013).
- [4] E. Grelet, *Phys. Rev. X* **4**, 021053 (2014).
- [5] E. Grelet and S. Fraden, *Phys. Rev. Lett.* **100**, 198302 (2003).
- [6] E. Grelet and R. Rana, *Soft Matter* **12**, 4621 (2016).
- [7] Z. Y. Chen, *Macromolecules* **26**, 3419 (1993).
- [8] M. A. Bates and D. Frenkel, *J. Chem. Phys.* **109**, 6193 (1998).
- [9] H. H. Wensink, *J. Chem. Phys.* **126**, 194901 (2007).

Nematic tactoids in an electric field

L. Metselaar,¹ I. Dozov,² K. Antonova,³ E. Belamie,⁴ P. Davidson,²
J. M. Yeomans,¹ and A. Doostmohammadi¹

¹ *The Rudolf Peierls Centre for Theoretical Physics, Oxford, United Kingdom*

² *Laboratoire de Physique des Solides, Université Paris-Sud, CNRS, Orsay, France*

³ *Institute of Solid State Physics, Bulgarian Academy of Sciences, Sofia, Bulgaria*

⁴ *Institut Charles Gerhardt Montpellier, ENSCM, Montpellier, France*

A ubiquitous behavior in lyotropic nematics is the emergence of nematic droplets, termed tactoids, which have been experimentally observed in material systems from carbon nanotubes and colloidal rods to F-actin viruses and cellulose nanocrystals. Despite their prevalence, the properties and dynamics of tactoids are currently poorly understood. This is partly due to their complex structure, which is affected by nematic elasticity, surface tension, and anchoring strength. To the best of our knowledge, direct simulations and numerical realizations of them are virtually non-existent.

Here, using both experiments and numerical simulations, we show that subjecting nematic tactoids to external electric fields can lead to the emergence of new nematic structures, where tactoids elongate up to 10 times their initial length to form highly aligned cigar-shaped inclusions. Importantly, our experiments show that the emergence of this new exotic phase is completely reversible upon removal of the electric field, and that the original shape of the tactoids can be recovered. We obtain pleasing agreement between experiment and the first fully dynamical simulations of tactoids, demonstrating the existence of a critical field needed to start the elongation with an associated small energy barrier.

Subjecting tactoids to shear flow improves the optical properties of liquid crystal films, by improving the internal alignment of the nematogens inside the tactoid. Our results demonstrate that using electric fields can achieve this same effect, but within an environment that is much more easily controlled. We therefore expect that these new findings will be of interest to a broad range of physicists, chemists and engineers concerned with the science and technology of liquid crystal materials.

Phantasmagoric liquid crystals: Continuous isotropic-nematic transition driven by shape transformation of micelles

J. Yamamoto,^{1,2} C. Ida,¹ H. Jo,³ G. Scalia,⁴ and J. P. Lagerwall⁴

¹ *Department of Physics, Graduate School of Science, Kyoto University, Kyoto, Japan*

² *JST-CREST, Japan Science and Technology Agency, Tokyo, Japan*

³ *Advanced Institutes of Convergence Technology, Seoul National University, Seoul, Korea*

⁴ *University of Luxembourg, Luxembourg, Luxembourg*

We have found that the new class of the continuous isotropic (I)-nematic (N) phase transition driven by the shape transformation of micelles near extremely dilute lyotropic nematic (LN) (3~9wt%). The system is made by the water solution of cationic and anionic surfactant mixture (sodium dodecyl sulfate; SDS and dodecyl trimethyl ammonium bromide; C12TAB, respectively). For thermotropic nematic (TN), orientation order is only broken by the order-disorder transition above weak but first order I-N transition keeping the anisotropy of the “building blocks” which is equivalent to the rod like one molecule. On the contrary, even the shape and size of building blocks can be changed dependent on temperature, concentration or other thermodynamic quantities in LN. It is easy to understand the shape change of building blocks strongly coupled with phase stabilities among LC phases.

We have investigated the phase transition phenomena in lyotropic liquid crystals by (i) polarizing microscope observation, (ii) dynamic light scattering, (iii) shear viscosity, and (iv) dynamics of flow induced birefringence by applying the sinusoidal change of the strength of the shear flow. All experiment were done by changing the temperature (T), concentration (ϕ) and charge compensation ratio ($\alpha = n\text{C12TAB}/n\text{SDS}$).

On the basis of the VH mode of DLS measurement in the isotropic phase near I-N transition, relaxation time of order parameter fluctuation strongly diverges just on the T_{IN} , which is exact identification of the continuous I-N transition. From the flow birefringence measurement, we can also confirms the continuous I-N transition with large pre-transitional shear induced birefringence. From the VV mode of DLS measurement, size of the micelle is estimated about few nm which is equivalent to the length of the surfactants in the higher temperature region, and drastically elongated near the I-N phase transition.

On the other hand, flow induced birefringence shows the sharp minimum under strong shear flow in the low temperature region of nematic, whereas it shows maximum in the high temperature region. Amplitude of the flow induced birefringence shows the minimum, where the phase of the response switch from maximum to minimum. It is reasonable that the change of the response to the shear flow is originated from the shape change of the micelles, namely, the rod like micelles transform to disk like ones in the low temperature region. Then we have concluded that Nc (rod)-Nd (disk) phase transition appears dependent on T , ϕ and α , associated with I-Nc continuous phase transition. These two types of nematic phases, Nc and Nd, can be stabilized even in extremely dilute regime ($\phi < 3\%$), but the range of α is become more narrow with decrease in ϕ .

Chiral symmetry breaking of confined lyotropic chromonic liquid crystals: Effects of saddle-splay elastic modulus and dopants

J. Jeong,^{1,2} J. Eun,¹ S.-J. Kim,² J. Kim,¹ H. Lee,¹ and M. Almukambetova¹

¹ *Department of Physics, Ulsan National Institute of Science and Technology (UNIST), Ulsan, Korea*

² *Center for Soft and Living Matter, Institute for Basic Science (IBS), Ulsan, Korea*

Water-based and biocompatible lyotropic chromonic liquid crystals (LCLCs) have received increasing attention because of their potential for bio-applications and unusual elastic properties such as a very small twist elastic modulus and an unprecedentedly large saddle-splay elastic modulus [1-4]. The peculiar elastic properties often result in spontaneous chiral symmetry breaking of confined LCLCs. The chiral symmetry-broken LCLCs exhibit new types of chiral director configurations and topological defects despite the absence of intrinsic chirality [3-8].

Here we report a series of experiments elucidating how water-soluble dopants added to LCLCs affect director configurations of confined LCLCs. First, we investigate director configurations of chiral LCLCs confined within cylindrical capillaries and demonstrate the competing roles of the saddle-splay elastic modulus and helical twisting power of the chiral dopants added. Additionally, we show that even minuscule amount of achiral dopants can alter significantly director configurations of confined LCLCs, presumably, by changing elastic moduli of the doped LCLCs. Lastly, based on our findings and smart design of confinements, i.e., confining geometry and anchoring conditions, we propose confined LCLC-based sensor platform to detect small amounts of water-soluble molecules.

Authors gratefully acknowledge support from the Korean Government through NRF-2015R1A2A2A01007613 and IBS-R020-D1.

- [1] S. Zhou, K. Neupane, Y. A. Nastishin, A. R. Baldwin, S. V. Shiyankovskii, O. D. Lavrentovich, and S. Sprunt, *Soft Matter* **10**, 6571 (2014).
- [2] S. Zhou, Y. A. Nastishin, M. M. Omelchenko, L. Tortora, V. G. Nazarenko, O. P. Boiko, T. Ostapenko, T. Hu, C. C. Almasan, S. N. Sprunt, J. T. Gleeson, and O. D. Lavrentovich, *Phys. Rev. Lett.* **109**, 037801 (2012).
- [3] Z. S. Davidson, L. Kang, J. Jeong, T. Still, P. J. Collings, T. C. Lubensky, and A. G. Yodh, *Phys. Rev. E* **91**, 050501 (2015).

- [4] K. Nayani, R. Chang, J. Fu, P. W. Ellis, A. Fernandez-Nieves, J. O. Park, and M. Srinivasarao, *Nat. Commun.* **6**, 8067 (2015).
- [5] J. Jeong, Z. S. Davidson, P. J. Collings, T. C. Lubensky, and A. G. Yodh, *Proc. Natl. Acad. Sci. USA* **111**, 1742 (2014).
- [6] J. Jeong, L. Kang, Z. S. Davidson, P. J. Collings, T. C. Lubensky, and A. G. Yodh, *Proc. Natl. Acad. Sci. USA* **112**, E1837 (2015).
- [7] L. Tortora and O. D. Lavrentovich, *Proc. Natl. Acad. Sci. USA* **108**, 5163 (2011).
- [8] A. Nych, U. Ognysta, I. Muševič, D. Seč, M. Ravnik, and S. Žumer, *Phys. Rev. E* **89**, 62502 (2014).

Annihilation dynamics of topological monopoles in nematic liquid crystal

M. Nikkhou,¹ M. Škarabot,² and I. Muševič^{2,3}

¹ *School of Physics and Astronomy, University of Leeds, Leeds, United Kingdom*

² *Jožef Stefan Institute, Ljubljana, Slovenia*

³ *Faculty of Mathematics and Physics, University of Ljubljana, Ljubljana, Slovenia*

Colloidal particles with various surface properties in uniformly oriented nematic liquid crystals are accompanied by topological defects [1]. The defects can be either singular points or closed loops, and appear in pairs with opposite topological charges to maintain the conservation of the total topological charge. Because of the elastic distortion of the director field around each defect, they move toward each other until they meet and annihilate into the vacuum, minimizing the elastic energy of the system.

Arbitrary number of pairs of oppositely charged topological monopoles can be created on a micrometre-diameter glass fibre, a topologically simple object, in the nematic liquid crystal (NLC) 5CB [2]. In this work, we demonstrate the dynamics of charge annihilation on a fibre set parallel to the nematic director of a planar cell and the effects of confinement on defect velocity [3]. A single pair of oppositely charged defect rings is created by laser quenching of the NLC around the fibre. Due to their opposite charge, these rings are attracted toward each other. Their relative velocity, v , shows a power-law dependence on the separation, d , of the rings: $v \propto 1/d^\alpha$ with $\alpha \approx 2 \pm 0.3$. This is a strong indication of a Coulomb-like force between the topological monopoles, $F \propto 1/d^2$. However, in a confined cell with a gap comparable to the fibre diameter, we observe the Coulomb-like attraction only at small separations of the defect rings. For larger separations ($> 15 \mu\text{m}$), the two rings are connected with a pair of line defects, which provide a constant, string-like force of attraction of this pair.

We further study the creation and annihilation of a pair of topological point defects on a fibre perpendicular to the bulk orientation of the NLC [4]. A gigantic Saturn ring with a -1 charge is created along its longer axis. This ring can be cut and reshaped using laser tweezers into an arbitrary number of topological point defect pairs, i.e., a hyperbolic and a radial hedgehog. The interaction force between a pair of monopoles on the fibre is divided into two regimes depending on the separation between the defects. In the far-field regime, when the monopoles are well separated from each other, the force between the monopoles is independent of separation and results in a constant velocity of approach. The far-field force may be either attractive

or repulsive, even for oppositely charged monopoles. This can be explained by the experimental inaccuracy in setting the fibre exactly perpendicular to the NLC director. In the near-field regime, when the two point defects begin to overlap, there is an additional power-law dependency to the velocity of approach, $v \propto 1/d^\alpha$, with $\alpha \approx 2 \pm 0.2$.

- [1] G. P. Alexander, B. G. Chen, E. A. Matsumoto, and R. D. Kamien, *Rev. Mod. Phys.* **84**, 497 (2012).
- [2] M. Nikkhou, M. Škarabot, S. Čopar, M. Ravnik, S. Žumer, and I. Muševič, *Nat. Phys.* **11**, 183 (2015).
- [3] M. Nikkhou, M. Škarabot, and I. Muševič, *Eur. Phys. J. E* **38**, 23 (2015).
- [4] M. Nikkhou, M. Škarabot, and I. Muševič, *Phys. Rev. E* **93**, 062703 (2016).

Hexatic phase of self-assembled micellar polymers

A. Pal, M. A. Kamal, and V. A. Raghunathan

Raman Research Institute, Bangalore, India

We have recently observed a thermodynamically stable line hexatic ($N + 6$) phase in a three-dimensional system made up of self-assembled polymer-like micelles of amphiphilic molecules [1]. The experimentally observed phase transition sequence, nematic (N) $\leftrightarrow N + 6 \leftrightarrow$ two-dimensional hexagonal (2D-H), is in agreement with theoretical predictions. Further, we have probed the effect of molecular chirality on the $N + 6$ phase. In the chiral $N + 6$ phase the bond-orientational order within each polymer bundle is found to be twisted about an axis parallel to the average polymer direction. This structure is consistent with the theoretically envisaged Moiré state. In addition to confirming predictions of fundamental theories of two-dimensional melting, these results are relevant in a variety of situations in chemistry, physics and biology, where parallel packing of polymer-like objects is encountered.

[1] A. Pal, Md. Arif Kamal, and V. A. Raghunathan, Sci. Rep. **6**, 32313 (2016).

Session 4: Polymers, Polyelectrolytes, Biopolymers

Drunken soft matter: Co-non-solvency based design of smart multi-responsive materials in aqueous alcohol mixtures

D. Mukherji,¹ M. D. Watson,² M. Wagner,¹ C. M. Marques,³ and K. Kremer¹

¹ *Max-Planck Institut für Polymerforschung, Mainz, Germany*

² *University of Kentucky, Lexington, KY, USA*

³ *Institut Charles Sadron, Université de Strasbourg, Strasbourg, France*

The design of multi-responsive smart polymers is fundamentally challenging, while at the same time it possesses immense potential for advanced functional soft materials. In this context, smart polymers are an important class of soft materials whose structure, function and stability drastically changes by a slight change in external stimuli. One of the puzzling and intriguing phenomena of smart polymers is co-non-solvency. Co-non-solvency occurs when a polymer is added to a mixture of two miscible good solvents.

As a result, the same polymer can collapse into a globule within intermediate mixing ratios [1,2]. More interestingly, polymer collapses despite the fact that the solvent quality remains good or even gets increasingly better by the addition of the better cosolvent [1,3]. Typical examples include thermoresponsive polymers in aqueous alcohol mixtures [4]. This puzzling phenomenon, where the solvent quality is decoupled from the polymer conformation, is driven by strong local preferential adsorption of the better cosolvent to the polymer [1-3].

In this work, combining molecular simulations and polymer synthesis in conjunction with the concept of co-non-solvency phenomenon, we propose design principle of a new class of copolymer architectures. We show how the relative solvent quality and the copolymer sequence can lead a fully flexible tuning of polymer conformation for desired applications.

- [1] D. Mukherji and K. Kremer, *Macromolecules* **46**, 9158 (2013).
- [2] D. Mukherji, C. M. Marques, and K. Kremer, *Nat. Commun.* **5**, 4882 (2014).
- [3] D. Mukherji, M. Wagner, M. D. Watson, S. Winzen, T. E. de Oliveira, C. M. Marques, and K. Kremer, *Soft Matter* **12**, 7995 (2016).
- [4] D. Mukherji, C. M. Marques, T. Stuehn and K. Kremer, *J. Chem. Phys.* **142**, 114903 (2015).

Artificial chaperonins

C. Tung,² I. Coluzza,¹ A. Maier,¹ and A. Cacciuto²

¹ *Computational Physics, Faculty of Physics, University of Vienna, Vienna, Austria*

² *Department of Chemistry, Columbia University, New York, NY, USA*

Incorrect folding of proteins in living cells may lead to malfunctioning of the cell machinery. To prevent such cellular disasters from happening, all cells contain molecular chaperones that assist nonnative proteins in folding into the correct native structure. One of the most studied chaperone complexes is the GroEL-GroES complex. The GroEL part has a "double-barrel" structure [1-4], which consists of two cylindrical chambers joined at the bottom in a symmetrical fashion. The hydrophobic rim of one of the GroEL chambers captures nonnative proteins. The GroES part acts as a lid that temporarily closes the filled chamber during the folding process. Several capture-folding-release cycles are required before the nonnative protein reaches its native state. We performed molecular simulations that suggest that translocation of the nonnative protein through the equatorial plane of the complex boosts the efficiency of the chaperonin action [5, 6]. If the target protein is correctly folded after translocation, it is released. However, if it is still nonnative, it is likely to remain trapped in the second chamber, which then closes to start a reverse translocation process. This shuttling back and forth continues until the protein is correctly folded. Our model provides a natural explanation for the prevalence of double-barreled chaperonins. Moreover, we argue that internal folding is both more efficient and safer than a scenario where partially refolded proteins escape from the complex before being recaptured. Here we present the results of an artificial device designed according to the proposed GroEL/GroES refolding mechanism. The device we propose consists in a cylindrical pore internally grafted with flexible chains. Using molecular dynamics simulations that include hydrodynamic interactions we observed that the translocation helps single protein to refold and forces cluster to break down [7].

- [1] Z. Xu, A. L. Horwich, and P. B. Sigler, *Nature* **388**, 741 (1997).
- [2] N. Papo, Y. Kipnis, G. Haran, and A. Horovitz, *J. Mol. Biol.* **380**, 717 (2008).
- [3] D. Yang, X. Ye, and G. H. Lorimer, *Proc. Natl. Acad. Sci. USA* **110**, E4298 (2013).
- [4] C. Ricci, M. G. Ortore, S. Vilasi, R. Carrotta, M. R. Mangione, D. Bulone, F. Librizzi, F. Spinozzi, G. Burgio, H. Amenitsch, and P. L. San Biagio, *Biophys. Chem.* **208**, 68 (2016).
- [5] I. Coluzza, S. M. van der Vies, and D. Frenkel, *Biophys. J.* **90**, 3375 (2006).
- [6] I. Coluzza, A. De Simone, F. Fraternali, and D. Frenkel, *PLoS Comput. Biol.* **4**, e1000006 (2008).
- [7] C. Tung, I. Coluzza, and A. Cacciuto, submitted.

The influence of charged-induced variations in the local permittivity on the static and dynamic properties of polyelectrolyte solutions

C. Holm, F. Fahrenberger, O. A. Hickey, and J. Smiatek

Institute for Computational Physics, University of Stuttgart, Stuttgart, Germany

There is a large body of literature investigating the static and dynamic properties of polyelectrolytes due both to their widespread application in industrial processes and their ubiquitous presence in biology. Because of their highly charged nature, polyelectrolytes can alter the local dielectric permittivity of the solution within a few nanometers of their backbone. The effect of having a gradient in the dielectric environment has been, however, almost entirely ignored in simulations and theoretical work, but this effect can lead to very interesting consequences [1]. In this article we apply our recently developed electrostatic solver based on Maxwell's equations [2] to examine the effects of the permittivity reduction in the vicinity of the polyelectrolyte. We first verify our new approach by calculating and comparing ion distributions around a linear fixed polyelectrolyte and find both quantitative and qualitative changes in the ion distribution. Further simulations with an applied electric field show that the reduction in the local dielectric constant increases the mobility of the chains by approximately ten percent [3]. Our new approach quantitatively reproduces experimental results on the conductivity of polyelectrolyte solutions unlike simulations with a constant permittivity that even qualitatively fail to describe the data [4]. We can relate this success to a change in the ion distribution close to the polymer due to the built-up of a permittivity gradient.

[1] F. Fahrenberger, Z. Xu, and C. Holm, J. Chem. Phys. **141**, 064902 (2014).

[2] F. Fahrenberger and C. Holm, Phys. Rev. E **90**, 063304 (2014).

[3] F. Fahrenberger, O. A. Hickey, J. Smiatek, and C. Holm, J. Chem. Phys. **143**, 243140 (2015).

[4] F. Fahrenberger, O. A. Hickey, J. Smiatek, and C. Holm, Phys. Rev. Lett. **115**, 118301 (2015).

On scenarios for dynamical arrest in protein solutions

F. Roosen-Runge,¹ R. Roth,² F. Zhang,³ F. Schreiber,³ T. Seydel,⁴
P. Schurtenberger,¹ and A. Stradner¹

¹ *Division of Physical Chemistry, Kemicentrum, Lund University, Lund, Sweden*

² *Institute for Theoretical Physics, University of Tübingen, Tübingen, Germany*

³ *Institute for Applied Physics, University of Tübingen, Tübingen, Germany*

⁴ *Institut Laue-Langevin, Grenoble, France*

In protein solutions, a complex interplay of anisotropic interactions causes a rich thermodynamic and dynamic behavior. The underlying link between statics and dynamics is not only important to understand biological (mal-)function, but also opens potentials for controlled assembly of biomatter.

We present multiscale results on protein diffusion using light scattering and quasielastic neutron scattering. A comparison between experimental protein systems reveals different scenarios for dynamical arrest driven by phase transitions.

In the first study on solutions of serum albumin, reentrant condensation and liquid-liquid phase separation is induced by an intermediate concentration of trivalent salt. Approaching the phase boundary, diffusion is slowed down following a master curve on a broad protein concentration range, both for nanosecond self-diffusion [1] and microsecond gradient diffusion [2]. The phase behavior is reproduced by cation crosslinks between proteins [3], and the related cluster fraction can explain the universal slowing down.

As the second system, solutions of α , β and γ crystallins are examined as model systems for the eye lens. α crystallin solutions behave as a polydisperse hard-sphere systems, with a repulsive glass transition at high volume fraction, corresponding arrest of the gradient diffusion [4], and a nanosecond cage diffusion consistent with colloidal short-time predictions up to the glass transition [5].

Solutions of γ crystallin show a liquid-liquid phase separation consistent with a shortrange attraction. The gradient diffusion correspondingly displays a critical slowing down, but furthermore evidences an arrest line due to attraction at low volume fractions around 35% [6]. The rapid decrease of nanosecond cage diffusion by more than a decade way before the macroscopic arrest line underlines the attractive origin of arrest [5, 6].

Based on the variety of arrest scenarios in protein solutions, we discuss implications and challenges for cases when different repulsive and attractive scenarios might compete.

- [1] M. Grimaldo, F. Roosen-Runge, M. Hennig, F. Zanini, F. Zhang, M. Zamponi, N. Jalarvo, F. Schreiber, and T. Seydel, *J. Phys. Chem. Lett.* **6**, 2577 (2015).
- [2] D. Soraruf, F. Roosen-Runge, D. Soraruf, F. Roosen-Runge, M. Grimaldo, F. Zanini, R. Schweins, T. Seydel, F. Zhang, R. Roth, M. Oettel, and F. Schreiber, *Soft Matter* **10**, 894 (2014).
- [3] F. Roosen-Runge, F. Zhang, F. Schreiber, and R. Roth, *Sci. Rep.* **4**, 7016 (2014).
- [4] G. Foffi, G. Savin, S. Bucciarelli, N. Dorsaz, G. M. Thurston, A. Stradner, and P. Schurtenberger, *Proc. Nat. Acad. Sci. USA* **111**, 16748 (2014).
- [5] S. Bucciarelli, J. S. Myung, B. Farago, S. Das, G. A. Vliegenthart, O. Holderer, R. G. Winkler, P. Schurtenberger, G. Gompper, A. Stradner, *Sci. Adv.* **2**, 1601432 (2016).
- [6] S. Bucciarelli, L. Casal-Dujat, C. De Michele, F. Sciortino, J. Dhont, J. Berghenoltz, B. Farago, P. Schurtenberger, and A. Stradner, *J. Phys. Chem. Lett.* **6**, 4470 (2015).

Quasicrystal formation in soft matter and a “crystal-liquid” state

A. J. Archer,¹ A. M. Rucklidge,² P. Subramanian,² and E. K. Knobloch³

¹ *Department of Mathematical Sciences, Loughborough University, Loughborough, United Kingdom*

² *Department of Applied Mathematics, University of Leeds, Leeds, United Kingdom*

³ *Department of Physics, University of California at Berkeley, Berkeley, CA, USA*

Complex quasiperiodic structures are observed in a variety of soft matter systems, including dendrimers. We investigate the formation and stability of such quasicrystals in both two [1,2] and three [3] dimensions using density functional theory and a phase field crystal model. The molecular interactions result in two length scales (in the golden ratio) being favoured, which in the model can be controlled independently. In addition to regular crystals, one-, two- and three-dimensional quasicrystals can be found. We compute the minima of the free energy of the competing structures to determine the phase diagram. In three dimensions, the icosahedral quasicrystal can be the global minimum free energy state. We find that strong nonlinear coupling between density waves at the two length scales are responsible for stabilizing the icosahedral quasicrystal. Density functional theory and Brownian dynamics simulations reveal that the two-dimensional system has a fluid phase and two crystalline phases with different lattice spacing. Of these the larger lattice spacing phase can form an exotic periodic state with a sizeable fraction of highly mobile particles: A “crystal-liquid”. Near the transition between this phase and the smaller lattice spacing phase, quasicrystalline structures may be created by a competition between linear instability at one scale and nonlinear selection of the other. This dynamic mechanism for forming quasicrystals is qualitatively different from mechanisms observed previously. The system first forms a small length scale crystal. Only when this phase is almost fully formed (i.e., the dynamics is far into the nonlinear regime) does the longer length scale start to appear, leading to the formation of quasicrystals.

[1] A. J. Archer, A. M. Rucklidge, and E. Knobloch, *Phys. Rev. Lett.* **111**, 165501 (2013).

[2] A. J. Archer, A. M. Rucklidge, and E. Knobloch, *Phys. Rev. E* **92**, 012324 (2015).

[3] P. Subramanian, A. J. Archer, E. Knobloch, and A. M. Rucklidge, *Phys. Rev. Lett.* **117**, 075501 (2016).

Single-chain polymer nanoparticles: From simple models for intrinsically disordered proteins to new soft colloids

A. J. Moreno,^{1,2} F. LoVerso,² P. Bacova,¹ M. Formanek,¹ A. Arbe,¹
J. Colmenero,^{1,2,3} and J. A. Pomposo^{1,3,4}

¹ *Centro de Física de Materiales (CSIC, UPV/EHU) and Materials Physics Center (MPC), San Sebastián, Spain*

² *DIPC, San Sebastián, Spain*

³ *Departamento de Física de Materiales, Universidad del País Vasco (UPV/EHU), San Sebastián, Spain*

⁴ *IKERBASQUE Foundation for Science, Bilbao, Spain*

Single chain nanoparticles (SCNPs) are an emergent and promising class of synthetic nano-objects. By combining chemical synthesis, large-scale molecular dynamics simulations and neutron scattering, we design and investigate different protocols leading to SCNPs with specific structures and different properties in solution. On one hand the analysis of the conformations of SCNPs synthesized in good solvent reveals that they share basic ingredients with intrinsically disordered proteins (IDPs), as topological polydispersity, sparse conformations, and compact local domains [1]. Unlike in the case of linear macromolecules, crowding leads to collapsed conformations of SCNPs resembling those of crumpled globules, at volume fractions (about 30%) that are characteristic of crowding in cellular environments. Our results for SCNPs — a model system free of specific interactions — propose a general scenario for the effect of steric crowding on IDPs.

On the other hand, dense solutions of globular SCNPs obtained via solvent-assisted routes exhibit soft caging, reentrant diffusivity and weak dynamic heterogeneity. This constitutes a realization, in a real macromolecular solution, of static and dynamic anomalies predicted by models of purely repulsive ultrasoft particles. Quantitative differences depend on the specific SCNP degree of compressibility, i.e. on the specific synthesis route adopted, as well as on the intrinsic topological polydispersity [2].

This new class of soft colloids opens up the possibility of getting insight into the mechanisms of diffusion in crowded environments (like globular proteins in cells or porous media) as well as to draw new strategies for tailoring rheological properties of polymer based nanomaterials. As an example, we discuss the effect of globular SCNPs on the rheological properties of concentrated polymer solutions. By

characterizing the tube path through isoconfigurational and primitive path analysis, we conclude that the universal effect of the globular SCNP architecture is to increase the degree of entanglement in the linear polymers [3].

- [1] A. J. Moreno, F. Lo Verso, A. Arbe, J. A. Pomposo, and J. Colmenero, *J. Phys. Chem. Lett.* **7**, 838 (2016).
- [2] F. LoVerso, A. J. Moreno, J. A. Pomposo, and J. Colmenero, *Soft Matter* **12**, 4805 (2016).
- [3] P. Bacova, F. LoVerso, A. Arbe, J. Colmenero, J. A. Pomposo, and A. J. Moreno, submitted.

Local chain segregation and entanglements in a confined polymer melt

H. Meyer,¹ N.-K. Lee,^{1,2} D. Diddens,¹ and A. Johner^{1,2}

¹ *Institut Charles Sadron, Université de Strasbourg, Strasbourg, France*

² *Institute of Fundamental Physics, Department of Physics, Sejong University, Seoul, Korea*

The reptation mechanism introduced by de Gennes and Edwards, where a polymer diffuses along a fluffy tube defined by the constraints imposed by its surroundings, convincingly describes the relaxation of long polymers in concentrated solution and melts. We propose that the scale for the tube diameter is set by local chain segregation which we study analytically. We show that the concept of local segregation is especially operational for confined geometries, where segregation extends over mesoscopic domains drastically reducing binary contacts, and provide an estimate of the entanglement length. Our predictions are quantitatively supported by extensive molecular dynamics simulations on systems consisting of long, entangled, chains. A qualitative disentanglement in thin films was already shown some time ago [1]. Combining molecular dynamics with double bridging MC moves it was now possible to equilibrate chains of length $N = 2048$ under various confinements in layers of 4 monomers up to twice the radius of gyration. This data is well described by the new theory [2].

- [1] H. Meyer, T. Kreer, A. Cavallo, J. P. Wittmer, and J. Baschnagel, *Eur. Phys. J. ST* **141**, 167 (2007).
- [2] N.-K. Lee, D. Diddens, H. Meyer, and A. Johner, *Phys. Rev. Lett.* in press.

Origin of spatial organization of DNA-polymer in chromosomes

A. Chatterji,¹ T. Agarwal,¹ G. P. Manjunath,² and F. Habib³

¹ Department of Physics, IISER-Pune, Pune, India

² Department of Biology, IISER-Mohali, Chandigarh, India

³ Department of Biology, IISER-Pune, Pune, India

Using data from contact maps of the DNA-polymer of *E. Coli* (at kilo base pair resolution) as an input to our model, we introduce cross-links between monomers in a bead-spring model of a flexible ring polymer at very specific points along the chain. By suitable Monte Carlo simulations we show that the presence of these cross-links lead to a specific architecture and organization of the chain at large (micrometer) length scales of the DNA. We also investigate the structure of a ring polymer with an equal number of cross-links at random positions along the chain. We find that though the polymer does get organized at the large length scales, the nature of organization is quite different from the organization observed with cross links at specific biologically determined positions. We used the contact map of *E. Coli* bacteria which has around 4642 kilo base pairs in a single chromosome. In our coarse grained flexible ring polymer model we used 4642 monomer beads and observe that around 82 cross-links are enough to induce large scale organization of the molecule accounting for statistical fluctuations induced by thermal energy. The length of a DNA chain of a even simple bacterial cell such as *E. Coli* is much longer than typical proteins, hence we avoided methods used to tackle protein folding problems. We define new suitable quantities to identify large scale structure of a polymer chain with a few cross-links. We have carried out similar studies with the DNA-bacteria of *C. Crecentus* with cross-links at specific points relevant to the DNA of *C. Crecentus*, and obtain identical conclusions. This assures us about the robustness of our results [1,2].

[1] T. Agarwal, G. P. Manjunath, F. Habib, and A. Chatterji,
<https://arxiv.org/abs/1701.05770>.

[2] T. Agarwal, G. P. Manjunath, F. Habib, P. Lakshmi, and A. Chatterji,
<https://arxiv.org/abs/1701.05068>.

Session 5: Colloids

Topologically protected multiparticle transport of magnetic colloids

J. Loehr, M. Loenne, A. Ernst, D. de las Heras, and T. M. Fischer

Institute of Physics and Mathematics, University of Bayreuth, Bayreuth, Germany

Topological protection is a widespread phenomenon in quantum systems. There, it allows robust transport of localized phenomena such as quantum information, solitons and dislocations. In contrast, classical techniques to control the motion of a collection of e.g. colloidal particles, such as gradient fields, thermal ratchets or active particles, results in a diffuse broadening of the trajectories due to the polydispersity of the particles.

Here, we apply the concept of topological protection to the dissipative transport of colloidal particles above a periodic hexagonal magnetic pattern. By driving the system with periodic modulation loops of an external and spatially homogeneous magnetic field, we achieve total control over the motion of diamagnetic and paramagnetic colloids. Using experiments, theory and simulations we show, that each type of colloid can be simultaneously and independently transported along any of the six crystallographic directions of the pattern via adiabatic or deterministic ratchet motion. The agreement across theory experiment and simulation is perfect. Both types of motion are topologically protected [1]. As a direct application, we implement an automatic topologically protected quality control of a chemical reaction between functionalized colloids.

Our results are not limited to our specific system but are also relevant to other systems with the same symmetry. Beyond that we could show that topological protection can also be found in systems with different symmetries and that the symmetry is deeply connected to the topology [2].

[1] J. Loehr, M. Loenne, A. Ernst, D. de las Heras, and T. M. Fischer, Nat. Commun. **7**, 11745 (2016).

[2] D. de las Heras, J. Loehr, M. Loenne, and T. M. Fischer, New J. Phys. **18**, 105009 (2016).

Optical trapping of colloids at a liquid-liquid interface

A. Caciagli, J. Kotar, D. Joshi, and E. Eiser

Cavendish Laboratory, University of Cambridge, Cambridge, United Kingdom

Optical tweezing is an established tool to examine interactions at the micro and nanometer level. Such forces are typically assessed by using an optically trapped particle as a probe. Since the size of an optical trap is usually of the same order of magnitude of the bead diameter, multiple particles can enter the same trap. This results in multiple scattering between the particles themselves, which display the tendency to reversibly form ordered structures: the phenomenon is dubbed optical binding [1]. The ordered structures are either chains of particles along the propagation axis or two dimensional crystalline patterns perpendicular to the laser beam [2]. The latter, referred to as lateral optical binding, is of particular interest as the creation of ordered, quasi-2D patterns of many distinct colloids or nano-particles is one of the key challenges in complex selfassembly. Complex cluster formation is however hindered by the scattering optical force along the beam propagation direction, which often destroys the crystal. Implementation of either complex or multiple beam trapping setups or the use of solid surface as a support for the crystal have been adopted to counteract the scattering force [3], but these approaches limits the study of extended clusters held together solely by optical forces.

In this talk, we will show that a liquid-liquid interface can be successfully employed to study lateral optical binding of colloids in a single-beam configuration. Here, we graft the colloids to an oil-water interface by using DNA tethers, as illustrated in our recent DNA functionalized oil droplet (OD) model system [4]. The tether provides full mobility to the colloids on the lateral plane while balancing the optical scattering force along the beam propagation direction, effectively confining their motion to a quasi-2D plane. Extended colloidal clusters can thus form under the action of a single-beam optical trap, where inter-particle interactions are only mediated by light and excluded volume effects. After a brief introduction of our emulsion model system, we report qualitative observation of lateral optical binding of colloidal particles grafted to the ODs. Then, we show how the obtained close-packing structures can be strengthened or relaxed upon adding additional inter-particle interactions. Finally, we report potential energy measurements and trap stiffness estimations of a single trapped particle at the liquid-liquid interface by tuning the light intensity and trap position. This clarifies under which assumptions the liquid-liquid interface under study can be considered “clean” and quasi-ideal 2D motion of the colloids is achieved. We conclude by stressing how the novelty of our system allows for interparticle

interactions only mediated by light and opens a new route toward the study and the realisation of extended photonic clusters.

- [1] R. W. Bowman and M. J. Padgett, Rep. Prog. Phys. **76**, 2 (2013).
- [2] K. Dholakia and P. Zemanek, Rev. Mod. Phys. **82**, 2 (2010).
- [3] M-T. Wei, J. Ng, C. T. Chan, and H. D. Ou-Yang, Sci. Rep. **6**, 38883 (2016).
- [4] D. Joshi, D. Bargteil, A. Caciagli et al., Sci. Adv. **2**, 8 (2016).

Localised plasticity in crystals formed by wireframe particles

J. M. McBride and C. Avendaño

School of Chemical Engineering and Analytical Science, University of Manchester, Manchester, United Kingdom

Particles with wireframe geometry, i.e. hollow, open structures comprised by interconnected edges, were first realised experimentally in 1991 when Chen et al. synthesised a cubic nanoframe from DNA strands [1]. By today a vast library of DNA wireframe geometries have been reported [2], alongside a growing number of metal nanoframes [3], ceramic networks [4], and open protein structures [5]. In this work, we study the phase behaviour and packing of a non-convex particle model that captures the main geometrical features of the experimental frame-like particles. In particular, we consider the case of cubic frame-like particles. The edges of the cubic frame are represented by twelve permanently bonded hard spherocylinders of varying thickness $t^* = \sigma/L$, where σ and L are the diameter and length of an edge respectively. Using Monte Carlo simulations and a tailored overlap algorithm, we have determined the unique phase behaviour of the model observing that thin cubic frames spontaneously form partially-plastic crystals upon increasing concentration. While these systems exhibit long-range orientational order typically characteristic of crystals, a dynamic fraction of particles occupy orientationally disordered states on a fixed lattice. This behaviour is in clear contrast to the observations reported in convex cubic particles [6]. As may be expected, the fraction of orientationally disordered particles, x_d , increases as the frames are made thinner. This behaviour enables the plastic crystals to exist at unusually high concentrations. To further assess the role of the symmetry on the phase behaviour of frame-like particles, we also report simulation results of systems of rhombic dodecahedra and triangular prisms – shapes with respectively lower and greater asphericity – to find that they too form partially plastic crystals. We argue that this novel phase behaviour is indicative of a wider trend for wireframe particles.

- [1] J. H. Chen and N. C. Seeman, *Nature* **350**, 6319 (1991).
- [2] R. Veneziano, S. Ratanaalert, K. Zhang, F. Zhang, H. Yan, W. Chiu, and M. Bathe, *Science* **352**, 6293 (2016).
- [3] X. Lu, L. Au, J. McLellan, Z.-Y. Li, M. Marquez, and Y. Xia, *Nano Lett.* **7**, 6 (2007).
- [4] L. R. Meza, S. Das, and J. R. Greer, *Science* **345**, 1322 (2014).
- [5] Y.-T. Lai, E. Reading, G. L. Hura, K.-L. Tsai, A. Laganowsky, F. J. Asturias, J. A. Tainer, C. V. Robinson, and T. O. Yeates, *Nat. Chem.* **6**, 12 (2014).
- [6] F. Smallenburg, L. Filion, M. Marechal, and M. Dijkstra, *Proc. Natl. Acad. Sci. USA.* **109**, 44 (2012).

MAD particles self-assemble into virus-like microcapsules

C. H. J. Evers,¹ J. A. Luiken,² P. G. Bolhuis,² and W. K. Kegel¹

¹ *Van 't Hoff Laboratory for Physical and Colloid Chemistry, Utrecht University, Utrecht, The Netherlands*

² *Van 't Hoff Institute for Molecular Sciences, University of Amsterdam, Amsterdam, The Netherlands*

In material sciences, anisotropic interactions have been induced by distributing mutually attractive domains anisotropically over the surface of colloids, or by making mutually attractive nanoparticles deformable. In biology, however, proteins incorporate mutual attraction, anisotropy as well as deformability and we abbreviate these three characteristics as MAD. Such MAD particles self-assemble, for example, into virus microcapsules.

Recently, we synthesized colloidal MAD particles that self-assemble into virus-like microcapsules [1]. We propose that mutual attraction and deformability (MD) induce anisotropic interactions via colloidal bond hybridization. Our particles contain both mutually attractive and repulsive surface groups that are flexible. Analogously to the simplest chemical bond—in which two isotropic orbitals hybridize into the molecular orbital of H₂—these flexible groups redistribute on binding.

Via colloidal bond hybridization, isotropic MD spheres self-assemble into planar monolayers, whereas anisotropic MAD particles form virus-like microcapsules. A modest change of the building blocks thus results in a significant leap in the complexity of the self-assembled structures. Finally, whereas details of viruses are different, the MAD characteristics of their building blocks could be important in the self-assembly of virus microcapsules as well.

[1] C. H. J. Evers, J. A. Luiken, P. G. Bolhuis, and W. K. Kegel, *Nature* **534**, 364 (2016).

Fabrication of homogeneous and structured polymeric nanoparticles through rapid solvent exchange

A. Nikoubashman,¹ N. Li,² V. E. Lee,² C. Sosa,² R. K. Prud'homme,²
R. D. Priestley,² and A. Z. Panagiotopoulos²

¹ *Institute of Physics, Johannes Gutenberg University Mainz, Mainz, Germany*

² *Department of Chemical and Biological Engineering, Princeton University, Princeton, NJ, USA*

Tailored nanoparticles are increasingly sought after for many scientific and technological applications, ranging from mesoscopic models for atomic systems, over soft optoelectronic devices, to highly selective catalysts. However, both research and commercialization of these systems has been impeded by the lack of suitable fabrication techniques. One promising approach for overcoming this hurdle is flash nanoprecipitation, where soft nanoparticles are assembled through rapid micromixing of polymers in solution with a miscible poor solvent. In principle, this continuous process allows for high yields as well as precise control over particle size and morphology. We performed both experiments [1] and computer simulations [2] to elucidate the underlying physics and to investigate the role of various process parameters. In particular, we discovered that no external stabilizing agents or charged end-groups are required to keep the colloids separated from each other, when water is used as the non-solvent. The size of the nanoparticles can be reliably tuned through the mixing rate and the ratio between polymer solution and nonsolvent. Furthermore, we were able to fabricate a wide variety of structured colloids, such as Janus and core-shell particles, when polymer blends were used in the feed stream. Our results demonstrate that this mechanism is highly promising for the mass fabrication of uniformly-sized polymeric nanoparticles, using a wide variety of polymeric feed materials.

[1] C. Sosa, R. Liu, C. Tang, F. Qu, S. Niu, M. Z. Bazant, R. K. Prud'homme, and R. D. Priestley, *Macromolecules* **49**, 3580 (2016).

[2] A. Nikoubashman, V. E. Lee, C. Sosa, R. K. Prud'homme, R. D. Priestley, and A. Z. Panagiotopoulos, *ACS Nano* **10**, 1425 (2016).

Direct measurement of sub-Debye-length forces between charged colloids

P. Bartlett,¹ S. Finlayson,¹ G. Smith,² F. Waggett,¹ and M. Shafiq¹

¹ School of Chemistry, University of Bristol, Bristol, United Kingdom

² Department of Chemistry, University of Sheffield, Sheffield, United Kingdom

Virtually all materials are charged at the micro-scale so electrostatics plays a key role in colloidal self assembly. For large particle-particle separations, the predictions of the classic Derjaguin-Landau-Verwey-Overbeek (DLVO) approach, based on linearization of the mean-field Poisson-Boltzmann (PB) theory, have been amply verified [1]. Charged particles interact via a screened-Coulombic potential on a scale which varies with the Debye screening length λ_D of the solvent. Far less is known about what happens at small separations $h < \lambda_D$ where polarization effects, which are normally neglected in linear treatments, make the charge on a colloidal surface spatially inhomogeneous. Using blinking optical tweezers, we have measured directly the forces between individual pairs of same-charged and oppositely-charged colloids at surface-surface separations h comparable to the Debye screening length λ_D . We use non-polar suspensions which make the mutual interactions between charged particles at $h \approx \lambda_D$ relatively easy to study quantitatively in the lab. At low salt concentrations, we find a short-range electrostatic attraction between same-charge particles combined with a longer-range repulsion. By contrast, oppositely-charged spheres interact via short-range repulsive and long-range attractive forces. We attribute these qualitative differences from DLVO to mutual polarization of the particle surfaces, resulting in regions of positive and negative surface charge density.

[1] S. Finlayson and P. Bartlett, J. Chem. Phys. **145**, 034905 (2016).

Non-touching charged colloidal particles near an oil-water interface

J. C. Everts,^{1,2} S. Samin,¹ N. A. Elbers,³ J. E. S. van der Hoeven,³
A. van Blaaderen,³ and R. van Roij¹

¹ *Institute for Theoretical Physics, Center for Extreme Matter and Emergent Phenomena, Utrecht University, Utrecht, The Netherlands*

² *Faculty of Mathematics and Physics, University of Ljubljana, Ljubljana, Slovenia*

³ *Soft Condensed Matter, Debye Institute for Nanomaterials Science, Utrecht, The Netherlands*

In this talk I will give a brief overview on the physics of charged colloidal particles with double layers larger than the particle size. In particular, I will show that the interaction of an oil-dispersed colloidal particle with an oil-water interface is highly tunable from attractive to repulsive, either by varying the sign of the colloidal charge via charge regulation, or by varying the difference in hydrophilicity between the dissolved cations and anions [1]. In addition, we investigate the yet unexplored interplay between the self-regulated colloidal surface charge distribution with the planar double layer across the oil-water interface and the spherical one around the colloid. We explain recent experiments where so-called "non-touching" oil-dispersed colloids were detached from an oil-water interface by the addition of an organic salt to the oil, while the particles were initially being trapped at a finite, but small distance from the interface [2,3].

[1] J. C. Everts, S. Samin, and R. van Roij, *Phys. Rev. Lett.* **117**, 098002 (2016).

[2] N. A. Elbers, J. E. S. van der Hoeven, D. A. M. de Winter, C. T. W. M. Schneijdenberg, M. N. van der Linden, L. Fillion, and A. van Blaaderen, *Soft Matter* **12**, 7265 (2016).

[3] J. C. Everts, N.A. Elbers, J. E. S. van der Hoeven, S. Samin, A. van Blaaderen, and R. van Roij, submitted.

Nonadditivity of critical Casimir forces

S. Paladugu,¹ A. Callegari,¹ Y. Tuna,^{1,2} L. Barth,¹ S. Dietrich,^{3,4}
A. Gambassi,⁵ and G. Volpe^{1,2,6}

¹ *Soft Matter Lab, Department of Physics, Bilkent University, Ankara, Turkey*

² *UNAM National Nanotechnology Research Center, Bilkent University, Ankara, Turkey*

³ *Max-Planck-Institut für Intelligente Systeme, Stuttgart, Germany*

⁴ *IV. Institut für Theoretische Physik, Universität Stuttgart, Stuttgart, Germany*

⁵ *SISSA International School for Advanced Studies and INFN, Trieste, Italy*

⁶ *Department of Physics, University of Gothenburg, Göteborg, Sweden*

In soft and condensed matter physics, effective interactions may emerge as a result of the spatial confinement of a fluctuating field. For instance, microscopic colloidal particles in a binary liquid mixture are subject to critical Casimir forces whenever their surfaces confine the thermal fluctuations of the order parameter of this solvent, emerging upon approaching its critical demixing point [1]. These critical Casimir forces are theoretically predicted to be non-additive and therefore many-body effects are expected to occur. However, until recently, a direct experimental evidence of this fact was lacking. In this contribution we report on the experimental measurement [2] of the associated three-body effects, which provides such evidence and confirms quantitatively the nonadditive nature of the critical Casimir effect.

[1] C. Hertlein, L. Helden, A. Gambassi, S. Dietrich, and C. Bechinger, *Nature* **451**, 172 (2008).

[2] S. Paladugu, A. Callegari, Y. Tuna, L. Barth, S. Dietrich, A. Gambassi, and G. Volpe, *Nat. Commun.* **7**, 11403 (2016).

Two-dimensional melting in binary hard disks

J. Russo¹ and N. Wilding²

¹ *School of Mathematics, University of Bristol, Bristol, United Kingdom*

² *Department of Physics, University of Bath, Bath, United Kingdom*

The melting of two-dimensional solids has attracted considerable interest since the pioneering work of Kosterlitz and Thouless [1], which showed the existence of a new type of continuous phase transition where topological defects play a crucial role, and for whose discovery they both won a share of the 2016 Nobel Prize in physics. The melting of monodisperse hard-disks has been recently shown to involve a KT transition between the solid and the hexatic phase, and a first order transition between the hexatic and the fluid phase [2], a result that has been generalised to soft potentials [3] and hard-sphere monolayers [4]. So far, most of the studies have focused on monodisperse systems, while there is still no clear understanding of the melting scenario in the important case of twodimensional binary mixtures [5]. In this contribution we explore the melting transition in two-dimensional hard-disk mixtures, where the ratio between the large and small disks is $r_L/r_S = 1.4$. We carry out extensive computer simulations and obtain the phase diagram of the mixture as a function of the concentration c of small disks, together with a detailed analysis of both the static and dynamic properties of the mixture along the melting line. Our results show that the hexatic phase is destabilised by the disorder induced by a small (but finite) concentration of small disks, at which point the KT transition is preempted by a first order solid-fluid phase transition. A study of the evolution of topological defects [6] helps us elucidate the conditions at which the hexatic phase becomes metastable with respect to the solid phase. Our results thus shed new light on the melting scenario of an important class of soft matter systems.

[1] J. M. Kosterlitz and D. J. Thouless, *J. Phys. C: Solid State Phys.* **5**, L124 (1972).

[2] E. P. Bernard and W. Krauth, *Phys. Rev. Lett.* **107**, 155704 (2011).

[3] S. C. Kapfer and W. Krauth, *Phys. Rev. Lett.* **114**, 035702 (2015).

[4] W. Qi, A. P. Gantapara, and M. Dijkstra, *Soft Matter* **10**, 5449 (2014).

[5] A. L. Thorneywork, R. Roth, D. G. A. L. Aarts, and R. P. A. Dullens, *J. Chem. Phys.* **140**, 161106 (2014).

[6] M. A. Bates and D. Frenkel, *Phys. Rev. E* **61**, 5223 (2000).

Self-assembly of cubes into 2D hexagonal and honeycomb lattices by hexapolar capillary interactions

G. Soligno,¹ M. Dijkstra,² and R. van Roij¹

¹ *Institute for Theoretical Physics, Center for Extreme Matter and Emergent Phenomena, Utrecht University, Utrecht, The Netherlands*

² *Soft Condensed Matter, Debye Institute for Nanomaterials Science, Utrecht University, Utrecht, The Netherlands*

Particles adsorbed at fluid-fluid interfaces can induce capillary deformations in the interface, generating interactions which drive them to self-assemble into ordered 2D structures. By a recently-introduced numerical method [1] to compute the equilibrium shape of a fluid-fluid interface, we calculate the capillary potential between adsorbed particles. We will present, in particular, results [2] for the capillary interactions and self-assembly of cubes. When Young's contact angle is close to 90, the cubes induce hexapolar capillary deformations in the interface height profile, which drive them to assemble into hexagonal and honeycomb lattices, as observed experimentally [3]. By a simple free energy model, we predict a temperature-density phase diagram where both the honeycomb lattice and hexagonal lattice appear as thermodynamic-stable states.

- [1] G. Soligno, M. Dijkstra, and R. van Roij, *J. Chem. Phys.* **141**, 244702 (2014).
- [2] G. Soligno, M. Dijkstra, and R. van Roij, *Phys. Rev. Lett.* **116**, 258001 (2016).
- [3] W. H. Evers, B. Goris, S. Bals, M. Casavola, J. de Graaf, R. van Roij, M. Dijkstra, and D. Vanmaekelbergh, *Nano Lett.* **13**, 2317 (2013).

Brownian Carnot engine

E. Roldan,^{1,2,5} I. A. Martinez,²⁻⁵ L. Dinis,^{4,5} D. Petrov,² J. M. R. Parrondo,^{4,5} and R. A. Rica²

¹ *Max Planck Institute for the Physics of Complex Systems, Dresden, Germany*

² *ICFO-Institut de Ciències Fotòniques, Castelldefels (Barcelona), Spain*

³ *Laboratoire de Physique, École Normale Supérieure, Lyon, France*

⁴ *Departamento de Física Atómica, Molecular y Nuclear, Universidad Complutense de Madrid, Madrid, Spain*

⁵ *GISC-Grupo Interdisciplinar de Sistemas Complejos, Madrid, Spain*

Sadi Carnot is considered the father of thermodynamics. In his seminal work “Reflexions sur la puissance motrice du feu” Carnot studied the conversion of heat into work by thermal engines. The Carnot cycle imposes a fundamental upper limit to the efficiency of a macroscopic motor operating cyclically between two thermal baths. Despite being at the core of classical thermodynamics, an experimental realization of the Carnot cycle has been elusive to experimentalists during almost two centuries.

Using an optically-trapped microscopic colloid immersed in water, we report on the first experimental realization of a Carnot engine at the microscale [1]. In our experiment, the microscopic particle is the working substance and the optical trap plays the role of the piston in a classical engine. The effective temperature of the colloid is controlled by applying time-dependent external noisy electrostatic fields, using a novel experimental technique that allows to tune the effective temperature of a colloid up to 3000K [2,3]. By concatenating a series of isothermal and microadiabatic protocols (where the entropy of the particle remains constant in time [4]), our microscopic engine attains Carnot efficiency when it is driven quasistatically.

We present an exhaustive study of the energetics of the engine and analyse the fluctuations of the finite-time efficiency, showing that the Carnot bound can be surpassed for a small number of non-equilibrium cycles. Our results characterize the sources of irreversibility in the engine and the statistical properties of the efficiency—an insight that could inspire new strategies in the design of efficient nano-motors [5].

[1] I. A. Martínez, É. Roldán, L. Dinis, J. M. R. Parrondo, D. Petrov, and R. A. Rica, *Nat. Phys.* **12**, 67 (2016).

[2] I. A. Martínez, É. Roldán, J. M. R. Parrondo, and D. Petrov, *Phys. Rev. E* **87**, 032159 (2013).

[3] P. Mestres, I. A. Martínez, A. Ortiz-Ambriz, R. A. Rica, and É. Roldán, *Phys. Rev. E* **90**, 032116 (2014).

[4] I. A. Martínez, É. Roldán, L. Dinis, D. Petrov, and R. A. Rica, *Phys. Rev. Lett.* **114**, 120601 (2015).

[5] I. A. Martínez, É. Roldán, L. Dinis, and R. A. Rica, *Soft Matter* **13**, 22 (2017).

Ultra low crosslinked microgels: How soft are soft particles?

A. Scotti, M. Brugnoni, and W. Richtering

Institute of Physical Chemistry, RWTH Aachen University, Aachen, Germany

Microgels are cross-linked polymeric network swollen by a solvent. They can go through volume phase transition depending on the variation of external stimuli, e.g. temperature or pH. Ultra-soft particles can be synthesized without the addition of crosslinking agents [1]. These ultra low crosslinked (ULC) microgels exhibit a higher capability of swelling with respect to the usual cross-linked particles and the highest possible softness. Due to their extreme softness, these particles represent an important system to build advanced soft materials in the field of food science, oil recovery, and biomedical applications. For instance, recently ULC poly(*N*-isopropylacrylamide) (pNIPAM) based microgels have been used to reproduce platelet-like behaviors [2]. These materials represent a new, challenging and fascinating system for technological applications, nevertheless, a deeper understanding of both, their internal structure and their properties in high concentrated environment are needed.

We present the first systematic and complete characterization of suspensions of ultra low crosslinked pNIPAM based microgels. Dynamic light scattering is used to obtain the hydrodynamic radius of the particles at different temperatures. Flory-Rehner theory, using a concentration dependent Flory solvency parameter, successfully describes the experimental swelling, despite the inhomogeneous character of the particles [3]. A series of ULC suspensions, at different concentrations, has been realized to study the phase behavior. Fluid, coexistence between fluid and crystals, fully crystalline and glassy phases are present. Due to the soft nature of microgels, the boundaries of the transitions are shifted to higher concentrations with respect both, hard spheres and normal pNIPAM-based microgels. The rheological response of the suspensions, at different concentrations, has been probed too. The suspensions show that the behavior is consistent with the one expected for normal microgels. Small-angle neutron scattering with contrast variation is used to directly observe the deformation of the ULC microgels in concentrated suspension and the results are compared with normal microgels [4]. Our findings highlight the main differences between this system and the normal pNIPAM-based microgels. This knowledge is crucial to synthesize ULC microgels tailored for innovative applications in the field of food science, oil recovery and biomedical applications.

- [1] O. L. J. Virtanen, A. Mourran, P. T. Pinard, and W. Richtering, *Soft Matter* **12**, 3919 (2016).
- [2] A. C. Brown, S. E. Stabenfeldt, B. Ahn, R. T. Hannan et al., *Nat. Mater.* **13**, 1108 (2014).
- [3] A. Fernandez-Barbero, A. Fernandez-Nieves, I. Grillo, and E. Lopez-Cabarcos, *Phys. Rev. E* **66**, 051803 (2002).
- [4] A. Scotti, U. Gasser, E. S. Herman, M. Pelaez-Fernandez, L. A. Lyon, and A. Fernandez-Nieves, *Proc. Natl. Acad. Sci. USA* **113**, 5576 (2016).

Can colloidal swarms settle faster than isolated particles?

E. Lattuada, S. Buzzaccaro, and R. Piazza

*Department of Chemistry, Materials Science, and Chemical Engineering “G. Natta”,
Politecnico di Milano, Milano, Italy*

Usually, the more concentrated a particle dispersion is, the slower it settles in natural gravity or in a centrifuge. Yet, we have recently shown [1] that this must not perforce be true: in fact, the sedimentation velocity $v(\phi)$ of a suspension of particles interacting via strong attractive forces depends non-monotonically on particle volume fraction. While at high particle concentration $v(\phi)$ does decrease with ϕ , like in the case of hard spheres, at sufficiently low ϕ the suspension settles even faster than a single particle. This evidence, obtained for a system where depletion interactions can be finely tuned and quantified, is favorably compared to recent numerical results [2] suggesting the occurrence of such a “promoted” sedimentation regime, which utterly contrasts with standard “hindered” settling.

Our results, however, also highlight an important and previously unnoticed consequence of promoted settling on the kinetics of sedimentation. In fact, the settling front, which for hindered settling takes on a time-invariant, shock-wave profile, conversely spreads with time, becoming liable to thermal instabilities that may lead to “stratification” of the profile into distinct concentration bands.

Promoted settling may actually be much more pronounced for systems of “patchy” particles interacting via short range anisotropic attractions that do not lead to phase separation, but rather to finite clustering effects. In fact, we suggest that our results may be specifically relevant for ultracentrifuge investigations of protein association effects, where promoted settling is sometimes observed and usually interpreted using semiphenomenological “clustering models”. Indeed, by investigating the specific case of β -lactoglobulin A (BLGA), a globular protein displaying strong attractive interactions in a narrow temperature and pH range [3], we show that the structural and dynamic information provided by light scattering measurements performed at equilibrium can be exploited to quantitatively predict the settling kinetics actually observed in an ultracentrifuge, without resorting to any detailed “chemical association” models.

[1] E. Lattuada, S. Buzzaccaro, and R. Piazza, *Phys. Rev. Lett.* **116**, 038301 (2016).

[2] A. Moncho-Jordá, A. A. Louis, and J. T. Padding, *Phys. Rev. Lett.* **104**, 068301 (2010).

[3] R. Piazza and S. Iacopini, *Eur. Phys. J. E* **7**, 45 (2002).

Self-assembly dynamics of flexible colloidal molecules

I. Chakraborty,¹ D. Pearce,² S. Matysik,¹ V. Meester,¹ C. van der Wel,¹
L. Giomi,² and D. J. Kraft¹

¹ *Soft Matter Physics, Huygens-Kamerlingh Onnes Laboratory, Leiden Institute of Physics, Leiden, The Netherlands*

² *Instituut Lorentz, Universiteit Leiden, Leiden, The Netherlands*

Colloidal molecules are designed to mimic their molecular analogues through their anisotropic shape and interactions. However, current experimental realizations are missing the structural flexibility present in real molecules thereby restricting their use as model systems. I will here show how this limitation can be overcome by assembling reconfigurable colloidal molecules in high yields using colloidal joints - silica particles functionalized with mobile DNA linkers. I will examine and quantify the various factors that influence the joint flexibility [1] and demonstrate how the self-assembly pathway can be steered towards the formation of finite-sized clusters with tunable valence [2]. I will examine the self-assembly dynamics of these flexible colloidal molecules by a combination of experiments, molecular dynamics simulations and an analytical model to elucidate the growth mechanism quantitatively [2]. These reconfigurable colloidal molecules are exciting building blocks for investigating and exploiting the self-assembly of complex hierarchical structures, photonic crystals and colloidal meta-materials.

[1] I. Chakraborty, V. Meester, C. van der Wel, and D. J. Kraft, arXiv:1610.04018.

[2] I. Chakraborty, D. J. Pearce, S. Matysik, L. Giomi, and D. J. Kraft (in preparation)

Observation of solid-solid transitions in 3D crystals of colloidal superballs

J. M. Meijer,^{1,2} A. Pal,¹ S. Ouhajji,¹ H. N. W. Lekkerkerker,¹ A. P. Philipse,¹ and A. V. Petukhov¹

¹ *Van 't Hoff Laboratory, Utrecht University, Utrecht, The Netherlands*

² *Department of Physics, University of Konstanz, Konstanz, Germany*

Self-organization in colloidal suspensions leads to a fascinating range of crystal and liquid crystal phases induced by shape alone. Simulations predict the phase behaviour of a plethora of shapes while experimental realisation often lags behind. Here we present the experimental phase behaviour of colloidal superballs, i.e. particles with a shape in between that of a sphere and a cube. We show that by tuning the shape, size and interactions we can probe the phase behaviour in a region where an enrichment of the phase behaviour is predicted [1]. Using a combination of confocal microscopy and high resolution x-ray scattering we find an even richer phase behavior than predicted as three distinct crystal phases are uncovered [2]. Particularly, we find a solid-solid transition from a plastic crystal phase into two different rhombohedral crystal phases, one with hollow-site stacking while the other possesses bridge-site stacking. We further investigate how the phase diagram depends on the exact superball shape and osmotic pressure in the system and additionally find that a slight softness causes a second solid-solid transition between the two stacking sequences at high osmotic pressures. Our investigation brings us closer to ultimately controlling the experimental superball self-assembly into functional materials, such as photonic crystals.

[1] R. Ni, A. P. Gantapara, J. de Graaf, R. van Roij, and M. Dijkstra, *Soft Matter*, **8**, 8826 (2012).

[2] J. M. Meijer, A. Pal, S. Ouhajji, H. N. W. Lekkerkerker, A. P. Philipse, and A. V. Petukhov, *Nat. Commun.*, in press (2017).

Dynamics of self-organization of network fluids

C. S. Dias,^{1,2} N. A. M. Araújo,^{1,2} and M. M. Telo da Gama^{1,2}

¹ *Departamento de Física, Faculdade de Ciências, Universidade de Lisboa, Lisboa, Portugal*

² *Centro de Física Teórica e Computacional, Universidade de Lisboa, Lisboa, Portugal*

Network fluids are structured fluids, consisting of chains and branches, product of limited valence interactions. They can be precursors of low-density liquids, photonic crystals, and other materials of enhanced physical properties. Prototypical examples are networks of patchy colloids, where the limited valence results from highly directional pairwise interactions. Here, we combine extensive Langevin simulations and Wertheim's theory of association to study the relaxation dynamics of these networks. In their kinetic route towards thermodynamically stable structures, for low enough temperatures, network fluids self-organize into intermediate (mesoscopic) structures that are much larger than the individual particles and become the relevant units for the dynamics [1]. A temperature driven crossover is observed from exponential to scale-free relaxation dynamics. The exponent of the latter is independent of temperature and initial configuration. We show that the typical coarsening dynamics at the coexistence phase is hindered by the dominant dynamics that falls into the random percolation universality class [2].

- [1] N. A. M. Araújo, C. S. Dias, and M. M. Telo da Gama, J. Phys.: Condens. Matter, **29**, 14001 (2017).
- [2] C. S. Dias, J. M. Tavares, N. A. M. Araújo, and M. M. Telo da Gama, arXiv: 1604.05279 (2016).

Session 6: Films, Foams, Surfactants, Emulsions

Micelles and emulsion droplets in amphiphilic Janus particle–water–oil ternary system

T. G. Noguchi, Y. Iwashita, R. Koike, and Y. Kimura

Department of Physics, Kyushu University, Fukuoka, Japan

An amphiphilic Janus particle (AJP), composed of hydrophilic and hydrophobic hemispheres, is the colloidal analog of a surfactant molecule, and much more: An AJP exhibits much higher surface activity than the molecule due to AJP's mesoscopic size. The high surface activity can make the Pickering emulsions thermodynamically stable, which is impossible in typical Pickering emulsions stabilized with homogeneous particles [1]. Those great features of AJPs have been studied predominantly in theory and numerical simulation [2,3], however the detail of self-assembled structures in a ternary system of AJP, water and oil has not been fully explored, especially for the composition range where the amount of the minority liquid phase and AJP are comparable; one would expect the Janus characteristics to be directly reflected there.

In this study, we changed the volume ratio of the particles and the minority liquid phase, water here, by two orders of magnitude around the comparable composition range, and observed the resultant structures at the resolution of the individual particle dimensions [4]. When the volume ratio of water is smaller than that of the Janus particles, capillary interactions between the hydrophilic hemispheres of the particles induce micelle-like clusters in which the hydrophilic sides of the particles face inward. With increasing water content, these clusters grow into a rod-like morphology. When the water volume exceeds that of the particles, the structure transforms into an spherical emulsion droplets, or colloidosomes, because of the surface activity of particles at the liquid–liquid interface. Thus, we found that a change in volume fraction alters the mechanism of structure formation in the ternary system, and large resulting morphological changes in the self-assembled structures reflect the anisotropy of the particles. The self-assembly shows essential commonalities with that in microemulsions of surfactant molecules, however the AJP system is stabilized only kinetically, in different from dynamic equilibrium structures in microemulsions. In addition, we have recently produced AJPs in polygonal shapes by soft lithography, and succeeded in realizing Pickering emulsions with them. The particle packing on spherical droplets exhibits apparent shape dependence.

- [1] R. Aveyard, *Soft Matter* **8**, 5233 (2012).
- [2] N. Glaser, D. J. Adams, A. Böker, and G. Krausch, *Langmuir* **22**, 5227 (2006).
- [3] F. Tu, B. J. Park, and D. Lee, *Langmuir* **29**, 12679 (2013).
- [4] T. G. Noguchi, Y. Iwashita, and Y. Kimura, *Langmuir* **33**, 1030 (2017).

Coarsening and coalescence of a liquid 2D-foam

E. Forel,¹ B. Dollet,² and E. Rio¹

¹*Laboratoire de Physique des Solides, UMR CNRS 8502, Université Paris Sud 11, Orsay, France*

²*Institut de Physique de Rennes, UMR UR1-CNRS 6251, Université Rennes 1, Rennes, France*

Foam destabilisation is crucial in many industrial processes such as food-processing or detergency. There are three processes leading to foam destabilisation: liquid drainage (gravity-driven liquid flow), coalescence (merging of two bubbles) and coarsening (gas transfer between neighbouring bubbles of different pressure). In a 3D foam, these three processes are interdependent and it is difficult to disentangle them. A way to separate drainage from coalescence and coarsening is to use horizontal quasi-2D-foams, which, in our case, consist of a monolayer of bubbles sandwiched between two horizontal plates. In this geometry, we can study coarsening, coalescence and the competition between both processes. If the coarsening is very well described in 2D-foams, the coalescence is poorly understood. There are many hypotheses to explain coalescence. Among them, one can cite a critical liquid fraction [1], a critical bubble size [2] or a critical capillary pressure [3].

To discriminate between these different mechanisms, we have built a 2D cell in order to control the liquid fraction in the 2D foam based on an experiment realized by Roth et al. [4]. We use direct visualisation to monitor the evolution in time of various foams, both monodisperse and polydisperse, at different liquid fractions and bubbles' size.

First, we show that the topology of a coalescing foam is very different from the one of a coarsening, but non-coalescing, foam. We quantify this difference using the averaged bubble convexity. This allows us to determine the time at which a cascade of coalescence starts in the foam. We show that this time increases with the foam humidity.

Using the 2D-foam, we also tested the three main hypotheses of coalescence by tracking bubbles and by measuring the correlation between the breaking of a film and the rearrangements in the foam.

[1] V. Carrier and A. Colin, *Langmuir* **19**, 4535 (2003).

[2] D. Georgieva, A. Cagna, and D. Langevin, *Soft Matter* **5**, 2063 (2009).

[3] K. Khristov, D. Exerowa, and G. Minkov, *Colloid Surface A* **210**, 159 (2002).

[4] A. Roth, C. Jones, and D. Durian, *Phys. Rev. E* **87**, 42304 (2013).

Foam rheology: Negative wake behind a penetrable obstacle

J. Koivisto,¹ T. Chevalier,¹ M. Alava,¹ S. Santucci,² C. Raufaste,² and
A. Puisto¹

¹ *Department of Applied Physics, Aalto University, Espoo, Finland*

² *Department of Physics, École Normale Supérieure de Lyon, Lyon, France*

³ *Laboratory of condensed matter physics, University of Nice-Sophia Antipolis, Nice, France*

Foams are one of the rare examples of simple yield stress fluids. Formed of bubbles embedded in liquid they are often studied in the context of jamming [1]. Foam flow is interesting not only because the start-up requires a dynamical unjamming transition (yielding), but also due to novel technological applications related to forming technologies [2]. Here, we study a foam flow through a 2D Hele-Shaw shell with an obstacle that partly fills the gap, effectively forming a constriction. For this purpose, we use bubble scale dynamics model (the Durian bubble model), which we extend with the appropriate descriptions for a permeable obstacle based on the bubble surface tension. We observe a negative wake behind the obstacle, analogous to the one observed in bubble motion in a viscoelastic medium. There, the medium is successfully described by an Oldroyd-B model. This suggests that in the present conditions, the foam acts as a typical viscoelastic fluid, rather than the expected elastoviscoplasticity [3]. In experiments, we find a quadrupolar flow field that vanishes at decreasing obstacle heights. The same holds for the velocity overshoot behind the obstacle. To enlighten the role of the overshoots in the formation of the experimentally observed quadrupole flow pattern around the obstacle, we compare the results of the bubble model and the Oldroyd B model to the experiments. We find a reasonable agreement in the flow dynamics and the overshoots between the experimental data, the bubble model, and the Oldroyd B model. Finally, we identify a viscoelastic timescale, which determines the magnitude of the velocity overshoot.

[1] G. Katgert, B. P. Tighe, and M. van Hecke, *Soft Matter* **9**, 9739 (2013).

[2] A. M. Al-Qararah, T. Hjelt, A. Koponen, A. Harlin, and J. A. Ketoja, *Colloids Surf. A* **467**, 97 (2015).

[3] S. Bénito, C.-H. Bruneau, T. Colin, C. Gay, and F. Molino, *Eur. Phys. J. E* **25**, 225 (2008).

Wall roughness effects in micro-channel flows of soft glassy materials

D. Filippi,¹ L. Derzsi,¹ G. Mistura,¹ M. Pierno,¹ M. Lulli,² M. Bernaschi,² and M. Sbragaglia²

¹ *Dipartimento di Fisica e Astronomia “G. Galilei”, Università di Padova, Padova, Italy*

² *Dipartimento di Fisica, Università di Roma “Tor Vergata” and INFN, Rome, Italy*

The flow of soft-glassy materials (SGM) like concentrated emulsions, foams and gels, occurs via successive elastic deformations and plastic rearrangements, which create fragile regions enhancing the “fluidization” of the material [1]. This behaviour is particularly emphasized in the flow of SGM on rough surfaces, which is also relevant for an ample variety of technological applications. Despite the fluidization of SGM is strongly affected by the surface roughness, the role played by the density of rough elements has not been quantitatively addressed so far [2,3].

We study the flow of concentrated emulsions in microfluidic channels, one wall of which is patterned with micron-size equally spaced grooves oriented perpendicularly to the flow direction [4]. We find a scaling law describing the roughness-induced fluidization as a function of the density of the grooves, thus fluidization can be predicted and quantitatively regulated. Furthermore we observe and characterize two distinct scenarios: For gap spacings comparable to the mean droplet diameter of the emulsion, droplets get trapped within the grooves and form a periodic and complimentary series of “deformable” posts, while for wider gaps droplets escape much more easily from the grooves, thus the plastic activity and local fluidization are significantly enhanced in the latter case. Our experimental observations are suitably complemented and confirmed by lattice Boltzmann simulations of a model emulsion [5]. These numerical simulations are key to highlight the change in the spatial distribution of the plastic rearrangements caused by surface roughness and to elucidate the micro-mechanics of the yielding scenario via the statistics of the droplets displacement field.

- [1] R. G. Larson, *The Structure and Rheology of Complex Fluids* (Oxford University Press, Oxford, 1999).
- [2] V. Mansard, L. Bocquet, and A. Colin, *Soft Matter* **10**, 6984 (2014).
- [3] J. Goyon, A. Colin, G. Ovarlez, A. Ajdari, and L. Bocquet, *Nature* **454**, 84 (2008).
- [4] L. Derzsi, D. Filippi, G. Mistura et al., arXiv:1611.01980 (2016).
- [5] A. Scagliarini, M. Sbragaglia & M. Bernaschi, *J. Stat. Phys.* **161**, 1482 (2015).

Session 7: Confined Fluids, Interfacial Phenomena

Three-dimensional structures of electrolyte aqueous solutions near a solid surface: 3D-AFM experiments and DFT

D. Martin-Jimenez,¹ E. Chacon,¹ P. Tarazona,² and R. Garcia¹

¹ *Instituto de Ciencia de Materiales de Madrid, CSIC, Madrid, Spain*

² *Departamento Fisica Teorica de la Materia Condensada, IFIMAC Condensed Matter Physics Center, UAM, Madrid, Spain*

The development of three-dimensional (3D) Atomic Force Microscopy (AFM) is opening a powerful experimental test to the molecular structure of solid-liquid interfaces. The time honored theoretical prediction of a layering structure in a dense fluid near a solid surface may be directly contrasted with the 3D-AFM phase contrast and force. We report 3D images of electrolyte solutions near a mica surface that show how the on-plane periodic structure of the mica surface propagates across that layered region in the liquid. The comparison of the 3D-AFM experimental results with model Density Functional Theory calculations gives the clue for the crucial aspects of the observed phenomena, from low to high salt concentrations [1].

[1] D. Martin-Jimenez, E. Chacon, P. Tarazona, and R. Garcia, Nat. Commun. **7**, 12164 (2016).

How does shape anisotropy affect the aggregation of colloidal particles at the edge of an evaporating drop

N. A. M. Araújo,^{1,2} C. S. Dias,^{1,2} P. J. Yunker,³ A. G. Yodh,⁴ and
M. M. Telo da Gama^{1,2}

¹ *Departamento de Física, Faculdade de Ciências, Universidade de Lisboa, Lisboa, Portugal*

² *Centro de Física Teórica e Computacional, Universidade de Lisboa, Lisboa, Portugal*

³ *School of Physics, Georgia Institute of Technology, Atlanta, GA, USA*

⁴ *Department of Physics and Astronomy, University of Pennsylvania, Philadelphia, PA, USA*

Experiments with suspensions of ellipsoidal colloidal particles suggest a transition in the statistical properties of the stain left by an evaporating drop, depending on the eccentricity of the particles [1]. The mechanism responsible for such transition is still elusive. We propose a stochastic model to show that the very-strong anisotropic capillary attraction between particles stemming from the deformation of the interface can be responsible for such transition [2, 3]. We map the ellipsoids into spherical particles with two types of patches and numerically study their aggregation at the edge of an evaporating drop. The same transition is observed for a range of parameters that is compatible with the experimental one. We will discuss the main mechanisms involved and compare the quantitative results with experiments.

[1] P. J. Yunker et al. *Phys. Rev. Lett.* **110**, 035501 (2013).

[2] C. S. Dias, N. A. M. Araújo, and M. M. Telo da Gama, *EPL* **107**, 56002 (2014).

[3] C. S. Dias et al. in preparation.

Observation of a roughening transition on the surface of ice

P. Llombart,¹ J. Benet,² E. Sanz,¹ and L. G. MacDowell¹

¹ *Departamento de Química Física, Universidad Complutense, Madrid, Spain*

² *Department of Physics, Durham University, Durham, United Kingdom*

The habit of ice crystals in the atmosphere change from plates, to columns, to plates and yet back to columns as temperature is cooled down below the triple point [1]. Attempts to explain this puzzling sequence of events rely on the formation of a thin quasi-liquid layer of premelted ice [2]. Many efforts have been devoted to determine the onset of premelting and the thickness of the layer as the triple point is approached [3]. But precisely what is the influence of this film on the global behavior of the ice/vapor interface, and how could it impact on the mechanism of crystal growth is far from being understood [1]. In this paper, we argue that a thin premelting layer of ice hardly one nanometer thick is able to induce a structural transition of the Kosterlitz-Thoules type on the ice surface.[4] Our computer simulations reveal that the two distinct surfaces bounding the quasi-liquid layer behave at small wavelengths as rough and independent ice/water and water/vapor interfaces. However, the finite thickness of the layer inhibits large scale fluctuations and drives the crystal surface smooth at long wave-lengths. Our results explain why ice crystal prisms retain a distinct hexagonal shape up to the triple point, and suggest the formation of a premelting film could slow down the growth rate of crystal facets. Understanding the structure and growth mechanisms of ice crystals also has important implications in atmospheric science, glaciology, and frost heaving [3].

In our study, we simulate the premelting layer of water a few Kelvin below the triple point. Using an adequate order parameter, it is possible to identify distinct ice/film and film/vapor, surfaces, which separate the premelting film from the bulk solid and vapor. The spectrum of surface fluctuations allow us to measure the wave-vector dependent components of the stiffness tensor, which are finite for a rough surface, but effectively diverge for smooth surfaces. At a temperature two Kelvin below the triple point, our results indicate that the stiffness coefficients for ice/film, film/vapor and coupled ice/film and film/vapor fluctuations converge to a finite value. Moreover, it is found that the fluctuations closely resemble those of independent ice/water and water/vapor interfaces at large wave-vectors, but eventually couple and produce an effective stiffness which is the sum of the stiffness coefficients of the independent interfaces. A few Kelvin below, however, the stiffness coefficients effectively diverge, and indicate the onset of a completely different regime with finite surface fluctuations that corresponds to a smooth surface. Accordingly, it is expected that the crystal

growth rate of the prismatic facet will slow down below this temperature, and promote the growth of columnar crystals as observed in the atmosphere.

- [1] K. G. Libbrecht, Rep. Prog. Phys. **68**, 855 (2005).
- [2] T. Kuroda and R. Lacmann, J. Cryst. Growth **56**, 189 (1982).
- [3] J. G. Dash, A. W. Rempel, and J. S. Wettlaufer, Rev. Mod. Phys. **78**, 695 (2006).
- [4] J. Benet, P. Llombart, E. Sanz, and L. G. MacDowell, Phys. Rev. Lett. **117**, 096101 (2016).

Energy transfer between colloids via critical interactions

I. A. Martínez,^{1,2} C. Devailly,^{1,3} A. Petrosyan,¹ and S. Ciliberto¹

¹ *Laboratoire de Physique, École Normale Supérieure, CNRS, Lyon, France*

² *Departamento de Física Atómica, Molecular y Nuclear, Universidad Complutense de Madrid, GISG, Madrid, Spain*

³ *SUPA and School of Physics and Astronomy, University of Edinburgh, JCMB, Edinburgh, United Kingdom*

We report the observation of a temperature controlled synchronization of two Brownian particles which are inside a binary mixture close to the critical point of the demixing transition. The two beads are trapped by two optical tweezers whose distance is periodically modulated. We show that the motion synchronization of the two beads appears when the critical temperature is approached and that it is induced by the critical Casimir forces. Instead when the fluid is far from its critical temperature the motions of the two beads are uncorrelated. Small changes in temperature can radically change the global dynamics of the system. Finally, the measured energy transfers inside the system produced by the critical interaction are presented too.

[1] I. A. Martínez, C. Devailly, A. Petrosyan, and S. Ciliberto, *Entropy* **19**, 77 (2017).

Negative pressure amplification by precipitation in a confined droplet and consequences for paleotemperature reconstruction

E. Guillermin,^{1,2} V. Gardien,² and F. Caupin¹

¹ *Université Claude Bernard Lyon 1, CNRS, Institut Lumière Matière, Lyon, France*

² *Université Claude Bernard Lyon 1, CNRS, Laboratoire de Géologie de Lyon Terre, Planètes et Environnement, Villeurbanne, France*

Fluid inclusions are confined liquids entrapped in minerals. The study of their physico-chemical properties offers a wealth of information to geologists, such as chemistry of past oceans, sea surface temperatures, pressure-temperature conditions in the Earth's crust, to name but a few. As fluid inclusions are comprised in rather rigid compartments, they are assumed to be quasi-isochoric systems. For the physicist this constitutes a Berthelot tube. Upon cooling in a Berthelot tube, the liquid occupies a larger volume than it would at equilibrium with its vapor. A negative pressure develops, and the liquid is in a metastable state which ends when cavitation (the nucleation of vapor) occurs. Fluid inclusions are thus intriguing objects which have been used to study metastable water [1-4], and which exhibit peculiar thermodynamic properties such as superstability against cavitation [5].

Here we consider another phenomenon which arises when the liquid is a saturated aqueous solution. Because the saturated solute concentration is a function of temperature and pressure, part of the solute may precipitate out of solution upon cooling. This changes both the solution volume and its mass, modifying the pressure generated in the Berthelot tube. For sodium chloride solutions, we calculate that the actual pressure is 50 % more negative than without precipitation. We validate our analytic model using Brillouin spectroscopy on fluid inclusions in salt crystals. Our results have implications on the use of these fluid inclusions for reconstruction of past temperatures. The large negative pressures generated can damage the inclusions and yield inaccurate values for the past temperatures. We show how Brillouin spectroscopy solves this issue.

- [1] A. Q. Zheng, D. J. Durben, G. H. Wolf, and C. A. Angell, *Science* **254**, 829 (1991).
- [2] G. Pallares, M. El Mekki Azouzi, M. A. González, J. L. Aragones, J. L. F. Abascal, C. Valeriani, and F. Caupin, *Proc. Natl. Acad. Sci. USA* **111**, 7936 (2014).
- [3] G. Pallares, M. A. Gonzalez, J. L. F. Abascal, C. Valeriani, and F. Caupin, *Phys. Chem. Chem. Phys.* **18**, 5896 (2016).
- [4] C. Qiu, Y. Krüger, M. Wilke, D. Marti, J. Ricka, and M. Frenz, *Phys. Chem. Chem. Phys.* **18**, 28227 (2016).
- [5] D. Marti, Y. Krüger, D. Fleitmann, M. Frenz, and J. Ricka, *Fluid Phase Equilib.* **13**, 314 (2012).

Evaporation of salt solutions from droplets and thin liquid films

N. Shahidzadeh and D. Bonn

Institute of Physics, WZI- University of Amsterdam, Amsterdam, The Netherlands

In many applications such as the purification of pharmaceuticals, inkjet printing, coating applications, and salt creeping, crystallization happens in a confined volume of liquid, i.e., droplets and thin liquid films. This can occur because of solvent evaporation, temperature changes or chemical reactions which consequently lead to crystallization. Although the resulting deposition patterns have been much studied for evaporating droplets of colloidal suspensions (also known as the coffee stain effect), very few studies exist of evaporating salt solutions. This is surprising since in many cases water contains dissolved salts, and in addition the much-studied colloidal systems are usually considered to be models for atomic systems.

We have investigated the crystallization patterns of salt solutions in droplets and thin films during evaporation. Our results show a more complex behavior compare to stains reported for evaporating colloidal suspensions. This happens because during the solvent evaporation, the salts start to crystallize and grow during the drying process. We find that the evaporation at the edge of the contact line drives a capillary flow in the liquid which consequently increases the probability of nucleation and growth at this location. However, the final salt deposition pattern is mainly controlled by two parameters [1,2]: (i) the interfacial properties of the emerging crystal which determine whether the crystallization happens at the solid/liquid, at the liquid/vapor or in the bulk and (ii) the pathway of nucleation and growth (i.e. one step or two step nucleation process). The impact of these parameters in relation with the evaporation rate on the creeping motion of salts will be discussed. We also show how the control over the confinement of the ionic solutions by means of change of wetting properties of the substrate can be used in order to control the precipitation of different polymorphs of the same salt crystal [1].

[1] N. Shahidzadeh, M. Schut, J. Desarnaud, M. Prat, and D. Bonn, *Sci. Rep.* **5**, 10335 (2015).

[2] M. Qazi, D. Bonn, and N. Shahidzadeh, submitted (2017).

Dynamic flow of confined poly-electrolyte solutions: Interfacial friction and complex slip length

B. Cross,¹ C. Barraud,¹ F. Restagno,² L. Léger,² and E. Charlaix¹

¹ LiPHY, Université Grenoble Alpes, Grenoble, France

² Laboratoire de Physique des Solides, Université Paris Sud, Orsay, France

Flow of complex liquids are familiar and usefull. Unlike Newtonian fluids, they display complex bulk rheological behaviours. But the way they flow also involves their boundary conditions on solid surfaces. This is particularly relevant at small scales, such as for instance in bio-medical applications, industrial applications, oil engineering, etc.

In order to understand the interfacial dynamics of complex fluids it is of interest to probe scales bridging the bulk to the molecular scale. We report here the study of visco-elastic, confined poly-electrolyte solutions with a Dynamic Surface Force Apparatus. The device allows us to investigate the visco-elastic response of the material at a low shear rate, in a frequency domain from 10 Hz to 300 Hz under a tunable confinement ranging from the nanometer to 15 micrometers.

On this example we demonstrate that the notion of usual slip length which is used to describe and understand the interfacial dynamics of simple liquids, it not appropriate for visco-elastic liquids. We show that the appropriate description lies in the original Navier's condition of partial slip boundary condition, and the associated interfacial friction coefficient. The proper use of this original Navier's condition describes accurately the complex hydrodynamic force up to scales of tens of micrometers, with a simple linear friction coefficient, not depending on frequency, and closely related to the existence of depletion effects at the solid/solution interface.

Temperature dependence and thermal response of electric double layer capacitors

M. Janssen and R. van Roij

Institute for Theoretical Physics, Utrecht University, Utrecht, The Netherlands

Where surfaces of charged electrodes meet fluids that contain mobile ions, so-called electric double layers (EDLs) form to screen the electric surface charge by a diffuse cloud of counterionic charge in the fluid phase. This double layer is of paramount importance to many processes in physical chemistry, soft matter, as well as in electric double layer capacitors (EDLCs). With the ongoing development of nanomaterials, electrodes can nowadays be made from porous carbon with huge internal surface areas that often exceed $1000 \text{ m}^2/\text{g}$. Due to their high capacitance, EDLCs made from these materials are a prime candidate for capacitive energy storage, water desalination [1] and harvesting so-called “blue energy” from capacitive mixing of sea and river water [2, 3].

In this talk we discuss the intricate interplay between temperature and EDL characteristics, looking both at fundamental physics and at possible applications. First, we show that varying the electrolyte temperature (at fixed electrode potential) gives rise to a temperature-induced charge variation. This phenomenon can be exploited in thermodynamic charging cycles to (i) significantly enhance blue energy harvesting [4] and to (ii) create a “capacitive heat engine” [5]. Second, we discuss thermally insulated EDLCs where variation of the electrode potential gives rise to a charge-induced temperature variation [6]. We argue that this thermal response, the capacitive analogue of adiabatic heating-by-compression of a gas, contains information on electric double layer formation that has remained largely unexplored. In particular, we derive a thermodynamic identity for adiabatic-heating-by-charging that replaces an earlier approximative expression [7].

- [1] S. Porada, R. Zhao, A. Van Der Wal, V. Presser, and P. M. Biesheuvel, *Prog. Mater. Sci.* **58**, 1388 (2013).
- [2] D. Brogioli, *Phys. Rev. Lett.* **103**, 058501 (2009).
- [3] A. Härtel, M. Janssen, S. Samin, and R. van Roij, *J. Phys. Condens. Matter* **27**, 194129 (2015).
- [4] M. Janssen, A. Härtel, and R. van Roij, *Phys. Rev. Lett.* **113**, 268501 (2014).
- [5] A. Härtel, M. Janssen, D. Weingarth, V. Presser, and R. van Roij, *Energy Environ. Sci.* **8**, 2396 (2015).
- [6] J. Schiffer, D. Linzen, and D. U. Sauer, *J. Power Sources* **160**, 765 (2006).
- [7] M. Janssen and R. van Roij, *Phys. Rev. Lett.* accepted (2017).

Power-law electrokinetic behavior as a direct probe of effective surface viscosity

Y. Uematsu,^{1,2} R. R. Netz,² and D. J. Bonthuis²

¹ *Department of Chemistry, Kyushu University, Fukuoka, Japan*

² *Fachbereich Physik, Freie Universität Berlin, Berlin, Germany*

Electro-osmosis is the motion of an electrolyte solution induced by an electric field along a surface, whereas electrophoresis is the electric-field-induced motion of a colloid suspended in an electrolyte. These electrokinetic effects play important roles in industry and bio-systems. Originating in the nanometer-wide electric double layer, both effects depend sensitively on the structure and the dynamic properties of this interfacial layer at a charged surface [1, 2]. Simulation studies demonstrate that the surface layer exhibits an increased viscosity at hydrophilic surfaces [3]. At hydrophobic surfaces, however, a depletion layer and a finite slip length are observed, indicating a decreased effective viscosity [3]. The interfacial dielectric profile of water has been studied using molecular dynamics simulations, revealing a highly inhomogeneous and oscillating profile near the interface [4]. Whereas an effective interfacial dielectric constant can be readily obtained from capacitance measurements, experimental determination of the interfacial viscosity has been controversial.

The traditional model describing electro-osmosis and electrophoresis is based on the Poisson-Boltzmann and Stokes equations. However, this model fails to capture many experimental observations, such as the saturation of the electrokinetic flow with rising surface charge density [5]. We construct an exact solution and derive analytical asymptotic expressions for the electrokinetic flow beyond the linear theory [2]. With these expressions, information about the subnanometer-scale interfacial properties can be directly acquired from standard electrokinetic experiments. In particular, in the limit of strongly charged surfaces and low salinity, we obtain an analytical power-law relation for the magnitude of the electrokinetic flow as a function of the surface charge density [1]. Remarkably, the power-law exponent is determined by the interfacial dielectric constant and viscosity, the latter of which has eluded experimental determination so far. Our approach provides a novel method to extract the effective interfacial viscosity from standard electrokinetic experiments. We find good agreement between our theory and experimental data.

[1] Y. Uematsu, R. R. Netz, and D. J. Bonthuis, *Chem. Phys. Lett.* **670**, 11 (2017).

[2] D. J. Bonthuis, Y. Uematsu, and R. R. Netz, *Phil. Trans. R. Soc. A* **374**, 20150033 (2016).

[3] C. Sendner, D. Horinek, L. Bocquet, and R. R. Netz, *Langmuir* **25**, 10768 (2009).

[4] D. J. Bonthuis, S. Gekle, and R. R. Netz, *Phys. Rev. Lett.* **107**, 166102 (2011).

[5] J. Lyklema, *Colloid Surf. A* **92**, 41 (1994).

Diverging time scale in the dimensional crossover for liquids in strong confinement

S. Mandal and T. Franosch

Institut für Theoretische Physik, Universität Innsbruck, Innsbruck, Austria

We study a strongly interacting dense hard-sphere system confined between two parallel plates by event-driven molecular dynamics simulations to address the fundamental question of the nature of the 3D to 2D crossover. As the fluid becomes more and more confined the dynamics of the transverse and lateral degrees of freedom decouple [1, 2], which is accompanied by a diverging time scale separating 2D from 3D behavior [3]. Relying on the time-correlation function of the transversal kinetic energy the scaling behavior and its density-dependence is explored. Surprisingly, our simulations reveal that its timedependence becomes purely exponential such that memory effects can be ignored. We rationalize our findings quantitatively in terms of an analytic theory which becomes exact in the limit of strong confinement [3].

- [1] T. Franosch, S. Lang, and R. Schilling, Phys. Rev. Lett. **109**, 240601 (2012).
- [2] S. Lang, T. Franosch, and R. Schilling, J. Chem. Phys. **140**, 104506 (2014).
- [3] S. Mandal and T. Franosch, Phys. Rev. Lett. **118**, 065901 (2017).

Precise colloidal assemblies in emulsion droplets

M. Engel,¹ J. Wang,^{1, 2} and N. Vogel²

¹ *Institute for Multiscale Simulation, FAU Erlangen-Nuremberg, Erlangen, Germany*

² *Institute for Particle Technology, FAU Erlangen-Nuremberg, Erlangen, Germany*

Colloids assemble upon increase of volume fraction into crystals. Complex structures can be achieved by varying composition, interaction, or shape of the constituent colloidal particles [1, 2]. Another method to modify the crystallization process is to utilize interfacial effects resulting from the introduction of confinement. Recently it has been shown that entropy favors icosahedral symmetry for colloids assembling in spherical confinement [3]. In this joint experimental-theoretical work we use droplet-based microfluidics to create homogeneous emulsion droplets as sources for defined spherical confinement, which are then analyzed and understood using computer simulations. This allows to systematically explore the assembly behavior of clusters containing between 100 and 10000 near-monodisperse colloidal spheres. We observe a discrete series of multiply twinned colloid clusters with icosahedral symmetry. To understand and explain the formation of the clusters, we propose a geometric model and extract extremal principles.

[1] M. A. Boles, M. Engel, and D. V. Talapin, *Chem. Rev.* **116**, 11220 (2016).

[2] N. Vogel, M. Retsch, C. A. Fustin, A. del Campo, and U. Jonas, *Chem. Rev.* **115**, 6265 (2015).

[3] B. de Nijs, S. Dussi, F. Smalenburg, J.D. Meeldijk, D.J. Groenendijk, L. Filion, A. Imhof, A. van Blaaderen, and M. Dijkstra, *Nat. Mater.* **14**, 56 (2015).

Interactions between charged particles in like-charged polyelectrolyte solutions: Interplay between non-exponential double-layer and depletion forces

G. Trefalt, M. Moazzami-Gudarzi, T. Kremer, V. Valmacco, P. Maroni, and M. Borkovec

Department of Inorganic and Analytical Chemistry, University of Geneva, Geneva, Switzerland

Depletion forces between colloidal particles are entropically driven and arise from the exclusion of the depletants from the area between the large colloidal particles. The pioneering work of Asakura and Oosawa gave a first understanding of this mechanism [1]. When colloids and depletants are charged the electrostatic forces also contribute to the total interaction. The electrostatics give rise to the double-layer (DL) forces, which can become important in these systems and in contrast to the exponential profile typical for such forces, they decay non-exponentially. Furthermore, the DL and depletion forces are intimately linked since charged depletants also contribute to screening. We study this interplay of DL and depletion forces between negatively charged colloidal particles in the presence of anionic polyelectrolytes. Specifically, we use atomic force microscopy (AFM) to measure the interactions between negatively charged silica particles in the presence of sodium poly(styrene sulfonate) (NaPSS) [2]. The force profiles can be decomposed into two parts: DL contribution important close to the surface, and oscillatory depletion force prominent at larger distances. Superposition of mean-field Poisson-Boltzmann theory and damped oscillatory profile can be used to quantitatively describe the measured data. The atypical non-exponential shape of the DL forces in these systems is due to the exclusion of like-charged polymers from the vicinity of the surface. This exclusion of the polyelectrolytes is electrostatically driven and defines the thickness of the double-layer. From this thickness the phase of depletion oscillations can be predicted.

[1] S. Asakura and F. Oosawa, J. Chem. Phys. **22**, 1255 (1954).

[2] M. Moazzami-Gudarzi, T. Kremer, V. Valmacco, P. Maroni, M. Borkovec, and G. Trefalt, Phys. Rev. Lett. **117**, 088001 (2016).

Hofmeister series of wettability in mica-water-alkane systems

B. Bera, A. Cavalli, N. Kumar, M. H. G. Duits, I. Siratanu,
M. A. Cohen Stuart, and F. Mugele

*Physics of Complex Fluids, MESA+ Institute for Nanotechnology, University of Twente,
Enschede, The Netherlands*

The competitive wetting of water and oil on solid surfaces is important in many areas of science and technology, including environmental science, separation technology, and oil recovery. In most practically relevant situations, both the aqueous phase as well as the oil phase contain various solutes that play an important role for determining the wettability of the surface. Here we demonstrate that water on mica in ambient pure decane chosen as a simple model oil displays a wetting transition from complete water wetting to partial wetting depending on the type and concentration of the salt dissolved as well as the pH of the aqueous phase [1]. Like the stability of protein solutions and various other soft matter systems, the wettability of the system displays a strong dependence on the specific type of ions. Using contact angle goniometry we identify for chloride salts of various alkali and earth alkali metal a Hofmeister series of increasing tendency of cations to induce partial water wetting: $\text{Na}^+ < \text{K}^+ < \text{Li}^+ < \text{Rb}^+ < \text{Cs}^+ < \text{Ca}^{2+} < \text{Mg}^{2+} < \text{Ba}^{2+}$ [2]. Water contact angles are found to range from $< 1^\circ$ up to $\approx 15^\circ$. A quantitative model of the disjoining pressure based on standard DLVO theory including charge regulation [3] shows that the transition is primarily controlled by changes of the surface charge of the mica-water interface due to cation adsorption. Complementary Atomic Force Microscopy measurements indeed confirm that the wetting transition is accompanied for many cations by a reversal of the mica surface charge at concentrations of a few tens of mM. Very strongly hydrated Li^+ ions, however, demonstrate the relevance of competing short range hydration effects consistent with molecular dynamics simulations[4]. The addition of small amounts polar fatty acid molecules to the oil phase synergistically enhances the effect of adsorbing cations leading to contact angles up to 70° [5].

[1] F. Mugele et al., Sci. Rep. **5**, (2015).

[2] B. Bera et al., (submitted).

[3] A. Cavalli et al., Phys. Rev. E **93**, 4 (2016).

[4] N. Schwierz, D. Horinek, and R. R. Netz, Langmuir **29**, 2602 (2013).

[5] B. Bera et al., Soft Matter **12**, 4562 (2016).

Visco-elastic drag force and crossover from no-slip to slip boundary conditions for flow near an air-water interface

A. Maali, R. Boisgard, H. Chraïbi, Z. Zhang, H. Kellay, and A. Würger

LOMA, Université de Bordeaux & CNRS, Talence, France

The “free” water surface is generally prone to contamination with surface impurities be they surfactants, particles or other surface active agents. The presence of such impurities can modify flow boundary near such interfaces in a drastic manner. Here we show that vibrating a small sphere mounted on an AFM cantilever near a gas bubble immersed in water, is an excellent probe of surface contamination.

We present recent findings, both experimental and theoretical, on the viscoelastic response of “free” air-water interfaces, and a control experiment on an interface contaminated with 60 μM SDS.

Both *viscous* and *elastic* forces are exerted by an air-water interface on the vibrating sphere even when very low doses of contaminants are present. When varying the frequency ω of the driving force in the range from 50 to 400 Hz, we observe for the viscous drag force a cross-over from no-slip to slip boundary conditions; the elastic force first increases linearly with ω , passes through a maximum at some intermediate frequency, and then decreases with $1/\omega$.

The experimental data are quantitatively described by a theory based on forced advection of the surfactant with the lubrication flow between sphere and bubble. Since the impurity content is the only adjustable parameter, our experimental setup provides an efficient tool for evaluating the concentration of such surface impurities. For experimental parameters, diffusion of surfactant is negligible, both in the bulk and along the liquid interface. We discuss different regimes with respect to the surfactant Péclet number.

- [1] A. Maali, R. Boisgard, H. Chraïbi, Z. Zhang, H. Kellay, and A. Würger, Phys. Rev. Lett., in press (2017).

Hysteresis phenomena concerning wetting of surfaces with nanoscale defects

A. Giacomello,^{1,2} L. Schimmele,² M. Tasinkevych,^{2,4} and S. Dietrich^{2,3}

¹ *Dipartimento di Ingegneria Meccanica e Aerospaziale, Sapienza Università di Roma, Rome, Italy*

² *Max-Planck-Institut für Intelligente Systeme, Stuttgart, Germany*

³ *IV. Institut für Theoretische Physik, Universität Stuttgart, Stuttgart, Germany*

⁴ *Department of Materials Science and Engineering, Northwestern University, Evanston, IL, USA*

Ubiquitous imperfections of surfaces can alter the way liquids wet them, giving rise to a variety of hysteresis phenomena. At the three-phase contact line the effect of defects becomes apparent as contact angle hysteresis, for which Joanny and de Gennes formulated a macroscopic theory bridging the experimental observable to the defect strength [1]. Here we show via microscopic density functional calculations combined with the string method devised for the study of rare events how wetting hysteresis can emerge even for subnanometric defects [2]. The barriers for thermally activated defect crossing, the pinning force, and hysteresis are quantified and related to the geometry and chemistry of the defects allowing for the occurrence of nanoscopic effects, for which the macroscopic picture does not apply by rescaling.

While at the three-phase contact line defects bring about contact angle hysteresis, for submerged surfaces, they can give rise to superhydrophobicity: owing to capillary forces, microscopic bubbles may be trapped within surface roughnesses. This (technologically relevant) superhydrophobic state may collapse into the fully wet state. Since these two states are reportedly metastable over a broad range of pressure, strong hysteresis in the intrusion and extrusion of liquids on superhydrophobic surfaces ensues [3]. Here we investigate the conditions under which such hysteresis can be decreased, with the final aim of realizing robust superhydrophobicity [4]. Results show that by a combination of nanoscale roughness and hydrophobic coatings it is possible to completely prevent the full wetting of the rough surface thus achieving perpetual superhydrophobicity over a broad range of pressure.

In conclusion, in this work we attempt to relate different conspicuous hysteresis phenomena emerging in wetting to the characteristics of nanoscale surface defects [2, 4]. The theoretical approach offers insights both on the fundamental phenomena occurring at the nanoscales and to the possibilities of controlling the properties of surfaces.

- [1] J. F. Joanny and P. G. de Gennes, J. Chem. Phys. **81**, 552 (1984).
- [2] A. Giacomello, L. Schimmele, and S. Dietrich, Proc. Natl. Acad. Sci. USA **113**, E262 (2016).
- [3] A. Checcho, B. M. Ocko, A. Rahman, C. T. Black, M. Tasinkevych, A. Giacomello, and S. Dietrich, Phys. Rev. Lett. **112**, 216101 (2014).
- [4] A. Giacomello, L. Schimmele, S. Dietrich, and M. Tasinkevych, Soft Matter **12**, 8927 (2016).

Session 8: Supercooled Liquids, Glasses, Gels

Unveiling dimensionality dependence of glassy dynamics: 2D infinite fluctuation eclipses inherent structural relaxation

H. Shiba,¹ Y. Yamada,^{1,2} T. Kawasaki,³ and K. Kim⁴

¹ *Institute for Materials Research, Tohoku University, Sendai, Japan*

² *Beijing Computational Science Research Center, Beijing, China*

³ *Department of Physics, Nagoya University, Nagoya, Japan*

⁴ *Graduate School of Engineering Science, Osaka University, Osaka, Japan*

Dimensionality plays a key role in the physics of solids and liquids. Fluctuation shows up differently in different spatial dimensions, as typically observed in phase transitions. Two-dimensional (2D) crystalline solids often exhibit enhanced fluctuations that span an infinite length that induces long-wavelength structural correlations. A glassy system, on the other hand, lacks the crystalline order and endows the random liquid-like structure. As a consequence, structural (static) correlations cannot represent the dimensionality dependence. We need to look into dynamical aspects to clarify the dimensionality dependence of such systems.

In this presentation, we will show that fluctuation is dependent on the spatial dimensions, but the modality of inherent structural relaxation is similar between 2D and 3D [1]. Extensive simulations are performed for both a 2D binary mixture of 12th-core repulsive potential and a 3D binary mixture of Kob-Andersen-type Lennard-Jones potential, with up to 256,000 and 10,240,000 particles, respectively. We first clarify enhancement of 2D fluctuation taking place due to a mechanism similar to Mermin-Wagner theorem for a 2D crystal, by direct calculation of the Debye-asymptote of the vibrational density of states, which also accounts for enhanced fluctuation recently observed in 2D systems [2,3]. It leads to system-size dependent behavior of the estimated relaxation time and dynamic correlation length in the 2D system in terms of the density-based correlation functions. However, such size dependence is eliminated by introduction of an alternative correlator that characterizes relative rearrangement motions of the particles. Our results are also supported by recent experiments [4,5].

[1] H. Shiba, Y. Yamada, T. Kawasaki, and K. Kim, Phys. Rev. Lett. **117**, 245701 (2016).

[2] H. Shiba, T. Kawasaki, and A. Onuki, Phys. Rev. E **86**, 041504 (2012).

[3] E. Flenner and G. Szamel, Nat. Commun. **6**, 7392 (2015).

[4] S. Vivek, C. P. Kelleher, P. M. Chaikin, and E. R. Weeks, Proc. Natl. Acad. Sci. **114**, 1850 (2017).

[5] B. Illing, S. Frischi, H. Kaiser, C. Klix, G. Maret, and P. Keim, Proc. Natl. Acad. Sci. **114**, 1856 (2017).

Dynamical and structural signatures of the glass transition in emulsions

C. Zhang,¹ N. Gnan,^{2,3} T. G. Mason,⁴ E. Zaccarelli,^{2,3} and F. Scheffold¹

¹ *Department of Physics, University of Fribourg, Fribourg, Switzerland*

² *CNR-ISC UOS Sapienza, Rome, Italy*

³ *Department of Physics, Sapienza University of Rome, Rome, Italy*

⁴ *Department of Chemistry & Biochemistry and Department of Physics and Astronomy, University of California Los Angeles, Los Angeles, CA, USA*

We investigate structural and dynamical properties of moderately polydisperse emulsions across an extended range of droplet volume fractions φ , encompassing fluid and glassy states up to jamming. The finite polydispersity of our samples, beyond the known terminal polydispersity above which a single-phase crystallization can occur [1,2], differentiates our system from previous studies, because of the absence of the growth of locally crystalline regions. In this talk, we compare 3D fluorescent microscopy measurements with numerical simulations. For the experimental part of the study we developed a refractive index and buoyancy matched micronscale emulsion system that is also fluorescently labelled [2]. In the current context, below the jamming point, the emulsion droplets behave as hard spheres, since the droplet deformation due to thermal fluctuations is negligible [1]. A key advantage of using such a well characterized emulsion system is the possibility to reversibly jam the system and thus access any state point at and below the jamming point with an absolute accuracy of φ -values better than 0.5% and a statistical error better than 0.3%, which we believe is unprecedented.

In our study we identify multiple signatures of the glass transition, analyzing both dynamical and structural quantities, highlighting a connection between the dynamic slowing down and growing dynamical and structural correlation lengths. First we show that when φ approaches the glass transition volume fraction φ_g , dynamical heterogeneities and amorphous order arise within the emulsion. In particular, we find an increasing number of clusters of particles having five-fold symmetry (i.e. the so-called locally favoured structures, LFS) as φ approaches φ_g , saturating to a roughly constant value in the glassy regime. However, contrary to previous studies, we do not observe a corresponding growth of medium-range crystalline order; instead, the emergence of LFS is decoupled from the appearance of more ordered regions in our system. We also find that the static correlation lengths associated with the LFS and with the fastest particles can be successfully related to the relaxation time of the system. By contrast, this does not hold for the length

associated with the orientational order. Our study reveals the existence of a link between dynamics and structure close to the glass transition even in the absence of crystalline precursors or crystallization. Furthermore, the quantitative agreement between our confocal microscopy experiments and Brownian dynamics simulations suggests that emulsions are very important model systems for the investigation of the glass transition and beyond.

- [1] C. Zhang, N. Gnan, T. G. Mason, E. Zaccarelli, and F. Scheffold, *J. Stat. Mech.-Theory E*, **2016**, 094003 (2016).
- [6] E. Zaccarelli, C. Valeriani, E. Sanz, W. C. K. Poon, M. E. Cates, and P. N. Pusey, *Phys. Rev. Lett.* **103**, 135704 (2009).

Structure and dynamics in glassy nanoparticles

W. Qi^{1,2} and R. K. Bowles¹

¹ *Department of Chemistry, University of Saskatchewan, Saskatoon, Canada*

² *Department of Mathematics and Statistics, University of Guelph, Guelph, Canada*

Molecular simulation is used to study the relationship between dynamics and structure in glassy nanoparticles formed by binary Lennard–Jones mixtures. We find the glass transition temperature, T_g , of these nanoparticles is significantly depressed relative to the bulk liquid and decreases further with decreasing nanoparticle size, which helps us to explore the dynamics of the liquid phase to low temperatures. Measurements of the structural relaxation time, τ_α , obtained from the intermediate scattering function, show that relaxation dynamics within the nanoparticles are inhomogeneous with the core becoming glassy above the nanoparticle T_g while the surface remains mobile at temperatures below T_g . Our work also reveals the presence of a crossover from fragile to strong liquid behaviour as the nanoparticles are cooled. An analysis of the local structure within the particles using Voronoi polyhedra shows that, like ultrastable glassy films formed through vapour deposition [1,2], the stability of the supercooled glass nanoparticles is characterised by a large, increasing fraction of bicapped square anti-prism motifs with Voronoi index (0; 2; 8; 0) [3]. Furthermore, we show that a structural length scale defined in terms of the radius of gyration of clusters of (0; 2; 8; 0) polyhedra grows as a power law, along with the increasing relaxation time, in the fragile liquid region. However, the scaling breaks down at the fragile-strong liquid crossover temperature.

[1] S. Singh, M. D. Ediger, and J. J. de Pablo, *Nat. Mater.* **12**, 139 (2013).

[2] I. Lyubimov, M. D. Ediger, and J. J. de Pablo, *J. Chem. Phys.* **139**, 144505 (2013).

[3] W. Qi and R. K. Bowles, *ACS Nano* **10**, 3416 (2016).

Emergence of long-ranged strain and stress correlations at the glass transition

M. Fuchs,¹ P. Keim,¹ and A. Zippelius²

¹ *Fachbereich Physik, Universität Konstanz, Konstanz, Germany*

² *Institut für Theoretische Physik, Georg-August-Universität Göttingen, Göttingen, Germany*

Strain and stress correlations are long-ranged in solids, while they fall-off rapidly in liquids. The emergence of rigidity at the glass transition thus requires the build-up of long-ranged spatial correlations. We report on recent measurements in colloidal dispersions and results from mode coupling theory for stresses and strains in supercooled liquids near their glass transition.

The strains reveal unexpected phenomena [1]. The shear strain correlation function $C_{xy}(\mathbf{r}, t)$ shows a $\cos(4\theta)/r^2$ symmetry, characteristic for elastic response, even in liquids at times longer than their structural relaxation time τ .

We present a mode-coupling theory for the strain correlation functions in supercooled liquids and data from video microscopy of a two-dimensional colloidal glass former [2]. The theory explains the emergence of rigidity and the existence of a well defined displacement field in glass [3]. Additionally, it provides an explanation for the occurrence of long-ranged strain-signatures in $C_{xy}(\mathbf{r}, t)$ of supercooled liquids at times t when density and shear stress fluctuations have already decayed to zero. The analysis of the video microscopy data provides the first experimental verification of these long-ranged strain fields in a supercooled liquid. Next we analyze the tensor of stress correlation functions in the supercooled liquid [4].

The crossover between viscous and elastic behavior is characterized by a rigidity length L , which increases together with the viscosity upon cooling. In a glass state, the transversal stress correlator develops a non-analytical structure for small wavevectors which links to the strain correlations according to a Hookian relation.

[1] J. Chattoraj and A. Lemaître, Phys. Rev. Lett. **111**, 066001 (2013).

[2] B. Illing, S. Fritschi, D. Hajnal, C. Klix, P. Keim, and M. Fuchs, Phys. Rev. Lett. **117**, 208002 (2016).

[3] C. Klix, F. Ebert, F. Weysser, M. Fuchs, G. Maret, and P. Keim, Phys. Rev. Lett. **109**, 178301 (2012).

[4] M. Maier, A. Zippelius, and M. Fuchs, in preparation (2017).

Catching up with experiments: Equilibrium simulations of supercooled liquids beyond laboratory time scales

D. Coslovich, L. Berthier, A. Ninarello, and M. Ozawa

Laboratoire Charles Coulomb, University of Montpellier, Montpellier, France

Computer simulations give precious insight into the microscopic behavior of disordered and amorphous materials, but their typical time scales are orders of magnitude shorter than the experimentally relevant ones. In particular, simulations of supercooled liquids cover at most 4-5 decades of viscous slowing down, which falls far short of the 13 decades commonly accessible in experimental studies. We close this enormous gap for a class of realistic models of liquids, which we successfully equilibrate beyond laboratory time scales by means of the swap Monte Carlo algorithm [1]. We show that combined optimization of selected features of the interaction potential, such as particle softness, polydispersity and non-additivity, leads to computer models with excellent glass-forming ability [2]. For such models, we achieve over 10 orders of magnitude speedup in equilibration time scale. This numerical advance allows us to address some outstanding questions concerning glass formation, such as the role of local structure and the relevance of an entropy crisis, in a dynamical range that remains inaccessible in experiments. Our results support the view that non-trivial static correlations continue to build up steadily in supercooled liquids even below the laboratory glass temperature.

[1] L. Berthier, D. Coslovich, A. Ninarello, and M. Ozawa, Phys. Rev. Lett. **116**, 238002 (2016).

[2] A. Ninarello, L. Berthier, and D. Coslovich, submitted (2017).

A biocompatible re-entrant DNA hydrogel

F. Bomboi,^{1,2} F. Romano,³ M. Leo,⁴ J. Fernandez-Castanon,² R. Cerbino,⁵ T. Bellini,⁵ F. Bordi,^{1,2} P. Filetici,⁶ and F. Sciortino^{1,2}

¹ ISC–CNR, Sapienza Università di Roma, Rome, Italy

² Dipartimento di Fisica, Sapienza Università di Roma, Rome, Italy

³ Dipartimento di Scienze Molecolari e Nanosistemi, Università Ca' Foscari di Venezia, Venezia Mestre, Italy

⁴ Dipartimento di Biologia e Biotecnologie C. Darwin, Sapienza Università di Roma, Rome, Italy

⁵ Dipartimento di Biotecnologie Mediche e Medicina Traslazionale, Università degli Studi di Milano, Segrate (MI), Italy

⁶ IBPM-CNR, Sapienza Università di Roma, Rome, Italy

After N. Seeman's pioneering intuition [1], DNA has rapidly become a key element in the development of novel materials based on its ability to self-assemble, in a controlled fashion, into supramolecular nanometric structures, which act as functional building blocks. Here we demonstrate the successful realization of an innovative material, a biocompatible and thermo-reversible DNA hydrogel, able to melt both on heating and on cooling [2], created by exploiting competitive interactions encoded in smartly designed DNA sequences. To reach this goal, we have focussed on a system, recently proposed in a theoretical work [3], consisting of a binary mixture of tetravalent (A) and monovalent (B) patchy particles, in which the competition between two different bonding possibilities (AA vs. AB bonds) leads to an unconventional phase behaviour. In this model, the relative strength of the AA and AB interactions determines the low temperature structure of the system: either a spanning network of AA bonds (a gel) either a fluid of diffusing AB₄ clusters (in which four B particles saturate all the bonding sites of particle A). This system shows a Safran's like re-entrant phase diagram [4], arising from the competition of the two possible bonding arrangements which generates upon cooling a transition from fluid to gel to fluid again, suggesting the possibility to create a material that can be hardened by heating. To move from the theoretical predictions to the experimental realization of this material, we exploited the addressability of DNA binding sites. Specifically, we used a mixture of tetravalent DNA nanostars (mimicking the A patchy particles) and monovalent single-stranded DNA sequences (B particles) to recreate in the laboratory the theoretical model. Our experimental results confirm that the relaxation time of the system, obtained via dynamic light scattering, slows down dramatically only in a restricted range of temperatures and that the phase diagram displays the expected re-entrant shape. We will thus present the aforementioned results and discuss how it is possible to create biocompatible

and fully thermo-reversible materials with uncommon phase diagrams and tailored properties by rationally enciphering into the DNA sequences not only the shape of the resulting particles but also the physics of the desired collective behaviour.

- [1] N. Seeman, *Nature* **421**, 427 (2003).
- [2] F. Bomboi, F. Romano, M. Leo, J. Fernandez-Castanon, R. Cerbino, T. Bellini, F. Bordi, P. Filetici, and F. Sciortino, *Nat. Commun.* **7**, 13191 (2016).
- [3] S. Roldàn-Vargas, F. Smallenburg, W. Kob, and F. Sciortino, *Sci. Rep.* **3**, 2451 (2013).
- [4] T. Tlusty and S. A. Safran, *Science* **290**, 1328 (2000).

Interplay of coarsening and aging impacting the mechanical properties of a colloidal gel

V. Trappe,¹ D. C. E. Calzolari,¹ I. Bischofberger,^{1,2} and F. Nazzani¹

¹ *Department of Physics, University of Fribourg, Fribourg, Switzerland*

² *Department of Mechanical Engineering, Massachusetts Institute of Technology, Cambridge, MA, USA*

We explore the dynamical and mechanical characteristics of an evolving gel, aiming to assess how the gel evolution impacts the creep response of the system. Our gel is formed by inducing the aggregation of thermosensitive colloids via a temperature quench. We find experimental evidence that the evolution of this gel is due to two distinct processes: a coarsening process that involves the incorporation of mobile particles into the network structure and an aging process that triggers intermittent large-scale rearrangements. While coarsening is the main process governing the evolution of the elastic properties of the gel, aging is the process determining the structural relaxation. The combination of both processes governs the creep behavior of the gel, a creep behavior that is determined by three distinct contributions: an instantaneous elastic, a delayed elastic and a loss contribution. The systematic investigation of these contributions along the creep profile allows for the conclusion that, upon approach of the yield stress, the rate of intermittent rearrangement events remains essentially unchanged, while the size of the restructured zones per event increases.

Correlation between dynamical and structural heterogeneities in metastable hard-sphere fluids

S. Golde¹ and H. J. Schöpe²

¹ PA Consulting Group GmbH, Frankfurt, Germany

² Institut für angewandte Physik, Eberhards Karls Universität Tübingen, Tübingen, Germany

A metastable fluid can either crystallize or vitrify. Crystallization and vitrification are the most fundamental non-equilibrium phenomena universal to a variety of materials. A unified understanding of solidification in view of the two competitive processes of crystallization and vitrification is still a great challenge.

A metastable fluid is not homogeneous and isotropic rather it is heterogeneous concerning structure and dynamics [1]. These heterogeneities refer to the appearance of spatially correlated domains of mobile and immobile particles as the temperature crosses the freezing temperature and approaches the glass transition temperature T_{GT} . Dynamical and structural heterogeneities have been proposed to play a key role in understanding crystallization and vitrification [2].

Theses heterogeneities are here studied by a novel and unique combination of dynamic and static light scattering techniques on the simplest model system showing crystallization and vitrification, the colloidal hard-sphere system. This allows us for the first time to quantify and correlate the temporal evolution of the amount of pronouncedly ordered clusters and the amount of slow particles [3]. Our analysis shows that their closely related temporal evolution may contribute to a more unified understanding of the correlation between the two competitive processes of crystallization and vitrification.

[1] L. Berthier and G. Biroli, Rev. Mod. Phys. **83**, 587 (2011).

[2] J. Taffs, S. R. Williams, H. Tanaka, and C. P. Royall, Soft Matter **9**, 297 (2013).

[3] S. Golde, T. Palberg, and H. J. Schöpe, Nat. Phys. **12**, 712 (2016).

Fluid flow speeds up the gravitational collapse of colloidal gels

J. de Graaf,¹ X. Zhou,¹ W. C. K. Poon,¹ and M. Hermes¹

¹ *School of Physics and Astronomy, University of Edinburgh, Edinburgh, United Kingdom*

Colloidal gels have a wide range of application, e.g., personal care products, pesticides, and oil-drilling muds. Such gels consist of solid particles that form a system-spanning, stress-bearing network, which is able to hold the gel up against gravity, when there is a mismatch between the density of the liquid and solid phase. However, the gel is intrinsically unstable and will eventually collapse under the influence of gravity. Understanding this process from a fundamental perspective offers opportunities for improving the stability of colloidal gels.

In this presentation, we study the collapse of a model colloidal gel using lattice-Boltzmann (LB) simulations to explain recent experimental observations of a fast collapse regime [1]. We first demonstrate that including fluid flow using the LB algorithm leads to the formation of thicker and stronger gels in the absence of gravity, compared to simulations where hydrodynamic and hydrostatic effects are not accounted for. This result is similar to that of Refs. [2,3] and thus gives confidence in our method. We then go beyond the formation process and show that including fluid flow significantly speeds up gel collapse, by a factor that is comparable to the one found in our recent experiments. We further relate the resistance of the gel against gravity to the gravitational Péclet number of the particles. Finally, we demonstrate that introducing hydrodynamics in the simulation can also reproduce the presence of volcano-like objects at the interface between the gel and liquid, as observed in the experiment.

Our analysis shows the importance of hydrodynamic interactions to the dynamic properties of colloidal gels and provides new understanding that has strong implications for improving real-world applications of gels.

- [1] R. Harich, T. W. Blythe, M. Hermes, E. Zaccarelli, A. J. Sederman, L. F. Gladden, and W. C. K. Poon, *Soft Matter* **12**, 4300 (2016).
- [2] Z. Varga, G. Wang, and J. Swan, *Soft Matter* **11**, 9009 (2015).
- [3] Z. Varga and J. Swan, *Soft Matter* **12**, 7670 (2016).

Temporarily arrested state in protein solutions studied using ultra-small angle X-ray scattering (USAXS)

S. Da Vela,¹ M. K. Braun,¹ J. Möller,² F. Zhang,¹ and F. Schreiber¹

¹ *Institut für Angewandte Physik, Universität Tübingen, Tübingen, Germany*

² *ESRF, Grenoble, France*

The interplay of liquid-liquid phase separation (LLPS) with the glass transition is a potential route to the formation of arrested states in colloidal and protein systems [1,2]. Previous studies have shown that the kinetics of the spinodal decomposition of such systems strongly depend on the quench depths: a shallow quench leads to a complete LLPS, an intermediate quench may result in a dynamic arrested state, and a deep quench ends up with a homogenous attractive glass state. However, many details regarding the interplay between LLPS and glass transition and their responses to the subtle changes of the quench depth are still not fully understood.

In our work, we have employed the USAXS technique which became available only recently with sufficient q range, to study the kinetics of LLPS and arrested state in protein systems with a high temporal and spatial resolution. The two protein systems studied were bovine γ -globulin in the presence of PEG1k, featuring an upper critical solution temperature (UCST) phase behavior, and bovine serum albumin with YCl_3 , featuring a lower critical solution temperature (LCST) phase behavior [3-5]. For both systems, the time evolution of the characteristic length (ξ) during phase separation was followed by USAXS over a broad range of time scales. The growth kinetics of ξ for shallow quenches was found to follow the classical coarsening kinetics with $\xi \sim t^{1/3}$. For deep quenches, a fully arrested state was obtained [5]. Interestingly, for intermediate quenches, we observed an unusual three-stage coarsening process: initially, the growth follows $\xi \sim t^{1/3}$, followed by a significant slow-down. After a short time, the coarsening accelerates again with $\xi \sim t^{1/3}$. We consider the state of the system following this type of kinetics as a temporarily arrested state. We interpret the finding in the light of simulations and experimental results on colloidal systems. The temporary nature of the arrested state is most likely due to the asymmetric quench. In this case, the minority phase is the dilute phase, which can still coarsen through the glassy majority phase.

[1] P. J. Lu, E. Zaccarelli, F. Ciulla, A. B. Schofield, F. Sciortino, and D. A. Weitz, *Nature* **453**, 499 (2008).

- [2] F. Cardinaux, T. Gibaud, A. Strander, and P. Schurtenberger, *Phys. Rev. Lett.* **99**, 118301 (2007).
- [3] F. Zhang, M. W. A. Skoda, R. M. J. Jacobs, S. Zorn, R. A. Martin, C. M. Martin, G. F. Clark, S. Weggler, A. Hildebrandt, O. Kohlbacher, and F. Schreiber, *Phys. Rev. Lett.* **101**, 148101 (2008).
- [4] O. Matsarskaia, M. K. Braun, F. Roosen-Runge, M. Wolf, F. Zhang, R. Roth, and F. Schreiber, *J. Phys. Chem. B* **120**, 7731 (2016).
- [5] S. Da Vela, M. K. Braun, A. Doerr, A. Greco, J. Mueller, Z. Fu, F. Zhang, and F. Schreiber, *Soft Matter* **12**, 9334 (2016).

Session 9: Driven Systems, Rheology, Nanofluidics

Nonlinear microrheological response to a step force

S. Leitmann,¹ S. Mandal,¹ M. Fuchs,² A. M. Puertas,³ and T. Franosch³

¹ *Institut für Theoretische Physik, Universität Innsbruck, Innsbruck, Austria*

² *Fachbereich Physik, Universität Konstanz, Konstanz, Germany*

³ *Group of Complex Fluids Physics, Departamento de Física Aplicada, Universidad de Almería, Almería, Spain*

In a microrheological experiment the thermal or forced motion of a colloidal particle is monitored to obtain information on mechanical properties of the surroundings [1]. While the linear response is well-characterized in terms of the fluctuation-dissipation theorem, few exact results are available for strong driving.

Here we consider the time-dependent velocity of a colloidal particle immersed in a dilute suspension of hard spheres in response to switching on a finite constant force at zero time. Our main quantity of interest is the time-dependent mobility and its approach to the stationary state mobility.

A stationary state solution for the mobility exact in first order of the packing fraction has been established earlier in terms of a power-series expansion in the force on the tracer particle [2]. We extend this results to the case of arbitrarily strong driving including the complete time-dependence of the response upon switching on the force. In the stationary state, our analytic solution recovers the anticipated limit for strong driving [2] and captures the nonlinear response in first order of the packing fraction for any strength of the force. Next, we consider the time-dependent response of the tracer and monitor the transition to the stationary state. In particular, we show that at finite times the response is an analytic function of the driving, but displays singular behavior for infinite times. The noncommutativity of the limits for vanishing driving and large times is traced back to the longtime tail in the velocity-autocorrelation function due to repeated encounters of the tracer with the same colloid. This scenario is strongly reminiscent of the nonlinear response of a driven particle in the lattice Lorentz model with frozen obstacles [3], and corroborates that in comparison to the linear response the time-dependent behavior becomes qualitatively different at long times even for arbitrarily small driving.

In the driven lattice Lorentz gas, the fluctuations of the tracer displacement along the force show a superdiffusive growth at intermediate times [4]. Such superdiffusively growing fluctuations have first been elaborated in computer

simulations of active microrheology [5] and one may anticipate a similar scenario in a dilute suspension of hard spheres.

- [1] T. M. Squires and T. G. Mason, *Annu. Rev. Fluid Mech.* **42**, 413 (2010).
- [2] T. M. Squires and J. F. Brady, *Phys. Fluids* **17**, 073101 (2005).
- [3] S. Leitmann and T. Franosch, *Phys. Rev. Lett.* **111**, 190603 (2013).
- [4] S. Leitmann and T. Franosch, *Phys. Rev. Lett.* **118**, 018001 (2017).
- [5] D. Winter, J. Horbach, P. Virnau, and K. Binder, *Phys. Rev. Lett.* **108**, 028303 (2012).

Nanoscale dynamics versus surface interactions: What dictates osmotic transport?

C. Lee,¹ C. Cottin-Bizonne,² R. Fulcrand,² L. Joly,² and C. Ybert²

¹ *Department of Mechanical Engineering, Kyung Hee University, Yongin, Korea*

² *Université Claude Bernard Lyon 1, CNRS, Institut Lumière Matière, Villeurbanne, France*

Osmotic effects refer to liquid (often water) flow between two regions with different salinity, driven by the presence of interfaces. Usually, these interfaces correspond to the walls of a porous medium – a membrane – connecting two liquid reservoirs. Osmotic effects play a key role in living systems, in sustainable energies (with for instance the “blue energy” systems), or in water treatment and desalination processes.

The classical paradigm for osmotic transport has long related the induced-flow direction to the solute membrane interactions, with the low-to-high concentration flow a direct consequence of the solute rejection from the semipermeable membrane. In principle, the same was thought to occur for the newly demonstrated membrane-free osmotic transport named diffusio-osmosis [1].

Combining nanofluidic experiments and simulations at the atomic scale, we revisit here this cornerstone of osmotic transport by studying the diffusio-osmotic flows generated at silica surfaces by either poly(ethylene)glycol polymers or ethanol molecules in aqueous solutions. Strikingly, we show that the standard description based on liquid-wall interactions can fail to describe the mere direction of osmotic flows [2].

Considering theoretically and numerically the intricate nature of the osmotic response that combines molecular-scale surface interaction and near-wall dynamics, these findings are rationalized within a generalized framework for osmotic transport. This better microscopic knowledge of osmotic effects paves the way for the development of new functionalities or for the optimization of performance in various fields going from sustainable energies to active matter.

[1] C. Lee, C. Cottin-Bizonne, A.-L. Biance, P. Joseph, L. Bocquet, and C. Ybert, *Phys. Rev. Lett.* **112**, 244501 (2014).

[2] C. Lee, C. Cottin-Bizonne, R. Fulcrand, L. Joly, and C. Ybert, *J. Phys. Chem. Lett.* **8**, 478 (2017).

The role of intercrystalline tie chains on plastic deformation of semicrystalline polymers

S. Jabbari-Farouji,¹ O. Lame,² J. Rottler,³ M. Perez,² and J.-L. Barrat⁴

¹*Institut für Physik, Johannes Gutenberg-Universität, Mainz, Mainz, Germany*

²*University of Lyon, INSA, MATEIS, Villeurbanne, France*

³*The University of British Columbia, Vancouver, Canada*

⁴*Université Grenoble Alpes, LIPHY, Grenoble, France*

The mechanical properties of polymeric materials strongly depend on their morphology and spatial arrangements. Solid-like polymers obtained from cooling of dense polymer melts are found in amorphous or semicrystalline states depending on the cooling-rate. Semicrystalline polymers, composed of ordered and amorphous regions, are of great technological interest as they combine the strength of purely crystalline materials with the strain-hardening feature of purely amorphous polymers.

We study the tensile response of semicrystalline polymers of a semiflexible bead-spring polymer model [1] via molecular dynamics simulations. By investigating the structural evolution of amorphous and crystalline regions, we provide a microscopic insight into the underlying mechanisms of plastic deformation [2, 3]. Particularly, we quantify the affinity of deformation by computing the microscopic stretch ratio of the polymers. We discuss the effect of chain length, crystallinity degree [2] and the entangled network of intercrystalline tie chains on the elastic and strain-hardening moduli of semicrystalline polymers [4].

[1] H. Meyer and F. Muller-Plathe, J. Chem. Phys. **115**, 7807 (2001).

[2] S. Jabbari-Farouji, J. Rottler, M. Perez, O. Lame, A. Makke, and J.-L. Barrat, ACS Macro Lett. **4**, 147 (2015).

[3] S. Jabbari-Farouji, J. Rottler, M. Perez, O. Lame, A. Makke, and J.-L. Barrat, J. Phys. Condens. Matter **27**, 194131 (2015).

[4] S. Jabbari-Farouji, O. Lame, J. Rottler, M. Perez, and J.-L. Barrat, under review.

Non-equilibrium separation: From biomimetic kidney-on-a-chip to active sieving

S. Marbach and L. Bocquet

Laboratoire de Physique Statistique, Ecole Normale Supérieure, PSL Research University, Paris, France

Filtering specific molecules is a challenge faced for several vital needs: from biomedical applications like dialysis to the intensive production of clean water. The domain has been boosted over the last decades by the possibilities offered by nanoscale materials, such as graphene or advanced membranes [1]. Filtration is however always designed according to an underlying sieving perspective: A membrane with small and properly decorated pores allows for the selection of the targeted molecules. This inevitably impedes the flux and transport, making separation processes costly in terms of energy.

Here we investigate two radically different approaches to separation and filtration.

First, we explore the filtering strategy of the human kidney. Building on a minimal model, we show that this separation device operates at a remarkably small energy cost as compared to traditional sieving processes. We show that this unique energetic efficiency originates in the serpentine geometry of the nephron – the central part of the kidney - which operates as an active osmotic exchanger [2].

Second, we explore the possibility of non-equilibrium sieving, harnessing the difference in the molecular dynamics of particles to separate them across nanopores. We investigate a simplified model for an "active pore", where gating is dynamically controlled, and mimic to some extent a minimal Maxwell demon process. Being analytically solvable, this model points to a rich variety of behaviors in terms of dynamical selectivity, and unravels the basic principles of active sieving [3].

These principles could be readily mimicked based on existing technologies to build artificial dialysis devices or alternatives for advanced water recycling.

[1] J. Werber, C. Osuji, and M. Elimelech, *Nat. Rev. Mater.* **1**, 16018 (2016).

[2] S. Marbach and L. Bocquet, *Phys. Rev. X* **6**, 031008 (2016).

[3] S. Marbach and L. Bocquet, submitted.

Liquid filled hourglass

N. Bremond, L. Rolland, J. Baudry, and J. Bibette

Laboratoire Colloïdes et Matériaux Divisés, Chemistry Biology & Innovation, ESPCI Paris, PSL Research University, Paris, France

An hourglass is a nice illustration of the complex feature of granular matter that exhibits a solid/liquid/gas like behavior depending on the level of the imposed stress [1,2]. Indeed, in contrast to a viscous fluid, the flow rate of particles through a bottleneck under gravity is constant, i.e. independent of the height of the granular medium. This peculiar behavior is a signature of solid friction. We revisit this well known phenomenon with particles composed of a hydrogel shell surrounding a liquid core and which are dispersed in water. Like for a classical hourglass, a constant flow rate of particles is observed. Moreover, the friction between particles and with the solid wall of the container can be tuned by adding surfactants into the continuous phase. The angle of repose can even tend to zero. Surprisingly, lowering friction does not influence the rate of discharge. The flow rate also follows the Bavelas scaling law that depends on the aperture size [2]. We rationalize these observations by making an analogy between the fluidization of the granular bed at the bottleneck due to the counter flow and the sedimentation of a suspension inside a tube having the same inner diameter. The law that links the particle settling velocity to the solid volume fraction leads to a maximum mass flow rate that depends on the tube diameter. The corresponding hourglass's flow rate converges to this maximum flow rate.

[1] P. Jop, Y. Forterre, and O. Pouliquen, *Nature* **441**, 727 (2006).

[2] L. Staron, P.-Y. Lagrée, and S. Popinet, *Phys. Fluids* **24**, 103301 (2012).

Onset of non-Newtonian viscosity in a DNA transient network

G. Nava,¹ T. Yang,² V. Vitali,² P. Minzioni,² F. Bragheri,³ R. Osellame,³ and T. Bellini¹

¹ *Department of Medical Biotechnology and Translational Medicine, Università di Milano, Milano, Italy*

² *Department of Information and Industrial Engineering, Università di Pavia, Pavia, Italy*

³ *Istituto di Fotonica e Nanotecnologie (IFN-CNR), Politecnico di Milano, Milano, Italy*

We present a thorough investigation of the thermodynamic and viscous properties of a model gel based on DNA colloids whose interaction strength, coordination number, network topology, and phase diagram are fully known. This system is based on DNA particles shaped as nano-stars (NS) interacting tip-to-tip via Watson-Crick pairing. At concentrations corresponding to less than 1% volume fraction, this system undergoes, in a temperature (T) range of 20°C, a continuous and reversible gelation transition with features analogous to the kinetic arrest of strong glass forming liquids [1,2].

We have investigated the rheological properties of this system, and in particular the onset of non-Newtonian viscosity by exploiting a novel microfluidic-based optical shooting technique. In a custom made optofluidic chip, two facing waveguides written via laser inscription technique can deliver a controlled optical force to a 5 μm PMMA bead and “shoot” it across the microchannel [3]. The motion of the bead under a controlled force profile reveals the effective viscosity at the different T and, in particular, through the continuous transition to a gel state. At higher T the system shows, as expected, Newtonian viscosity. Upon lowering T , the stabilization of the network and the strengthening of its bonds has an enormous effect on the viscosity, that sharply increases and acquires a power-law shear-thinning dependence on bead velocity. We demonstrate that the whole viscous behavior can be described through a universal curve dependent on dimensionless reduced quantities, which in turn depend solely on the bond lifetime, as independently measured by dynamic light scattering. This behavior can be understood on the basis of simple models which rely on the detailed knowledge of this simple DNA network topology and interaction strength.

Our results offer new understanding of the rheological behavior of transient networks in complex fluids and of network-forming liquids close to their glass transition.

- [1] S. Biffi, R. Cerbino, G. Nava, F. Bomboi, F. Sciortino, and T. Bellini, *Soft Matter* **11**, 3132 (2015).
- [2] S. Biffi, R. Cerbino, F. Bomboi, E. M. Paraboschi, R. Asselta, F. Sciortino, and T. Bellini, *Proc. Natl. Acad. Sci. USA* **110**, 15633 (2013).
- [3] T. Yang, F. Bragheri, G. Nava, I. Chiodi, C. Mondello, R. Osellame, K. Berg-Sørensen, I. Cristiani, and P. Minzioni, *Sci. Rep.* **6**, 23946 (2016).

Session 10: Active Matter

Interactions of chemical microswimmers with microscale objects

J. Simmchen,^{1,2} J. Katuri,^{1,3} W. E. Uspal,¹ M. Popescu,¹ and S. Sánchez^{1,3}

¹ *Physical Chemistry, TU Dresden, Dresden, Germany*

² *MPI for Intelligent Systems, Stuttgart, Germany*

³ *Institute for Bioengineering of Catalonia (IBEC), Barcelona, Spain*

Catalytic microswimmers developed into a broad, interdisciplinary field of science during the last decades with catalytic Janus particles as one of the most studied types of micromotors due to their simple geometry that offers a well defined interface to join theory and experiment.

The interaction of Janus microswimmers with substrates and other microscale objects that they might encounter in their path is influenced by many factors from hydrodynamic interactions, gravity and phoretics. Previously we presented a guiding method based on step-like submicrometre topographical features, engineered through a photo-lithography based process and thin film deposition [1]. The Janus particles reliably dock on sub-micron sized steps based on their phoretic and hydrodynamic interactions and move along the edges for significantly long times, which systematically increase with fuel concentration. Using especially engineered system this principle can be used to develop autonomous devices at the micron-scale [2] and we extend those studies to different microobjects.

[1] J. Simmchen, J. Katuri, W. E. Uspal, M. N. Popescu, M. Tasinkevych, and S. Sanchez, *Nat. Commun.* **7**, 10598 (2016).

[2] C. Maggi, J. Simmchen, F. Saglimbeni, J. Katuri, M. Dipalo, F. De Angelis, S. Sanchez, and R. Di Leonardo, *Small* **12**, 446 (2016).

Pressure and phase equilibria in active Brownian particles

J. Stenhammar,¹ A. Solon,² M. E. Cates,³ and J. Tailleur⁴

¹ *Division of Physical Chemistry, Lund University, Lund, Sweden*

² *Department of Physics, Massachusetts Institute of Technology, Cambridge, MA, USA*

³ *DAMTP, Centre for Mathematical Sciences, University of Cambridge, Cambridge, United Kingdom*

⁴ *Laboratoire Matière et Systèmes Complexes, Université Paris Diderot, Paris, France*

The phenomenon of motility-induced phase separation (MIPS), whereby suspensions of self-propelled particles will phase separate into coexisting dense and dilute phases even in the absence of attractive or aligning interactions, has attracted significant interest over the last few years. While the onset and kinetics of this phase transition has been successfully described in terms of an “effective chemical potential” which depends on a single-particle swim-speed that decreases with density due to collisional slow-down [1-2], a quantitative theoretical description of the phase boundaries for a system undergoing MIPS is still lacking. In this contribution, we will show how the concept of “active pressure” [3-4] can be used to fully describe these phase boundaries by employing a modified version of the Maxwell equal-area construction used in equilibrium thermodynamics. We show that the details of this “unequal-area construction” depends on the exact form of the gradient terms in the pressure, which are non-zero only near interfaces, and that the phase diagram thus cannot be fully described in terms of a bulk equation of state, as is the case for systems in thermodynamic equilibrium. By measuring these interfacial pressure terms from computer simulations of active Brownian particles (ABPs) in two dimensions, we furthermore show how the binodals can be reconstructed, thus providing a quantitative description of phase equilibria in ABPs.

[1] J. Tailleur and M. E. Cates, *Phys. Rev. Lett.* **100**, 218103 (2008).

[2] J. Stenhammar, A. Tiribocchi, R. J. Allen, D. Marenduzzo, and M. E. Cates, *Phys. Rev. Lett.* **111**, 145702 (2013).

[3] A. Solon, J. Stenhammar, R. Wittkowski, M. Kardar, Y. Kafri, M. E. Cates, and J. Tailleur, *Phys. Rev. Lett.* **114**, 198301 (2015).

[4] A. Solon, J. Stenhammar, M. E. Cates, Y. Kafri, and J. Tailleur, arXiv:1609.03483.

Confined and complex: when shape and interfaces modify active trajectories

I. Buttinoni,¹ K. Dietrich,¹ S. Ni,^{1,2} D. Renggli,¹ G. Volpe,³ H. Wolf,² and L. Isa¹

¹ *Department of Materials, ETH Zürich, Zürich, Switzerland*

² *IBM Research – Zurich, Rüschlikon, Switzerland*

³ *Department of Physics, University of Gothenburg, Gothenburg, Sweden*

Active colloids are self-propelled micro and nanoparticles that convert uniform sources of “fuel” (e.g. chemical) or uniform external driving fields (e.g. magnetic or electric) into directed motion by virtue of asymmetry in their shape or composition. In most cases, the direction of motion is along the asymmetry axis of the particle (e.g., for patchy colloids the axis that links the two different poles of the particle surface) and reorients with a characteristic time set by rotational diffusion. However, physical confinements or complex particle shapes defy this simple picture.

I will present two experiments. In the first experiment, we investigate the active behavior of Pt-coated particles at flat oil-water interfaces that constrain the rotational and translational motion to the *xy*-plane. The colloids self-propel due to H₂O₂ “fuel” dispersed in the water phase [1]. The particle orientation with respect to the interfacial plane also determines the effective swimming speed: slow and fast particles correspond to Pt-coatings immersed mostly in the water or in the oil phase, respectively [2]. In the second experiment, we fabricate colloidal clusters of prescribed shapes (“colloidal molecules”) by linking microspheres of different materials [3] and actuate their active motion using electro-hydrodynamic flows in vertical AC fields [4]. Depending on the shape and composition, the clusters translate at various speeds, circulate, rotate, or switch between these modes of motion and even perform simple transport tasks [5].

All in all, we demonstrate that the properties of the trajectories of active colloids are dramatically affected by complex environments and particle shape.

- [1] J. Palacci, C. Cottin-Bizonne, C. Ybert, and L. Bocquet, *Phys. Rev. Lett.* **105**, 088304 (2010).
- [2] K. Dietrich, D. Renggli, M. Zanini, G. Volpe, I. Buttinoni, and L. Isa, submitted.
- [3] S. Ni, J. Leemann, I. Buttinoni, L. Isa, and H. Wolf, *Sci. Adv.* **2**, e1501779 (2016).
- [4] F. Ma, X. Yang, H. Zhao, and N. Wu, *Phys. Rev. Lett.* **115**, 208302 (2015).
- [5] S. Ni, E. Marini, I. Buttinoni, H. Wolf, and L. Isa, arxiv.org/abs/1701.08061 (2017).

Flocking through disorder

A. Morin, N. Desreumaux, J.-B. Caussin, and D. Bartolo

ENS de Lyon, Lyon, France

How do flocks, herds and swarms proceed through disordered environments? This question is not only crucial to animal groups in the wild, but also to virtually all applications of collective robotics, and active materials composed of synthetic motile units. In stark contrast, apart from very rare exceptions, our physical understanding of flocking has been hitherto limited to homogeneous media. Here we explain how collective motion survives to geometrical disorder. To do so, we combine experiments on motile colloids cruising through random microfabricated obstacles, and analytical theory. We explain how disorder and bending elasticity compete to channel the flow of polar flocks along sparse river networks akin those found beyond plastic depinning in driven condensed matter. Further increasing disorder, we demonstrate that collective motion is suppressed in the form of a first-order phase transition generic to all polar active materials.

Synchronization and pattern formation in active matter

D. Levis,¹ B. Liebchen,² A. Diaz-Guilera,¹ and I. Pagonabarraga¹

¹ *Departamento de Física de la Materia Condensada, Universidad de Barcelona, Barcelona, Spain*

² *SUPA, School of Physics and Astronomy, University of Edinburgh, Edinburgh, United Kingdom*

Synchronization processes by which a population of mobile units organize into a cooperative state play an important role in very diverse contexts, from physics to biology going through social sciences. Here, we address the general question of how self-propulsion affects the synchronization of motile physical entities - like fireflies or bacteria synchronizing their internal clocks- and how this tendency to synchronize can be exploited to generate and control self-sustained patterns in active matter.

We introduce a generic model to describe such a variety of situations by considering the synchronization of (Kuramoto-like) oscillators carried by self-propelled physical interacting units (thus generating time evolving networks). We focus first on identical oscillators with an internal dynamics that does not affect the motion of the particles [1]. This allows us to identify different dynamic regimes and understand the role played by the network time-dependent topology, the motion of the agents and their mutual interaction. While for point-like particles, self-propulsion accelerates synchronization, the presence of excluded volume interactions gives rise to a richer scenario, where self-propulsion has a non-monotonic impact on synchronization. We show that the synchronization of locally coupled mobile oscillators generically proceeds through coarsening verifying the dynamic scaling hypothesis, with the same scaling laws as the the 2D XY model following a quench.

Then, we consider the case where the internal phase of the oscillators dictates the direction of self-propulsion. Our model extends the Vicsek model to describe the collective behaviour of polar circle swimmers with local alignment interactions [2]. While the phase transition leading to collective motion in 2D (flocking) occurs at the same interaction to noise ratio as for linear swimmers, circular motion enhances the polarization in the ordered phase and induces secondary instabilities leading to structure formation. We analyze the impact of self-rotations in chiral active matter and find that the feedback between the orientation dynamics and the motion of the agents gives rise to a novel generic route to pattern formation, absent both in the standard Vicsek model and in synchronization Kuramoto-like models in static networks. We discuss the connexions between these results and the experimental studies of chiral colloidal systems, sperm cells and robots swarms.

[1] D. Levis, I. Pagonabarraga, and A. Diaz-Guilera, *Phys. Rev. X* **7**, 011028 (2017).

[2] B. Liebchen and D. Levis, *arXiv:1701.00091* (2017).

Flowing crystals – the liquid solid transition of monodisperse active particles

D. Vågberg and L. Berthier

Laboratoire Charles Coulomb, CNRS, Université Montpellier, Montpellier, France

We simulate a dense system of athermal monodisperse self propelled particles in two dimensions. We use Langevin dynamics where the activity is introduced as an Ornstein-Uhlenbeck process with a persistence time τ_p and a noise strength D_f . More details about the model can be found in [1, 2].

We explore static and dynamic properties across a wide section of the three dimensional phase space given by the packing fraction ϕ , τ_d and D_f . We find that phase space can be reduced to an almost two dimensional form by suitable choice of parameters. By defining an effective temperature T_e and switching from the persistence time τ_p to the persistence length l_p it is possible to capture the important features of the phase space by looking at the $\phi - l_p$ plane while keeping T_e constant. The resulting phase diagram can be described as the intersection of two different phenomena, the liquid-solid transition at high ϕ and the motility induced phase separation at high l_p . Interesting dynamics is observed in the region where these two transitions meet. In order to better understand this crossover regime we study the liquid-solid transition as a function of ϕ and l_p from the Brownian limit at $l_p \rightarrow 0$ to the highly active regime where the dynamics is dominated by the motility induced phase separation.

Close to the intersection of the two transitions, at high l_p but still below the motility induced phase separation we observe systems that remains dynamically active even at packing fractions far above the liquid-solid transition point seen in the Brownian limit. In these active systems we observe the formation of short lived crystal like structures that constantly forms, melts and flows giving rise to some very interesting dynamics. Our results seems consistent with the observations in the recent experimental work by Briand and Dauchot [3] however our simulations allows us to extend their findings by probing a wider parameter range than were accessible in their experiment.

[1] G. Szamel, Phys. Rev. E **90**, 012111 (2014).

[2] G. Szamel, E. Flenner, and L. Berthier, Phys. Rev. E **91**, 062304 (2015).

[3] G. Briand and O. Dauchot, Phys. Rev. Lett. **117**, 098004 (2016).

Painting with bacteria

J. Arlt,¹ V. A. Martinez,¹ A. Dawson,¹ T. Pilizota,² and W. C. K. Poon¹

¹*School of Physics & Astronomy, University of Edinburgh, Edinburgh, United Kingdom*

²*School of Biological Sciences, University of Edinburgh, Edinburgh, United Kingdom*

Suspensions of swimming bacteria, such as *Escherichia coli*, are widely used as model active colloids [1], but a real-time tuneable control of their swimming speed is lacking. Here, we construct strains of *Escherichia coli* for which their swimming speed can be controlled by the intensity of incident green light [1]. We show how to ‘paint pictures’ using such bacteria and externally-imposed spatially-structured light fields and discuss the physical principles that control various features of the resulting patterns. We also use these bacteria to verify a fundamental prediction from the statistical mechanics of active particles [2], namely, that the product of the local density of swimmers and their local swimming speed $\rho(x)v(x) = \text{constant}$.

[1] J. Schwarz-Linek, J. Arlt, A. Jepson, A. Dawson, T. Vissers, D. Miroli, T. Pilizota, V. A. Martinez, and W. C. K. Poon, *Colloids Surf. B* **137**, 2(2016).

[2] J. Tailleur and M. E. Cates, *Phys. Rev. Lett.* **100**, 3 (2008).

Dynamics of self-propelled colloidal particles in viscoelastic fluids

J. R. Gomez-Solano,¹ N. Narinder,¹ M. Sahebdivani,¹ A. Blokhuis,¹ and C. Bechinger^{1,2}

¹ *Physikalisches Institut, Universität Stuttgart, Stuttgart, Germany*

² *Max-Planck-Institute for Intelligent Systems, Stuttgart, Germany*

The motion of many microorganisms, such as bacteria and spermatozoa, commonly takes place in viscoelastic fluids, which can display either liquid- or solid-like behavior depending on the induced strain rate [1]. The understanding of the dynamics of natural microswimmers has triggered a lot of experimental and theoretical work in recent years as well as the development of synthetic self-propelled Janus particles. Although the motion of such synthetic microswimmers in Newtonian fluids has been extensively studied [2], so far only few investigations have focused on the swimming of living microorganisms in Non-Newtonian fluids [3]. In this work, we experimentally investigate the dynamics of spherical Janus colloidal particles in a viscoelastic fluid. The particles are self-propelled by local demixing of a critical polymer mixture induced by laser illumination. We observe a pronounced enhancement of both translational and rotational diffusion with increasing particle velocity even at low Weissenberg number, where the drag force on the particle exerted by the fluid obeys the Stokes law [4]. In addition, we find that a self-propelled particle undergoes a strong repulsion induced by the surrounding viscoelastic liquid when moving close to a solid wall. We show that these effects, which originate from the coupling between the directed particle motion and the slow microstructural relaxation of the fluid, have dramatic consequences for the particle dynamics in more complex confined geometries, as well as for their collective motion in crowded environments.

[1] J. R. Gomez-Solano and C. Bechinger, *New J. Phys.* **17**, 103032 (2015).

[2] C. Bechinger, R. Di Leonardo, H. Löwen, C. Reichhardt, G. Volpe, and G. Volpe, *Rev. Mod. Phys.* **88**, 045006 (2016).

[3] A. Patteson, A. Gopinath, and P. E. Arratia, *Curr. Opin. Colloid Interface Sci.* **21**, 86 (2016).

[4] J. R. Gomez-Solano, A. Blokhuis, and C. Bechinger, *Phys. Rev. Lett.* **116**, 138301 (2016).

Control of active nematics by means of addressable soft interfaces

P. Guillamat, J. Hardoüin, J. Ignés-Mullol, and F. Sagués

Department of Materials Science and Physical Chemistry, and Institute of Nanoscience and Nanotechnology, Universitat de Barcelona, Barcelona, Spain

Motor-proteins are responsible for transport inside cells. Harnessing their activity is key towards developing new nano-technologies or functional biomaterials. Cytoskeleton-like networks, recently tailored in vitro, result from the self-assembly of subcellular autonomous units. Taming this biological activity bottom-up may thus require molecular level alterations compromising protein integrity.

We have taken a top-down perspective consisting on tuning the anisotropic viscosity of a contacting thermotropic liquid crystal oil. We show that the seemingly chaotic flows of a tubulin-kinesin aqueous active gel with nematic-like order [1] can be forced to adopt well-defined spatial directions that correlate with the structure of the responsive oil/water interface. Different configurations of the active material are realized, when the passive liquid crystal is either unforced [2] or commanded by a magnetic field [3]. The inherent instability of the extensile active fluid (*active turbulence*) is thus spatially regularized, leading to organized flow patterns, endowed with characteristic length and time scales whose role is redefined under the imposed geometrical confinements. Other control strategies, including the use of thermosensitive depleting agents that enable to tune the order of the active gel will be discussed.

[1] T. Sanchez, D. T. Chen, S. J. De Camp, M. Heymann, and Z. Dogic, *Nature* **491**, 431 (2012).

[2] P. Guillamat, J. Ignés-Mullol, and F. Sagués, arXiv:1511.03880v1.

[3] P. Guillamat, J. Ignés-Mullol, and F. Sagués, *Proc. Natl. Acad. Sci. USA* **113**, 5498 (2016).

Reawakening of motility in glassy confluent epithelia

C. Malinverno,¹ S. Corallino,¹ F. Giavazzi,² G. Scita,^{1,3} and R. Cerbino²

¹ IFOM-FIRC Institute of Molecular Oncology, Milan, Italy

² BIOMETRA Department, University of Milan, Milan, Italy

³ DIPO Department, University of Milan, Milan, Italy

Cells in confluent epithelial layers may remain quiescent for a long time to suddenly get motile and migrate far away from their original location. Very often, such migration events exhibit a cooperative and collective character, as observed for instance during morphogenesis, wound healing and cancer spreading. Despite recent advances, much remains to be uncovered about the physical and molecular factors behind this collective behaviour and a complete description of collective cellular migration is still lacking. In this framework, an important analogy has been recently drawn between confluent cell monolayers and inert systems exhibiting, due to density constraints, a jamming transition between a fluid-like and a solid-like state [1]. However, while the transition in inert systems invariably occurs at a critical density, epithelial monolayers display limited density fluctuations. Therefore, material parameters that encode cell properties such as cell-cell adhesion and cortical tension, rather than density alone, have been shown to describe the rigidity transition in cells [2]. The general validity of this theoretical framework remains to be investigated, as the link with relevant molecular determinants. Here we present recent experimental and modelling results [3] obtained with confluent monolayers of epithelial MCF-10A cells. We show that over-expression of RAB5A, a key endocytic protein, is sufficient to induce large-scale, coordinated motility over tens of cells, and ballistic motion in otherwise kinetically arrested monolayers. This reawakening of motility is accompanied by increased traction forces and to the extension of cell protrusions, which align with local velocity. This RAB5A-induced collective motility is abrogated by impairing endocytosis, macropinocytosis or by increasing fluid flux. To elucidate how these different contributions combine in our experiments, we performed numerical simulations of monolayer dynamics. Our simulations are based on a self-propelled Voronoi (SPV) model that incorporate mechanical junctional tension and an active cell reorientation mechanism for the velocity of self-propelled cells. Our model explains endocytic reawakening of locomotion in terms of a combination of large-scale directed migration and local unjamming. These changes in multicellular dynamics enable collectives to migrate under physical constraints and may be exploited by tumours for metastatic dissemination.

[1] T. E. Angelini et al., Proc. Natl. Acad. Sci. USA **108**, 4714 (2011).

[2] J.-A. Park et al., Nat. Mater. **14**, 1040 (2015).

[3] C. Malinverno et al., Nat. Mater. **16**, 587 (2017).

Active matter logic for autonomous microfluidics

F. G. Woodhouse¹ and J. Dunkel²

¹ *Department of Applied Mathematics and Theoretical Physics, University of Cambridge, Cambridge, United Kingdom*

² *Department of Mathematics, Massachusetts Institute of Technology, Cambridge, MA, USA*

The ability of chemically or optically powered active matter to self-organise and spontaneously flow makes these concepts an increasingly attractive option in smart microfluidics and materials design. Active matter has the potential to serve as the bedrock of customisable, controllable transport and processing systems, but in order to fully harness this potential, its intrinsic tendency toward turbulence must be tamed. Geometric confinement has recently emerged as an excellent stabilising scheme, allowing complex yet controllable behaviours to be engineered by careful design of the flow environment. Drawing on recent work showcasing a geometrically-realised bacterial analogue of the Ising model [1], I will describe a new model for incompressible active flow in networks [2] before using this framework to introduce active matter logic [3]. We will see how the synchronised self-organisation of individual network components across carefully chosen flow topologies can be harnessed to construct logic gates and to store data within SR latches, laying the foundation for autonomous microfluidic logic devices driven by bacterial fluids, active liquid crystals or chemically engineered motile colloids.

[1] H. Wioland, F.G. Woodhouse, J. Dunkel, and R. E. Goldstein, *Nat. Phys.* **12**, 341 (2016).

[2] F. G. Woodhouse, A. Forrow, J. B. Fawcett, and J. Dunkel, *Proc. Natl. Acad. Sci. USA* **113**, 8200 (2016).

[3] F. G. Woodhouse and J. Dunkel, [arXiv:1610.05515](https://arxiv.org/abs/1610.05515).

Chemotaxis and autochemotaxis in self propelling liquid crystal droplets

C. C. Maass,¹ C. Jin,¹ C. Krüger,¹ and C. Bahr¹

¹*Max Planck Institute for Dynamics and Self-Organization, Göttingen, Germany*

Chemotaxis and auto-chemotaxis are key mechanisms in the dynamics of micro-organisms, e.g. in the acquisition of nutrients and in the communication between individuals, influencing the collective behaviour. However, chemical signalling and the natural environment of biological swimmers are generally complex, making them hard to access analytically.

We present a well-controlled, tunable artificial model to study chemotaxis and autochemotaxis in complex geometries, using microfluidic assays of self-propelling liquid crystal droplets in an aqueous surfactant solution. Droplets gain propulsion energy by micellar solubilisation, with filled micelles acting as a chemical repellent by diffusive phoretic gradient forces [1, 2].

We have studied these effects in a series of microfluidic geometries.

In a first demonstration setup, droplets are guided along the shortest path through a maze by surfactant diffusing into the maze from the exit [3].

Second, we let auto-chemotactic droplet swimmers pass through bifurcating microfluidic channels and record anticorrelations between the branch choices of consecutive droplets. We present an analytical model based on balancing stochastic forces versus a diffusing chemical gradient matching the experimental data.

Last, pillar arrays of variable sizes and shapes provide a convex wall interacting with the swimmer and in the case of attachment bending its trajectory and forcing it to revert to its own trail. We observe different behaviour based on the interplay of wall curvature and negative autochemotaxis, i. e., no attachment for highly curved interfaces, stable trapping at large pillars, and a narrow transition region where negative autochemotaxis makes the swimmers detach after a single orbit.

- [1] S. Herminghaus, C. C. Maass, C. Krüger, S. Thutupalli, L. Goehring, and C. Bahr, *Soft Matter* **10**, 7008 (2014).
- [2] C. C. Maass, C. Krüger, C. Bahr, and S. Herminghaus, *Annu. Rev. Condens. Matter Phys.* **7**, 171 (2016).
- [3] C. Jin, K. Krüger, and C. C. Maass, *Proc. Natl. Acad. Sci. U.S.A.* **114**, 5089 (2017).

Active micromachines: Novel propulsion and control strategies

C. Maggi,¹ F. Saglimbeni,¹ G. Vizsnyiczai,² and R. Di Leonardo^{1,2}

¹ NANOTEC-CNR, Institute of Nanotechnology, Soft and Living Matter Laboratory, Rome, Italy

² Dipartimento di Fisica Università di Roma "Sapienza", Rome, Italy

In the first part of the talk I will present a new type of light-activated motors with unprecedented efficiency [1]. These consist in asymmetric micro-fabricated gears produced by laser lithography covered by an absorbing film of amorphous carbon deposited by sputtering converting the energy of wide-field illumination into rotational motion. These micromotors are suspended at an air-liquid interface and induce a non-homogeneous heating of the fluid that, in turn, causes a surface tension-driven torque spinning the rotor up to 300 rpm. Moreover we demonstrate that these micro-devices have an efficiency orders of magnitude higher than rotors relying on direct optical momentum transfer or on thermophoresis and therefore can be actuated without using strongly focused (laser) radiation. In the second part of the talk I will show how we were able to design self-assembling micro-motors from catalytic (Janus) self-propelling particles and passive microgears [2]. This combination leads to the fully autonomous construction and propulsion of rotors via the almost perfect alignment of Janus particles with the gear's edge. This is achieved by carefully designing the size and of the gears with respect to the diameter of the Janus particles that display a strikingly deterministic aligning interactions with walls. It will be discussed how the performances of these motors are affected by hydrodynamics and competition for fuel. Finally I will present new synthetic micromachines where bacteria act as biological propellers [3]. These are composed by two-photon polymerized synthetic structures inducing the self-assembly of genetically engineered *E. coli* bacteria. These rotors capture individual swimming bacteria into an array of micro-chambers so that every cell contributes optimally to the applied torque. Bacterial cells are genetically modified smooth swimmers expressing a light-driven proton pump that allows to optically control their swimming speed. Employing a spatial light modulator we can address individual motors with tunable light intensities allowing the dynamic control of their rotational speeds. Using a real time feedback control loop, we can also command a set of micromotors to rotate in unison with a prescribed angular speed.

[1] C. Maggi, F. Saglimbeni, M. Dipalo, F. De Angelis, and R. Di Leonardo, *Nat. Commun.* **6**, 7855 (2015).

[2] C. Maggi, J. Simmchen, F. Saglimbeni, J. Katuri, M. Dipalo, F. De Angelis, S. Sanchez, and R. Di Leonardo, *Small* **12**, 446 (2016).

[3] G. Vizsnyiczai, C. Maggi, G. Frangipane, R. Di Leonardo et al., submitted.

Session 11: Biological and Biomimetic Fluids

Direct observations of transition dynamics from macro- to micro-phase separation in asymmetric lipid bilayers

S. F. Shimobayashi,¹ M. Ichikawa,² and T. Taniguchi³

¹ *Department of Mathematical science and Advanced Technology, Japan Agency for Marine-Earth Science and Technology, Kanagawa, Japan*

² *Department of Physics, Kyoto University, Kyoto, Japan*

³ *Department of Chemical Engineering, Kyoto University, Kyoto, Japan*

We present the first direct observations of morphological transitions from macro- to micro-phase separation in asymmetric lipid vesicles to mimic biological membranes. The transition occurs via an intermediate stripe-shaped state. During the transition, monodisperse micro domains emerge through repeated scission events of the stripe domains. Moreover, we numerically confirmed such transitions with a time-dependent Ginzburg-Landau model, which describes phase separation in three-dimensional bending elastic lipid vesicles. Our findings could provide important mechanistic clues for understanding the dynamics of the heterogeneities existing in cell membranes.

[1] S. F. Shimobayashi, M. Ichikawa, and T. Taniguchi, EPL **113**, 56005 (2016).

Active shape control as an adaptive strategy in phytoplankton

A. Sengupta, F. Carrara, and R. Stocker

Institute for Environmental Engineering, ETH Zurich, Zurich, Switzerland

Phytoplankton are unicellular photosynthetic organisms that form the basis of life in the oceans and contribute a major fraction of global oxygen production. They are frequently exposed to turbulence, which has long been known to affect phytoplankton fitness and species succession, generally by harming motile species and thus favoring a transition to non-motile species. Here we report on a striking, unexpected behavioral response of motile species to hydrodynamic cues mimicking those experienced in ocean-scale turbulence. In the absence of turbulence, the cells exhibit upward swimming – or ‘negative gravitaxis’ – observable as cell accumulations at the top of an experimental chamber. When we exposed cells to overturning in the vertical plane, mimicking Kolmogorov-scale turbulent eddies, the population robustly split into two subpopulations, one swimming upward and one swimming downward. Experiments with overturning in the horizontal plane, in which no population split was observed, revealed that the cue inducing this active switch in motility is the reversal of the gravitational acceleration. Microscopic observation at the single-cell level showed that the behavioral switch was accompanied by a rapid morphological change, and a mechanistic model of gravitaxis confirms that such a shape change can alter the cell’s stability and induce downward migration. The results indicate that, over timescales smaller than the cell cycle, certain species of phytoplankton can actively switch between two alternative stable states, in response to mechanical cues. This active response to fluid flow, whereby nearly half of a phytoplankton population in the ocean invert its direction of migration in response to turbulence, could be part of a bet-hedging strategy to maximize the chances of at least a fraction of the population evading high-turbulence microzones.

[1] A. Sengupta, F. Carrara, and R. Stocker, *Nature* (in press).

Wire active microrheology to differentiate viscoelastic liquids from soft solids: Applications to biophysics

J.-F. Berret

*Matière et Systèmes Complexes, UMR 7057 CNRS Université Denis Diderot Paris-VII,
Bâtiment Condorcet, Paris, France*

Being able to reduce the size of a rheometer down to the micron scale is a unique opportunity to explore the mechanical response of expensive and/or confined liquids and gels. In this work, we used micron-size magnetic wires to measure the viscoelastic response of complex fluids. We exploit the technique of rotational magnetic spectroscopy in which wires are submitted to a rotational magnetic field (as a function of the frequency) and their motion is monitored by time-lapse microscopy.

We also provide for the first time the constitutive equations for the wire rotation in viscoelastic materials in general [1]. Prior to biomechanical studies on living cells, the rotational magnetic spectroscopy is assessed using known rheological model systems, such as wormlike micelles and polysaccharide gels [2].

With living cells, we address here the question of the viscoelastic nature of the interior of living cells, an issue that is relevant to understand how cells adapt to their environment. Cytoplasm viscosity measurements on three cells lines, including murine NIH/3T3 fibroblasts, HeLa cervical cancer cells and A549 lung carcinoma epithelial cells are obtained from the determination of a critical frequency between synchronous and asynchronous wire rotation regime. The values of the shear viscosity (10 – 100 Pa s) and for the elastic modulus (20 – 200 Pa) for the three cell lines confirm the viscoelastic character of the cytoplasm. In contrast to earlier studies however, it is concluded that the living cell interior is best described as a viscoelastic liquid, and not as an elastic gel [3].

The present work finally demonstrates the potential of the wire-based magnetic rotation spectroscopy as an accurate rheological tool to distinguish between flow and yield stress behaviors in highly confined environments.

[1] L. Chevy, N. K. Sampathkumar, A. Cebers, and J.-F. Berret, *Phys. Rev. E* **88**, 062306 (2013).

[2] F. Loosli, M. Najm, R. Chan, E. Oikonomou, A. Grados, M. Receveur, and J.-F. Berret, *Chem. Phys. Chem* **17**, 4134 (2016).

[3] J.-F. Berret, *Nat. Commun.* **7**, 10134 (2016).

Selective activation of immune response by non-specific multivalent interactions

J. Dobnikar,^{1,2} N. W. Schmidt,³ T. Curk,^{1,2} E. Y. Lee,³ F. Jin,^{3,4} R. Lande,^{5,6} W. Xian,³ L. Frasca,^{5,6} D. Frenkel,² M. Gilliet,⁵ and G. C. L. Wong³

¹ *Institute of Physics, Chinese Academy of Sciences, Beijing, China*

² *Department of Chemistry, University of Cambridge, Cambridge, United Kingdom*

³ *Bioengineering Department, Chemistry & Biochemistry Department, California Nano Systems Institute, University of California, Los Angeles, CA, USA*

⁴ *Hefei National Laboratory for Physical Sciences at Microscale, Department of Polymer Science and Engineering, CAS Key Laboratory of Soft Matter Chemistry, University of Science and Technology of China, Hefei, China*

⁵ *Department of Dermatology, Lausanne University Hospital, Lausanne, Switzerland*

⁶ *Department of Infectious, Parasitic and Immunomediated Diseases, Istituto Superiore di Sanità, Rome, Italy*

Complex biological processes are often controlled by specific molecular interactions. An example of this is immune system response by plasmacytoid dendritic cells that is activated when single-stranded viral DNA specifically binds to TLR9 receptors in the cells. However, the TLR9 receptors are sometimes activated also when no viral DNA is present leading to an unwanted autoimmune response. It has been known that complexes of double-stranded self-DNA and antimicrobial peptides such as LL37 can cause autoimmune disorders but the mechanism of the receptor activation was not understood until recently.

We [1] have combined X-ray scattering, computer simulations, statistical mechanics and in-vitro measurements of interferon production in the cells to demonstrate that a broad range of antimicrobial peptides and other cationic molecules cause similar effects upon forming liquid-crystalline complexes with DNA molecules present in the intercellular medium. TLR9 activation super-selectively depends on inter-DNA spacing and multiplicity of parallel DNA ligands in the self-assembled complex. Complexes at the optimum spacing can interlock with multiple TLR9 like a zipper, leading to multivalent electrostatic interactions that drastically amplify binding and thereby trigger the immune response.

Our results suggest a plausible mechanism of receptor activation in certain autoimmune disorders and further suggest that the TLR9-mediated immune response can be modulated deterministically offering new treatment possibilities [2]. Moreover, the discovered universal mechanism elucidates how non-specific interactions can be turned into specific by multivalent effects. It is expected that this

universal mechanism is underlying many biological processes; other systems exhibiting similar behaviour have been studied recently [3].

- [1] N. W. Schmidt, F. Jin, R. Lande, T. Curk, W. Xian, L. Frasca, D. Frenkel, J. Dobnikar, M. Gilliet, and G. C. L. Wong, *Nat. Mater.* **14**, 696 (2015).
- [2] E. Y. Lee, C. K. Lee, N. W. Schmidt, F. Jin, R. Lande, T. Curk, A. Kaplan, D. Frenkel, J. Dobnikar, M. Gilliet, and G. C. L. Wong, *Adv. Col. Int. Sci.* **232**, 17 (2016).
- [3] E. Y. Lee, T. Curk, J. Dobnikar, and G. C. L. Wong, submitted (2017).

Multiscale MD-GFRD simulations of the effect of rebinding kinetics in dilute diffusion-reaction systems

A. Vijaykumar,^{1,2} P. R ten Wolde,¹ and P. G. Bolhuis²

¹ FOM Institute AMOLF, Amsterdam, The Netherlands

² van 't Hoff Institute for Molecular Sciences, University of Amsterdam, Amsterdam, The Netherlands

Many important systems can be modelled as reaction-diffusion systems. Examples are biochemical networks, gene regulatory networks, or self-assembly of complex molecules in living cells. Also in materials science reaction-diffusion plays a central role, e.g. in the self-assembly of colloidal particles, the formation of micro-emulsions, or the phase behavior of polymer solutions. In industry, reaction-diffusion systems find applications in catalytic reactions, e.g. fuel cells.

However, in dilute systems, diffusion typically occurs on the mesoscopic scales of micrometers and milliseconds while the reactions take place on the microscopic scales of nanometers and microseconds, thus making the reaction a rare event. Such systems are notoriously difficult to simulate. While the mean-field rate equation cannot accurately describe such processes, the recently developed Green's function reaction dynamics (GFRD) [1] is a computationally efficient, exact, event-driven algorithm to simulate systems at the particle level. However, in GFRD the particles have an idealized shape, while it is now known that the microscopic dynamics, such as the rapid rebinding between a catalyst and its substrate, can dramatically change the behavior of the system at the macroscopic scale [1]. In these cases, the conformational and/or orientational dynamics of the particles has to be described explicitly and cannot be integrated out. While (ab initio) Molecular Dynamics (MD) could, in principle, simulate the system at the required microscopic scale, such a scheme would be highly inefficient. To alleviate this problem, we developed a multiscale algorithm [2, 3] that simulates reaction-diffusion systems. The scheme uses Green's function reaction dynamics (GFRD) to treat the diffusion at the mesoscopic scales and Brownian Dynamics (BD) or full atom MD to handle the reactions at the microscopic scales.

In this work, we first discuss the general need for these kinds of multiscale simulation algorithms, and then present the MD-GFRD scheme using a simple system. Next, we apply this multiscale scheme to study the response of a Mitogen Activated Protein Kinase (MAPK) pathway. In this system, the substrate has two binding sites, and the response of the system depends on whether these sites are modified according to a

processive or a distributive mechanism. We study the response as a function of the distance between these bindings sites and the orientational dynamics of the substrate and enzyme molecules.

- [1] K. Takahashi, S. Tanase-Nicola, and P. R. ten Wolde, *Proc. Natl. Acad. Sci. USA* **107**, 2473 (2010).
- [2] A Vijaykumar, P. G. Bolhuis, and P. R. ten Wolde, *J. Chem. Phys.* **143**, 214102 (2015).
- [3] A. Vijaykumar, T. E. Ouldridge, P. R. ten Wolde, and P. G. Bolhuis, arXiv: 1611.09239v1.

List of Posters

Topic 1: Ionic Liquids, Liquid Metals

- 1.001 **Solid Liquid Equilibria and Molecular Modeling Predictions of Glucose in Tetra Butyl Ammonium Bromide based Deep Eutectic Solvents**
Banerjee T., Paul S., Naik P. K., Goud V. V., Mohan M.
- 1.002 **A molecular dynamics study for dibenzo-18-crown-6 assisted metal ion extraction in ionic liquid-water biphasic systems**
Biswas R., Ghosh P., Banerjee T., Musharaf Ali S.
- 1.003 **Metal ion partitioning with calix[4]arene-benzo-crown-6 in ionic liquid-water biphasic systems**
Biswas R., Ghosh P., Banerjee T., Musharaf Ali S.
- 1.004 **Selective Thermal Dehydrogenation of Ethylene Diamine Bisborane Facilitated by Phosphonium Based Ionic Liquids**
Banerjee T., Kundu D., Pugazenthi G., Banerjee B.
- 1.005 **The Internal Pressure and Cohesive Energy Density of Liquid Metallic Elements**
Marcus Y.
- 1.006 **Vapour-liquid phase behaviour of ionic fluids in disordered porous media: application of the scaled particle theory and the ion-association concept**
Holovko M., Patsahan T., Patsahan O.
- 1.007 **Frenkel line: Theoretical background and experimental evidences**
Brazhkin V. V.
- 1.008 **Analysis of local bond-orientational order for liquid gallium at ambient pressure**
Wu T. M., Chen L. Y., Tang P. H.
- 1.009 **The polymorphic plethora of Wigner bilayer systems**
Kahl G., Antlanger M., Mazars M., Šamaj L., Trizac E.
- 1.010 **Influence of alkyl chain length on the diffusion of a nitroxide radical in imidazolium-based ionic liquids**
Merunka D., Peric M.
- 1.011 **The influence of multivalent ions on charge-regulation interaction**
Adžić N., Podgornik R.
- 1.012 **Rheology of nano-confined ionic liquids between metallic surfaces**
Garcia L., Charlaix E., Cross B.
- 1.013 **Equilibrium Studies on the Separation of Acetic Acid from Aqueous Solutions by Bulk Ionic Liquid Membrane Containing Tributyl Phosphate**
Baylan N., Çehreli S.
- 1.014 **Removal of Acetic Acid from Water by using Tributyl Phosphate Dissolved in Ionic Liquid [BMIM][Tf₂N]**
Baylan N., Çehreli S.
- 1.015 **Electrochemical behavior of uranyl ions in ionic liquid, 1-butyl-3-methylimidazolium chloride**
Kim I. S., Kwon S. M., Chung D. Y.
- 1.016 **Phase behaviors of ionic liquids and ionic liquid crystals**
Cao W., Wang Y.
- 1.017 **A Simple Method for Efficient Synthesis of Tetraarylporphyrin using Acidic Ionic Liquids**
Kitaoka S., Nobuoka K., Yamamoto A.

- 1.018 **Dielectric constant of ionic liquids – theoretical estimation**
Rybińska A., Sosnowska A., Puzyn T.
- 1.019 **Effect of Anionic Structure of Ionic Liquids on Thermal Cyclization of Chromene Derivatives with Polar Substituents**
Nobuoka K., Kitaoka S., Sano R., Ohga Y., Ishikawa Y.
- 1.020 **Topology of Liquid Aluminium**
Valladares R. M., Díaz-Celaya J. A., Valladares A., Valladares A. A.
- 1.021 **Shear Viscosity of liquid alloys**
Meyer N., Xu H., Wax J. F.
- 1.022 **Phase behaviour of primitive models of ionic fluids confined in disordered matrices: collective variables approach**
Patsahan T., Patsahan O., Holovko M.
- 1.023 **Molecular dynamics investigation of a coarse-grained model of ionic liquid under confinement and shear**
Dašić M., Stanković I., Gkagkas K.
- 1.024 **Thermodynamic and structural properties of 2D ionic liquids and charge ordering**
Urbič T., Perera A.
- 1.025 **Electrochemical four-electron reduction of dioxygen by diiron complex promoted in an ionic liquid-modified electrode**
Masuda H.
- 1.026 **The Intrinsic Structure of the Interface of Partially Miscible Fluids: an Application to Ionic Liquids**
Hantal G., Sega M., Kantorovich S. S., Schröder C., Jorge M.
- 1.027 **Efficient 3d Ewald summation method for simulating inhomogeneous charged systems with slab geometry**
Levin Y., Pereira Dos Santos A., Giroto M.
- 1.028 **Transverse excitations in a van der Waals-like liquid Hg**
Hosokawa S., Inui M., Kajihara Y., Chiba A., Tsutsui S., Baron A. Q. R.
- 1.029 **Simple liquids’ quasiuniversality and the hard-sphere paradigm**
Dyre J. C.
- 1.030 **The influence of electronic polarizability on the properties of ionic liquids**
Zeman J., Uhlig F., Smiatek J., Holm C.

Topic 2: Water, Solutions

- 2.001 **Common microscopic structural origin for water’s thermodynamic and dynamic anomalies**
Shi R., Russo J., Tanaka H.
- 2.002 **Characterization of dynamic crossovers in bulk liquid water by molecular dynamics simulations**
Suffritti G. B., Sant M., Gabrieli A., Demontis P., Izadi S., Shabane P. S., Onufriev A. V.
- 2.003 **COSMO-RS: The currently most tool for the prediction of free energies of molecules in solution**
Klamt A.
- 2.004 **Ultrafast energy fluxes during solvation dynamics in liquid water**
Rey R., Hynes J. T.

- 2.005 **Ion-specific effects in aqueous polyelectrolyte solutions - volumetric and calorimetric properties of ionene salts**
Hribar-Lee B., Lukšič M.
- 2.006 **Droplet-like nanoscale heterogeneity in aqueous solutions of polar organic compounds**
Shkirin A., Bunkin N., Lyakhov G., Penkov N., Molchanov I.
- 2.007 **Experimental investigation of critical Casimir forces in binary liquid mixture by blinking optical tweezers**
Magazzù A., Schmidt F., Callegari A., Gambassi A., Dietrich S., Volpe G.
- 2.008 **Characterization of water confined into nanoscale hydrophobic pores**
Grzimek V., Schlegel M. C., Hoser A., Karanikolos G., Veziri M., Stein W. D., Bewley R., Russina M.
- 2.009 **New Potential Model for Propylene Glycol: Insight to Local Structure and Dynamics**
Ferreira E. S. C., Voroshylova I. V., Pereira C. M., Cordeiro M. N. D. S.
- 2.010 **Viscosity of supercooled water under pressure and two-state interpretation of water anomalies**
Issenmann B., Singh L. P., Caupin F.
- 2.011 **Molecular dynamics study of curcumin in water, methanol and dimethyl sulfoxide**
Patsahan T., Ilnytskyi J., Pizio O.
- 2.012 **Liquid polymorphism driven by interconvertible states in a single-component fluid**
Amrhein L., Anisimov M., Caupin F., Duška M., Rosenbaum A., Sadus R.
- 2.013 **A review of classical interatomic potentials applied to aqueous lithium chloride solutions**
Pethes I.
- 2.014 **On the existence of a scattering pre-peak in the mono-ols and diols**
Pożar M., Perera A.
- 2.015 **Modeling water as a continuous medium**
Berthoumieux H., Maggs A. C.
- 2.016 **Estimation of direct transition mechanism for molecular diffusion in type I gas hydrates using Density Functional Theory**
Piñeiro M. M., Vidal-Vidal Á., Pérez-Rodríguez M.
- 2.017 **Evaporation of water droplets on inclination**
Kim J. Y., Hwang I. G., Weon B. M.
- 2.018 **Temperature induced changes in the hydrogen-bond network of water-ethanol mixtures in the water-rich composition range**
Pothoczki S., Pusztai L., Bakó I.
- 2.019 **Modification of the Stokes law in confinement at the nanoscale due to memory effects**
Kowalik B., Daldrop J. O., Netz R. R.
- 2.020 **Activity coefficients of individual ions in multivalent electrolytes: Comparison of experiment and the Π +IW theory**
Valiskó M., Henderson D., Boda D.
- 2.021 **Calculating the partition coefficient of pyrene and asphaltenes using computer simulations**
Wand C., Frenkel D., Totton T.

- 2.022 **Intramolecular structure and energetics in supercooled water and aqueous solutions**
Lehmkuhler F., Forov Y., Büning T., Sahle C. J., Steinke I., Elbers M., Julius K., Buslaps T., Tolan M., Hakala M., Sternemann C.
- 2.023 **Modelling of liquid 1,4-butanediol: Molecular dynamics and x-ray scattering studies**
Tomšič M., Cerar J., Jamnik A.
- 2.024 **Various models for n-butanol: Molecular dynamics and x-ray scattering studies**
 Cerar J., Lajovic A., Jamnik A., Tomšič M.
- 2.025 **Modelling the thermodynamic properties of aqueous electrolyte solutions with a free energy perturbation approach**
Lazarou G., Jackson G., Adjiman C. S., Galindo A.
- 2.026 **Hydration states of phospholipids studied by THz spectroscopy**
Hishida M., Hemmi Y., Yamamura Y., Saito K.
- 2.027 **Fast molecular dynamics and phase transition of water confined inside carbon nanotubes**
Kyakuno H., Matsuda K., Ichimura R., Saito T., Maniwa Y.
- 2.028 **Total Neutron Scattering: the order of disorder**
Imberti S.
- 2.029 **Simple models of alcohols**
Urbič T., Papež P.
- 2.030 **Properties of bulk and confined water-alcohol mixture**
Urbič T., Pršlja P., Gonzalez Noya E.
- 2.031 **Ammonia clathrate hydrate as seen from Grand Canonical Monte Carlo Simulations**
Fabián B., Picaud S., Jedlovsky P., Guilbert-Lepoutre A., Mousis O.
- 2.032 **Influence of the interaction model on dynamic properties of liquid water**
 Meyer N., Wax J. F., Xu H., Friant-Michel P., Millot C.
- 2.033 **Mercedes-Benz like model for methanol**
Primorac T., Sokolić F., Zoranić L., Požar M., Urbič T.
- 2.034 **Molecular emulsions: from charge order to domain order**
Perera A.
- 2.035 **Viscosities of antibody solutions depend on their binding sites**
Kastelic M., Dill K. A., Kalyuzhnyi Y. V., Vlachy V.
- 2.036 **Molecular dynamics simulation of a binary mixture near the lower critical point**
Maciolek A., Pousaneh F., Edholm O.
- 2.037 **Phase behaviour of a core-softened fluid from the chemical potential perspective**
Lukšič M., Hribar-Lee B., Pizio O.
- 2.038 **Adaptive resolution simulation methods: fundamental aspects, applications, and perspectives**
Potestio R.
- 2.039 **Equilibrium properties in the thermodynamic limit from small-sized molecular dynamics simulations**
Cortes-Huerto R., Kremer K., Potestio R.
- 2.040 **Calculation of Excess Chemical Potential of Liquids via Hamiltonian Adaptive Resolution Simulation**
Heidari M., Cortes-Huerto R., Kremer K., Potestio R.

- 2.041 **Probing Supercooled Liquid Water at 229.5 K by Raman Spectroscopy**
Grisenti R. E., Goy C., Potenza M. A. C., Dederá S., Guillerm E., Caupin F., Glasmacher U.
- 2.042 **The effect of organic co-solutes on local water dynamics**
Zeman J., Holm C., Smiatek J.
- 2.043 **Ice nucleation near the liquid-liquid critical point in simulations of supercooled water**
Poole P. H.
- 2.044 **Fast and accurate prediction of solvation free energies of proteins The Molecular Density Functional Theory**
Gageat C., Borgis D., Levesque M.
- 2.045 **The surface affinity of the hydrated proton calculated by thermodynamically consistent simulations**
Mamatkulov S. I., Allolio C., Netz R. R., Bonthuis D. J.
- 2.046 **Equations of state through simple thermodynamic integration**
Kournopoulos S., Schoen M., Galindo A., Jackson G.
- 2.047 **Competition between inter- and intramolecular association within a SAFT framework**
Febrá S. A., Galindo A., Adjiman C. S., Jackson G.
- 2.048 **Viscosity in supercooled water-glycerol solutions**
Berthelard R., Issenmann B., Caupin F.
- 2.049 **Probing the equation of state of deeply supercooled TIP4P/2005 water with nanodroplets**
Malek S. M., Poole P. H., Saika-Voivod I.
- 2.050 **Simulating the gold nanoparticle-water interface**
Ruiz Lopez V. G., Dzubiella J.
- 2.051 **Bulk melting of water ice**
Moritz C., Dellago C.

Topic 3: Liquid Crystals

- 3.001 **Heat-driven micro turbines with chiral liquid crystalline droplets in an oligomeric solvent**
Yoshioka J., Araoka F.
- 3.002 **Electro-driven director-deformation wave propagating in chiral liquid crystals confined to pillar geometries**
Yoshioka J., Araoka F.
- 3.003 **A study of nematic wetting near free surfaces**
Izzo D., de Oliveira M. J.
- 3.004 **Smectic monolayer confined on a sphere: topology at the particle scale**
Allahyarov E., Löwen H.
- 3.005 **Programmable pattern formation in anisotropic liquids mediated by topological defects**
Aya S., Araoka F.
- 3.006 **Unusual temperature dependence of anchoring torque in liquid crystals triggered by surface-localized structures**
Aya S., Araoka F.

- 3.007 **Liquid crystalline properties of chain complexes based on dinuclear ruthenium carboxylates**
Mikuriya M., Ishida H., Ujiie S., Handa M.
- 3.008 **Structure, Dynamics and Phase Behavior of a Discotic Liquid Crystal Confined in Nanoporous Anodic Aluminum Oxide Membranes**
Yildirim A., Sentker K., Huber P., Schönhals A.
- 3.009 **Monte Carlo studies on the phase behavior of model chiral liquid-crystals using the hybrid anchoring approach**
Nozawa T., Brumby P. E., Yasuoka K.
- 3.010 **Extensional Rheology of Liquid Crystal Fibers**
Kress O., Ostapenko T.
- 3.011 **Ultraviolet irradiation caused structural transitions in nematic liquid crystal droplets**
Repnik R., Dubtsov A. V., Shmeliova D. V., Pasechnik S. V., Kralj S.
- 3.012 **Topological defects and structures formed by defects in smectic films in free and confined geometry**
Dolganov P. V., Shuravin N. S., Dolganov V. K.
- 3.013 **Long-period polar structures in smectic liquid crystals**
Dolganov P. V.
- 3.014 **Molecular ordering lowers cavitation threshold in complex anisotropic liquids**
 Stieger T., Agha H., Schoen M., Mazza M. G., Sengupta A.
- 3.015 **Slippery Interfaces -localization and luburication of director rotations**
Yamamoto J., Sakatsuji W., Nishiyama I.
- 3.016 **A Landau-de Gennes theory for hard colloidal rods: defects and tactoids**
Everts J. C., Punter M. T. J. J. M., Samin S., van der Schoot P., van Roij R.
- 3.017 **Large electrocaloric effect in smectic liquid crystals**
 Kutnjak Z., Trček M., Kralj S., Klemenčič E.
- 3.018 **Stabilization of topological defects on micro-helices and ribbed colloids in nematic liquid crystal**
Nikkhou M., Mušević I.
- 3.019 **Large elastocaloric effect in main-chain liquid crystal elastomers**
Lavric M., Sánchez-Ferrer A., Zalar B., Kutnjak Z.
- 3.020 **Oriented gold nanorods and gold nanorod chains within smectic liquid crystal topological defects**
Rožič B., Gallas B., Fiorini-Debuisschert C., Kraus T., Hegmann T., Lacaze E.
- 3.021 **Magnetic domains in ferromagnetic nematic and chiral nematic liquid crystals**
Mertelj A., Medle Rupnik P., Lisjak D., Čopić M.
- 3.022 **Dynamics of ferromagnetic liquid crystals**
Sebastian N., Lisjak D., Čopić M., Mertelj A.
- 3.023 **The impact of local interactions on the formation of smectic mesophases and cybotactic domain formation within nematics**
Walker M., Wilson M. R.
- 3.024 **Liquid crystalline organization in spindle-shape confinement**
Gårlea I. C., Notenboom V., Alvarado J., Aarts D. G. A. L., Lettinga M. P., Koenderink G. H., Mulder B. M., Dammone O., Jia Y.

- 3.025 **Chiral columns from achiral chromonic mesogens and the formation of a new layered chromonic phase**
Wilson M. R., Walker M.
- 3.026 **Direct observation of microscopic molecular dynamics in liquid crystal 8CB: Intralayer liquid-like dynamics and interlayer non-liquid-like dynamics**
 Saito M., Masuda R., Yoda Y., Yamamoto J., Seto M.
- 3.027 **Geometry-induced topological defect states in nematic colloids**
Hashemi S. M.
- 3.028 **Optothermal effects in nematic microflows**
Tkalec U., Emeršič T., Zhang R., Martinez-Gonzalez J. A., de Pablo J. J.
- 3.029 **Helical induction in nematic liquid crystals by using chiral metal complexes**
Yoshida J., Watanabe G.
- 3.030 **Observation of chiral structures from achiral micellar lyotropic liquid crystals under capillary confinement**
Dietrich C. F., Giesselmann F., Rudquist P.
- 3.031 **Liquid Crystalline Behavior of Bio-Inspired Polymer-Clay Nano-Composites**
Xu P., Eiser E.
- 3.032 **Liquid crystal droplet as a magnetically tunable whispering gallery mode laser**
Mur M., Sofi J. A., Kvasić I., Mertelj A., Lisjak D., Niranjan V., Mušević I., Dhara S.
- 3.033 **Micro-structured liquid crystal alignment with out-of-plane surface relief gratings**
 Ji Z., Gao S., Zhang X., Li W., Wu Q., Xu J., Drevenšek-Olenik I.
- 3.034 **Phase diagram of a smectic-nematic liquid crystal elastomer network based on stress - strain measurements**
Milavec J., Rešetič A., Domenici V., Zupančič B., Zalar B.
- 3.035 **Density-functional theory of lyotropic nematic order in semiflexible dimers**
 Vaghela A., Teixeira P. I. C., Terentjev E. M.
- 3.036 **Active particle filtering by liquid crystal microfluidics**
 Salamon P., Jevšček V., Drevenšek-Olenik I., Osterman N.
- 3.037 **Dissipative Particle Dynamics simulations of surfactants**
Gray S., Walker M., Wilson M. R.
- 3.038 **Nematodynamics in microcapillary junctions**
Kos Ž., Ravnik M., Žumer S.
- 3.039 **Chiral Nitroxide Radical Liquid Crystals as Novel Magneto-Optical Soft Materials**
Akita T., Yamazaki T., Uchida Y., Nishiyama N.
- 3.040 **A molecular dynamics study of physical properties of chiral metal complex dopants in nematic liquid crystals**
Watanabe G., Yamazaki A., Yoshida J.
- 3.041 **Nanosecond optical imaging of phase transitions dynamics in liquid crystals**
 Jagodič U., Ryzhkova A. V., Mušević I.
- 3.042 **The Induction of the Ntb Phase in Mixtures of non-Ntb Forming Cyanobiphenyl Dimers**
Ramou E., Hussey J., Ahmed Z., Welch C., Karahaliou P. K., Mehl G. H.
- 3.043 **Dielectric anisotropy studies of CBnCB/5CB and CBnCB/CBOnOCB mixtures exhibiting two nematic phases**
Zavvou E. E., Ramou E., Ahmed Z., Welch C., Karahaliou P. K., Vanakaras A. G., Mehl G. H.

- 3.044 **Particle diffusion in ferromagnetic liquid crystals**
 Majaron H., Cmok L., Vilfan M., Lisjak D., Mertelj A.
- 3.045 **Molecular Dynamics in a “de Vries” Liquid Crystal: ^1H NMR Relaxometric Study**
 Gradišek A., Apih T., Domenici V., Sebastião P. J.
- 3.046 **Switching dynamics in cholesteric liquid crystal emulsions**
Fadda F., Gonnella G., Marenduzzo D., Orlandini E., Tiribocchi A.
- 3.047 **Localization of low-molecular-weight molecules at the defect of a liquid crystal**
 Ohzono T., Katoh K., Fukuda J.
- 3.048 **Hydrodynamic cavitation in Stokes flow of anisotropic fluids: Simulations and Theory**
 Stieger T., Agha H., Schoen M., Mazza M. G., Sengupta A.
- 3.049 **Molecular simulations elucidate soft elasticity in polydomain liquid crystal elastomers**
Skacej G., Zannoni C.
- 3.050 **Spontaneous breaking of chiral symmetry due to octupolar (tetrahedral) order**
Pleiner H., Brand H. R.
- 3.051 **Colloidal liquid crystals in confinement: isotropic, nematic and smectic phases**
Cortes L. B. G., Gao Y., Dullens R. P. A., Aarts D. G. A. L.
- 3.052 **Characterization of the thermotropic phase behavior and microscopic structure of a confined discotic liquid crystal**
Sentker K., Yildirim A., Lippmann M., Hofmann T., Kityk A., Schönhals A., Huber P.
- 3.053 **Confinement-induced topological defects in a tetratic liquid crystal**
de las Heras D., Renner J., González-Pinto M., Borondo F., Martínez-Ratón Y., Velasco E.
- 3.054 **Percolation theory of aligned polydisperse carbon nanotubes in composite materials**
Finner S. P., van der Schoot P.
- 3.055 **Topological formations in chiral nematic droplets**
Posnjak G., Čopar S., Mušević I.
- 3.056 **Dislocations in blue phases**
Wang S., Ravnik M., Žumer S.
- 3.057 **Development of coarse grained models for chromonic liquid crystals**
Potter T. D., Tasche J., Barrett E., Walker M., Wilson M. R.
- 3.058 **Role of the anchoring energy on the texture of cholesteric droplets: finite element simulations and experiments**
Poy G., Bunel F., Oswald P.
- 3.059 **Isotropic and nematic liquid crystalline phases of 2-state rotaxane switch**
He H., Sevick E. M., Williams D. R. M.
- 3.060 **Waveguiding with liquid crystal director profiles**
Bregar A., Ravnik M.
- 3.061 **Liquid crystal gyroids as photonic crystals**
Aplinc J., Štimulak M., Čopar S., Ravnik M.
- 3.062 **Compensated cholesterics of helical mesogens: insights from simple microscopic models**
Wensink H. H., Ruzicka S., Ferreiro-Córdova C.

- 3.063 **Impact of CdSe-ZnS quantum dots upon the nematic liquid crystalline orientational order**
Kyrou C., Kralj S., Raptis Y. S., Nounesis G., Lelidis I.

Topic 4: Polymers, Polyelectrolytes, Biopolymers

- 4.001 **Star - long chain mixtures: a novel coarse-graining approach**
Locatelli E., Capone B., Likos C. N.
- 4.002 **Condensation and demixing in solutions of DNA nanostars and their mixtures**
Locatelli E., Handle P. H., Likos C. N., Sciortino F., Rovigatti L.
- 4.003 **Structure of ionic microgels driven by an alternating electric field: theory, experiments and simulations**
Colla T. E., Likos C. N., Mohanty P. S., Schurtenberger P., Dhont J. K. G.
- 4.004 **Magnetically functionalized star-polymers**
Blaak R., Likos C. N.
- 4.005 **Equilibrium properties of DNA-dendrimers in electrolyte solutions**
Jochum C., Adžić N., Kahl G., Likos C. N.
- 4.006 **Magnetically Functionalized Star Polymers in Equilibrium and under Shear**
Toneian D., Blaak R., Kahl G., Likos C. N.
- 4.007 **Telechelic star polymer micelles under shear**
Gârlea I. C., Likos C. N.
- 4.008 **Closing a Gap - Polymer Ring Brushes pushed together: a DPD simulation study**
Jehser M., Likos C. N.
- 4.009 **Study of silica nanoparticles / polymer hydrogel nanocomposite**
Perrin E., Coudert F. X., Boutin A., Schoen M.
- 4.010 **Conformation evolution of hydrophobic polyelectrolyte in aqueous solution as a function of solvent quality: a SANS study**
Essafi W., Ben Mahmoud S., Boué F.
- 4.011 **Polymer brush/gold nanoparticle composite materials for the application as colorimetric sensors**
Kesal D., Krause P., von Klitzing R.
- 4.012 **Bimolecular reactions in stimuli-responsive nanoreactors**
Roa R., Kim W. K., Kanduč M., Angioletti-Uberti S., Dzubiella J.
- 4.013 **Association of alkali metal and tetraalkylammonium counterions to poly(thiophen-3-ylacetate) as seen by NOESY NMR spectroscopy and molecular dynamics**
Hostnik G., Podlipnik Č., Mériguet G., Bren U., Ancian B., Cerar J.
- 4.014 **Weak Intramolecular Complexation within Star-like Copolymers: A Generic Model**
Hebbeker P., Steinschulte A. A., Plamper F. A., Schneider S.
- 4.015 **Colloidal stability and reversible aggregation of oxidized tannins**
Millet M., Zanchi D., Poupard P., Le Quéré J., Guyot S.
- 4.016 **Evolution and Correlation of Morphology and Mechanical Properties in Polymorphic Phases of PVDF**
Suresh G., Mallikarjunachari G., Ghosh P., Satapathy D. K.
- 4.017 **Comparison between micro- and macro-scale kinetics of water sorption in textile fibers**
Glavan G., Kurečić M., Maver U., Stana-Kleinschek K., Drevenšek-Olenik I.

- 4.018 **Elastomeric PDMS stiffness influence on adhesion, culture and mechanics of endothelial cells**
Iturri J., Miholich J., Zemljic S., Toca-Herrera J. L.
- 4.019 **Coarse-grained Mie force field for the molecular dynamics simulation of water - polyethylene glycol systems**
Lindeboom T., Galindo A., Jackson G.
- 4.020 **Temperature phase behaviour of PMEO₂MA-b-POEGMA₃₀₀ co-polymer in water by molecular dynamics**
Tatlipinar H., Dalgakiran E.
- 4.021 **Statistical theory of co-nonsolvency: comparison with MD simulation results**
Budkov Y. A., Kolesnikov A. L.
- 4.022 **Light induced patterning in transparent polydiene solutions**
Bogris A., Burger N., Fytas G., Loppinet B.
- 4.023 **Polyelectrolyte Behavior of G-Quadruplex DNA Structures**
Tašić B., Drevenšek-Olenik I., Spindler L.
- 4.024 **Towards Predicting Protein Aggregation in Biopharmaceuticals**
Zidar M., Ravnik M., Kuzman D.
- 4.025 **Simulation and experimental analysis of the structure and antimicrobial activity of linear peptoids**
Woodhouse V. J., Bromley E., Wilson M. R.
- 4.026 **Universal criterion for designability of heteropolymers**
Cardelli C., Bianco V., Rovigatti L., Nerattini F., Tubiana L., Dellago C., Coluzza I.
- 4.027 **Designing highly specific probes with tunable affinity**
Nerattini F., Tubiana L., Cardelli C., Bianco V., Coluzza I.
- 4.028 **Towards Stable Water-in-Water Emulsions through Interfacial Adsorption of Polyelectrolytes**
Tromp R. H., Tuinier R., Vis M.
- 4.029 **On the mechanism of LCST and its variation with co-solvents in thermoresponsive polymer solutions**
Bharadwaj S., Kumar P. B. S., Komura S., Deshpande A. P.
- 4.030 **Modeling of pH-responsive polyelectrolyte solutions and gels**
Nová L., Uhlík F., Rud O. V., Košovan P., Borisov O. V., Richter T., Holm C.
- 4.031 **Open Boundary Molecular Dynamics of Star-Polymer Melts**
Praprotnik M., Sablić J., Delgado-Buscalioni R.
- 4.032 **Process-directed self-assembly of copolymer materials**
Müller M., Sun D. W.
- 4.033 **Temperature responses of polymer mediated interactions**
Forsman J., Xie F., Woodward C. E.
- 4.034 **Tube Concept for Entangled Stiff Fibers Predicts Their Dynamics in Space and Time**
Leitmann S., Höfling F., Franosch T.
- 4.035 **Chirality-mediated interaction between knots on tensioned polymers**
Potestio R.
- 4.036 **Non-monotonous polymer translocation time: an analytical perspective**
Malgaretti P., Bianco V.

- 4.037 **Diffusion of a protein: the role of fluctuation-induced hydrodynamic coupling**
Illien P., Golestanian R.
- 4.038 **Confinement effects in biopolymer thin films**
Pradipkanti L., Satapathy D. K.
- 4.039 **Mechanism of chain collapse of strongly charged polyelectrolytes**
Tom A. M., Vemparala S., Rajesh R., Brilliantov N. V.
- 4.040 **A coarse-grained dsDNA model optimized for electrokinetic applications**
Weik F., Holm C., Rau T.
- 4.041 **Bayesian optimization of coarse-grain molecular models by statistical trajectory matching**
Dequidt A., Solano Canchaya J. G., Goujon F., Malfreyt P.
- 4.042 **Modeling of Polyelectrolyte Adsorption from Micellar Solutions onto Biomimetic Substrates**
Léonforte F., Banerjee S., Cazeneuve C., Baghdadli N., Ringeissen S., Leermakers F. A. M., Luengo G. S.
- 4.043 **Hydration Effects Turn a Highly Stretched Polymer from an Entropic into an Energetic Spring**
Liese S., Gensler M., Krysiak S., Schwarzl R., Hugel T., Rabe J. P., Netz R. R., Achazi A.
- 4.044 **Local pH of linear weak polyelectrolytes**
Nová L., Uhlík F., Košovan P.
- 4.045 **Droplet model to investigate watermark defects in immersion lithography**
van der Heijden T. W. G., Darhuber A. A., Harting J. D. R., van der Schoot P.
- 4.046 **Mechanical properties of bimodal gels under tension**
Kamerlin N., Elvingson C.
- 4.047 **Molecular simulations of functionalised copolymers in bulk and in confinement: uncovering the role of functional-group distribution**
Apóstolo R. F. G., Camp P. J., Dowding P. J., Schwarz A. D., Cattoz B. N.
- 4.048 **Universal shape properties of mesoscopic polymer chains, polymer stars and their aggregates**
Kaliuzhnyi O., Ilnytskyi J., Holovatch Y., von Ferber C.
- 4.049 **Inhibition of self-replication of protein fibrils**
Curk S., Micheals T. C. T., Frenkel D., Knowles T. P. J., Šarić A.
- 4.050 **Improving the coupling between Molecular Dynamics and Lattice Boltzmann**
Tretyakov N., Dünweg B.

Topic 5: Colloids

- 5.001 **Ferromagnetic phases in colloidal suspensions**
Zarubin G., Bier M.
- 5.002 **Hierarchical self-assembling of colloidal hard hemispheres**
Lei Q., Ni R.
- 5.003 **Colloidal suspensions in one-phase mixed solvents under shear flow**
Barbot A., Araki T.
- 5.004 **Electrostatic interaction between colloids at a liquid interface**
Majee A., Bier M., Dietrich S.

- 5.005 **Model-dependent phase behavior of hard and soft particle mixtures**
Dhumal U., Erigi U., [Tripathy M.](#)
- 5.006 **Colloidal grain boundary loops: creation, shrinkage, and condition of existence**
[Lavergne F. A.](#), Curran A., Aarts D. G. A. L., Dullens R. P. A.
- 5.007 **Direct observation of dislocation and particle dynamics during grain boundary migration**
[Lavergne F. A.](#), Curran A., Aarts D. G. A. L., Dullens R. P. A.
- 5.008 **Liquid-state approaches to protein solutions: from protein phase behaviour to the second virial coefficient**
Platten F., [Hansen J.](#), Wagner D., Egelhaaf S. U.
- 5.009 **Electrophoretic mobility of low salt aqueous charged sphere suspensions**
[Botin D.](#), Palberg T.
- 5.010 **Dramatic influence of anisotropic interactions on short time diffusion and arrest of protein solutions**
[Myung J. S.](#), Winkler R. G., Gompper G., Schurtenberger P., Stradner A.
- 5.011 **Double layer structure of topological colloids**
[Everts J. C.](#), Ravnik M.
- 5.012 **Crowding and interaction effects in multi-component diffusion-controlled reactions**
[Roa R.](#), Siegl T., Lin Y., Dzubiella J.
- 5.013 **Elasticity, structure and kinetics in binary microgel systems**
[Immink J.](#), Maris E., Månsson L., Crassous J. J., Stenhammar J., Schurtenberger P.
- 5.014 **Dynamic assembly of magnetic colloidal vortices**
[Dobnikar J.](#), Mohorić T., Kokot G., Osterman N., Snezhko A., Vilfan A., Babić D.
- 5.015 **Freezing monolayers of colloidal particles in water**
[Chen S.](#), Pei K., Dullens R. P. A., Aarts D. G. A. L.
- 5.016 **Screw-dislocation handedness driven by growth rate in chiral colloidal self-assemblies**
[Grelet E.](#), Sung B., de la Cotte A.
- 5.017 **Effective interaction potentials in binary mixtures of thermoresponsive microgels**
[Bergman M.](#), Obiols-Rabasa M., Meijer J. M., Gnan N., Zaccarelli E., Schurtenberger P.
- 5.018 **Two dimensional melting of deformable particle systems**
[Pica Ciamarra M.](#), Li Y.
- 5.019 **Two-dimensional non-close-packed nematic colloidal assemblies and their electrical response**
Tamura Y., [Kimura Y.](#)
- 5.020 **Investigation of thermo-responsive microgels at flat liquid-liquid interfaces: Connection between microgel softness and monolayer properties**
[Bochenek S.](#), Richtering W.
- 5.021 **On the propensity of inverse patchy colloids to self-organize in stable, lamellar structures**
[Kahl G.](#), Bianchi E., Gonzalez Noya E., Ferrari S.
- 5.022 **Formation of Laves Phases in Repulsive and Attractive Hard Sphere Suspensions**
Schaertel N., Palberg T., [Bartsch E.](#)

- 5.023 **Colloidal aggregates of tricationic porphyrin on inorganic polyphosphate**
Ryazanova O., Zozulya V., Voloshin I., Ilchenko M., Dubey I., Glamazda A., Karachevtsev V.
- 5.024 **Sorption and spatial distribution of protein globules in charged hydrogel particles**
Adroher-Benítez I., Moncho-Jordá A., Dzubiella J.
- 5.025 **Hydrophobically-coated gold nanoparticles: from interaction to superlattices**
Pansu B., Hajiw S., Imperor-Clerc M., Schmitt J.
- 5.026 **Diffusion and Arrest of Ellipsoidal Particles in the Presence of an External Field**
Pal A., Martinez V. A., Ito T., Arlt J., Crassous J. J., Poon W. C. K., Schurtenberger P.
- 5.027 **Phase behaviour and gravity-directed self-assembly of spherical caps**
McBride J. M., Avendaño C.
- 5.028 **First passage times in a model membrane channel**
Thorneywork A. L., Gladrow J., Tan Y., Keyser U.
- 5.029 **Drying-mediated deposit patterns in dilute colloid-polymer suspensions**
Kim J. Y., Ryu S., Kim S. Y., Weon B. M.
- 5.030 **Hard X-ray nanotomography of randomly packed colloidal particles**
Kim Y., Lim J., Weon B. M.
- 5.031 **Microgels in computer simulations**
Minina E., Kantorovich S. S., Likos C. N.
- 5.032 **Exploring a new class of effective interactions in crowded environment**
Gnan N., Garcia N. A., Zaccarelli E.
- 5.033 **State of the art of the interaction between cytolytic proteins and lipid-cholesterol bilayers**
Moreno-Cencerrado A., Tharad S., Bogataj T., Iturri J., Toca-Herrera J. L., Promdonkoy B., Krittanaï C.
- 5.034 **Effects of ligand mobility on self-assembly of hairy disks**
Rzysko W., Borowko M., Sokolowski S., Staszewski T.
- 5.035 **Vesicular structure formation of a triple-chain ion pair amphiphile**
Chang C. C., Su Y., Chang C. H.
- 5.036 **Colloidal Motion under the Action of a Thermophoretic Force**
Burelbach J., Zupkauskas M., Lamboll R., Eiser E.
- 5.037 **Adsorption of soft particles at supported lipid bilayer**
Wang M., Dabkowska A. P., Crassous J. J., Sparr E.
- 5.038 **Colloidal crystal size evaluation: Scherrer vs. Laue**
Heidt S., Jung G., Hofmann M., Palberg T.
- 5.039 **On the interaction of dipolar filaments**
Spiteri L., Messina R.
- 5.040 **Heterogeneous Dynamics of concentrated PNIPAm core-shell systems**
Frenzel L., Lehmkuhler F., Lokteva I., Grübel G.
- 5.041 **Forces between similar and disimilar interfaces in solutions of the multivalent ions**
Moazzami-Gudarzi M., Adam P., Trefalt G., Szilágyi I., Maroni P., Borkovec M.
- 5.042 **Thermo-optical trapping and manipulation of individual nanoparticles**
Stergar J., Osterman N.

- 5.043 **Eutectic Crystal Structures in Binary and Ternary Charged Colloids due to Depletion Attraction**
Toyotama A., Yamanaka J., Okuzono T.
- 5.044 **pH reversible encapsulation of oppositely charged colloids mediated by polyelectrolytes**
Guo Y., van Ravensteijn B. G. P., Evers C. H. J., Kegel W. K.
- 5.045 **Pressure mediated phase transition in phoretic nematic colloids**
 Pages-Casas J., Straube A. V., Tierno P., Ignés-Mullol J., Sagués F.
- 5.046 **Synthesis of bi-functional Janus colloids**
Chang F., Kegel W. K.
- 5.047 **Microscopy of colloidal particles at an oil/water interface with an external electric field**
Rogier F., Ern  B. H., Kuipers B., Kegel W. K.
- 5.048 **Static structure factor for a fluid with interaction of hard spheres plus two Yukawa tails**
Herrera-Pacheco N., Cruz-Vera A., Escobar-Ortega Y.
- 5.049 **The stability of high concentration whey protein systems and the influence of pH and salt**
Grace M., Brodkorb A., Rooney D., Fenelon M., McManus J. J.
- 5.050 **Spatial confinement governs orientational order in one-patch particles**
Iwashita Y., Kimura Y.
- 5.051 **Density dependence of orientational order in one-patch particles**
Iwashita Y., Kimura Y.
- 5.052 **Adsorption and Crystallization of Charged Colloids on Polymer Modified Glass Substrates**
Aoyama Y., Toyotama A., Okuzono T., Yamanaka J.
- 5.053 **Modulating protein-protein interactions in high concentration protein formulations**
Jacobs M. R., Mittag J. J., James S., McManus J. J.
- 5.054 **Dynamics of Charged Colloids in Inhomogeneous Concentration Fields**
Seki T., Okuzono T., Toyotama A., Yamanaka J.
- 5.055 **Fractal Nematic Colloids**
Jagodi  U., Hashemi S. M., Mozaffari M. R., Ejtahadi M. R., Mu ević I., Ravnik M.
- 5.056 **Optically Transparent Dense Colloidal Gels**
Zupkauskas M., Lan Y., Joshi D., Ruff Z., Eiser E.
- 5.057 **Aggregation and phase transition of colloids induced by optical tweezers and thermophoresis**
Bruot N., Tanaka H.
- 5.058 **One-dimensional fluids with second nearest-neighbor interactions**
 Fantoni R., Santos A.
- 5.059 **Structural properties of the Jagla fluid**
 L pez De Haro M., Rodr guez-Rivas A., Yuste S. B., Santos A.
- 5.060 **Anisotropic colloidal systems as models for island formation in monolayer growth**
Camargo M., Gonz lez D. L.

- 5.061 **Effect of polymer addition on a colloidal model for CSH aggregation**
Álvarez C. E., Camargo M.
- 5.062 **Screening, hyperuniformity, and instability in the sedimentation of irregular objects**
Diamant H., Goldfriend T., Witten T.
- 5.063 **Microscopic engine powered by critical demixing**
Schmidt F., Magazzù A., Callegari A., Biancofiore L., Cichos F., Volpe G.
- 5.064 **Equilibrium and dynamical density functional theory in the canonical ensemble**
de las Heras D., Brader J. M., Fortini A., Schmidt M.
- 5.065 **Self-assembly and magnetization of colloidal magnetic tubes**
Stanković I.
- 5.066 **Interplay between self-assembly and condensation in models with asymmetric patches**
Tavares J. M., Teixeira P. I. C.
- 5.067 **Thermo-reversible colloidal gels from fluorinated particles**
Buzzaccaro S., Lattuada E., Canova C. T., Moscatelli D., Piazza R.
- 5.068 **Effective interactions between Janus particles in critical solvents**
Labbé-Laurent M., Dietrich S.
- 5.069 **Dipolar colloids: From filaments to helices**
Messina R., Spiteri L., Stanković I.
- 5.070 **How roughness affects the depletion mechanism**
Anzini P., Parola A.
- 5.071 **Direct Measurement of Thermodynamic Properties of Dense 2D Colloidal Fluids using a Repulsive Optical Landscape**
Stones A. E., Lavergne F. A., Curran A., Dullens R. P. A., Aarts D. G. A. L.
- 5.072 **Dynamics of polydisperse colloidal systems: a mean-field lattice-gas theory**
de Castro P., Sollich P.
- 5.073 **Dynamical density functional theory for colloid-polymer mixtures**
Stopper D., Roth R., Hansen-Goos H.
- 5.074 **Motion in diffusivity landscapes: Towards analytic correlation functions**
Roosen-Runge F., Bicout D., Barrat J. L.
- 5.075 **Chiral Colloids from Isotropic Spheres**
Ouhajji S., van Ravensteijn B. G. P., Fernández Rico C., Philipse A. P., Petukhov A. V.
- 5.076 **Iterative Reconstruction of Memory Kernels**
Jung G., Schmid F.
- 5.077 **Structures of Binary Colloidal Mixtures in Emulsion Droplets**
Mravlak M., Schilling T., Kister T., Kraus T.
- 5.078 **The chimera state in small arrays of colloidal phase oscillators**
Hamilton E., Bruot N., Cicuta P.
- 5.079 **Free Energy Calculation of Colloidal Crystals. Application to Low Temperature Phases of the Lennard-Jones System**
Calero C., Knorowski C., Travasset Å.
- 5.080 **Single-File Escape of Colloidal Particles from Microfluidic Channels**
Locatelli E., Pierno M., Baldovin F., Orlandini E., Tan Y., Pagliara S.

- 5.081 **Defects in simple cubic crystals: Revealing the vacancy-analogue of the crowdfion interstitial**
van der Meer B., van Damme R., Smalenburg F., Dijkstra M., Filion L.
- 5.082 **Two-step melting in Two Dimensions with Long-ranged forces**
Kapfer S., Krauth W.
- 5.083 **From a driven passive to an active colloid in spatially periodic potentials**
Straube A. V., Höfling F.
- 5.084 **Chains and Rings in Dipolar Fluids**
Ronti M., Rovigatti L., Tavares J. M., Ivanov A. O., Kantorovich S. S., Sciortino F.
- 5.085 **Glassy orientational dynamics in plastic crystals of aspheric colloids**
Karner C., Burian M., Dellago C., Lechner R. T.
- 5.086 **Dynamic Pair Correlations and Superadiabatic Forces in a Dense Brownian Liquid**
Schindler T., Schmidt M.
- 5.087 **Phase transitions on the surface of a sphere**
Law J. O., Wong A., Kusumaatmaja H., Miller M. A.
- 5.088 **Crystallization of star polymer under shear flow**
Ruiz-Franco J., Marakis J., Lettinga M. P., Gnan N., Vlassopoulos D., Zaccarelli E.
- 5.089 **Structure formation in soft nanocolloids: Liquid-drop model**
Doukas A. K., Likos C. N., Zihlerl P.
- 5.090 **Phase diagram of soft nanoparticles at interface**
Doukas A. K., Zihlerl P.
- 5.091 **Elasticity of soft nanocolloidal crystals**
Frontini J., Zihlerl P.
- 5.092 **A model colloidal microphase former with anisotropic competing interactions**
Stopper D., Roth R.
- 5.093 **Exact results for the counter-ion condensation in two-dimensions**
Téllez G., Mallarino J. P.
- 5.094 **A model of self-electrophoresis of isotropic colloidal particles with chemical reactions**
Okuzono T., Seki T., Toyotama A., Yamanaka J.
- 5.095 **Crystallization of ultra-soft particles on periodic substrates: A systematic density functional theory study of surface-induced phase transitions**
Kraft A., Klapp S. H. L.
- 5.096 **Force linearization closure for noisy systems with time-delay**
Loos S. A. M., Klapp S. H. L.
- 5.097 **Comparison of different methods for calculating effective interactions and pressure in charge-stabilized dispersions**
Brito M., Riest J., Denton A., Nägele G.
- 5.098 **Effective potential and crystallization by depletion effect in binary hard-sphere systems**
Suematsu A., Yoshimori A., Akiyama R.
- 5.099 **Melting, growth and surfaces of colloidal quasicrystals**
Martinsons M., Schmiedeberg M.

- 5.100 **Depletion interaction in charged colloidal systems: excluded volume and electrostatic coupling**
Reščič J.
- 5.101 **Melting upon cooling and freezing upon heating: Fluid-solid phase diagram for Shvejk-Hashek model of dimerizing hard spheres**
Kalyuzhnyi Y. V., Jamnik A., Cummings P. T.
- 5.102 **Phase transitions of the one component plasma with inverse power law interactions**
Salazar R., Mazars M.
- 5.103 **One-component log-gas: Exact Expansion of the pair correlation function for Odd Values of $\Gamma/2$**
Salazar R., Téllez G.
- 5.104 **Towards a realistic description of computer-generated nano- and microgels: assembly protocol, form factors, density profiles and swelling curves of single soft particles**
Rovigatti L., Gnan N., Zaccarelli E.
- 5.105 **The Second Virial coefficient of the Mie Potential and predictions of the critical temperature for short range attractive potential fluids.**
Heyes D. M., Pieprzyk S., Branka A. C., Rickayzen G.
- 5.106 **Morphological transition of adsorbed aggregates and micelles onto a gold surface**
Llombart P., Alcolea Palafox M., Guerrero-Martínez A., MacDowell L. G.
- 5.107 **Equation of state for short-range square-well potentials**
Herrera-Pérez D., Sastre F., Benavides A. L.
- 5.108 **Transitions between ordered and disordered phases of patchy particles in two dimensions**
Wagner S., Kahl G., Gonzalez Noya E.
- 5.109 **Colloidal Dynamics in Random Potential Energy Landscapes**
Zunke C., Bewerunge J., Platten F., Egelhaaf S. U.
- 5.110 **The Constant Force Continuous Molecular Dynamics for potentials with multiple discontinuities**
Padilla L. A., Benavides A. L.
- 5.111 **The effect of Brownian fluctuations on the behaviour of self-orienting dumbbell particles driven by an external flow in a microchannel**
Fiorucci G., Padding J., Dijkstra M.
- 5.112 **Phase behaviour of colloidal rod-sphere mixtures**
Kennedy C. L., van Blaaderen A.
- 5.113 **Universal self-assembly of one-component three-dimensional decagonal and dodecagonal quasicrystals**
Ryltsev R., Chetchelatchev N.
- 5.114 **Elastic behavior of crystals of charged colloids close to melting**
Smallenburg F., Löwen H.
- 5.115 **Magneto-optically driven colloidal microrheometer**
Ortiz-Ambriz A., Tierno P.
- 5.116 **Self-assembly of patchy nanoparticles with various patch arrangements using molecular simulation**
Kobayashi Y., Arai N., Nomura K.

Topic 6: Films, Foams, Surfactants, Emulsions

- 6.001 **Effect of molecules which have a core and an alkyl chain on lipid bilayers**
Usuda H., Hishida M., Yamamura Y., Saito K.
- 6.002 **Influence of formulation on the oxidative stability of water-in-oil emulsions**
Essafi W., Dridi W., Toutain J., Sommer A., Leal Calderon F., Cansell M.
- 6.003 **A conductimetric study of alkyl carboxylate surfactants as a function of length chain, counter-ions and temperature. Interpretation below and above the critical micellar concentration using a transport theory.**
Durand-Vidal S., Bernard O., Medoš Ž., Bešter-Rogač M.
- 6.004 **Theory of spreading and contraction behavior of benzene drop on water**
Emelyanenko K. A., Emelyanenko A. M., Boinovich L. B.
- 6.005 **Ultra-slow dynamic surface tension of surfactants induced by salts**
Qazi M., Schlegel S., Backus E., Bonn M., Bonn D., Shahidzadeh N.
- 6.006 **Stabilization of food-grade oil-in-water emulsions by chitosan-modified nanoparticles as a function of pH**
Alison L., Demirörs A., Tervoort E., Teleki A., Studart A. R.
- 6.007 **Outstanding stability of free-standing co-polymer films above the glass transition – an interfacially-driven micro-phase separation?**
Kaushal M., Gaillard T., Rio E., Poulard C., Scheid B., Davidson P., Roché M., Drenckhan W.
- 6.008 **Surface and interfacial activity of pH-responsive surfactant-free amphiphilic Janus nanoparticles**
Honciuc A., Wu D.
- 6.009 **Photoregulating the self-assembly of lipophilic guanosine derivatives at the air-water interface**
Ličen M., Čoga L., Masiero S., Drevenšek-Olenik I.
- 6.010 **When is a surface foam-phobic?**
Teixeira M. A. C., Arscott S., Cox S. J., Teixeira P. I. C.
- 6.011 **Formation of long thread-like micelles and association of functionalised nanoparticles: A large-scale molecular dynamics study**
Gujt J., Bešter-Rogač M., Spohr E.
- 6.012 **What determines the value of the surface tension at the critical micelle concentration?**
Blokhuis E. M.
- 6.013 **Coarsening and mechanics in the bubble model for wet foams**
Khakalo K., Puisto A., Baumgarten K., Tighe B. P.
- 6.014 **A theoretical Model of the frame-guided Assembly Process**
Raschke S., Heuer A.
- 6.015 **The non-equilibrium surface growth of anisotropically interacting patchy particles**
Martynek T., Klapp S. H. L.

Topic 7: Confined Fluids, Interfacial Phenomena

- 7.001 **PYTIM: a Multi-Platform Software Package for Molecular Surface Analysis**
Sega M., Hantal G., Fábíán B., Jedlovský P.

- 7.002 **Distribution of the surface tension along the interface normal in various liquids**
Sega M., Fábián B., Horvai G., Jedlovsky P.
- 7.003 **Intrinsic and layer-by-layer properties of fluid interfaces**
Sega M.
- 7.004 **Spontaneous electrification of fluoropolymer-water interfaces probed by electrowetting**
Banpurkar A., Sawane Y., Wandhai S., Murade C., Siretanu I., van den Ende D., Mugele F.
- 7.005 **Toroidal seeds for investigation of heterogeneous crystal nucleation of colloids**
Blatman D., Chang Y. W., Fragkopoulos A. A., Ellis P. W., Gasser U., Fernandez-Nieves A.
- 7.006 **Anomalous Diffusion in Crowding Biomimetic Confinements**
Watanabe C., Yanagisawa M.
- 7.007 **Predictive modeling of molecular self-assembly at an electrochemical solid-liquid interface**
Hartl B., Kahl G., Cui K., De Feyter S., Walter M., Mertens S. F. L.
- 7.008 **Effects of water dissolution on the dispersion forces in nanosized alkane**
Emelyanenko K. A., Emelyanenko A. M., Boinovich L. B.
- 7.009 **Responsive surface coating with magneto-elastic filaments**
Dobnikar J., Wei J.
- 7.010 **Estimating Differential Capacitance of the Electric Double Layer in Ionic Liquids using Computer Simulations**
Voroshlyova I. V., Mišin M., Ivaništšev V., Lembinen M., Pereira C. M., Cordeiro M. N. D. S.
- 7.011 **Evaporation and boiling in thin gap**
Matsumoto M., Ogawa K., Xu D., Yasumoto Y.
- 7.012 **Coarse-grained molecular simulations for semi-flexible polyelectrolyte brush**
Washizu H.
- 7.013 **Dynamics of a colloidal Particle near a Gas-Liquid Interface**
Villa S., Stocco A., Blanc C., Nobili M.
- 7.014 **T-ramp tracking of colloids with controlled adsorption on flat substrate**
Boniello G., Marie E., Tribet C., Croquette V., Zanchi D.
- 7.015 **Crowdedness of fluids in confinement**
Qiao C. Z., Zhao S. L., Liu H. L., Dong W.
- 7.016 **Co-assembly of amphiphilic Janus disks and small molecules in two-dimensional systems**
Borowko M., Rzyśko W., Sokolowski S., Staszewski T.
- 7.017 **Field-driven population inversion in a confined colloidal mixture: following the time evolution by Langevin dynamics simulation**
Amokrane S., Chung S., Samin S., Holm C., Malherbe J. G.
- 7.018 **Explaining the Cassie-Wenzel transition with X-ray microscopy**
Lim S. J., Kim Y., Jeong S., Kim D., Ryu S., Pang C., Weon B. M.
- 7.019 **Three-dimensional force balance of asymmetric droplets**
Kim Y., Lim S. J., Weon B. M.
- 7.020 **Nano-Mechanics with the force feedback microscope: from capillary bridge dynamics to noncontact indentation**
Rodrigues M. S., Carpentier S., Vitorino M. V., Costa L., Charlaix E., Chevrier J.

- 7.021 **Drop impacts onto mobile and fixed particles rafts**
Planchette C., Biance A. L., Lorenceau E.
- 7.022 **Study of intercalation complexes of kaolinite with primary intercalation reagents**
Kristóf T., Sarkadi Z., Ható Z.
- 7.023 **Using nanopores as sensors: a Monte Carlo modeling study**
Valiskó M., Máдай E., Boda D.
- 7.024 **Multiscale modeling of rectifying bipolar nanopore: explicit-water versus implicit-water simulations**
Valiskó M., Ható Z., Kristóf T., Gillespie D., Boda D.
- 7.025 **Droplets, capillary interactions and self-assembly from the equilibrium shape of fluid-fluid interfaces**
Soligno G., Dijkstra M., van Roij R.
- 7.026 **Magnetically tunable wettability of soft magnetoactive elastomers**
Glavan G., Salamon P., Belyaeva I. A., Shamonin M., Drevenšek-Olenik I.
- 7.027 **Melting scenarios and unusual crystal structures in two-dimensional core-softened potential systems**
Ryzhov V. N., Fomin Y. D., Kruchkov N., Tsiok E. N., Yurchenko S. O.
- 7.028 **Structural forces acting between negatively charged surfaces in micellar solutions studied by CP-AFM**
Ludwig M., Schoen S., von Klitzing R.
- 7.029 **Leidenfrost effect dynamics with conical surfaces**
Escobar-Ortega Y., Herrera-Pacheco N., Pacheco-Vázquez F.
- 7.030 **Hertzian disks system: phase diagrams and melting scenario**
Tsiok E. N., Fomin Y. D., Gaiduk E., Ryzhov V. N.
- 7.031 **Selectivity of large hard sphere on a hard wall immersed in binary hard-sphere fluid**
Oshima A., Chiba A., Akiyama R.
- 7.032 **Application of design of experiments to coarse-grained molecular dynamics simulations: wettability of liquid resins**
Ito H., Matsumoto S., Suzuki T., Sugii T., Terasaki T., Moriya H.
- 7.033 **Experimental studies on the detachment of multiwalled carbon nanotubes by a mobile liquid interface**
Ahlskog M., Hokkanen M., Lautala S.
- 7.034 **The study on the confinement effect of self-assembly process and structure in surfactant solution using coarse-grained molecular simulation**
Yoshimoto Y., Arai N.
- 7.035 **Cavitation within a liquid micro-confined by a porous hydrogel**
Scognamiglio C., Magaletti F., Izmaylov Y., Gallo M., Casciola C. M., Noblin X.
- 7.036 **Contact angle of spheres floating at air-water interfaces by solving the Young-Laplace equation**
Garrido P. F., Rubio M. A., Domínguez-García P.
- 7.037 **Hydration forces in water nanofilms confined between calcium carbonate surfaces**
Svaland G. B., Bresme F.
- 7.038 **Study of the kinetic effects in homogeneous and heterogeneous bubble cavitation via atomistic simulations**
Marchio S., Giacomello A., Meloni S., Casciola C. M.

- 7.039 **Simulating cavitation in hydrophobic nanopores: the effect of the line tension**
Tinti A., Giacomello A., Casciola C. M.
- 7.040 **The Salvinia prototype: stability and recovery of superhydrophobicity on nanotextured surface in submerged conditions**
Amabili M.
- 7.041 **Theoretical Principles of Self-Recovery Superhydrophobic Surfaces**
Meloni S.
- 7.042 **Electric double layer in electrode slit pores. Grand canonical Monte Carlo simulation at constant electrode potential**
Lamperski S.
- 7.043 **Electric Double Layer for Charged Hard Spheres With an Off-center Charge**
Henderson D., Bhuiyan L. B., Lamperski S.
- 7.044 **Liquid drops on surfaces: using density functional theory to calculate the binding potential and drop profiles and comparing with results from mesoscopic modelling**
Archer A. J., Hughes A. P., Yin H., Sibley D. N., Thiele U.
- 7.045 **Solvent fluctuations around solvophobic, solvophilic and patchy nanostructures and the accompanying solvent mediated interactions**
Archer A. J., Chacko B., Evans R.
- 7.046 **Non-equilibrium interfaces in fluids**
Bier M.
- 7.047 **Phase diagram and critical phase transitions of driven granular matter in quasi 2d**
Schindler T., Kapfer S.
- 7.048 **The magic numbers of equal spheres on triply periodic minimal surfaces**
Dotera T., Tanaka H., Takahashi Y.
- 7.049 **Phase separation under gravity: sample height and non-equilibrium**
Geigenfeind T., de las Heras D., Schmidt M.
- 7.050 **Diffusion in Quasi-One Dimensional Channels: A Small System Isobaric-Isothermal (n, p, T) Transition State Theory for Hopping Times**
Ahmadi S., Bowles R. K.
- 7.051 **Thin Films of Anisotropic Particles: Equilibrium and Growth**
Dixit M., Klopotek M., Shreiber F., Oettel M., Schilling T.
- 7.052 **Boundary conditions and correlation functions for Stokes' law**
Yoshimori A.
- 7.053 **Tricritical Casimir forces and order parameter profiles in wetting films of ^3He - ^4He mixtures**
Farahmand Bafi N., Maciolek A., Dietrich S.
- 7.054 **Onset of anomalous diffusion in colloids confined to quasi-monolayers**
Bleibel J., Dominguez A., Oettel M.
- 7.055 **Solvent mediated forces in critical fluids**
Anzini P., Parola A.
- 7.056 **Drag coefficient of a raft-like domain having the membrane viscosity different from the one outside the domain**
Tani H., Ohtsuka Y., Fujitani Y.

- 7.057 **Dynamical behavior of hydrated water molecules between phospholipid membranes**
Yamada T., Takahashi N., Tominaga T., Takata S., Seto H.
- 7.058 **Transient Casimir forces from quenches in thermal and active matter**
Rohwer C. M., Krüger M., Kardar M.
- 7.059 **Interaction of inclusions in overheated free-standing smectic films**
Pikina E. S., Ostrovskii B. I.
- 7.060 **Enhanced wavelength-dependent surface tension of liquid-vapour interfaces**
Höfling F., Dietrich S.
- 7.061 **Solid-liquid interfacial premelting and droplet spreading**
Laird B. B., Yang Y.
- 7.062 **Temperature dependence of surface tension of 1-butanol aqueous solution**
Sakaguchi Y., Kaneko T., Ueno I.
- 7.063 **Stretching of viscoelastic drops by steady sliding**
Pierno M., Varagnolo S., Filippi D., Mistura G., Sbragaglia M.
- 7.064 **Critical adsorption on a line defect**
Parisen Toldin F., Assaad F. F., Wessel S.
- 7.065 **Electrolytes between dielectric charged surfaces: Simulations and theory**
Pereira Dos Santos A., Levin Y.
- 7.066 **Analytical theory for colloids on spherical surfaces**
Marechal M., Gimperlein M., Mecke K.
- 7.067 **Confined interfaces at the nanoscale: continuous thermodynamics and line tension**
Bey R., Picard C., Charlaix E., Coasne B.
- 7.068 **Additive Modified Crystallization in Binary Lennard Jones System**
Sen Gupta B., Radu M., Kremer K.
- 7.069 **Origin of the hydration force between phospholipid membranes**
Schlaich A., Daldrop J. O., Kowalik B., Kanduč M., Schneck E., Netz R. R.
- 7.070 **Fluid-Solid Interactions in Nanoporous Media: From Vapour Condensation-Induced Deformations and Capillarity-Driven Transport to Switchable Imbibition**
Huber P.
- 7.071 **Molecular simulation of aqueous electrolytes in nanoporous carbons: Blue Energy and water desalination**
Ganfoud N., Simoncelli M., Salanne M., Haefele M., Rotenberg B.
- 7.072 **Critical drying of liquid water at a hydrophobic surface**
Wilding N., Stewart M., Evans R.
- 7.073 **Interplay between the critical Casimir and dispersion forces in ellipsoid/sphere - plate systems immersed in non-polar fluid**
Valchev G., Dantchev D.
- 7.074 **The effect of spatial confinement on the phase behavior of Heisenberg fluids**
Wandrei S. M., Schoen M.
- 7.075 **Friction at the interface between solid self-assembled monolayers and liquid polymers or solid metal nanotips**
McGraw J.
- 7.076 **Experimental study of snow and ice friction**
Canale L., Laborieux A., Niguès A., Cohen C., Clanet C., Siria A., Bocquet L.

- 7.077 **Mean-field theory of adsorption induced deformation of mesoporous materials**
Kolesnikov A. L., Georgi N., Möllmer J., Hofmann J., Adolphs J.
- 7.078 **Computing Thermo-Osmotic Slip**
Ganti R., Liu Y., Frenkel D.
- 7.079 **Molecular Simulations of Surfactant Adsorption and Self-assembly under Static and Shear Conditions**
Tsagkaropoulou G., Warrens C. P., Camp P. J.
- 7.080 **The influence of the topological defects in the two dimensional melting**
Mazars M., Salazar R.
- 7.081 **Non-equilibrium phase behavior of sheared confined molecular films under pressure using Nonequilibrium Molecular Dynamics**
Maćkowiak S., Pieprzyk S., Branka A. C., Heyes D. M., Dini D.
- 7.082 **Snap evaporation of droplets on smooth topographies**
Wells G. G., Ruiz-Gutiérrez É., Le Lirzin Y., Nourry A., Pradas M., Ledesma-Aguilar R.
- 7.083 **Curvature effects for multicomponent droplets**
Aasen A., Blokhuis E. M., Wilhelmsen Ø.

Topic 8: Supercooled Liquids, Glasses, Gels

- 8.001 **Higher-order correlations in glass- and crystal-forming complex liquids**
Lehmkuhler F., Schroer M. A., Fischer B., Grübel G.
- 8.002 **Low and high density liquid structures in the polarizable BK3 model of water**
Skvara J., Moucka F., Nezbeda I.
- 8.003 **TOApy program for investigation of the phase transitions**
Osiecka N., Massalska-Arodz M., Galewski Z.
- 8.004 **Shrinking water's no man's land in the intermediate pressure regime**
Stern J., Loerting T.
- 8.005 **Integral equation theories, configurational overlap, effective potential and the Random First Order Glass Transition**
Bomont J. M., Pastore G., Hansen J. P.
- 8.006 **Effect of temperature jump on physical aging of gelatin gels**
Maki Y., Katakai M., Watabe S., Dobashi T., Matsuo K.
- 8.007 **Intimate link between crystallization and glass transition**
Tanaka H., Russo J., Romano F.
- 8.008 **Revealing the structural origin of dynamic heterogeneity in glass-forming liquids**
Tong H., Tanaka H.
- 8.009 **The reversibility and first-order nature of liquid-liquid transition in a molecular liquid**
Kobayashi M., Tanaka H.
- 8.010 **A transient amorphous solid formed from low density aqueous charged sphere suspension**
Palberg T., Niu R., Heidt S., Hofmann M.
- 8.011 **Dynamical instability causes the demise of a supercooled tetrahedral liquid**
Gautam A. K., Pingua N., Goyal A., Apte P. A.

- 8.012 **Non-equilibrium self-assembly in cement hydration**
Dobnikar J., Ioannidou K., Kanduč M., Li L., Frenkel D., Del Gado E.
- 8.013 **Cosolute partitioning and gel permeability in swell-collapse transitions of random tetra-functional hydrogels**
Kim W. K., Roa R., Kanduč M., Dzubiella J.
- 8.014 **Nano-particle resolved studies of deeply supercooled liquids**
Hallett J. E., Turci F., Royall C. P.
- 8.015 **Combined Cononsolvency and Temperature Effects on PNIPAM Microgels in Bulk Phase and at Interfaces**
Backes S., Krause P., Nasilowska W., Witt M., Mukherji D., Kremer K., von Klitzing R.
- 8.016 **Fatigue in colloidal gels**
Verweij J. E., van Doorn J. M., Leermakers F. A. M., Sprakel J., van der Gucht J.
- 8.017 **Percolation threshold in the gelation process of DNA self-assembled structures**
Fernandez-Castanon J., Sciortino F.
- 8.018 **Thermodynamic anomalies and network topology in liquids**
Fijan D., Wilson M.
- 8.019 **Shape effects on the rheological behavior of polymer-grafted nanoparticles in solution**
Parisi D., Loppinet B., Ruan Y., Liu Y., Vlassopoulos D.
- 8.020 **Static structure of densified GeSe₂ glass**
Koura A., Shimojo F.
- 8.021 **Inhomogeneous local packing densities and bonding natures of melt-quenching Ni₆₇Zr₃₃ amorphous alloy**
Itoh K., Saida J., Otomo T.
- 8.022 **X-ray cross-correlation of supercooled water via coherent x-ray scattering**
Jain A., Lehmkuhler F., Grübel G.
- 8.023 **Gravity, Hydrodynamics and Fivefold Symmetry in Hard Sphere Nucleation Discrepancy**
Wood N., Russo J., Turci F., Royall C. P.
- 8.024 **Formation and characterisation of tough protein gels**
Moran L., Blumlein A., McManus J. J.
- 8.025 **Complex disorder in binary mixtures (Analysis of the thermodynamic factor)**
Primorac T., Sokolić F., Zoranić L., Munoz-Munoz Y. M., Požar M., Perera A., Vrabec J.
- 8.026 **Adiabatic Calorimetry Study of Surface-Induced Melting of Ice Confined in Controlled Porous Glass**
Podnek V., Voronov V.
- 8.027 **Percolation of Patchy Colloids on Patterned Substrates**
Treffenstädt L. L., Araújo N. A. M., de las Heras D.
- 8.028 **Glass Transition in Supercooled Liquids with Medium Range Crystalline Order**
Tah I., Sengupta S., Sastry S., Dasgupta C., Karmakar S.
- 8.029 **Common mechanism for the devitrification and ageing of hard sphere glasses**
Yanagishima T., Russo J., Tanaka H.
- 8.030 **Simple scenario for glass transition phenomena based on liquid-liquid transition framework**
Kajihara Y., Inui M., Chiba A.

- 8.031 **Controlling fragility from strong to fragile using an isotropic short-ranged pairwise potential**
Ozawa M., [Kim K.](#), Miyazaki K.
- 8.032 **Mermin-Wagner fluctuations in 2D amorphous solids**
Illing B., Fritsch S., Kaiser H., Klix C. L., Maret G., [Keim P.](#)
- 8.033 **Connectivity, Dynamics, and Structure in a Tetrahedral Network Liquid**
[Roldán-Vargas S.](#), Rovigatti L., Sciortino F.
- 8.034 **Identification of time-scales that support violation or preservation of Stokes-Einstein relation in supercooled water**
[Kawasaki T.](#), Kim K.
- 8.035 **Potential Energy Landscape of the TIP4P/2005 model and the water anomalies**
[Handle P. H.](#), Sciortino F.
- 8.036 **Coordination number statistics of cluster formation in 2D colloid-polymer mixtures**
[Mordan M. A.](#), Reynolds C. P., Sampson W. W., Aarts D. G. A. L., Dullens R. P. A.
- 8.037 **Releasing frustration for better relaxation**
[Turci F.](#), Crowther P., Tarjus G., Royall C. P.
- 8.038 **Shear thinning in glassy liquids**
[Furukawa A.](#)
- 8.039 **Theory of thermodynamics of freezing and melting**
[Pedersen U. R.](#), Costigliola L., Bailey N. P., Schröder T. B., Dyre J. C.
- 8.040 **Yield in Amorphous Solids: The Ant in the Energy Landscape Labyrinth**
[Regev I.](#), Lookman T.
- 8.041 **Selectivity of reactants through a thermoresponsive hydrogel**
[Kanduč M.](#), Chudoba R., Palczynski K., Kim W. K., Roa R., Dzubiella J.
- 8.042 **Mechanical response of ultrastable glasses**
[Ozawa M.](#), Ninarello A., Berthier L.
- 8.043 **Structural characterization of relaxation of supercooled tetrahedral liquids in terms of boat and chair rings**
[Pingua N.](#), Apte P. A.
- 8.044 **Calculation of displacement correlation tensor indicating vortical collective motion in two-dimensional systems of Brownian particles**
[Ooshida T.](#), Goto S., Matsumoto T., Otsuki M.
- 8.045 **Cooling rate dependence of simulated Cu-Zr-(Al) metallic glasses structure**
[Ryltsev R.](#), Klumov B., Chchelatchev N., Ryltseva A., Shunyaev K.
- 8.046 **Crystallization kinetics of $(\text{Cu}_{0.5}\text{Zr}_{0.5})_{100-x}\text{Al}_x$ bulk metallic glasses**
Ryltseva A., Kulikova T., Bykov V., Estemirova S., Shunyaev K., [Ryltsev R.](#)
- 8.047 **Enhanced Sampling Calculation of Chemical Potential in Fluids**
[Perego C.](#), Parrinello M.
- 8.048 **Heat transport coefficients from optimally short molecular dynamics simulations**
[Ercole L.](#), Marcolongo A., Baroni S.

Topic 9: Driven Systems, Rheology, Nanofluidics

- 9.001 **Polymer flow and polymer topology: linear chains, rings and knots flow differently**
Liebetreu M., Likos C. N., Weiß L. B.
- 9.002 **Designing a topological filter: Transport of linear and ring polymers in micro-fluidic devices**
Weiß L. B., Nikoubashman A., Likos C. N.
- 9.003 **Rheological properties of isolated telechelic star polymers under linear shear flow**
Jaramillo-Cano D. F., Camargo M., Likos C. N.
- 9.004 **Colloidal particles driven across an oscillating periodic optical potential energy landscape**
Abbott J. L., Straube A. V., Aarts D. G. A. L., Dullens R. P. A.
- 9.005 **Viscosity of the Lennard-Jones fluid**
Costigliola L., Heyes D. M., Schröder T. B., Dyre J. C.
- 9.006 **Experimental and simulated study of nearly-hard sphere suspensions in an oscillatory shear**
Xing Z., Ness C., Eiser E.
- 9.007 **Nonequilibrium dynamic clustering of hydrodynamically coupled particles driven by optical force**
Saito K., Okubo S., Kimura Y.
- 9.008 **DDM is a new track to microrheology, without tracking**
Giavazzi F., Edera P., Bergamini D., Cerbino R.
- 9.009 **Dynamics of a Driven Colloidal Particle under Time-delayed Feedback Control**
Curran A., Liu Y., Balin A. K., Aarts D. G. A. L., Dullens R. P. A.
- 9.010 **Brillouin viscoelastometry of hydrocarbon binary mixture liquids**
Rakhymzhanov A. M., Baptayev B., Utegulov Z. N.
- 9.011 **Resilience of a thermoresponsive rod-like gel**
Barabé B., Gunes D. Z., Lettinga M. P.
- 9.012 **Friction controls submerged granular flows**
Koivisto J., Korhonen M., Alava M., Durian D. J., Puisto A.
- 9.013 **Non-Newtonian behavior of hydrated polymer under shear with ultrasmall amplitude**
Kageshima M., Itoh S., Fukuzawa K.
- 9.014 **Rheological properties of mixtures of anisotropic colloids using molecular dynamics and stochastic rotation dynamics**
Olarte Plata J. D., Bresme F.
- 9.015 **Intrinsically Complex Fluids in Multiparticle Collision Dynamics**
Toneian D., Kahl G., Gompper G., Winkler R. G.
- 9.016 **Electro-osmotic flow and Droplet Electrophoresis in a bicomponent fluid**
Bazarenko A., Sega M.
- 9.017 **From collective transport to temperature gradient driven coarsening in near critical binary mixtures**
Roy S., Maciolek A., Höfling F., Dietrich S.
- 9.018 **Power functional theory for nonequilibrium many-body systems**
Schmidt M.

- 9.019 **Granular Mpemba effect: A hotter granular fluid can cool faster than a cooler one**
Lasanta A., Vega Reyes F., Prados A., Santos A.
- 9.020 **Threshold force to melt a glass locally: Theory and Simulations of microrheology on a colloidal glass**
Puertas A. M., Gruber M., Abade G., Fuchs M.
- 9.021 **Diffusive-convective transition in simple driven electrolytes**
Lobaskin V., Netz R. R.
- 9.022 **Elastic wake instabilities in a creeping flow between two obstacles**
Varshney A., Steinberg V.
- 9.023 **Theory of Nonequilibrium Fluids**
Krüger M., Basu U., Helden L., Bechinger C., Maes C.
- 9.024 **Nonlinear motion in viscoelastic media**
Müller B., Krüger M.
- 9.025 **Monolayers of hard rods: A soft matter model for non-equilibrium growth**
Klopotek M., Hansen-Goos H., Dixit M., Schilling T., Oettel M.
- 9.026 **Rheology of Pluronic-Hyaluronic acid thermoreversible gelling systems**
Ramya K. A., Deshpande A. P.
- 9.027 **The analog of discontinuous shear thickening flows under confining pressure**
Dong J., Trulsson M.
- 9.028 **Brownian dynamics simulations of sheared colloidal nanoclutches**
Gerloff S., Klapp S. H. L.

Topic 10: Active Matter

- 10.001 **Emergent forces in active hard spheres**
Ni R., Cohen-Stuart M. A., Bolhuis P. G.
- 10.002 **Dynamical coupling between structural rearrangements and self-propelled particle motion in colloidal glasses**
Lozano C., Gomez-Solano J. R., Bechinger C.
- 10.003 **Modular Micro-Swimmers**
Niu R., Kreissl P., Botin D., de Graaf J., Brown A. T., Oğuz E. C., Speck T., Holm C., Löwen H., Palberg T.
- 10.004 **Motion of Bio-hybrid Microswimmers in Optical Potentials**
Helgadottir S., Verre R., Volpe G.
- 10.005 **Phase co-existence in bidimensional passive and active dumbbell systems**
Digregorio P., Cugliandolo L. F., Gonnella G., Suma A.
- 10.006 **Towards Van 't Hoff's Law for Active Dispersions: Shape, Speed, Stroke, and Stress of Swimmers**
van Roij R., Samin S., Rodenburg J., Bet B., Paliwal S., Boosten G., Dijkstra M.
- 10.007 **A dynamic preferred direction model for the self-organization dynamics of a bacterial microfluidic pump**
Svenšek D., Pleiner H., Brand H. R.
- 10.008 **Light controlled polymer microcrawlers**
Rehor L., Maslen C., Eral H. B., Kegel W. K.

- 10.009 **Adaptive Resolution Simulations of Biomolecular Systems**
Fiorentini R., Fogarty A., Potestio R., Kremer K.
- 10.010 **Experimental investigation of a Brownian Gyrotor**
Soni J., Argun A., Dabelow L., Bo S., Eichhorn R., Pesce G., Volpe G.
- 10.011 **Switching of characteristic motions for swimming oil droplets in concentrated surfactant solution**
Suga M., Kobayashi S., Eitoku H., Ikeda T., Ichikawa M., Maeda Y., Kimura Y.
- 10.012 **Giant migrating clusters in tunable active Janus colloids**
van der Linden M., Alexander L., Dauchot O., Aarts D. G. A. L.
- 10.013 **Active transport of mucus driven by the self organization of ciliary activity in reconstituted human bronchial epithelium**
Loiseau E., Khelloufi K., Gras D., Chanez P., Viallat A.
- 10.014 **Theory on chemotactic migration of eukaryotic cells**
Hiraiwa T.
- 10.015 **Thermomechanically functionalized rubber**
Rešetič A., Milavec J., Zupančič B., Domenici V., Zalar B.
- 10.016 **Throwers and rowers - artificial hydrodynamic swimmers**
Vilfan M., Osterman N., Vilfan A.
- 10.017 **Bacterial swimmers in a critical binary mixture**
Koumakis N., Devailly C., Poon W. C. K.
- 10.018 **Bacteria E.coli swimming in high molecular-weight polymers: a universal scaling**
Devailly C., Martinez V. A., Dawson A., Arlt J., Schwarz-Linek J., Morozov A., Poon W. C. K.
- 10.019 **Hydrogen-Peroxide-Fuelled Janus Colloids are Active Brownian Particles**
Kurzthaler C., Devailly C., Arlt J., Franosch T., Poon W. C. K., Martinez V. A., Brown A. T.
- 10.020 **Non-Boltzmann stationary distributions and nonequilibrium relations in active baths**
Argun A., Moradi A., Pinçe E., Bağcı G. B., Imparato A., Volpe G.
- 10.021 **Power Functional Theory for Active Brownian Particles**
Krinninger P., Schmidt M., Brader J. M.
- 10.022 **Disorder-mediated crowd control in an active matter system**
Callegari A., Pinçe E., Velu S. K. P., Elahi P., Gigan S., Volpe G., Volpe G.
- 10.023 **Mechanical and chemical equilibrium in mixtures of active spherical particles: predicting phase behaviour from bulk properties alone**
Prymidis V., van der Meer B., Dijkstra M., Filion L.
- 10.024 **The sound of active liquids**
Geyer D., Bartolo D.
- 10.025 **Effective interactions between active swimmers and fluid interfaces**
Malgaretti P., Dominguez A., Popescu M. N., Dietrich S.
- 10.026 **From effective interactions to the interfacial phase behavior and pressure of active particles**
Wittmann R., Brader J. M.
- 10.027 **Collective motion of cells crawling on a substrate: roles of cell shape and contact inhibition**
Schnyder S. K., Molina J. J., Yamamoto R.

- 10.028 **Dynamics of model bacteria in dense polymer suspensions and networks**
Zöttl A., Yeomans J. M.
- 10.029 **E. coli swims faster in tight microtunnels**
Vizsnyiczai G., Saglimbeni F., Frangipane G., Bianchi S., Maggi C., Di Leonardo R.
- 10.030 **Hydrodynamics of microswimmers: Phase separation and the influence of gravity**
Blaschke J., Rühle F., Kuhr J. T., Stark H.
- 10.031 **Size zero Vs. fat bodies: cell-size effects on swimming behavior**
Adhyapak T. C., Jabbari-Farouji S.
- 10.032 **Shape-dependent guidance of active Janus particles by chemically patterned noindent surfaces**
Uspal W. E., Popescu M. N., Tasinkevych M., Dietrich S.
- 10.033 **Small activity differences drive phase separation in active-passive polymer mixtures**
Smrek J., Kremer K.
- 10.034 **Multistability in the actin motility assay**
Huber L., Krüger T., Suzuki R., Bausch A., Frey E.
- 10.035 **Collective Hydrodynamics of Active Polymers**
Manna R. K., Kumar P. B. S., Adhikari R.
- 10.036 **Dynamics of active deformable particles in Poiseuille flow**
Tarama M.
- 10.037 **Gating of mechanosensitive channels: computational study**
Paraschiv A., Šarić A.
- 10.038 **Influences of orienting external fields on the dynamics of mesoscale turbulence**
Reinken H., Heidenreich S., Bär M., Klapp S. H. L.
- 10.039 **Collective dynamics of Squirmer in Poiseuille flow**
Sorathiya S., Stark H.
- 10.040 **The polar order formation in model microswimmer dispersion**
Oyama N., Molina J. J., Yamamoto R.
- 10.041 **Dynamics of epithelial cells in microchannels of varying height: Experiments and modelling as active nematic**
Doostmohammadi A., Kempf F., Müller R., Zorn M., Frey E., Rädler J. O., Yeomans J. M.
- 10.042 **Vapor-Liquid Coexistence and Non-Equilibrium Surface Tension of Active Lennard-Jones Particles**
Paliwal S., Prymidis V., Filion L., Dijkstra M.

Topic 11: Biological and Biomimetic Fluids

- 11.001 **Athermal driven glass like behavior in living cytoplasm**
Nishizawa K., Mizuno D.
- 11.002 **Supra-folding and unfolding of DNA origamis on polymeric substrates**
Nakazawa K., Rossi-Gendron C., Rudiuk S., Hishida M., Saito K., Baigl D.
- 11.003 **The flow of a bacterial suspension around a pillar: broken simmetry and biofilm formation**
Secchi E., Rusconi R., Stocker R.

- 11.004 **Collective dynamics of motile cilia**
Feriani L., Juenet M., Fowler C. J., Bruot N., Chioccioli M., Holland S. M., Bryant C. E., Cicuta P.
- 11.005 **Lasers inside live cells**
Humar M., Cho S., Yun S.
- 11.006 **A microtubule dynamics and signaling feedback-loop induced cell self-polarization**
Li Y., ten Wolde P. R.
- 11.007 **Influence of various buffering agents and excipients on stability of biological drug Pertuzumab in liquid formulation**
Jančar J., Tompa G., Brus B., Šušterič A., Kuzman D.
- 11.008 **Thermodynamic and structural properties of a simple model for amyloid fibrils**
Urbič T., Dias C.
- 11.009 **Material transport through a binary lamellar stack**
Hoshino T., Komura S., Andelman D.
- 11.010 **Modeling of the phase equilibria in protein solutions of lysozyme and binary mixture of $\beta - \gamma$ lens crystallins**
Kalyuzhnyi Y. V., Kastelic M., Hribar-Lee B., Dill K. A., Vlachy V.
- 11.011 **Universal entrainment mechanism controls contact times of freely swimming organisms and passive objects**
Jeanneret R., Mathijssen A., Kantsler V., Polin M.
- 11.012 **Flow generation and sensing in the vertebrate left-right organizer**
Vilfan A., Ferreira R. R., Jülicher F., Supatto W., Vermot J.
- 11.013 **Optimal multivalent targeting of membranes with many distinct receptors**
Curk T., Dobnikar J., Frenkel D.
- 11.014 **Fluidization of three-dimensional cell sheets by forced rearrangements**
Krajnc M., Dasgupta S., Zihler P., Prost J.
- 11.015 **Simulating the effect of microwaves on biological macromolecules**
Gladović M., Oostenbrink C., Kocbek S., Predin M., Veselič U., Bren U.
- 11.016 **Mechano-chemical model for directive processive motility of cytoplasmic dynein**
Šarlah A., Vilfan A.
- 11.017 **Interplay between optical, viscous and elastic forces on an optically trapped Brownian particle immersed in a viscoelastic fluid**
Domínguez-García P., Forró L., Jeney S.
- 11.018 **Surface-Tension-Based Model of Confined Epithelial Tissues: Buckled Tubular Morphologies**
Rozman J., Krajnc M., Zihler P.

Author Index

Aarts D. G. A. L. P4, 3.024, 3.051, 5.006, 5.007, 5.015, 5.071, 8.036, 9.004, 9.009, 10.012
 Aasen A. **7.083**
 Abade G. 9.020
 Abascal J. F. L. K2.1
 Abbott J. L. P4, **9.004**
 Achazi A. 4.043
 Ackerman P. J. K3.2
 Adam P. 5.041
 Adhikari R. 10.035
 Adhyapak T. C. **10.031**
 Adjiman C. S. 2.025, 2.047
 Adolphs J. 7.077
 Adroher-Benítez I. 5.024
 Adžić N. **1.011**, 4.005
 Agarwal T. O4.8
 Agha H. 3.014, 3.048
 Ahlskog M. **7.033**
 Ahmadi S. **7.050**
 Ahmed Z. 3.042, 3.043
 Akita T. **3.039**
 Akiyama R. 5.098, 7.031
 Alava M. O6.3, 9.012
 Alcolea Palafox M. 5.106
 Alexander L. 10.012
 Alison L. **6.006**
 Allahyarov E. **3.004**
 Allolio C. 2.045
 Almukambetova M. O3.5
 Alvarado J. 3.024
 Álvarez C. E. 5.061
 Amabili M. **7.040**
 Amokrane S. **7.017**
 Amrhein L. 2.012
 Anachkov S. K7.2
 Ancian B. 4.013
 Andelman D. 11.009
 Angell C. A. O2.6
 Angioletti-Uberti S. 4.012
 Anisimov M. 2.012
 Antlanger M. 1.009
 Antonova K. O3.3
 Anzini P. **5.070**, **7.055**
 Aoyama Y. **5.052**
 Apih T. **3.045**
 Aplinc J. **3.061**
 Apóstolo R. F. G. **4.047**
 Apte P. A. **8.011**, 8.043
 Arai N. 5.116, 7.034
 Araki T. **5.003**
 Araoka F. 3.001, 3.002, 3.005, 3.006
 Araújo N. A. M. O5.16, **O7.2**, 8.027
 Arbe A. O4.6
 Archer A. J. **O4.5**, **7.044**, **7.045**
 Argun A. 10.010, **10.020**
 Arlt J. 5.026, **O10.7**, 10.018, 10.019
 Arscott S. 6.010
 Assaad F. F. 7.064
 Avendaño C. O5.3, 5.027
 Aya S. **3.005**, **3.006**
 Babić D. 5.014
 Backes S. **8.015**
 Backus E. 6.005
 Bacova P. O4.6
 Bagci G. B. 10.020
 Baghdadli N. 4.042
 Bahr C. O10.12
 Baigl D. 11.002
 Bailey N. P. 8.039
 Bakó I. 2.018
 Baldovin F. 5.080
 Balin A. K. 9.009
 Banerjee B. 1.004
 Banerjee S. 4.042
 Banerjee T. **1.001**, **1.002**, **1.003**, **1.004**
 Banpurkar A. 7.004
 Baptyayev B. 9.010
 Bär M. 10.038
 Barabé B. **9.011**
 Barbot A. 5.003
 Baron A. Q. R. 1.028
 Baroni S. 8.048
 Barrat J. L. 5.074, O9.3
 Barraud C. O7.7
 Barrett E. 3.057
 Barth L. O5.8
 Bartlett P. **O5.6**
 Bartolo D. O10.4, 10.024
 Bartsch E. **5.022**
 Bartsch H. **O1.1**
 Basu U. 9.023
 Baudry J. O9.5
 Baumgarten K. 6.013
 Bausch A. 10.034
 Baylan N. 1.013, 1.014
 Bazarenko A. **9.016**

Bechinger C. K10.1, 9.023, O10.8, 10.002
 Behler J. K5.1
 Belamie E. O3.3
 Belli S. O3.1
 Bellini T. O8.6, O9.6
 Belyaeva I. A. 7.026
 Benavides A. L. 5.107, 5.110
 Benet J. O7.3
 Ben Mahmoud S. 4.010
 Bera B. O7.13
 Bergamini D. 9.008
 Bergman M. **5.017**
 Bernard O. 6.003
 Bernaschi M. O6.4
 Berret J. F. **O11.3**
 Berthelard R. **2.048**
 Berthier L. O8.5, 8.042, O10.6
 Berthoumieux H. **2.015**
 Bešter-Rogač M. 6.003, 6.011
 Bet B. 10.006
 Bewerunge J. 5.109
 Bewley R. 2.008
 Bey H. K6.3
 Bey R. **7.067**
 Bharadwaj S. **4.029**
 Bhuiyan L. B. 7.043
 Biance A. L. 7.021
 Bianchi E. 5.021
 Bianchi S. 10.029
 Bianco V. O2.1, **O2.5**, 4.026, 4.027, 4.036
 Biancofiore L. 5.063
 Bibette J. O9.5
 Bicout D. 5.074
 Bier M. O1.1, 5.001, 5.004, **7.046**
 Bischofberger I. O8.7
 Biswas R. 1.002, 1.003
 Blaak R. **4.004**, 4.006
 Black W. L. K2.2
 Blanc C. 7.013
 Blaschke J. **10.030**
 Blatman D. **7.005**
 Bleibel J. **7.054**
 Blokhuis A. O10.8
 Blokhuis E. M. **6.012**, 7.083
 Blumlein A. 8.024
 Bo S. 10.010
 Bochenek S. **5.020**
 Bocquet L. K10.2, O1.3, 7.076, O9.4
 Boda D. 2.020, 7.023, 7.024
 Bogataj T. 5.033
 Bogris A. **4.022**
 Boinovich L. B. 6.004, 7.008
 Boisgard R. O7.14
 Bolhuis P. G. O5.4, 10.001, O11.5
 Bomboi F. **O8.6**
 Bomont J. M. 8.005
 Boniello G. 7.014
 Bonn D. **P9**, 6.005, O7.6
 Bonn M. 6.005
 Bonthuis D. J. **2.045**, O7.9
 Boosten G. 10.006
 Bordi F. O8.6
 Borgis D. O2.3, 2.044
 Borisov O. V. 4.030
 Borkovec M. 5.041, O7.12
 Borondo F. 3.053
 Borowko M. 5.034, **7.016**
 Botin D. **5.009**, 10.003
 Boué F. 4.010
 Boutin A. 4.009
 Bowles R. K. 7.050, **O8.3**
 Brader J. M. 5.064, 10.021, 10.026
 Bragheri F. O9.6
 Brand H. R. 3.050, 10.007
 Branka A. C. 5.105, 7.081
 Braun M. K. O8.10
 Brazhkin V. V. **1.007**
 Bregar A. **3.060**
 Bremond N. **O9.5**
 Bren U. 4.013, 11.015
 Bresme F. 7.037, 9.014
 Brilliantov N. V. 4.039
 Brito M. **5.097**
 Brodtkorb A. 5.049
 Bromley E. 4.025
 Brown A. T. 10.003, 10.019
 Brugnoni M. O5.12
 Bruijn J. R. O2.6
 Brujic J. **K6.1**
 Brumby P. E. 3.009
 Bruni F. O2.2
 Bruot N. **5.057**, 5.078, 11.004
 Brus B. 11.007
 Bryant C. E. 11.004
 Budkov Y. A. **4.021**
 Bunel F. 3.058

Büning T. 2.022
 Bunkin N. 2.006
 Burelbach J. **5.036**
 Burger N. 4.022
 Burian M. 5.085
 Buslaps T. 2.022
 Buttinoni I. **O10.3**
 Buzzaccaro S. 05.13, **5.067**
 Bykov V. 8.046
 Cacciuto A. 04.2
 Caciagli A. **O5.2**
 Calero C. **5.079**
 Callegari A. 2.007, 05.8, 5.063, **10.022**
 Calzolari D. C. E. 08.7
 Camargo M. **5.060, 5.061**, 9.003
 Camp P. J. 4.047, 7.079
 Canale L. **7.076**
 Canova C. T. 5.067
 Cansell M. 6.002
 Cantat I. **K6.2**
 Cao W. **1.016**
 Capone B. 4.001
 Cardelli C. **4.026**, 4.027
 Carpentier S. 7.020
 Carrara F. 011.2
 Casciola C. M. 7.035, 7.038, 7.039
 Cates M. E. 010.2
 Cattoz B. N. 4.047
 Caupin F. K2.1, 2.010, **2.012**, 2.041, 2.048, 07.5
 Caussin J. B. 010.4
 Cavalli A. 07.13
 Cazeneuve C. 4.042
 Çehreli S. **1.013, 1.014**
 Cerar J. **4.013**
 Cerar J. 2.023, 2.024
 Cerbino R. 08.6, 9.008, **O10.10**
 Chacko B. 7.045
 Chacon E. 07.1
 Chakraborty I. 05.14
 Chanez P. 10.013
 Chang C. C. 5.035
 Chang C. H. **5.035**
 Chang F. **5.046**
 Chang Y. W. 7.005
 Charbonneau P. **K8.1**
 Charlaix E. 1.012, **O7.7**, 7.020, 7.067
 Chatterji A. **O4.8**
 Chen J. Z. Y. K4.2
 Chen L. Y. 1.008
 Chen Q. **K7.1**
 Chen S. **5.015**
 Chevalier T. 06.3
 Chevrier J. 7.020
 Chiba A. 1.028, 7.031, 8.030
 Chioccioli M. 11.004
 Cho S. 11.005
 Chraïbi H. 07.14
 Chtchelatchev N. 5.113, 8.045
 Chudoba R. 8.041
 Chung D. Y. 1.015
 Chung S. 7.017
 Cichos F. 5.063
 Cicuta P. 5.078, 11.004
 Ciliberto S. 07.4
 Clanet C. 7.076
 Cmok L. 3.044
 Coasne B. 01.3, 7.067
 Cohen C. 7.076
 Cohen-Addad S. **K6.3**
 Cohen-Stuart M. A. 07.13, 10.001
 Colla T. E. **4.003**
 Colmenero J. 04.6
 Coluzza I. **O4.2**, 4.026, 4.027
 Comtet J. **O1.3**
 Corallino S. 010.10
 Cordeiro M. N. D. S. 2.009, 7.010
 Cortes L. B. G. **3.051**
 Cortes-Huerto R. **2.039**, 2.040
 Coslovich D. **O8.5**
 Costa L. 7.020
 Costigliola L. 8.039, **9.005**
 Cottin-Bizonne C. **K10.2**, 09.2
 Coudert F. X. 4.009
 Cox S. J. 6.010
 Crassous J. J. 5.013, 5.026, 5.037
 Croquette V. 7.014
 Cross B. **1.012**, 07.7
 Crowther P. 8.037
 Cruz-Vera A. 5.048
 Cugliandolo L. F. 10.005
 Cui K. 7.007
 Cummings P. T. 5.101
 Curk S. **4.049**
 Curk T. 011.4, **11.013**
 Curran A. 5.006, 5.007, 5.071, **9.009**
 Čoga L. 6.009

Čopar S. 3.055, 3.061
 Čopič M. 3.021, 3.022
 Dabelow L. 10.010
 Dabkowska A. P. 5.037
 Daldrop J. O. 2.019, 7.069
 Dalgakiran E. 4.020
 Dammone O. 3.024
 Dantchev D. 7.073
 Daoulas K. C. **K4.2**
 Darhuber A. A. 4.045
 Darmon A. K3.1
 Dasgupta C. 8.028
 Dasgupta S. 11.014
 Dašić M. **1.023**
 Dauchot O. 10.012
 Da Vela S. O8.10
 Davidson P. O3.3, 6.007
 Dawson A. O10.7, 10.018
 de Castro P. **5.072**
 Dederá S. 2.041
 De Feyter S. 7.007
 de Graaf J. **O8.9**, 10.003
 de la Cotte A. 5.016
 de las Heras D. **3.053**, O5.1, **5.064**, 7.049, 8.027
 Del Gado E. 8.012
 Delgado-Buscalioni R. 4.031
 Dellago C. **K5.1**, 2.051, 4.026, 5.085
 Demirörs A. 6.006
 Demontis P. 2.002
 Dennison M. O3.1
 Denton A. 5.097
 de Oliveira M. J. 3.003
 de Pablo J. J. 3.028
 Dequidt A. **4.041**
 Derzsi L. O6.4
 Deshpande A. P. 4.029, 9.026
 Desreumaux N. O10.4
 Detcheverry F. K10.2
 Devailly C. O7.4, **10.017**, **10.018**, 10.019
 Dhara S. 3.032
 Dhont J. K. G. 4.003
 Dhumal U. 5.005
 Diamant H. **5.062**
 Dias C. 11.008
 Dias C. S. **O5.16**, O7.2
 Díaz-Celaya J. A. 1.020
 Diaz-Guilera A. O10.5
 Diddens D. O4.7
 Dietrich C. F. **3.030**
 Dietrich K. O10.3
 Dietrich S. O1.1, 2.007, O5.8, 5.004, 5.068, O7.15, 7.053, 7.060, 9.017, 10.025, 10.032
 Digregorio P. **10.005**
 Dijkstra M. **O3.1**, O5.10, 5.081, 5.111, 7.025, 10.006, 10.023, 10.042
 Di Leonardo R. O10.13, 10.029
 Dill K. A. 2.035, 11.010
 Dini D. 7.081
 Dinis L. O5.11
 Dixit M. **7.051**, 9.025
 Dobashi T. 8.006
 Dobnikar J. **5.014**, **7.009**, **8.012**, **O11.4**, 11.013
 Dolganov P. V. **3.012**, **3.013**
 Dolganov V. K. 3.012
 Dollet B. O6.2
 Domenici V. 3.034, 3.045, 10.015
 Dominguez A. 7.054, 10.025
 Domínguez-García P. **7.036**, **11.017**
 Dong J. **9.027**
 Dong W. 7.015
 Doostmohammadi A. O3.3, 10.041
 Dotera T. **7.048**
 Doukas A. K. **5.089**, **5.090**
 Dowding P. J. 4.047
 Dozov I. O3.3
 Drenckhan W. 6.007
 Drevénšek-Olenik I. **3.033**, 3.036, **4.017**, 4.023, 6.009, 7.026
 Dridi W. 6.002
 Dubey I. 5.023
 Dubtsov A. V. 3.011
 Duits M. H. G. O7.13
 Dullens R. P. A. **P4**, 3.051, 5.006, 5.007, 5.015, 5.071, 8.036, 9.004, 9.009
 Dunkel J. O10.11
 Dünweg B. 4.050
 Durand-Vidal S. **6.003**
 Durey G. K3.1
 Durian D. J. 9.012
 Dussi S. O3.1
 Duška M. 2.012
 Dyre J. C. **1.029**, 8.039, 9.005
 Dzubiella J. 2.050, 4.012, 5.012, 5.024, 8.013, 8.041
 Edera P. 9.008
 Edholm O. 2.036
 Egelhaaf S. U. 5.008, 5.109

Eichhorn R. 10.010
 Eiser E. 3.031, O5.2, 5.036, 5.056, 9.006
 Eitoku H. 10.011
 Ejtahadi M. R. 5.055
 Elahi P. 10.022
 Elbers M. 2.022
 Elbers N. A. O5.7
 Ellis P. W. 7.005
 Elvingson C. 4.046
 Emelyanenko A. M. 6.004, 7.008
 Emelyanenko K. A. **6.004, 7.008**
 Emeršič T. 3.028
 Engel M. **O7.11**
 Eral H. B. 10.008
 Ercole L. **8.048**
 Erigi U. 5.005
 Ern   B. H. 5.047
 Ernst A. O5.1
 Escobar-Ortega Y. 5.048, **7.029**
 Essafi W. **4.010, 6.002**
 Estemirova S. 8.046
 Eun J. O3.5
 Evans R. 7.045, **7.072**
 Evers C. H. J. **O5.4**, 5.044
 Everts J. C. **3.016, O5.7, 5.011**
 F  bi  n B. **2.031**, 7.001, **7.002**
 Fadda F. **3.046**
 Fahrenberger F. O4.3
 Fantoni R. 5.058
 Farahmand Bafi N. **7.053**
 Febra S. A. **2.047**
 Fedosov D. A. K11.1
 Fenelon M. 5.049
 Feriani L. **11.004**
 Fernandez-Castanon J. O8.6, **8.017**
 Fernandez-Nieves A. 7.005
 Fern  ndez Rico C. 5.075
 Ferrari S. 5.021
 Ferreira E. S. C. **2.009**
 Ferreira R. R. 11.012
 Ferreiro-C  rdova C. 3.062
 Fielding S. M. **K9.1**
 Fijan D. **8.018**
 Filetici P. O8.6
 Fillion L. 5.081, 10.023, 10.042
 Filippi D. **O6.4, 7.063**
 Finlayson S. O5.6
 Finner S. P. **3.054**
 Fiorentini R. **10.009**
 Fiorini-Debuisschert C. 3.020
 Fiorucci G. **5.111**
 Fischer B. 8.001
 Fischer T. M. O5.1
 Fogarty A. 10.009
 Fomin Y. D. 7.027, 7.030
 Forel E. **O6.2**
 Formanek M. O4.6
 Forov Y. 2.022
 Forr   L. 11.017
 Forsman J. **O1.2, 4.033**
 Fortini A. 5.064
 Fowler C. J. 11.004
 Fragkopoulos A. A. 7.005
 Frangipane G. 10.029
 Franosch T. **4.034**, O7.10, O9.1, 10.019
 Frasca L. O11.4
 Frenkel D. 2.021, 4.049, 7.078, 8.012, O11.4, 11.013
 Frenzel L. **5.040**
 Frey E. **P6**, 10.034, 10.041
 Friant-Michel P. 2.032
 Fritschi S. 8.032
 Frontini J. **5.091**
 Fuchs M. **O8.4**, O9.1, 9.020
 Fujitani Y. 7.056
 Fukuda J. **3.047**
 Fukuzawa K. 9.013
 Fulcrand R. O9.2
 Furukawa A. **8.038**
 Fytas G. 4.022
 Gabrieli A. 2.002
 Gageat C. O2.3, **2.044**
 Gaiduk E. 7.030
 Gaillard T. 6.007
 Galewski Z. 8.003
 Galindo A. 2.025, 2.046, 2.047, 4.019
 Gallas B. 3.020
 Gallo M. 7.035
 Gambassi A. 2.007, **O5.8**
 Ganfoud N. **7.071**
 Ganti R. **7.078**
 Gao S. 3.033
 Gao Y. 3.051
 Garcia L. 1.012
 Garcia N. A. 5.032
 Garcia R. O7.1
 Gardien V. O7.5

Gârlea I. C. **3.024, 4.007**
 Garrido P. F. 7.036
 Gasser U. 7.005
 Gautam A. K. 8.011
 Geigenfeind T. **7.049**
 Gensler M. 4.043
 Georgi N. 7.077
 Gerloff S. **9.028**
 Geyer D. **10.024**
 Ghosh P. 1.002, 1.003
 Ghosh P. 4.016
 Giacomello A. **07.15**, 7.038, 7.039
 Giavazzi F. **9.008**, O10.10
 Giesselmann F. 3.030
 Gigan S. 10.022
 Gillespie D. 7.024
 Gilliet M. O11.4
 Gimperlein M. 7.066
 Ginot F. K10.2
 Giomi L. O5.14
 Girotto M. 1.027
 Gkagkas K. 1.023
 Gladović M. **11.015**
 Gladrow J. 5.028
 Glamazda A. 5.023
 Glasmacher U. 2.041
 Glavan G. 4.017, **7.026**
 Gnan N. 5.017, **5.032**, 5.088, 5.104, O8.2
 Golde S. O8.8
 Goldfriend T. 5.062
 Golestanian R. **P7**, 4.037
 Gomez-Solano J. R. **O10.8**, 10.002
 Gompfer G. **K11.1**, 5.010, 9.015
 Gonnella G. 3.046, 10.005
 González D. L. 5.060
 Gonzalez Noya E. 2.030, 5.021, 5.108
 González-Pinto M. 3.053
 Goto S. 8.044
 Goud V. V. 1.001
 Goujon F. 4.041
 Goy C. 2.041
 Goyal A. 8.011
 Grace M. **5.049**
 Gradišek A. 3.045
 Gras D. 10.013
 Gray S. **3.037**
 Greco C. K4.2
 Grelet E. **O3.2, 5.016**
 Grisenti R. E. **2.041**
 Grübel G. 5.040, 8.001, 8.022
 Gruber M. 9.020
 Grzimek V. **2.008**
 Guardia E. **O2.8**
 Guerrero-Martínez A. 5.106
 Guilbert-Lepoutre A. 2.031
 Guillamat P. O10.9
 Guillerm E. **O7.5**, 2.041
 Gujt J. **6.011**
 Gunes D. Z. 9.011
 Guo Y. **5.044**
 Guyot S. 4.015
 Guzman-Lastra F. K10.1
 Habib F. O4.8
 Haefele M. 7.071
 Hajiw S. 5.025
 Hakala M. 2.022
 Hallett J. E. K8.3, **8.014**
 Hamilton E. **5.078**
 Handa M. 3.007
 Handle P. H. 4.002, **8.035**
 Hansen J. **5.008**
 Hansen J. P. 8.005
 Hansen-Goos H. **5.073**, 9.025
 Hantal G. **1.026**, 7.001
 Hardoüin J. O10.9
 Harting J. D. R. 4.045
 Hartl B. **7.007**
 Hashemi S. M. **3.027**, 5.055
 Ható Z. 7.022, 7.024
 He H. **3.059**
 Hebbeker P. **4.014**
 Hegmann T. 3.020
 Heidari M. **2.040**
 Heidenreich S. 10.038
 Heidt S. **5.038**, 8.010
 Helden L. 9.023
 Helgadottir S. **10.004**
 Hemingway E. J. K9.1
 Hemmi Y. 2.026
 Henao A. O2.8
 Henderson D. 2.020, 7.043
 Hermes M. O8.9
 Herrera-Pacheco N. **5.048**, 7.029
 Herrera-Pérez D. **5.107**
 Heuer A. 6.014
 Heyes D. M. **5.105**, 7.081, 9.005

Hickey O. A. O4.3
 Hilbers M. O2.6
 Hiraiwa T. **10.014**
 Hishida M. **2.026**, 6.001, 11.002
 Höfling F. 4.034, 5.083, **7.060**, 9.017
 Hofmann J. 7.077
 Hofmann M. 5.038, 8.010
 Hofmann T. 3.052
 Höhler R. K6.3
 Hokkanen M. 7.033
 Holland S. M. 11.004
 Holm C. 1.030, 2.042, **O4.3**, 4.030, 4.040, 7.017, 10.003
 Holovatch Y. 4.048
 Holovko M. **1.006**, 1.022
 Honciuc A. **6.008**
 Horvai G. 7.002
 Hoser A. 2.008
 Hoshino T. **11.009**
 Hosokawa S. **1.028**
 Hostnik G. 4.013
 Hribar-Lee B. **2.005**, 2.037, 11.010
 Huber L. **10.034**
 Huber P. 3.008, 3.052, **7.070**
 Hugel T. 4.043
 Hughes A. P. 7.044
 Humar M. **11.005**
 Hussey J. 3.042
 Hwang I. G. 2.017
 Hynes J. T. 2.004
 Ichikawa M. 10.011, O11.1
 Ichimura R. 2.027
 Ida C. O3.4
 Ignés-Mullol J. 5.045, **O10.9**
 Ikeda T. 10.011
 Ilchenko M. 5.023
 Illien P. **4.037**
 Illing B. 8.032
 Ilnytskyi J. 2.011, 4.048
 Imberti S. O2.2, **2.028**
 Immink J. **5.013**
 Imparato A. 10.020
 Imperor-Clerc M. 5.025
 Inui M. 1.028, 8.030
 Ioannidou K. 8.012
 Isa L. **K7.2**, O10.3
 Ishida H. 3.007
 Ishikawa Y. 1.019
 Issenmann B. **2.010**, 2.048
 Ito H. **7.032**
 Ito T. 5.026
 Itoh K. **8.021**
 Itoh S. 9.013
 Iturri J. **4.018**, 5.033
 Ivaništšev V. 7.010
 Ivanov A. O. 5.084
 Iwashita Y. **5.050**, **5.051**, **O6.1**
 Izadi S. 2.002
 Izmaylov Y. 7.035
 Izzo D. **3.003**
 Jabbari-Farouji S. **O9.3**, 10.031
 Jackson G. 2.025, 2.046, 2.047, 4.019
 Jacobs M. R. **5.053**
 Jagodič U. **3.041**, **5.055**
 Jain A. **8.022**
 James S. 5.053
 Jamnik A. **2.023**, 2.024, 5.101
 Jančar J. 11.007
 Janssen L. M. C. K10.1
 Janssen M. **O7.8**
 Jaramillo-Cano D. F. **9.003**
 Jeanneret R. **11.011**
 Jedlovsky P. 2.031, 7.001, 7.002
 Jehser M. **4.008**
 Jeney S. 11.017
 Jeong J. **O3.5**
 Jeong S. 7.018
 Jevšček V. 3.036
 Ji Z. 3.033
 Jia Y. 3.024
 Jiang Y. K4.2
 Jin C. O10.12
 Jin F. O11.4
 Jo H. O3.4
 Jochum C. **4.005**
 Johner A. O4.7
 Joly L. O9.2
 Jorge M. 1.026
 Joshi D. O5.2, 5.056
 Juenet M. 11.004
 Jülicher F. 11.012
 Julius K. 2.022
 Jung G. 5.038, **5.076**
 Kageshima M. **9.013**
 Kahl G. **1.009**, 4.005, 4.006, **5.021**, 5.108, 7.007, 9.015

Kaiser A. K10.1
 Kaiser H. 8.032
 Kaiser V. O1.3
 Kajihara Y. 1.028, **8.030**
 Kalyuzhnyi O. **4.048**
 Kalyuzhnyi Y. V. 2.035, **5.101**, **11.010**
 Kamal M. A. O3.7
 Kamerlin N. **4.046**
 Kamien R. D. K3.1
 Kanduč M. 4.012, 7.069, 8.012, 8.013, **8.041**
 Kaneko T. **7.062**
 Kantorovich S. S. 1.026, 5.031, 5.084
 Kantsler V. 11.011
 Kapfer S. **5.082**, 7.047
 Kappler J. K11.2
 Karachevtsev V. 5.023
 Karahaliou P. K. 3.042, 3.043
 Karanikolos G. 2.008
 Kardar M. 7.058
 Karmakar S. 8.028
 Karner C. **5.085**
 Kastelic M. **2.035**, 11.010
 Katakai M. 8.006
 Katoh K. 3.047
 Katuri J. O10.1
 Kaushal M. **6.007**
 Kawasaki T. O8.1, **8.034**
 Kegel W. K. O5.4, 5.044, 5.046, 5.047, 10.008
 Keim P. O8.4, **8.032**
 Kellay H. O7.14
 Kempf F. **10.041**
 Kennedy C. L. **5.112**
 Kervil R. K6.2
 Kesal D. **4.011**
 Keyser U. 5.028
 Khakalo K. **6.013**
 Khelloufi K. 10.013
 Kim D. 7.018
 Kim I. S. **1.015**
 Kim J. Y. **2.017**, **5.029**
 Kim J. O3.5
 Kim K. O8.1, **8.031**, 8.034
 Kim S. Y. 5.029
 Kim S. J. O3.5
 Kim W. K. 4.012, **8.013**, 8.041
 Kim Y. **5.030**, 7.018, **7.019**
 Kimura Y. **5.019**, 5.050, 5.051, O6.1, 9.007, 10.011
 Kister T. 5.077
 Kitaoka S. **1.017**, 1.019
 Kityk A. 3.052
 Klamt A. **2.003**
 Klapp S. H. L. 5.095, 5.096, 6.015, 9.028, 10.038
 Klein J. **LMP**
 Klemenčič E. 3.017
 Klix C. L. 8.032
 Klopotek M. 7.051, **9.025**
 Klumov B. 8.045
 Knobloch E. K. O4.5
 Knorowski C. 5.079
 Knowles T. P. J. **K4.1**, 4.049
 Kobayashi M. **8.009**
 Kobayashi S. 10.011
 Kobayashi Y. **5.116**
 Kocbek S. 11.015
 Koenderink G. H. 3.024
 Koike R. O6.1
 Koivisto J. O6.3, **9.012**
 Kokot G. 5.014
 Kolesnikov A. L. 4.021, **7.077**
 Komura S. 4.029, 11.009
 Korhonen M. 9.012
 Kornyshev A. A. **K1.1**
 Kos Ž. **3.038**
 Košovan P. **4.030**, 4.044
 Kotar J. O5.2
 Koumakis N. 10.017
 Koura A. **8.020**
 Kournopoulos S. **2.046**
 Kowalik B. **2.019**, 7.069
 Kraft A. **5.095**
 Kraft D. J. **O5.14**
 Krajnc M. **11.014**, 11.018
 Kralj S. 3.011, 3.017, 3.063
 Kraus T. 3.020, 5.077
 Krause P. 4.011, 8.015
 Krauth W. 5.082
 Kreissl P. 10.003
 Kremer K. K4.2, 2.039, 2.040, O4.1, 7.068, 8.015, 10.009, 10.033
 Kremer T. O7.12
 Kress O. **3.010**
 Krinninger P. **10.021**
 Kristóf T. **7.022**, 7.024
 Krittanaï C. 5.033
 Kruchkov N. 7.027
 Krüger C. O10.12

Krüger M. 7.058, **9.023**, 9.024
 Krüger T. 10.034
 Krysiak S. 4.043
 Kuhr J. T. 10.030
 Kuipers B. 5.047
 Kulikova T. 8.046
 Kumar N. 07.13
 Kumar P. B. S. 4.029, 10.035
 Kundu D. 1.004
 Kurečić M. 4.017
 Kurzthaler C. **10.019**
 Kusumaatmaja H. K9.1, 5.087
 Kutnjak Z. **3.017**, 3.019
 Kuzman D. 4.024, **11.007**
 Kvasić I. 3.032
 Kwon S. M. 1.015
 Kyakuno H. **2.027**
 Kyrrou C. **3.063**
 Labbé-Laurent M. **5.068**
 Laborieux A. 7.076
 Lacaze E. 3.020
 Lagerwall J. P. 03.4
 Laird B. B. **7.061**
 Lajovic A. 2.024
 Lamboll R. 5.036
 Lame O. 09.3
 Lamperski S. **7.042**, **7.043**
 Lan Y. 5.056
 Lande R. 011.4
 Lasanta A. 9.019
 Lattuada E. **05.13**, 5.067
 Lautala S. 7.033
 Lavergne F. A. **5.006**, **5.007**, 5.071
 Lavrentovich M. O. K3.1
 Lavrentovich O. D. **P3**
 Lavric M. **3.019**
 Law J. O. **5.087**
 Lazarou G. **2.025**
 Leal Calderon F. 6.002
 Lechner R. T. 5.085
 Ledesma-Aguilar R. 7.082
 Lee C. 09.2
 Lee E. Y. 011.4
 Lee H. 03.5
 Lee N. K. 04.7
 Lee V. E. 05.5
 Leermakers F. A. M. 4.042, 8.016
 Léger L. 07.7
 Lehmkuhler F. **2.022**, 5.040, **8.001**, 8.022
 Lei Q. **5.002**
 Leitmann S. 4.034, **09.1**
 Lekkerkerker H. N. W. 05.15
 Lelidis I. 3.063
 Le Lirzin Y. 7.082
 Lembinen M. 7.010
 Leo M. 08.6
 Léonforte F. **4.042**
 Le Quéré J. 4.015
 Lettinga M. P. 3.024, 5.088, 9.011
 Levesque M. **02.3**, 2.044
 Levin Y. **1.027**, 7.065
 Levis D. **010.5**
 Li B. 01.2
 Li L. 8.012
 Li N. 05.5
 Li W. 3.033
 Li Y. 5.018
 Li Y. **11.006**
 Ličen M. **6.009**
 Liebchen B. 010.5
 Liebetreu M. **9.001**
 Liese S. **4.043**
 Likos C. N. 4.001, 4.002, 4.003, 4.004, 4.005, 4.006,
 4.007, 4.008, 5.031, 5.089, 9.001, 9.002, 9.003
 Lim J. 5.030
 Lim S. J. **7.018**, 7.019
 Lin Y. 5.012
 Lindeboom T. **4.019**
 Lippmann M. 3.052
 Lisjak D. 3.021, 3.022, 3.032, 3.044
 Liu H. L. 7.015
 Liu Y. 8.019
 Liu Y. 9.009
 Liu Y. 7.078
 Llombart P. 5.106, 07.3
 Lobaskin V. **9.021**
 Locatelli E. **4.001**, 4.002, **5.080**
 Loehr J. **05.1**
 Loenne M. 05.1
 Loerting T. **P8**, 8.004
 Loher J. K5.2
 Loiseau E. **10.013**
 Lokteva I. 5.040
 Lookman T. 8.040
 Loos S. A. M. **5.096**
 López De Haro M. 5.059

Lopez-Leon T. **K3.1**
 Loppinet B. 4.022, 8.019
 Lorenceau E. 7.021
 Loverso F. O4.6
 Löwen H. **K10.1**, 3.004, 5.114, 10.003
 Lozano C. K10.1, **10.002**
 Lu H. K2.2
 Lu H. O1.2
 Ludwig M. **7.028**
 Luengo G. S. 4.042
 Luiken J. A. O5.4
 Lukšić M. 2.005, **2.037**
 Lulli M. O6.4
 Lyakhov G. 2.006
 Maali A. O7.14
 Maass C. **O10.12**
 MacDowell L. G. **5.106**, **O7.3**
 Maciolek A. **2.036**, 7.053, **9.017**
 Maćkowiak S. **7.081**
 Má dai E. 7.023
 Maeda Y. 10.011
 Maes C. 9.023
 Magaletti F. 7.035
 Magazzù A. **2.007**, 5.063
 Maggi C. **O10.13**, 10.029
 Maggs A. C. 2.015
 Maier A. O4.2
 Majaron H. 3.044
 Majee A. **5.004**
 Maki Y. **8.006**
 Malek S. M. O2.7, **2.049**
 Malfreyt P. 4.041
 Malgaretti P. **4.036**, **10.025**
 Malherbe J. G. 7.017
 Malinverno C. O10.10
 Mallarino J. P. 5.093
 Mallikarjunachari G. 4.016
 Mamatkulov S. I. 2.045
 Mandal S. **O7.10**, O9.1
 Maniwa Y. 2.027
 Manjunath G. P. O4.8
 Manna R. K. **10.035**
 Månsson L. 5.013
 Marakis J. 5.088
 Marbach S. **O9.4**
 Marchio S. **7.038**
 Marcolongo A. 8.048
 Marcus Y. **1.005**
 Marechal M. **7.066**
 Marenduzzo D. 3.046
 Maret G. 8.032
 Marie E. 7.014
 Marini E. K7.2
 Maris E. 5.013
 Maroni P. 5.041, O7.12
 Marques C. M. O4.1
 Marschelke C. K7.2
 Martínez V. A. 5.026, O10.7, 10.018, 10.019
 Martínez I. A. O5.11, **O7.4**
 Martínez-Gonzalez J. A. 3.028
 Martínez-Ratón Y. 3.053
 Martín-Jimenez D. O7.1
 Martinsons M. **5.099**
 Martynec T. **6.015**
 Masiero S. 6.009
 Maslen C. 10.008
 Mason T. G. O8.2
 Massalska-Arodz M. 8.003
 Masuda H. **1.025**
 Masuda R. 3.026
 Mathijssen A. 11.011
 Matsuda K. 2.027
 Matsumoto M. **7.011**
 Matsumoto S. 7.032
 Matsumoto T. 8.044
 Matsuo K. 8.006
 Matysik S. O5.14
 Maver U. 4.017
 Mazars M. 1.009, **5.102**, **7.080**
 Mazza M. G. 3.014, **3.048**
 McBride J. M. **O5.3**, **5.027**
 McGraw J. **7.075**
 McLain S. E. O2.2
 McManus J. J. 5.049, 5.053, 8.024
 McMullen A. K6.1
 Mecke K. 7.066
 Medle Rupnik P. 3.021
 Medoš Ž. 6.003
 Meester V. O5.14
 Mehl G. H. 3.042, 3.043
 Meijer J. M. **O5.15**, 5.017
 Meloni S. 7.038, **7.041**
 Mériguet G. 4.013
 Mertelj A. **3.021**, 3.022, 3.032, 3.044
 Mertens S. F. L. 7.007
 Merunka D. **1.010**

Merzel F. **O2.4**
 Messina R. 5.039, **5.069**
 Metselaar L. **O3.3**
 Meyer H. **O4.7**
 Meyer N. **1.021**, 2.032
 Micheals T. C. T. 4.049
 Miholich J. 4.018
 Mikuriya M. **3.007**
 Milavec J. **3.034**, 10.015
 Miller M. A. 5.087
 Millet M. 4.015
 Millot C. 2.032
 Minina E. **5.031**
 Minzioni P. O9.6
 Mistura G. O6.4, 7.063
 Mišin M. 7.010
 Mittag J. J. 5.053
 Miyazaki K. 8.031
 Mizuno D. 11.001
 Moazzami-Gudarzi M. **5.041**, O7.12
 Mohan M. 1.001
 Mohanty P. S. 4.003
 Mohorič T. 5.014
 Molchanov I. 2.006
 Molina J. J. 10.027, 10.040
 Möller J. O8.10
 Möllmer J. 7.077
 Moncho-Jordá A. **5.024**
 Moradi A. 10.020
 Moran L. **8.024**
 Morawietz T. K5.1
 Mordan M. A. **8.036**
 Moreno A. J. **O4.6**
 Moreno-Cencerrado A. **5.033**
 Morin A. **O10.4**
 Moritz C. **2.051**
 Moriya H. 7.032
 Morozov A. 10.018
 Moscatelli D. 5.067
 Moucka F. 8.002
 Mousis O. 2.031
 Mozaffari M. R. 5.055
 Mravlak M. **5.077**
 Mugele F. **O7.13**, **7.004**
 Mukherji D. **O4.1**, 8.015
 Mulder B. M. 3.024
 Müller B. **9.024**
 Müller M. **4.032**
 Müller R. 10.041
 Munoz-Munoz Y. M. 8.025
 Mur M. **3.032**
 Murade C. 7.004
 Musharaf Ali S. 1.002, 1.003
 Mušević I. O3.6, 3.018, 3.032, 3.041, 3.055, 5.055
 Myung J. S. **5.010**
 Nägele G. 5.097
 Naik P. K. 1.001
 Nakazawa K. **11.002**
 Narinder N. O10.8
 Nasilowska W. 8.015
 Nava G. **O9.6**
 Nazzani F. O8.7
 Nerattini F. 4.026, **4.027**
 Ness C. 9.006
 Netz R. R. **K11.2**, 2.019, 2.045, 4.043, O7.9, 7.069, 9.021
 Nezbeda I. **8.002**
 Ni R. 5.002, **10.001**
 Ni S. O10.3
 Niguès A. O1.3, 7.076
 Nikkhou M. **O3.6**, **3.018**
 Nikoubashman A. **O5.5**, 9.002
 Ninarello A. O8.5, 8.042
 Niranjana V. 3.032
 Nishiyama I. 3.015
 Nishiyama N. 3.039
 Nishizawa K. **11.001**
 Niu R. 8.010, **10.003**
 Nobili M. 7.013
 Noblin X. 7.035
 Nobuoka K. 1.017, **1.019**
 Noguchi T. G. O6.1
 Nomura K. 5.116
 Nordholm S. O1.2
 Notenboom V. 3.024
 Nou S. K6.2
 Nounesis G. 3.063
 Nourry A. 7.082
 Nová L. 4.030, **4.044**
 Nozawa T. **3.009**
 Obiols-Rabasa M. 5.017
 Oettel M. 7.051, 7.054, 9.025
 Ogawa K. 7.011
 Oğuz E. C. 10.003
 Ohga Y. 1.019
 Ohtsuka Y. 7.056

Ohzono T. 3.047
 Okubo S. 9.007
 Okuzono T. 5.043, 5.052, 5.054, **5.094**
 Olarte Plata J. D. **9.014**
 Onufriev A. V. 2.002
 Ooshida T. **8.044**
 Oostenbrink C. 11.015
 Orlandini E. 3.046, 5.080
 Ortiz-Ambriz A. K5.2, **5.115**
 Osellame R. 09.6
 Oshima A. **7.031**
 Osiecka N. **8.003**
 Ostapenko T. 3.010
 Osterman N. **3.036**, 5.014, **5.042**, 10.016
 Ostrovskii B. I. 7.059
 Oswald P. 3.058
 Otomo T. 8.021
 Otsuki M. 8.044
 Ouhajji S. 05.15, **5.075**
 Oyama N. **10.040**
 Ozawa M. 08.5, 8.031, **8.042**
 Pacheco-Vázquez F. 7.029
 Padding J. 5.111
 Padilla L. A. **5.110**
 Pages-Casas J. **5.045**
 Pagliara S. 5.080
 Pagonabarraga I. 010.5
 Pal A. 03.7, 05.15, **5.026**
 Paladugu S. 05.8
 Palberg T. 5.009, 5.022, 5.038, **8.010**, 10.003
 Palczynski K. 8.041
 Paliwal S. 10.006, **10.042**
 Panagiotopoulos A. Z. 05.5
 Pang C. 7.018
 Pansu B. **5.025**
 Papež P. 2.029
 Paraschiv A. **10.037**
 Pardo L. C. 02.8
 Parisen Toldin F. **7.064**
 Parisi D. **8.019**
 Parola A. 5.070, 7.055
 Parrinello M. 8.047
 Parrondo J. M. R. 05.11
 Pasechnik S. V. 3.011
 Pastore G. **8.005**
 Patsahan O. 1.006, 1.022
 Patsahan T. 1.006, **1.022**, **2.011**
 Paul S. 1.001
 Pearce D. 05.14
 Pedersen U. R. **8.039**
 Pei K. 5.015
 Penkov N. 2.006
 Perego C. **8.047**
 Pereira C. M. 2.009, 7.010
 Pereira Dos Santos A. 1.027, **7.065**
 Perera A. 1.024, 2.014, **2.034**, 8.025
 Perez M. 09.3
 Pérez-Rodríguez M. 2.016
 Peric M. 1.010
 Perkin S. **P10**
 Perrin E. **4.009**
 Pesce G. 10.010
 Pethes I. **2.013**
 Petrosyan A. 07.4
 Petrov D. 05.11
 Petukhov A. V. 05.15, 5.075
 Philipse A. P. 05.15, 5.075
 Piazza R. 05.13, 5.067
 Pica Ciamarra M. **5.018**
 Picard C. 7.067
 Picaud S. 2.031
 Pieprzyk S. 5.105, 7.081
 Pierno M. 5.080, 06.4, 7.063
 Pikina E. S. **7.059**
 Pilizota T. 010.7
 Pinçe E. 10.020, 10.022
 Piñeiro M. M. **2.016**
 Pingua N. 8.011, **8.043**
 Pizio O. 2.011, 2.037
 Plamper F. A. 4.014
 Planchette C. **7.021**
 Platten F. 5.008, 5.109
 Pleiner H. **3.050**, 10.007
 Podgornik R. 1.011
 Podlipnik Č. 4.013
 Podnek V. **8.026**
 Polin M. 11.011
 Pomposo J. A. 04.6
 Poole P. H. 02.7, **2.043**, 2.049
 Poon W. C. K. 5.026, 08.9, 010.7, 10.017, 10.018, 10.019
 Popescu M. 010.1
 Popescu M. N. 10.025, 10.032
 Posnjak G. **3.055**
 Potenza M. A. C. 2.041
 Potestio R. **2.038**, 2.039, 2.040, **4.035**, 10.009

Pothoczki S. **2.018**
 Potter T. D. **3.057**
 Poulard C. 6.007
 Poupard P. 4.015
 Pousaneh F. 2.036
 Poy G. **3.058**
 Požar M. **2.014**, 2.033, 8.025
 Pradas M. 7.082
 Pradipkanti L. **4.038**
 Prados A. 9.019
 Praprotnik M. **4.031**
 Predin M. 11.015
 Priestley R. D. O5.5
 Primorac T. **2.033**, **8.025**
 Promdonkoy B. 5.033
 Prost J. 11.014
 Pršlja P. 2.030
 Prud'Homme R. K. O5.5
 Prymidis V. **10.023**, 10.042
 Puertas A. M. O9.1, **9.020**
 Pugazenthi G. 1.004
 Puisto A. **O6.3**, 6.013, 9.012
 Punter M. T. J. J. M. 3.016
 Pusztai L. 2.018
 Puzyn T. 1.018
 Qazi M. **6.005**
 Qi W. O8.3
 Qiao C. Z. **7.015**
 Rabe J. P. 4.043
 Rädler J. O. 10.041
 Radu M. 7.068
 Raghunathan V. A. **O3.7**
 Rajesh R. 4.039
 Rakhymzhanov A. M. 9.010
 Ramou E. **3.042**, 3.043
 Ramya K. A. **9.026**
 Rana R. O3.2
 Raptis Y. S. 3.063
 Raschke S. **6.014**
 Rau T. 4.040
 Raufaste C. O6.3
 Ravnik M. 3.038, 3.056, 3.060, 3.061, 4.024, 5.011, 5.055
 Regev I. **8.040**
 Rehor I. **10.008**
 Reinken H. **10.038**
 Renggli D. O10.3
 Renner J. 3.053
 Repnik R. **3.011**
 Restagno F. O7.7
 Reščič J. **5.100**
 Rešetič A. 3.034, **10.015**
 Rey R. **2.004**
 Reynolds C. P. 8.036
 Rhys N. O2.2
 Rica R. A. O5.11
 Ricci M. A. **O2.2**
 Richter T. 4.030
 Richtering W. O5.12, 5.020
 Rickayzen G. 5.105
 Riest J. 5.097
 Ringeissen S. 4.042
 Rio E. O6.2, 6.007
 Roa R. **4.012**, **5.012**, 8.013, 8.041
 Robin A. K2.2
 Roché M. 6.007
 Rodenburg J. 10.006
 Rodrigues M. S. **7.020**
 Rodriguez-Rivas A. 5.059
 Rogier F. **5.047**
 Rohwer C. M. **7.058**
 Roldan E. **O5.11**
 Roldán-Vargas S. **8.033**
 Rolland L. O9.5
 Romano F. O8.6, 8.007
 Ronsin O. K6.3
 Ronti M. **5.084**
 Rooney D. 5.049
 Roosen-Runge F. **O4.4**, **5.074**
 Rosenbaum A. 2.012
 Rossi-Gendron C. 11.002
 Rotenberg B. **K1.2**, 7.071
 Roth R. O4.4, 5.073, 5.092
 Rottler J. **K8.2**, O9.3
 Rovigatti L. O2.1, **4.002**, 4.026, 5.084, **5.104**, 8.033
 Roy S. 9.017
 Royall C. P. **K8.3**, 8.014, 8.023, 8.037
 Rozman J. **11.018**
 Rožič B. **3.020**
 Ruan Y. 8.019
 Rubio M. A. 7.036
 Rucklidge A. M. O4.5
 Rud O. V. 4.030
 Rudiuk S. 11.002
 Rudquist P. 3.030
 Ruff Z. 5.056

Rühle F. 10.030
 Ruiz-Franco J. **5.088**
 Ruiz-Gutiérrez É. **7.082**
 Ruiz Lopez V. G. **2.050**
 Rusconi R. 11.003
 Russina M. 2.008
 Russo J. K8.3, 2.001, **O5.9**, 8.007, 8.023, 8.029
 Ruzicka S. 3.062
 Ryazanova O. **5.023**
 Rybińska A. **1.018**
 Ryltsev R. **5.113**, **8.045**, **8.046**
 Ryltseva A. 8.045, 8.046
 Ryu S. 5.029
 Ryu S. 7.018
 Ryzhkova A. V. 3.041
 Ryzhov V. N. **7.027**, 7.030
 Rzysko W. **5.034**, 7.016
 Sablić J. 4.031
 Sadus R. 2.012
 Saglimbeni F. O10.13, 10.029
 Sagués F. 5.045, O10.9
 Sahebdivani M. O10.8
 Sahle C. J. 2.022
 Saida J. 8.021
 Saika-Voivod I. **O2.7**, 2.049
 Saito K. 2.026, 6.001, 11.002
 Saito K. **9.007**
 Saito M. **3.026**
 Saito T. 2.027
 Sakaguchi Y. 7.062
 Sakatsuji W. 3.015
 Salamon P. 3.036, 7.026
 Salanne M. 7.071
 Salazar R. 5.102, **5.103**, 7.080
 Samin S. 3.016, O5.7, 7.017, 10.006
 Sampson W. W. 8.036
 Sanchez S. O10.1
 Sánchez-Ferrer A. 3.019
 Sano R. 1.019
 Sant M. 2.002
 Santiago M. K2.2
 Santos A. **5.058**, **5.059**, **9.019**
 Santucci S. O6.3
 Sanz E. K2.1, O7.3
 Sarkadi Z. 7.022
 Sastre F. 5.107
 Sastry S. 8.028
 Satapathy D. K. 4.016, 4.038
 Sawane Y. 7.004
 Sbragaglia M. O6.4, 7.063
 Scalia G. O3.4
 Schaertel N. 5.022
 Scheffold F. O8.2
 Scheid B. 6.007
 Schilling T. 5.077, 7.051, 9.025
 Schimmele L. O7.15
 Schindler T. **5.086**, **7.047**
 Schlaich A. K11.2, **7.069**
 Schlegel M. C. 2.008
 Schlegel S. 6.005
 Schmid F. 5.076
 Schmidt F. 2.007, **5.063**
 Schmidt M. 5.064, 5.086, 7.049, **9.018**, 10.021
 Schmidt N. W. O11.4
 Schmiedeberg M. 5.099
 Schmitt J. 5.025
 Schneck E. 7.069
 Schneider S. 4.014
 Schnyder S. K. **10.027**
 Schoen M. 2.046, 3.014, 3.048, 4.009, 7.074
 Schoen S. 7.028
 Schönhals A. 3.008, 3.052
 Schöpe H. J. **O8.8**
 Schreiber F. O4.4, O8.10
 Schröder C. 1.026
 Schröder T. B. 8.039, 9.005
 Schroer M. A. 8.001
 Schurtenberger P. O4.4, 4.003, 5.010, 5.013, 5.017,
 5.026
 Schwarz A. D. 4.047
 Schwarzl R. 4.043
 Schwarz-Linek J. 10.018
 Sciortino F. **O2.1**, 4.002, 5.084, O8.6, 8.017, 8.033,
 8.035
 Scita G. O10.10
 Scognamiglio C. **7.035**
 Scotti A. **O5.12**
 Sebastian N. **3.022**
 Sebastião P. J. 3.045
 Secchi E. **11.003**
 Segá M. 1.026, **7.001**, 7.002, **7.003**, 9.016
 Seiwert J. K6.2
 Seki T. **5.054**, 5.094
 Sengupta A. **3.014**, 3.048, **O11.2**
 Sengupta S. 8.028
 Sen Gupta B. **7.068**

Sentker K. 3.008, **3.052**
 Seto H. **7.057**
 Seto M. 3.026
 Sevvick E. M. 3.059
 Seydel T. O4.4
 Shabane P. S. 2.002
 Shafiq M. O5.6
 Shahidzadeh N. 6.005, **O7.6**
 Shamoin M. 7.026
 Shi R. **2.001**
 Shiba H. **O8.1**
 Shimobayashi S. F. **O11.1**
 Shimojo F. 8.020
 Shkirin A. **2.006**
 Shmeliova D. V. 3.011
 Shreiber F. 7.051
 Shunyaev K. 8.045, 8.046
 Shuravin N. S. 3.012
 Sibley D. N. 7.044
 Siegl T. 5.012
 Simmchen J. **O10.1**
 Simoncelli M. 7.071
 Singh L. P. 2.010
 Singraber A. K5.1
 Siretanu I. O7.13, 7.004
 Siria A. O1.3, 7.076
 Skacej G. **3.049**
 Skarmoutsos I. O2.8
 Skvara J. 8.002
 Smallenburg F. 5.081, **5.114**
 Smalyukh I. I. **K3.2**
 Smiatek J. 1.030, 2.042, O4.3
 Smith G. O5.6
 Smrek J. **10.033**
 Snezhko A. 5.014
 Sofi J. A. 3.032
 Sohn H. O. K3.2
 Sokolić F. 2.033, 8.025
 Sokolowski S. 5.034, 7.016
 Solano Canchaya J. G. 4.041
 Soligno G. **O5.10, 7.025**
 Sollich P. 5.072
 Solon A. O10.2
 Sommer A. 6.002
 Soni J. **10.010**
 Sorathiya S. **10.039**
 Sosa C. O5.5
 Sosnowska A. 1.018
 Sparr E. 5.037
 Speck T. 10.003
 Spindler L. **4.023**
 Spiteri L. **5.039**, 5.069
 Spohr E. 6.011
 Sprakel J. 8.016
 Squires T. M. **K9.2**
 Stana-Kleinschek K. 4.017
 Stanković I. 1.023, **5.065**, 5.069
 Stark H. 10.030, 10.039
 Staszewski T. 5.034, 7.016
 Stebe K. J. **P2**
 Stein W. D. 2.008
 Steinberg V. 9.022
 Steinke I. 2.022
 Steinschulte A. A. 4.014
 Stenhammar J. 5.013, **O10.2**
 Stergar J. 5.042
 Stern J. **8.004**
 Sternemann C. 2.022
 Stewart M. 7.072
 Stieger T. 3.014, 3.048
 Stocco A. 7.013
 Stocker R. O11.2, 11.003
 Stones A. E. **5.071**
 Stopper D. 5.073, **5.092**
 Stradner A. O4.4, 5.010
 Straube A. V. 5.045, **5.083**, 9.004
 Stroock A. D. **K2.2**
 Studart A. R. 6.006
 Su Y. 5.035
 Subramanian P. O4.5
 Suematsu A. **5.098**
 Suffritti G. B. **2.002**
 Suga M. **10.011**
 Sugii T. 7.032
 Suma A. 10.005
 Sun D. W. 4.032
 Sung B. 5.016
 Supatto W. 11.012
 Suresh G. **4.016**
 Suzuki R. 10.034
 Suzuki T. 7.032
 Svaland G. B. **7.037**
 Svenšek D. **10.007**
 Synytska A. K7.2
 Szilágyi I. 5.041
 Šamaj L. 1.009

Šarić A. 4.049, 10.037
 Šarlah A. **11.016**
 Škarabot M. O3.6
 Štimulak M. 3.061
 Šušterič A. 11.007
 Tah I. **8.028**
 Tai B. J. S. K3.2
 Tailleur J. O10.2
 Takahashi N. 7.057
 Takahashi Y. 7.048
 Takata S. 7.057
 Tamura Y. 5.019
 Tan Y. 5.028, 5.080
 Tanaka H. 2.001, 5.057, **8.007**, 8.008, 8.009, 8.029
 Tanaka H. 7.048
 Tang P. H. 1.008
 Tani H. **7.056**
 Taniguchi T. O11.1
 Tarama M. **10.036**
 Tarazona P. **O7.1**
 Tarjus G. **P1**, K8.3, 8.037
 Tasche J. 3.057
 Tasinkevych M. O7.15, 10.032
 Tašič B. 4.023
 Tatlipinar H. **4.020**
 Tavares J. M. O2.1, **5.066**, 5.084
 Teixeira M. A. C. 6.010
 Teixeira P. I. C. **3.035**, 5.066, **6.010**
 Teleki A. 6.006
 Téllez G. **5.093**, 5.103
 Telo Da Gama M. M. O5.16, O7.2
 ten Hagen B. K10.1
 ten Wolde P. R. O11.5, 11.006
 Terasaki T. 7.032
 Terentjev E. M. 3.035
 Tervoort E. 6.006
 Tharad S. 5.033
 Thiele U. 7.044
 Thorneywork A. L. P4, **5.028**
 Tierno P. **K5.2**, 5.045, 5.115
 Tighe B. P. 6.013
 Tinti A. **7.039**
 Tiribocchi A. 3.046
 Tkalec U. **3.028**
 Toca-Herrera J. L. 4.018, 5.033
 Tolan M. 2.022
 Tom A. M. **4.039**
 Tominaga T. 7.057
 Tompa G. 11.007
 Tomšič M. 2.023, **2.024**
 Toneian D. **4.006**, **9.015**
 Tong H. **8.008**
 Totton T. 2.021
 Toutain J. 6.002
 Toyotama A. **5.043**, 5.052, 5.054, 5.094
 Tran L. K3.1
 Trappe V. **O8.7**
 Traveset A. 5.079
 Trček M. 3.017
 Trefält G. 5.041, **O7.12**
 Treffenstädt L. L. **8.027**
 Tretyakov N. **4.050**
 Tribet C. 7.014
 Tripathy M. **5.005**
 Trizac E. 1.009
 Tromp R. H. 4.028
 Trulsson M. 9.027
 Tsagkaropoulou G. **7.079**
 Tsiok E. N. 7.027, **7.030**
 Tsutsui S. 1.028
 Tubiana L. 4.026, 4.027
 Tuinier R. 4.028
 Tuna Y. O5.8
 Tung C. O4.2
 Turci F. K8.3, 8.014, 8.023, **8.037**
 Uchida Y. 3.039
 Uematsu Y. **O7.9**
 Ueno I. 7.062
 Uhlig F. 1.030
 Uhlík F. 4.030, 4.044
 Ujje S. 3.007
 Urbič T. **1.024**, **2.029**, **2.030**, 2.033, **11.008**
 Uspal W. E. O10.1, **10.032**
 Usuda H. **6.001**
 Utegulov Z. N. **9.010**
 Vågberg D. **O10.6**
 Vaghela A. 3.035
 Valchev G. **7.073**
 Valeriani C. **K2.1**
 Valiskó M. **2.020**, **7.023**, **7.024**
 Valladares A. 1.020
 Valladares A. A. 1.020
 Valladares R. M. **1.020**
 Valmacco V. O7.12
 Vanakaras A. G. 3.043
 van Blaaderen A. O5.7, 5.112

van Damme R. 5.081
 van den Ende D. 7.004
 van der Gucht J. 8.016
 van der Heijden T. W. G. **4.045**
 van der Hoeven J. E. S. O5.7
 van der Linden M. **10.012**
 van der Loop T. H. O2.6
 van der Meer B. **5.081**, 10.023
 van der Schoot P. 3.016, 3.054, 4.045
 van der Wel C. O5.14
 van Doorn J. M. 8.016
 van Ravensteijn B. G. P. 5.044, 5.075
 van Roij R. O3.1, 3.016, O5.7, O5.10, O7.8, 7.025,
 10.006
 Varagnolo S. 7.063
 Varshney A. **9.022**
 Vega C. K2.1
 Vega Reyes F. 9.019
 Velasco E. 3.053
 Velu S. K. P. 10.022
 Vemparala S. 4.039
 Vermot J. 11.012
 Verre R. 10.004
 Verweij J. E. **8.016**
 Veselić U. 11.015
 Veziri M. 2.008
 Viallat A. 10.013
 Vidal-Vidal Á. 2.016
 Vijaykumar A. **O11.5**
 Vilfan A. 5.014, 10.016, **11.012**, 11.016
 Vilfan M. **3.044**, **10.016**
 Villa S. **7.013**
 Vincent O. K2.2
 Vis M. **4.028**
 Vitali V. O9.6
 Vitorino M. V. 7.020
 Vizsnyiczai G. O10.13, **10.029**
 Vlachy V. 2.035, 11.010
 Vlassopoulos D. **P5**, 5.088, 8.019
 Vogel N. O7.11
 Voloshin I. 5.023
 Volpe G. 10.022
 Volpe G. **K5.3**, 2.007, O5.8, 5.063, O10.3, 10.004,
 10.010, 10.020, 10.022
 von Ferber C. 4.048
 von Klitzing R. 4.011, 7.028, 8.015
 Voronov V. 8.026
 Voroshylova I. V. 2.009, **7.010**
 Vrabec J. 8.025
 Waggett F. O5.6
 Wagner D. 5.008
 Wagner M. O4.1
 Wagner S. **5.108**
 Waisbord N. K10.2
 Walker M. **3.023**, 3.025, 3.037, 3.057
 Walter M. 7.007
 Wand C. **2.021**
 Wandhai S. 7.004
 Wandrei S. M. **7.074**
 Wang J. O7.11
 Wang M. **5.037**
 Wang S. **3.056**
 Wang Y. 1.016
 Warrens C. P. 7.079
 Washizu H. **7.012**
 Watabe S. 8.006
 Watanabe C. **7.006**
 Watanabe G. 3.029, **3.040**
 Watson M. D. O4.1
 Wax J. F. 1.021, **2.032**
 Wei J. 7.009
 Weik F. **4.040**
 Weiß L. B. 9.001, **9.002**
 Welch C. 3.042, 3.043
 Wells G. G. 7.082
 Wensink H. H. **3.062**
 Weon B. M. 2.017, 5.029, 5.030, 7.018, 7.019
 Wessel S. 7.064
 Wilding N. O5.9, 7.072
 Wilhelmsen Ø. 7.083
 Williams D. R. M. 3.059
 Wilson M. 8.018
 Wilson M. R. 3.023, **3.025**, 3.037, 3.057, 4.025
 Winkler R. G. 5.010, 9.015
 Wintzenrieth F. K6.3
 Witt M. 8.015
 Witten T. 5.062
 Wittmann R. **10.026**
 Wolf H. O10.3
 Wong A. 5.087
 Wong G. C. L. O11.4
 Wood N. K8.3, **8.023**
 Woodhouse F. G. **O10.11**
 Woodhouse V. J. **4.025**
 Woodward C. E. O1.2, 4.033
 Woutersen S. **O2.6**

Wu D. 6.008
 Wu Q. 3.033
 Wu T. M. **1.008**
 Würger A. **07.14**
 Xian W. O11.4
 Xie F. 4.033
 Xing Z. **9.006**
 Xu D. 7.011
 Xu H. 1.021, 2.032
 Xu J. 3.033
 Xu P. **3.031**
 Yamada T. 7.057
 Yamada Y. O8.1
 Yamamoto A. 1.017
 Yamamoto J. **03.4, 3.015**, 3.026
 Yamamoto R. 10.027, 10.040
 Yamamura Y. 2.026, 6.001
 Yamanaka J. 5.043, 5.052, 5.054, 5.094
 Yamazaki A. 3.040
 Yamazaki T. 3.039
 Yanagisawa M. 7.006
 Yanagishima T. **8.029**
 Yang T. O9.6
 Yang Y. 7.061
 Yasumoto Y. 7.011
 Yasuoka K. 3.009
 Ybert C. K10.2, **09.2**
 Yeomans J. M. O3.3, 10.028, 10.041
 Yildirim A. **3.008**, 3.052
 Yin H. 7.044
 Yoda Y. 3.026
 Yodh A. G. O7.2
 Yoshida J. **3.029**, 3.040
 Yoshimori A. 5.098, **7.052**
 Yoshimoto Y. **7.034**
 Yoshioka J. **3.001, 3.002**
 Yun S. 11.005
 Yunker P. J. O7.2
 Yurchenko S. O. 7.027
 Yuste S. B. 5.059
 Zaccarelli E. **K5.4**, 5.017, 5.032, 5.088, 5.104, O8.2
 Zalar B. 3.019, 3.034, 10.015
 Zanchi D. **4.015, 7.014**
 Zanini M. K7.2
 Zannoni C. 3.049
 Zarubin G. **5.001**
 Zavvou E. E. **3.043**
 Zeman J. **1.030, 2.042**
 Zemljic S. 4.018
 Zhang C. **08.2**
 Zhang F. O4.4, **08.10**
 Zhang R. 3.028
 Zhang X. 3.033
 Zhang Z. O7.14
 Zhao S. L. 7.015
 Zhao Z. O2.6
 Zhou X. O8.9
 Zhu S. K2.2
 Zidar M. **4.024**
 Zihlerl P. 5.089, 5.090, 5.091, 11.014, 11.018
 Zippelius A. O8.4
 Zoranić L. 2.033, 8.025
 Zorn M. 10.041
 Zöttl A. **10.028**
 Zozulya V. 5.023
 Zunke C. **5.109**
 Zupančič B. 3.034, 10.015
 Zupkauskas M. 5.036, **5.056**
 Žumer S. 3.038, 3.056

Advertisements



Turn-key laser tweezers system



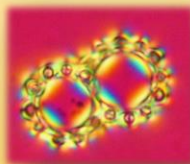
Tweez 250si



Colloids / Microfluidics



Biology / Biophysics



Liquid crystals

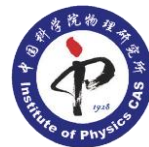
Visit us at booth no. 3

www.aresis.com



中国科学院物理研究所

Institute of Physics (IoP)
Chinese Academy of Sciences (CAS)
http://sm.iphy.ac.cn/English/index_en.htm



Soft Matter positions in Beijing

As a part of a strategic investment into **Soft Matter & Biological Physics** research, we are seeking to appoint **new staff members on all levels**.

Requirements

We are looking for internationally competitive candidates of experimental and theoretical background who will complement the research profile of the IoP Soft/Bio Matter division, establish an independent state of the art research activity and contribute to the institute's international collaboration program.

Commensurate with the candidate's experience, positions will be offered at the (equivalent of) **Full, Associate** or **Assistant Professor** level.

We are also looking for outstanding **postdoctoral** and **PhD candidates** to join us by applying to the prestigious **CAS International Fellowship Program**.

Benefits

IoP is a leading research institution in China. We are offering excellent research conditions, a **substantial start-up** budget and **competitive salary** with benefits package including housing assistance, health and social insurance. Please contact us to discuss further details.

Contact

- **Prof. Jure Dobnikar** (jd489@cam.ac.uk; *Find me at Liquids*)
- **Prof. Fangfu Ye** (fye@iphy.ac.cn)
- **Ms. Zhaoping Xie**, Academic Secretary (zpxie@iphy.ac.cn)
- **Ms. Qi Fu**, IoP HR office (fuqi@iphy.ac.cn)



INDUSTRIAL-GRADE ULTRAFAST LASERS TO ADVANCE **YOUR** RESEARCH

Whether you are working at 1 kHz or 1 MHz, Coherent femtosecond amplifiers operate at extraordinary levels of quality, accuracy, and repeatability. Our **HALT** designed, **HASS** verified scientific lasers deliver industrial-grade reliability.

Join the Industrial Revolution in Ultrafast Science

coherent.com/industrial-revolution



COHERENT®

Superior Reliability & Performance

VersaSCAN™

Electrochemical Scanning System



AMETEK

supported by

LKB



Malvern
www.malvern.com

supported by

LKB



WATER TREATMENT SOLUTIONS

COST-EFFICIENT WATER TREATMENT WITH
ONLINE ZETA POTENTIAL MEASUREMENT

RK TECH Ltd. distributor of Newport & Spectra-Physics

RK TECH

Our company was established in 1999.

We provide the utmost information and help to our customers in connection with the instruments and the applications during the trade and service work. With our help the customers can find the appropriate equipment for their needs. We even provide support for special technical questions.

In case you would like to ask for more information, or an offer, or you would like to place an order you can contact us via e-mail or phone.

Contact:
managing director:

Dr. László Kovács

Sales:
Balazs Domonkos
+ 36306677115
domonkos.balazs@rktech.hu

Krisztian Hátori, PhD
+ 36305320285
hamori.krisztian@rktech.hu

Our company is the authorised distributor of the following companies in the territory of the following Eastern – European Countries: Slovenia, Croatia, Serbia, Bosnia Herzegovina, Montenegro, Romania, Albania and Hungary.

Newport Corporation (USA) including ILXLightwave, NewFocus (optical mounts), Oriel Instruments (solar simulators, tunable light sources), Richardson Gratings, Corion Filters and Femtolasers Optics. Newport offers the most extensive selection of high-quality light sources and instrumentation, as well as optical tables, mounts and mirrors, motion and vibration control, and optics and opto-mechanical instrumentation. web: www.newport.com

Spectra-Physics (USA) offers high quality lasers such as fibre lasers, high energy pulsed lasers, laser accessories, Q-switched DPSS lasers, tuneable lasers, ultrafast lasers and diode lasers. All of these products are built according to the highest quality standards, and out of the finest materials. web: www.spectra-physics.com

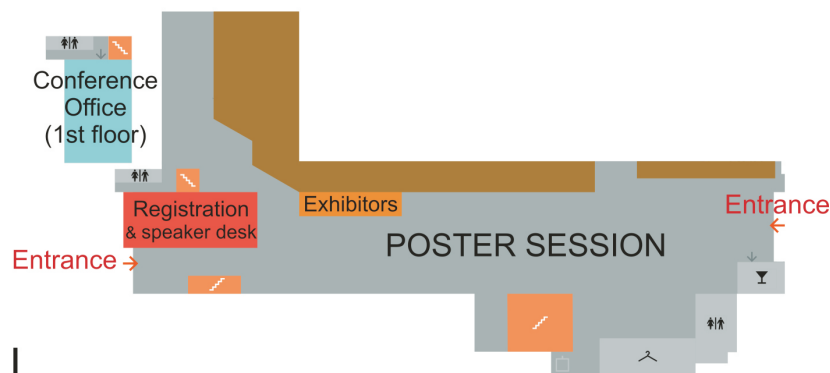
Last year these companies joined to MKS Instruments.

Won tenders – international:

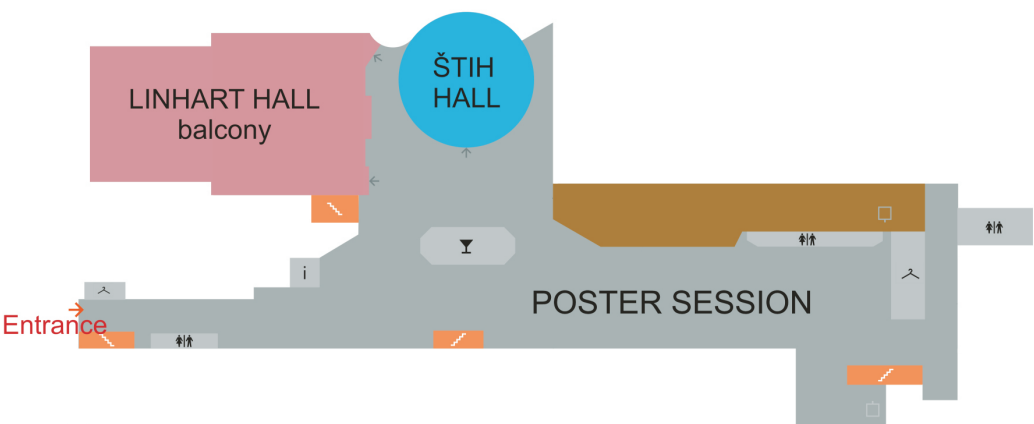
- University of Maribor
- University of Zagreb
- University of Rijeka

Floor plans

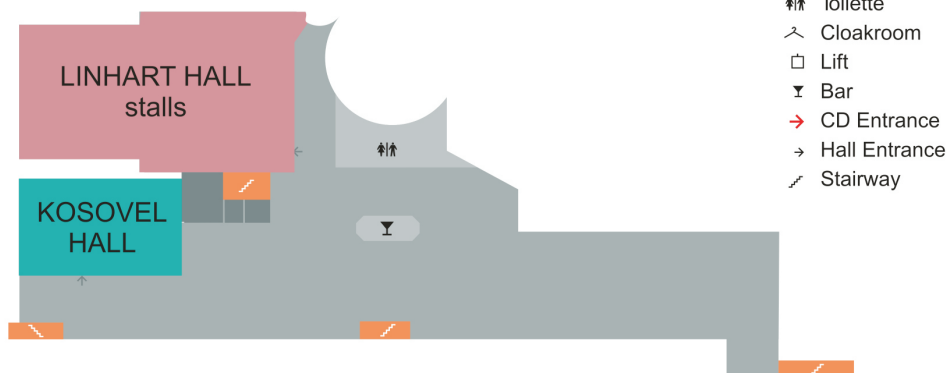
0 | Grand Reception Hall



-1 | Foyer I



-2 | Foyer II



LIQUIDS 2017 – Conference Program

Monday July 17			Tuesday July 18			Wednesday July 19			Thursday July 20			Friday July 21					
Kosovel Hall			Linhart Hall			Šišin Hall			Kosovel Hall			Linhart Hall			Šišin Hall		
8-45			8-45			8-45			8-45			8-45			8-45		
OPENING SESSION			OPENING SESSION			OPENING SESSION			OPENING SESSION			OPENING SESSION			OPENING SESSION		
9:00			9:00			9:00			9:00			9:00			9:00		
P1 Tarjus			P3 Lavrenovich			P5 Vlassopoulos			P7 - de Gennes Lecture Golestanian			P9 Bonn			P10 Perkin		
10:00			10:00			10:00			10:00			10:00			10:00		
K8.1 Charbonneau			K5.1 Dellago			K8.2 Rotler			K3.1 Lopez Leon			K1.2 Rotenberg			K3.2 Smalyukh		
O8.1 Shiba			O5.1 Loehr			O1.1 Bartsch			O8.6 Bomboi			O3.1 Dijkstra			O1.3 Comet		
O8.2 C. Zhang			O5.2 Caciagli			O1.2 Forsman			O8.7 Trappe			O3.2 Gretel			O3.6 Nikhrou		
															O3.7 Ragunathan		
															O5.14 Kraft		
															O4.2 Coluzzi		
															O10.2 Magli		
															Dias		
															K6.1 Briic		
															K9.2 Squires		
															K2.2 Stroock		
															K6.3 Cohen-Addad		
															O9.4 Marbach		
															O2.6 Woutersen		
															O6.2 Forel		
															O9.5 Brenond		
															O2.7 Puisio		
															O8.6 Guardia		
															O6.4 Filippi		
11:10			11:10			11:10			11:10			11:10			11:10		
COFFEE BREAK POSTERS			COFFEE BREAK POSTERS			COFFEE BREAK POSTERS			COFFEE BREAK POSTERS			COFFEE BREAK POSTERS			COFFEE BREAK POSTERS		
Topics: 1, 3, 7, 8, 10			Topics: 1, 3, 7, 8, 10			Topics: 1, 3, 7, 8, 10			Topics: 2, 4, 5, 6, 9, 11			Topics: 2, 4, 5, 6, 9, 11			Topics: 2, 4, 5, 6, 9, 11		
12:30			12:30			12:30			12:30			12:30			12:30		
14:00			14:00			14:00			14:00			14:00			14:00		
P2 Stebe			P4 Dullens			P6 Frey			P8 Loetting			P10 Perkin			P10 Perkin		
15:00			15:00			15:00			15:00			15:00			15:00		
K10.1 Löwen			K5.2 Tienno			K7.1 Chen			K8.3 Royall			O5.9 Russo			O10.4 Mornin		
O10.1 Simnichen			O5.3 McBride			O7.1 Tarazona			O8.8 Schlope			O5.10 Soligno			O10.5 Levis		
															O10.6 Leitmann		
															O9.2 Yvoert		
															O4.4 Rosen-Bunge		
															O11.2 Sengupta		
															O2.2 Ricci		
															O7.11 Engel		
															O2.3 Trefalt		
															O11.5 Vijayarani		
16:30			16:30			16:30			16:30			16:30			16:30		
Nikousterman Buttironi			MacDowell			F. Zhang			Scotti			Aht			Jabbari-Farouji		
17:00			17:00			17:00			17:00			17:00			17:00		
O8.3 Bowles			O5.6 Bartlett			O7.4 Martinez			O3.3 Meiselaar			O7.7 Charlaix			O10.8 Gomez-Solano		
O8.4 Fuchs			O5.7 Everts			O7.5 Guillelm			O3.4 Yamanoto			O7.8 Janssen			O10.9 Ignes-Muller		
O8.5 Coslovich			O5.8 Gambassi			O7.6 Shahzadeh			O3.5 Jeong			O7.9 Uematsu			O10.10 Cebirio		